



UNIVERSIDAD NACIONAL AUTÓNOMA DE MÉXICO

Maestría y Doctorado en Ciencias Bioquímicas

**“SELECCIÓN DE UN ANTICUERPO DE UN SOLO DOMINIO HUMANO
ESPECÍFICO PARA EL COMPLEJO PROTEÍCO FORMADO ENTRE HLA-
A*0201 Y UN PÉPTIDO PERTENECIENTE AL ANTÍGENO Ag85B de
Mycobacterium tuberculosis”**

TESIS

PARA OPTAR POR EL GRADO DE:

Doctora en Ciencias

PRESENTA:

Paola Andrea Ortega Portilla

TUTOR PRINCIPAL

Dra. Clara Inés Espitia Pinzón
Instituto de Investigaciones Biomédicas

MIEMBROS DEL COMITÉ TUTOR

Dra. Gohar Gevorkian Markosian
Instituto de Investigaciones Biomédicas

Dr. Rogelio Enrique Hernández Pando
Instituto Nacional de Ciencias Médicas y Nutrición Salvador Zubirán

Ciudad Universitaria, CD. MX. Noviembre, 2021



Universidad Nacional
Autónoma de México



UNAM – Dirección General de Bibliotecas
Tesis Digitales
Restricciones de uso

DERECHOS RESERVADOS ©
PROHIBIDA SU REPRODUCCIÓN TOTAL O PARCIAL

Todo el material contenido en esta tesis esta protegido por la Ley Federal del Derecho de Autor (LFDA) de los Estados Unidos Mexicanos (México).

El uso de imágenes, fragmentos de videos, y demás material que sea objeto de protección de los derechos de autor, será exclusivamente para fines educativos e informativos y deberá citar la fuente donde la obtuvo mencionando el autor o autores. Cualquier uso distinto como el lucro, reproducción, edición o modificación, será perseguido y sancionado por el respectivo titular de los Derechos de Autor.

Este trabajo de tesis fue realizado en el Instituto de Investigaciones Biomédicas de la Universidad Nacional Autónoma de México (UNAM)

La propuesta y trabajo de investigación fue desarrollado durante la formación doctoral gracias al apoyo de:

Consejo Nacional de Ciencia y Tecnología (CONACYT)
CVU/Becarios: 707238

Programa de investigación institucional Nuevas Alternativas para el Tratamiento de Enfermedades Infecciosas “NUATEI” del Instituto de Investigaciones Biomédicas-UNAM

Programa de Apoyo a Proyectos de Investigación e Innovación Tecnológica “PAPIIT”/
CV-201220, del Instituto de Investigaciones Biomédicas-UNAM

Proyecto EC/H2020.PHC-2014/EMI-TB -“Eliciting Mucosal Immunity to Tuberculosis”-
King`s College London.

DEDICATORIA

A mi familia...

A mi hermana Nancy, por su apoyo y amor incondicional.

A mis tíos Bernardo, Juan Carlos y Ligia Ortega, por ser mis pilares, mi ejemplo e inspiración.

A mis sobrinos que adoro.

AGRADECIMIENTOS

A la Dra. Clara Inés Espítia Pinzón, por abrirme las puertas de su laboratorio, brindándome la oportunidad de crecer no solamente en la academia si no también como persona. Gracias por su guía, paciencia, comprensión y por compartir su sabiduría día a día.

A la Maestra María Cristina Parada Colín, por sus enseñanzas en el manejo y desarrollo de proteínas recombinantes, representando uno de los apoyos técnicos principales para el desarrollo del presente trabajo. De igual manera, agradezco su apoyo a nivel personal, por estar ahí cuando lo necesite, y por permitirme compartir momentos inolvidables de mucha alegría.

A la Dra. Mayra Silva Miranda, por depositar su confianza al compartir su conocimiento en el área técnica de cultivo celular y microscopia de fluorescencia, enseñanzas que permitieron la culminación de esta propuesta investigativa. Gracias por mostrarme las pautas necesarias para desarrollar un criterio con bases suficientemente sólidas, pero siempre acompañadas de la humanidad requerida. Realmente, las palabras se quedan cortas para expresar mi agradecimiento por su invaluable amistad.

A Jose Alberto, quien fue un pilar constante, gracias por escuchar y comprender cada una de las situaciones a las que tuve que enfrentarme, gracias por ser una luz.

A Laura Cancino y Wenceslao Coronada, quienes hicieron de la etapa final, un momento inolvidable que siempre recordaré con alegría puesto que, a pesar de la situación mundial, unimos fuerzas, aprendiendo, creciendo y apoyándonos cada día. Gracias.

A mis compañeros de laboratorio: Erika Segura, Laura Guzmán, Omar Aliaga, Luis Eduardo, por sus enseñanzas, acompañamiento y por momentos que recordaré con gratitud.

A todas las personas que me acompañaron en los malos, buenos y excelentes momentos en mi estancia en México, gracias por hacer de esta, una de las mejores experiencias de vida. Tony, Rafa, Rafita, Alonso y Jesús.

A mi familia biológica, quienes fueron un apoyo sentimental a la distancia, representando un estímulo suficiente para continuar en este camino.

ÍNDICE GENERAL

A.	RESUMEN.....	1
B.	ABSTRACT	2
C.	ABREVIATURAS.....	3
D.	INTRODUCCIÓN.....	4
	D.1 Datos epidemiológicos tuberculosis.....	5
	D.2 Respuesta inmune en tuberculosis.....	6
	D.2.1 Presentación antigénica	9
	D.3 Proteína Ag85B.....	11
	D.3.1 Péptido Ag85Bp _(199KLCANNTRL207)	14
	D.4 Proteínas de complejo principal de histocompatibilidad y Tuberculosis en México.....	15
	D.5 Anticuerpos tipo TCR.....	17
	D.6 Anticuerpos de un solo dominio.....	19
	D.6.1 Desarrollo y selección de anticuerpos de un solo dominio.....	21
	D.6.2 Aplicación de anticuerpos de un solo dominio.....	23
E.	JUSTIFICACIÓN.....	26
F.	HIPÓTESIS.....	26
G.	OBJETIVO GENERAL.....	26
H.	OBJETIVOS ESPECÍFICO.....	26
I.	DISEÑO EXPERIMENTAL.....	27
J.	MATERIALES Y MÉTODOS.....	27
	J.1 Complejos proteicos recombinante: HLA-A*0201/péptidos de <i>Mycobacterium tuberculosis</i>	28
	J.1.2. Evaluación de complejos recombinantes.....	28
	J.2. Selección anticuerpos de un solo dominio contra el complejo Ag85Bp/HLA- A*0201.....	28
	J.2.1 Rondas de selección usando despliegue en fago.....	28
	J.2.2 Fusión con partículas fágicas.....	29
	J.2.3 Precipitación de partícula fágica con PEG30.....	30
	J.3 Evaluación de clonas post rondas de selección por despliegue en fago.....	30
	J.3.1 Selección y fusión de clonas con partículas fágicas.....	30
	J.3.2 Evaluación de clonas por inmunoensayo (anticuerpo de un solo dominio-fago)	31
	J.4 Secuenciación de anticuerpos de un solo dominio.....	31
	J.5 Producción de anticuerpos de un solo dominio solubles.....	32
	J.5.1 Transformación de <i>E. coli</i> cepa HB2151.....	32
	J.5.2 Expresión, extracción y purificación de anticuerpos de un solo dominio.....	32
	J.5.3 Evaluación purificación de anticuerpos de un solo dominio.....	33
	J.6 Evaluación de anticuerpos de un solo dominio.....	34
	J.6.1 Especificidad de anticuerpos de un solo dominio en un inmunoensayo.....	34
	J.6.2 Reconocimiento de anticuerpo de un solo dominio sobre superficie celular.....	34

J.6.2.1 Evaluación de la exposición de HLA-A*0201 en superficie de células T2.....	35
J.6.2.2 Evaluación reconocimiento de anticuerpos de un dominio sobre superficie de células T2.....	35
J.7 Determinación de la constante de afinidad del anticuerpo de un solo dominio 2C.....	36
J.8. Análisis estadístico.....	37
K. RESULTADOS.....	37
K.1. Evaluación de complejos recombinantes mediante inmunoensayo.....	37
K.2. Selección de anticuerpos de un solo dominio contra el complejo Ag85Bp/HLA-A*0201.....	38
K.2.1 Rondas de selección por despliegue en fago.....	38
K.2.2 Evaluación y selección por inmunoensayo (anticuerpos de un solo dominio-fago).....	39
K.3 Secuenciación de clonas seleccionadas.....	40
K.4. Expresión y purificación anticuerpos de un solo dominio.....	41
K.5. Evaluación de anticuerpos de un solo dominio.....	41
K.5.1 Especificidad de anticuerpos de un solo dominio en un inmunoensayo.....	41
K.5.2 Reconocimiento del anticuerpo de un solo dominio 2C sobre superficie celular.....	42
K.5.2.1 Expresión de HLA-A*0201 en superficie de células T2.....	42
K.5.2.2 Reconocimiento de 2C en superficie de células T2.....	43
K.6 Determinación de la constante de afinidad del anticuerpo de un solo dominio 2C.....	45
L. DISCUSIÓN.....	46
M. CONCLUSIÓN.....	49
N. PERSPECTIVAS.....	50
REFERENCIAS	

ANEXOS

- a. Ortega, P. A., Silva-Miranda, M., Torres-Larios, A., Campos-Chávez, E., Franken, K., Ottenhoff, T., Ivanyi, J., & Espitia, C. (2020). Selection of a Single Domain Antibody, Specific for an HLA-Bound Epitope of the Mycobacterial Ag85B Antigen. *Frontiers in immunology*, 11, 577815. <https://doi.org/10.3389/fimmu.2020.577815>.
- b. Valdez-Cruz, N. A., García-Hernández, E., Espitia, C., Cobos-Marín, L., Altamirano, C., Bando-Campos, C. G., Cofas-Vargas, L. F., Coronado-Aceves, E. W., González-Hernández, R. A., Hernández-Peralta, P., Juárez-López, D., Ortega-Portilla, P. A., Restrepo-Pineda, S., Zelada-Cordero, P., & Trujillo-Roldán, M. A. (2021). Integrative overview of antibodies against SARS-CoV-2 and their possible applications in COVID-19 prophylaxis and treatment. *Microbial cell factories*, 20(1), 88. <https://doi.org/10.1186/s12934-021-01576-5>

ÍNDICE DE FIGURAS

Figura 1. Esquema de la estructura de granuloma en infección con <i>Mycobacterium tuberculosis</i>	8
Figura 2: Esquema comparativo de la estructura de anticuerpos tradicionales y de cadena pesada	21
Figura 3: Evaluación de los complejos recombinantes (péptidos/HLA-A*0201)	38
Figura 4: Evaluación de clonas post bio-selección mediante inmunoensayo.....	40
Figura 5: Expresión y purificación de anticuerpos de un solo dominio 2C y 7E a partir de <i>E. coli</i> HB2151.....	41
Figura 6: Evaluación de especificidad de anticuerpos de un solo dominio solubles 2C y 7E (Inmunoensayo).....	42
Figura 7: Expresión de HLA-A*02 en superficie de células T2.....	43
Figura 8: Reconocimiento de 2C y 7E en superficie de células T2.....	44
Figura 9: Determinación de la constante de afinidad por interferometría de biocapa en tiempo real.	45
Figura 10: Potencial de aplicación de anticuerpos de un solo dominio en Tuberculosis.	50

ÍNDICE DE TABLAS

Tabla 1: Proteínas de complejo principal de histocompatibilidad y tuberculosis.....	17
Tabla 2: Aplicación anticuerpo tipo TCR.....	18
Tabla 3: Bibliotecas de anticuerpos	22
Tabla 4: Aplicación anticuerpos de un solo dominio	24
Tabla 5: Resultados rondas de selección	38

A. RESUMEN

La tuberculosis es una enfermedad infecciosa causada por *Mycobacterium tuberculosis*, en la cual la respuesta inmunológica del hospedero desempeña un papel fundamental en el control y/o desarrollo de la enfermedad. La función protectora que se le ha adjudicado a los linfocitos T inicia con el reconocimiento de péptidos micobacterianos desplegados con proteínas del complejo principal de histocompatibilidad, expuestos en la superficie de las células infectadas. Dentro del arsenal de antígenos micobacterianos, se destaca el Ag85B que gracias a su naturaleza secretora e inmunodominante, es considerado un blanco atractivo para el diseño de vacunas. A lo largo de su secuencia proteica, se han identificado epítopes interaccionando específicamente con la proteína HLA-A*0201, con la cual forma complejos proteicos que son reconocidos por linfocitos TCD8 de ratón y de humano infectados con *M. tuberculosis*. El reconocimiento de estos complejos por parte del receptor de las células T (TCR) es altamente específico, puesto que reconoce la interacción péptido-proteína HLA, cualidad que ha llevado al desarrollo de anticuerpos que emulan este reconocimiento conocidos como anticuerpos tipo TCR. En el presente trabajo, se desarrolló una estrategia de selección e identificación de anticuerpos de un solo dominio, dirigidos contra el complejo proteico formado por el péptido de Ag85B_{p199-207} y la proteína HLA-A*0201, a partir de una biblioteca de anticuerpos de un solo dominio de origen humano. Para lograr este objetivo, se realizaron tres rondas de selección mediante la metodología de despliegue en fago, usando al complejo proteico como molécula blanco, lo cual permitió la identificación de un anticuerpo de un solo dominio humano, nombrado 2C, que al estar desplegado en una partícula fágica y también como secuencia proteica independiente reconoció al complejo proteico recombinante Ag85Bp/HLA-A*0201 en un inmunoensayo y sobre una superficie celular.

B. ABSTRACT

Tuberculosis is an infectious disease caused by *Mycobacterium tuberculosis*, where the host's immune response plays a fundamental role in controlling and developing the disease. The protective function assigned to T lymphocytes begins with recognizing mycobacterial peptides displayed with proteins belonging to the major histocompatibility complex, exposed on the surface of infected cells. Within the arsenal of mycobacterial antigens, Ag85B stands out, which, thanks to its secretory and immunodominant nature, is considered an attractive target for vaccine design. Throughout its protein sequence, epitopes have been identified that are displayed specifically by the HLA-A*0201 protein, forming a protein complex recognized by mouse and human TCD8 lymphocytes infected with *M. tuberculosis*. The recognition of these complexes by the T cell receptor (TCR) is highly specific since it recognizes the peptide-HLA protein interaction, a quality that has led to the development of antibodies that emulate this recognition, known as antibodies TCR-like. In the present work, a strategy for selecting and identifying single-domain antibodies, directed against the protein complex formed by the Ag85B_{p199-207} peptide and the HLA-A*0201 protein, was made using a library of human single-domain antibodies. To achieve this objective, three rounds of selection were carried out, using the phage display methodology, using the protein complex as a target molecule, which allowed the identification of a human single domain antibody, named 2C, which, when displayed in a phage particle and also as an independent protein sequence, recognized the protein complex Ag85Bp / HLA-A * 0201 in an immunoassay and on a cell surface.

C. ABREVIATURAS:

ADN: Ácido desoxirribonucleico

BCG: *Mycobacterium bovis* bacillus Calmette-Guérin

BSA: Albúmina sérica bovina

CAR-T: Chimeric Antigen Receptor- T cells.

HLA-A: Human Leukocyte Antigen

HRP: Peroxidasa de rábano

IFN- γ : interferón gamma

IgG: Inmunoglobulina G

IL-10: Interleucina 10

IPTG: Isopropil β -D- tiogalactopiranosido

Mtb: *Mycobacterium tuberculosis*

MDRTB: Tuberculosis multidrogorresistente

OPD: O-Phenylenediamine dihydrochloride

PBS-T0.05: solución amortiguadora con Tween 20 al 0.05%

PBS-TBSA: solución amortiguadora con Tween20 al 0.05%- BSA 2%

PBS: solución amortiguadora o amortiguador de fosfato de sodio

PEG: Polyetiological

PFA: Paraformaldehído

PRRs: Pattern Recognition Receptors.

PAMPs: Pathogen associated molecular patterns.

SDS PAGE: Electroforesis en gel de poliacrilamida con dodecilsulfato de sodio

TCD4: Linfocitos T CD4+

TCD8: Linfocitos T CD8+

TMB:3,3',5,5'-tetramethylbenzidine

TCR: T cells receptor

TLR: Toll like Receptor

UFC_s: Unidades formadoras de colonias

VIH: Virus Inmunodeficiencia Humana

VHH: Variable domain heavy chain

V-NAR: Variable domain new antigen receptor.

D. INTRODUCCIÓN

Mycobacterium tuberculosis (Mtb) es el agente causal de Tuberculosis, enfermedad crónica que afecta principalmente los pulmones, su transmisión ocurre mediante inhalación de gotas de *flügge* que contienen a los bacilos. Se calcula que un cuarto de la población mundial tiene tuberculosis latente y aproximadamente el 10% de estas personas infectadas desarrollarán la enfermedad por reactivación de la bacteria en edad avanzada o en condiciones de inmunosupresión (Manangan y col, 2001). La dinámica pos-infección, depende de factores propios de la micobacteria y de la respuesta inmune del hospedero, donde la población de linfocitos T desempeña un importante papel en la protección contra la enfermedad. La activación de los diferentes mecanismos efectores de esta población celular, depende de su receptor de superficie, conocido como TCR (del inglés *T-Cell Receptor*) el cual reconoce complejos formados entre péptidos de origen micobacteriano y proteínas del complejo principal de histocompatibilidad desplegados en la superficie de células previamente infectadas.

Dentro del arsenal antigénico micobacteriano, los antígenos de secreción se caracterizan por inducir una fuerte respuesta inmunológica, donde la proteína Ag85B es uno de los más abundantes en fase aguda de infección y gracias a su inmunodominancia, es uno de los antígenos más estudiados por su potencial a candidato vacunal (Kwon y col, 2018). A lo largo de su secuencia proteica, se han identificado péptidos específicos reconocidos por los linfocitos TCD8, presentados de manera específica con la proteína HLA-A*0201 (Geluk y col, 2000).

Esta cualidad de interacción entre péptido-HLA-I, fue utilizada para construir complejos recombinantes, permitiendo la identificación de linfocitos TCD8-péptido específicos en pacientes con tuberculosis activa (Axelsson R. y col, 2013). Tal identificación, incentivó al desarrollo de moléculas que simularán el reconocimiento del receptor de linfocitos T conocidas como anticuerpos tipo TCR. Esta estrategia ha sido ampliamente explorada en enfermedades como el cáncer, donde se busca su aplicación como herramientas de identificación y eliminación específica del tejido afectado (Høydahl L. y col, 2019).

Una de las estrategias más utilizadas para su desarrollo, es la técnica de despliegue en fago, la cual, mediante rondas de exposición entre la molécula blanco y las bibliotecas de

anticuerpos desplegados en la superficie de una partícula fágica, permite su selección de manera específica. Uno de los formatos más utilizados para la construcción de estas bibliotecas, son los fragmentos de anticuerpo de un solo dominio, los cuales han mostrado ciertas ventajas con respecto a anticuerpos completos, como el reconocimiento de epítopes de difícil acceso, menor respuesta inmunológica inespecífica (ausencia de fracción cristalizante), bajos costos en producción y la opción de obtener moléculas de reconocimiento cien por ciento humanas. Gracias a sus cualidades como mayor solubilidad, alta estabilidad estructural, este formato ha sido uno de los más explorados actualmente para el desarrollo de herramientas a fin de contrarrestar la pandemia causada por SARS-CoV-2 (Huo y col., 2020) (Li W. y col., 2020).

En el presente trabajo, se describe la selección y evaluación de un anticuerpo de un solo dominio humano, que tiene la capacidad de reconocer un péptido de Ag85B, desplegado con la proteínas HLA-A*0201, en formato recombinante y también en superficie celular. La obtención de este anticuerpo, no sólo representa una herramienta con el potencial para identificar células infectadas con la micobacteria, sino también la estandarización de una metodología que podría ser aplicada para seleccionar y evaluar anticuerpos con el mismo formato y naturaleza, dirigidos contra otros epítopes inmunogénicos pertenecientes a antígenos tanto de Mtb como de otros microorganismos.

D.1 Datos epidemiológicos de Tuberculosis

En 2019, 10 millones de personas desarrollaron la enfermedad, causando 1.2 millones de muertes (Reporte mundial de tuberculosis, 2020). En los individuos con tuberculosis latente coinfectados con el Virus de Inmunodeficiencia Humana (VIH), se aumenta en un 10% la probabilidad de desarrollar tuberculosis activa, siendo la causa principal de muerte en estos pacientes con 208,000 muertes reportadas en 2019. En México, la incidencia estimada y tasa de muerte por cada 100,000 habitantes reportada en el 2019, se encontró en el rango de 10-99 casos, y 1 a 4.9 por año respectivamente, según el reporte mundial de tuberculosis 2020 (8). A nivel nacional, 31,724 nuevos casos de tuberculosis respiratoria, fueron reportados por la Dirección general de epidemiología en el año 2020 (Dirección general de epidemiología, 2020). Estas cifras, muestran que no se ha logrado el control de la enfermedad a pesar de

contar con una vacuna y tratamiento establecidos. La protección de la vacuna Bacillus Calmette-Guérin (BCG), en recién nacidos e infantes contra tuberculosis meníngea y miliar, tiene una eficacia del 70% (Colditz y col., 1995), y en adultos, la protección contra tuberculosis pulmonar está en el rango de 0 a 80% (Brewer T., 2000). A este panorama, se suma la presencia de cepas resistentes a Rifampicina, con 465,000 casos en el 2019, de los cuales, 78% también son resistentes a Isoniacida, catalogándose como tuberculosis multirresistente.

En cuanto a su diagnóstico, la baciloscopia sigue siendo utilizada, aún con una sensibilidad de alrededor del 50%, y en donde el cultivo micobacteriano que tarda aproximadamente 12 semanas. La prueba rápida Xpert MTB/RIF, que permite detectar tuberculosis y resistencia a rifampicina, la cual fue aprobada por la Organización Mundial de Salud (OMS), desde el 2010, sin embargo, no todos los centros de atención médica tiene acceso a esta. Desde la declaración por parte de la OMS de la pandemia causada por el virus SARS CoV-2 a inicios del año 2020, la identificación y manejo de pacientes con tuberculosis, se vio afectada negativamente. Según el reporte mundial de tuberculosis 2020, el número de casos detectados y tratados, disminuyó en el primer semestre del año, en comparación con el mismo periodo del 2019, además, el incremento en desempleo, hacinamiento y mal nutrición, resultado del impacto económico causado por la pandemia, podría incrementar el número de casos con tuberculosis en el periodo comprendido entre los años 2020 a 2025. Organismos internacionales como la OMS y la Organización de las Naciones Unidas, se han planteado estrategias para lograr la reducción de la incidencia de tuberculosis, meta que se plantea alcanzar para el 2035. En este sentido, la búsqueda y desarrollo de nuevas alternativas, que permitan estudiar más a fondo la enfermedad, diagnosticar y explorar opciones a nuevos tratamientos, van de la mano con la meta planteada.

D.2 Respuestas inmunológica en tuberculosis

Mtb agente causal de tuberculosis, es un patógeno intracelular que ingresa por el tracto respiratorio superior mediante inhalación, una vez que el bacilo alcanza las vías respiratorias inferiores, los macrófagos alveolares, las células dendríticas y los neutrófilos, células de la respuesta inmune innata, responden reconociendo y fagocitando al microorganismo. Esta respuesta desempeña una función importante en el control inicial de la infección, y a través

de la presentación de antígenos hacia células de la respuesta adaptativa, constituye el enlace entre las dos respuestas.

La interacción inicial entre la micobacteria y las células del sistema inmune innato, se presenta mediante receptores de las células del hospedero ubicados en la superficie celular y el citoplasma, más conocidos por sus siglas en inglés PRRs (*pattern recognition receptors*), que reconocen patrones moleculares asociados a patógenos, más conocidos por sus siglas en inglés PAMPs (*Pathogen associated molecular patterns*) (Court N. y col, 2010). Una vez las células del sistema inmune reconocen al microorganismo, se da inicio a la activación y desarrollo de mecanismos antimicobacterianos, como la formación del fago-lisosoma conteniendo al microorganismo y la producción de Óxido nítrico (Flesch IE y col, 1991) (MacMicking JD y col., 1997).

Durante la fase temprana de infección, tanto los macrófagos alveolares como las células epiteliales de pulmón, secretan quimiocinas que inducen el reclutamiento de fagocitos al sitio de infección, con el fin de potenciar la respuesta inmune del hospedero (Lin Y. y col., 1998) (Nouailles G. y col., 2014). El movimiento de macrófagos alveolares a través del epitelio alveolar, hacia el tejido pulmonar, induce el reclutamiento celular dando inicio a la formación del granuloma, estructura definida como agregado celular que se forma en respuesta a un estímulo persistente de naturaleza infecciosa o no (Ramakrishnan L. 2012). Esta estructura característica de la tuberculosis, está relacionada con la contención física de la infección, sin embargo, algunos estudios han identificado una relación directa entre la presencia de factores de virulencia micobacterianos y la formación de los mismos. En el trabajo de Volkman, H. E y colaboradores en 2004, compararon el efecto sobre el granuloma, al infectar con *Mycobacterium marinum* con y sin RD1 (*Region of differences 1*). A diferencia de lo esperado, la formación de los granulomas fue más lenta y en menor número al infectar con la micobacteria atenuada. Lo que les llevó a sugerir que la presencia de RD1 va de la mano con su formación adecuada (Volkman H. y col., 2004). Otro grupo, evaluó el efecto de la reinfección con Mtb en granulomas ya establecidos, encontrando, que las micobacterias pertenecientes a la segunda oleada de infección, mostraron predilección y un mayor crecimiento en los macrófagos que formaban parte del granuloma, sugiriendo que esta estructura incluso completamente formada, ofrece un microambiente idóneo para flujo y crecimiento micobacteriano (Cosma C. y col, 2008).

El granuloma, está compuesto por macrófagos infectados, células dendríticas, células epitelioides, células gigantes multinucleadas, macrófagos espumosos y neutrófilos, rodeado por una capa de linfocitos T. (Figura 1)(Ndlovu H. y col., 2016). La fusión de membranas plasmáticas de macrófagos, da lugar a la formación de células gigantes multinucleadas, macrófagos espumosos y macrófagos epitelioides (Puissegur M. y col., 2007). Los linfocitos T y B son los últimos en llegar a las zona de infección y forman la capa celular externa, brindando estabilidad estructural permitiendo la restricción micobacteriana, sin embargo, cuando algunas células infectadas ubicadas en el centro del granuloma mueren por necrosis, se forma un espacio hipóxico con alta concentración de lípidos, conocido como granuloma caseoso, el cual puede ganar inestabilidad y dar lugar a la destrucción de la organización celular, permitiendo la liberación de la micobacteria(Ndlovu H. y col, 2016). En cuanto a citocinas, TNF- α e IFN- γ están relacionados con la formación y mantenimiento del granuloma (Clay H. y col., 2008) (Cooper A. y col., 1993).

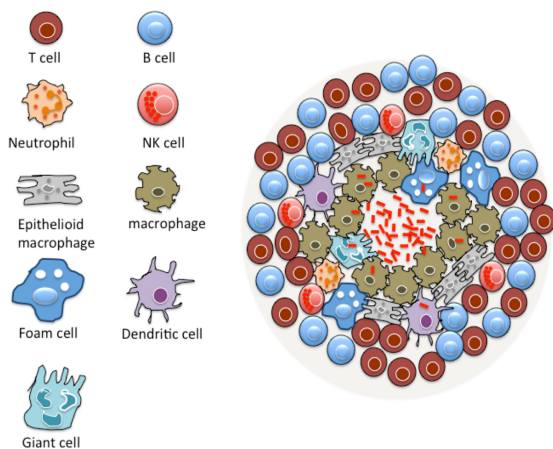


Figura 1: **Esquema de la estructura del granuloma en infección con Mtb.** Tomada de (Ndlovu H. y col., 2016)

Por otro lado, las células dendríticas que han fagocitado a la micobacteria, sus productos y restos de células previamente infectadas, migran hacia nódulos linfáticos locales, para iniciar la presentación antigénica a linfocitos T, actuando como un enlace entre respuesta inmune innata y adaptativa (Wolf A. y col., 2007). Esta presentación inicial, da lugar a la formación, proliferación y activación de linfocitos TCD4 y TCD8 antígeno específicos, donde los LTCD4 representan las principales células efectoras, mediante la producción de citocinas como IFN- γ y TNF- α , e inducción de la activación de funciones antimicobacterianas en fagocitos mononucleares como la producción de óxido nítrico y la fusión fagolisosomal (Scanga C. y col., 2000). La activación de células dendríticas y macrófagos mediante la unión

CD40-CD40L y la inducción de citotoxicidad en células infectadas por expresión de FAS ligando, también son mecanismos de inducción de los LTCD4. Los linfocitos TCD8, también producen IFN- γ y TNF- α y se caracterizan por inducir la muerte de las células infectadas y de la micobacteria directamente, mediante degranulación de moléculas citotóxicas como perforinas y proteasas, se ha descrito que su principal papel está en la fase crónica (Prezzemolo T. y col., 2014). Estas células también inducen apoptosis de células infectadas mediante FAS y TNF-R (receptor de muerte celular). La presencia de linfocitos TCD8-antígeno específicos, está relacionada con la carga micobacteriana, por esta razón algunos trabajos de investigación los proponen como posibles indicadores de la respuesta ante el tratamiento.

D.2.1 Presentación antigénica

La activación de linfocitos TCD4 y TCD8, requiere la presentación antigénica por parte de células infectadas, para tal fin un complejo proceso que abarca, la internalización micobacteriana, tráfico intracelular, cortes proteolíticos, interacciones bioquímicas y exposición en superficie del epítipo antigénico seleccionado son necesarios. Dada la naturaleza de la infección, se esperaría que las células del sistema inmune que fagocitaron a la micobacteria presenten péptidos a los linfocitos TCD4, en el contexto de las moléculas de presentación antigénica clase II (Prezzemolo T. y col., 2014), sin embargo, en la infección con Mtb, se han identificado linfocitos TCD8 antígeno específicos. Además, algunos mecanismos han sido propuestos para explicar el efecto negativo que ejerce la micobacteria en la presentación antigénica:

- Presentación retrasada hacia la respuesta inmune adaptativa: los antígenos de secreción son altamente expresados en fase temprana de la infección, sin embargo, la respuesta de los linfocitos T, es detectada a partir del día 12, esto ha sido adjudicado al tiempo prolongado que tardan las células dendríticas infectadas en llegar hasta los nódulos linfáticos (Wolf A. y col., 2008). La relación entre expresión antigénica y el tiempo de respuesta de los linfocitos T, ha sido catalogado como un mecanismo de evasión a la respuesta adaptativa, permitiendo el tiempo necesario para proliferación y establecimiento inicial de una infección persistente (Baena A. y col., 2009).

- Modificación en la vía de procesamiento antigénica por clase II:

Disminución de la expresión en superficie: esto se ha relacionado directamente con la infección micobacteriana y antígenos específicos. En el trabajo de Pecora y colaboradores, observaron que las células presentadoras de antígenos pulmonares, pertenecientes a ratones expuestos a BCG-GFP, mostraron disminución en la superficie de proteínas de MHC-II, a diferencia de aquellas células no infectadas (Pecora N. y col., 2009).

La naturaleza de los antígenos presentados: los ensayos *in vitro* respaldan el papel supresor sobre la expresión de MHC-II que ejercen algunos antígenos proteicos como la lipoproteína de 19kDa, al ser un ligando de TLR-2, el cual ejerce una prolongada estimulación interviniendo con la señalización de IFN- γ (Fulton S. y col., 2004). Teniendo en cuenta, que la micobacteria cuenta con otros antígenos que actúan como ligandos para TLR-2, (lipoproteína de 38kDa, Esat-6 entre otros), este mecanismo podría ser indicativo de un proceso sinérgico por parte de la micobacteria, enfocado en la disminución de la expresión de moléculas necesarias para la presentación antigénica.

Efecto negativo en el tráfico intracelular de proteínas: el ambiente ácido del compartimento endolisosomal conocido como MHIIC, donde se lleva a cabo la unión de los péptidos micobacterianos con las moléculas de MHC-II, es catalogado como un blanco en el procesamiento antigénico. Esto fue evaluado en un ensayo *in vitro*, comparando la expresión de moléculas MHC-II en células THP-1 expuestas a BCG ureasa negativa y positiva, donde encontraron una relación directa, entre la expresión de ureasa, acompañada de un aumento en la cantidad de amonio, con una disminuida exposición en superficie de moléculas MHC-II (Sendide K. y col, 2004) En este mismo compartimento, se encuentra, Catepsina S, una proteasa de cisteínas, implicada en la degradación de la cadena invariante Li, que permite la unión entre péptidos micobacterianos y las proteínas de MHC-II (Chow A. y col., 2005).

Algunos trabajos han adjudicado un efecto inhibitorio a la IL-10, puesto que se ha relacionado con la disminución de la expresión de catepsina S y la exposición de las moléculas de MHC-II “inmaduras” (en presencia de proteínas li) en superficie, interfiriendo con una adecuada presentación antigénica (Sendide K. y col., 2005).

Presentación antigénica por moléculas clase I:

La fuente de péptidos presentados por las proteínas de clase I, es principalmente del citoplasma celular como consecuencia de infecciones virales y proteínas mal plegadas en el retículo endoplasmático, sin embargo, esta fuente puede ser también a partir de microorganismos que han entrado a la célula por fagocitosis pero que logran escapar al citoplasma, donde sus proteínas serán procesadas y su péptidos serán presentados por moléculas de presentación antigénica clase I. El grupo liderado por Wel N. y col, 2007, mediante inmunofluorescencia y microscopía electrónica, demostró la presencia de Mtb en citoplasma, evidenciando mayor duplicación en comparación con aquellas presentes en fagolisosomas (Wel N. y col., 2007). Mediante microscopía confocal y citometría de flujo, Sreejit y colaboradores, evidenciaron la colocalización del complejo proteico Esat-6/CFP-10 en el lumen del retículo endoplasmático, interaccionando específicamente con la proteína β 2Microglobulina, lo cual se vio reflejado en el incremento de cadenas alfa de moléculas MHC-I libres de β 2M en superficie de macrófagos THP-1(Sreejit G. y col., 2014).

La internalización de cuerpos apoptóticos, provenientes de macrófagos previamente expuestos a proteínas de *Mycobacterium smegmatis*, fue propuesta como una condición que induce presentación cruzada (Espinosa-Cueto P. y col., 2017).

La presentación cruzada y los mecanismos para disminuir la presentación antigénica clase II, identificados en la infección con *Mycobacterium tuberculosis*, ha incentivado la búsqueda de antígenos que despierten la respuesta de linfocitos TCD8. Los antígenos de secreción se caracterizan por inducir una fuerte respuesta en los linfocitos TCD4 y TCD8, dentro de este grupo antigénico, el complejo proteico Ag85B se han destacado por desempeñar diferentes funciones en la infección micobacteriana, por lo tanto, su selección para estudio permitiría ampliar el campo de aplicación para el diseño de estrategias vacunales y el desarrollo de terapias inmunológicas que complementen el tratamiento actualmente existente.

D.3 Proteína Ag85B

El Ag85B, pertenece al complejo Ag85, formado por tres proteínas, Ag85A (31kDa), Ag85B (30kDa) y Ag85C (31.5kDa), codificadas por los genes *fbpA*, *fbpB*, y *fbpC2* respectivamente.

El Ag85 es un complejo antigénico altamente conservado en otras especies micobacterianas y representa la mayor parte de proteínas de secreción en cultivo (60%), la cual se encuentra en el cultivo desde el día tres y representa hasta un 41% durante la fase logarítmica de la micobacteria (Harth G. y col., 1996) (Babaki M. y col., 2017). Ag85B es una proteína de secreción en fase aguda, sin embargo, exhibe disminución de su RNA mensajero (RNAm), tres semanas post-infección (Rogerson B. y col, 2006). Utilizando PCR en tiempo real, Wilkinson y colaboradores, midieron la cantidad (RNAm) de Ag85B en monocitos infectados con Mtb y encontraron un aumento de 54 veces comparado con el RNAm 16S micobacteriano después de 24 horas de infección, proponiendo a Ag85B como indicador de crecimiento intracelular de la micobacteria (Wilkinson R. y col., 2001).

El complejo Ag85, tiene actividad de micolil-transferasa que cataliza la transferencia de ácido micólico al arabinogalactan presente en la pared micobacteriana, dando lugar a una barrera altamente impermeable que brinda protección a fármacos y sustancias hidrofílicas; esta actividad enzimática también participa en la biosíntesis de Trehalosa Dimicolato TDM, que consiste en la unión entre una trehalosa y dos grupos de ácido micólico (Kuo C. y col., 2012), siendo el glicolípido más abundante de la envoltura micobacteriana (Dulberger C. y col, 2020). Dentro de algunos mecanismo de virulencia, adjudicados a TDM, está la resistencia a antibióticos y la formación de granulomas (Hunter R. y col, 2006). Además, su eliminación de la pared micobacteriana por extracción química (Indrigo J y col., 2003) o mediante la eliminación de expresión de las proteínas Ag85A en la cepa H37Rv, evidenciaron menor replicación intracelular y velocidad de crecimiento (Armitige L y col, 2000). La unión del complejo Ag85 a fibronectina y elastina se ha relacionado con adherencia, invasión y diseminación micobacteriana en células del hospedero (Kou C. y col., 2013).

Al complejo Ag85, se le ha adjudicado un papel tipo protector dado que contiene proteínas inmunodominantes que inducen la producción de IFN- γ y IL-2 por linfocitos Th1 (Forrellad M. y col, 2013) (Huygen K., 2014). Por esta razón, ha sido ampliamente explorado su potencial como candidato vacunal, siendo evaluado en diversos formatos. Como vacuna micobacteriana recombinante rBCG30, donde BCG contiene un plásmido que codifica a Ag85B, mostrando disminución de unidades formadoras de colonia a nivel pulmonar y bazo

(Horwitz M. y col., 2000) (Khan A. y col., 2019). *Mycobacterium smegmatis*, transformada con un plásmido que codifica epítopes específicos del Ag85B (rMs064), evidenció un aumento significativo en la producción de IFN- γ e IL-12 (Kadir N. y col., 2016).

El Ag85B también se ha evaluado como vacuna de subunidad, en combinación con otros antígenos de secreción, por ejemplo, (Hybrid1-IC31), que contiene Ag85B y Esat-6, esta vacuna se encuentra actualmente en fase II de evaluación clínica. Los resultados obtenidos evidenciaron la inmunogenicidad y la respuesta predominante de los linfocitos TCD4+ específicos para Ag85B, coexpresando INF- γ , TNF- α y IL-2, en comparación con Esat-6 (Mearns H. y col., 2017). En combinación con proteínas específicas de latencia, como H56:IC31, (Ag85B-Esat-6-Rv2660), donde la respuesta inducida por el Ag85B en LTCD4 específicos, fue predominante y sostenida en el modelo de evaluación, en comparación con la respuesta no uniforme hacia los otros dos antígenos presentes en la vacuna (Suliman S. y col., 2019). También se ha evaluado el Ag85, utilizando virus como vectores, AERAS-402 es un adenovirus que contiene las secuencias de Ag85A, Ag85B y TB10.4, esta vacuna fue evaluada en fase clínica II, y se observó la inducción de una fuerte respuesta en los linfocitos TCD4 y TCD8. A bajas dosis se evidenciaron células T polifuncionales, siendo predominante para el Ag85A/B (Van Z. y col., 2017).

Las vacunas basadas en DNA, también han sido evaluadas con secuencias génicas del Ag85, por ejemplo Ag85B-T-bet, donde utilizaron al gen de Ag85B y T-bet como adyuvante, después de la inmunización se obtuvo una significativa producción de INF- γ e IL-2, acompañada de una disminución de las citocinas IL-4 e IL-10 (Hu D. y col., 2012). Y finalmente MTBVAC, la única vacuna de una cepa atenuada de Mtb, tiene dos genes eliminados, *phoP* que controla aproximadamente el 2% del todo el contenido genómico y *fadD26* relacionado con la ruptura fagosomal. Esta vacuna también ha sido evaluada en fase clínica II (ClinicalTrials.gov identifier: NCT02729571) y se le ha adjudicado parte de su eficacia, a la antigenicidad incrementada por la secreción del Ag85 (Kauffman S. y col., 2014).

Las referencias anteriormente mencionadas, representan algunos trabajos de investigación en los últimos años, en donde se ha evaluado el potencial del complejo Ag85 como agente vacunal. El patrón de respuesta antígeno-específica predominante, post-vacunación de los linfocitos TCD4 y TCD8, ante las proteínas de Ag85, han incentivado la búsqueda de

epítopes que son reconocidos por el TCR. Su identificación podría representar un blanco adicional, que permitiría estudiar más a fondo la interacción entre respuesta inmune del hospedero y la micobacteria, como también el desarrollo de herramientas que ayuden a contrarrestar el desarrollo de la infección.

D.3.1 Péptido Ag85Bp_(199KLVANNTRL207)

La inmunodominancia de Ag85B llevó a Geluk y colaboradores en el 2000, al desarrollo de un trabajo, donde, usando el modelo de ratón HLA-transgénico, identificaron dos secuencias de 9 residuos de aminoácidos, presentadas por la proteína HLA-A*0201 mediante la cuantificación de linfocitos TCD8 péptido-específicos, siendo la secuencia (KLVANNTRL) una de la identificadas (Geluk A. y col., 2000). El grupo de FF Weichold, en el 2007, analizaron interacciones bioquímicas entre 49 péptidos pertenecientes al antígeno Ag85B y 7 alelos de proteínas pertenecientes al complejo principal de histocompatibilidad clase I. Sus resultados evidenciaron que la interacción entre el péptido (KLVANNTRL) y la proteína HLA-A*0201 es altamente específica, puesto que el mismo péptido no es plegado con alelos diferentes. (Weichold F. y col., 2007).

El análisis comparativo entre secuencias completas de 21 cepas filo-geográficamente diversas, pertenecientes al complejo de Mtb, realizado por el grupo de Iñaki y colaboradores en el 2010, permitió concluir que los epítopes que despiertan respuesta de los linfocitos T (donde se encuentra la secuencia KLVANNTRL), son altamente conservados en comparación con el resto del genoma, su grado de conservación fue cercano al reportado para genes esenciales (Comas I., y col, 2010).

Axelsson y colaboradores en el 2013, midieron la frecuencia de linfocitos TCD8 de 27 pacientes con tuberculosis activa previa al tratamiento, utilizando tetrámeros recombinantes, formados entre proteínas del antígeno leucocitario humano más frecuentes en la población africana y los péptidos KLVANNTRL de Ag85B y AMASTEGNV de Esat-6. Esto, permitió la identificación de los linfocitos TCD8 péptido-específicos con mayor frecuencia en la población evaluada, incluso comparada con otras secuencias del mismo antígeno, estos hallazgos permitieron reafirmar la inmunodominancia de la secuencia KLVANNTRL (Axelsson R. y col., 2013) Este mismo grupo del Instituto Karolinska, en el 2015, aplicando una metodología similar, en una población de Korea del sur donde los alelos HLA-A*02 y

HLA-A*24 son unos de los más frecuentes, identificaron linfocitos TCD8 en pacientes con tuberculosis activa, donde el tetrámero formado entre HLA-A*0201 y la secuencia KLVANNTRL de Ag85B, mostró la mayor frecuencia a linfocitos TCD8 péptido-específicos(Axelsson R. y col., 2015). Siguiendo la misma estrategia, pero ahora realizando una comparación antes y después del tratamiento en pacientes sudafricanos diagnosticados con tuberculosis, se evidenció una disminución de 0.11% en la frecuencia de linfocitos TCD8 específicos para los antígenos de secreción evaluados (Esat-6, Ag85B y TB10.4), en comparación con una disminución de tan solo 0.01% para antígenos de naturaleza no secretora, además, este grupo encontró que a diferencia de la población total de linfocitos TCD8, la población identificada con tetrámeros evidenció un mayor porcentaje de marcadores de degranulación post tratamiento(Axelsson R., y col., 2015).

Estos trabajos demostraron que el péptido KLVANNTRL presente en la secuencia del Ag85B, es expuesto en conjunto con la proteína HLA-A*0201 en la superficie de células infectadas con Mtb y son reconocidos por linfocitos TCD8. También fue evidenciada una alta especificidad de interacción con la proteína HLA-A*0201 y un alto grado de conservación. Todas estas características, convierten al complejo protéico entre Ag85B_{p199-207} y HLA-A*0201, en un blanco ideal para el desarrollo de moléculas para su reconocimiento.

D.4 Proteínas del complejo principal de histocompatibilidad y Tuberculosis en México

Dada la importancia que tiene la presentación antigénica en el desarrollo de la enfermedad causada por Mtb, algunos grupos de investigación se han enfocado en encontrar o descartar la relación entre proteínas pertenecientes al complejo principal de histocompatibilidad y predisposición o protección a tuberculosis. Según estudios de meta-análisis, la presencia de HLA-DRB1*04 y HLA-DRB1*08 fueron los más comunes en pacientes con tuberculosis, por otro lado HLA-DRB1*03 y HLA-DRB1*07 fueron relacionados con protección (Li C. y col., 2015)(Oliveira C. y col., 2016).

En trabajos experimentales, realizados en diferentes grupos poblacionales en México, determinaron que los alelos DQA1*0101 (62%), DQB1*0501 (44%), DRB1*1501 (48%) fueron los más frecuentes en pacientes con tuberculosis pulmonar en condiciones no

inmunosuprimidas y DRB1*1101 (46%) fue el más frecuente en pacientes VIH positivos. (Tabla 1) (Teran E. y col., 1999). Al norte de México, 50 pacientes con tuberculosis pulmonar fueron analizados, encontrando una relación positiva entre tuberculosis y los alelos DR11-16 y DQ7, y una relación negativa con DR17 y DQ8 (De lo Angeles R. y col., 2008). En una publicación más reciente, Ocaña-Guzman y colaboradores a inicios del año 2021, reportaron una asociación entre pacientes con tuberculosis pulmonar-multidrogorresistente de origen mexicano y HLA-DRB1*04 (35%), y en pacientes fármaco sensibles con HLA-DRB1*08 con (40%) (Ocaña G. y col., 2021)

HLA-DRB1*04 fue reportado como uno de las más frecuentes con 32.17%, en un estudio de identificación de frecuencia alélica del antígeno leucocitario humano clase I y II, en tres poblaciones de México (Del Angel P., y col., 2020). HLA-DRB1*04 también fue reportado en otro estudio realizado en Brasil, donde la población de pacientes con tuberculosis pulmonar evaluada fue de 316, sin embargo, en este caso, la evaluación alélica fue más específica y logró identificar a DRB1*04:11:01 con 50%, y a DRB1*04:07:01 con 0% en pacientes con tuberculosis pulmonar. En este grupo también se identificó mediante un análisis *in silico* que la interacción entre DRB1*04:07:01 y los péptidos de Esat-6 fue muy alta en comparación con el alelo más frecuente en pacientes con tuberculosis pulmonar. (Souza de L. y col., 2016). Sin embargo, se han reportado trabajos contrastantes, por ejemplo, en India, donde a 109 pacientes diagnosticados con tuberculosis, se identificó a DRB1*14 como uno de los alelos más frecuentes en la población de pacientes multidrogorresistentes y a DRB1*04, como uno de los predominantes en los pacientes farmacosenibles (Sharma S. y col., 2003).

En cuanto a alelos de HLA clase I y su relación con tuberculosis en México, se encuentran muy pocos reportes en la bibliografía. En 34 pacientes mexicanos, el grupo de Soto y colaboradores identificaron a HLA-B*39 y HLA-B*35 como los alelos más frecuentes en pacientes con tuberculosis extrapulmonar y pulmonar respectivamente (Soto M. y col., 2007). HLA-B*35, también identificado fue como uno de los más frecuentes (52%) de 35 pacientes con tuberculosis en Argentina, en este caso, la diferencia significativa se obtuvo comparando con dos grupos control: contactos familiares y controles sanos (De Sorrentino A. y col., 2014). En la publicación de Del Angel P, en el 2020, evaluaron la distribución de alelos y haplotipos en más de 500 mexicanos, donde a pesar de la alta variabilidad alélica

identificada en las tres poblaciones evaluadas, los alelos HLA-A*0201 y HLA-B*3501 fueron los más frecuentes, coincidiendo con reportes de frecuencia alélica a nivel mundial (Neville M. y col., 2017)

Encontrar una asociación entre el desarrollo de tuberculosis y proteínas pertenecientes al complejo principal de histocompatibilidad clase I y II resulta controversial, debido a que la interpretación va de la mano con la frecuencia alélica predominante de la población evaluada, prevalencia de tuberculosis y factores de riesgo. Sin embargo, la identificación de una tendencia alélica y su interacción con péptido micobacterianos, podrían brindar un panorama que permita identificar un aspecto adicional, direccionado hacia el entendimiento del éxito de Mtb como agente patógeno en los humanos.

Tabla 1: Proteínas del complejo principal de histocompatibilidad y tuberculosis

País	Número de pacientes con tuberculosis pulmonar	Alelos más frecuentes		Referencia
		predisposición	protección	
México	50	DQA1*0101(62%)	DQA1*0501(46.3%)	Terán E. y col., 1999.
México	50	DR11-16, DQ7	DR17, DQ8	De los Ángeles y col., 2008.
México	20	DRB1*04♦	---	Ocaña G. y col., 2020.
Brasil	316	HLA-DRB1*04:11:01 (50%)	DRB1*04:07:01♠	Souza de Lima y col., 2016.
India	109	DRB1*14 (30%)♦	---	Sharma y col., 2003.
México	34	HLA-B*39, 35	---	Soto y col., 2007.
Argentina	35	HLA-B*35 (52%)	---	De Sorrentino y col., 2014.

♦ alelo relacionado con el desarrollo de multidrogorresistencia a tuberculosis.

♠ alelo ausente en pacientes con tuberculosis pulmonar.

D.5 Anticuerpos tipo TCR

La importancia del perfil peptídico en conjunto con proteínas pertenecientes al complejo principal de histocompatibilidad, expuestos en superficie celular, durante el cáncer y algunos procesos infecciosos, ha impulsado el desarrollo de moléculas que simulen el reconocimiento

del receptor de linfocitos T. Tales moléculas de reconocimiento son conocidos como anticuerpos tipo TCR.

La interacción con su molécula blanco (péptido/HLA-I), ha sido dilucidada mediante cristalografía, mostrando solo algunas diferencias de reconocimiento con el receptor de linfocitos T, lo cual se le adjudica a la ausencia de moléculas accesorias, (por ejemplo CD8), sin embargo, en todos los casos se conserva el patrón de unión entre el anticuerpo CDR3 y el péptido blanco (Høydahl L. y col., 2019). El tipo de reconocimiento de los anticuerpos tipo TCR, ha permitido detectar y cuantificar péptidos expuestos en superficie, en conjunto con proteínas del complejo principal de histocompatibilidad, brindando un panorama más completo para una evaluación específica del reconocimiento y activación de los linfocitos T (Reay P., y col., 2000).

Gracias a que su blanco de reconocimiento (péptido/HLA-I), está expuesto en las células cancerígenas o células infectadas, su aplicación está enfocada tanto a su identificación como en la eliminación de las mismas. Anticuerpos tipo TCR conjugados con fluorocromos y toxinas, han permitido evaluar su capacidad para identificar e inducir apoptosis y fagocitosis mediada por anticuerpos. En plataformas con nanopartículas y lentivirus también permitido eliminación de células de forma específica (He Q. y col., 2019). Se ha propuesto, su acoplamiento a superficie de células citotóxicas, específicamente al dominio de señalización intracelular (CD3), conllevando a la activación de mecanismos efectores de producción de citocinas, perforinas y granzimas (Chames P., y col 2000).

Tabla 2: Aplicación anticuerpos tipo TCR

HLA-I, II	Nombre	Método de selección	Formato de anticuerpo	Referencia
Cuantificación de péptido/HLA-I				
I-E ^k	D4	Hibridoma	completo	Reay P. y col, 2000.
HLA-A0201	E1, L1 y L2	Hibridoma	completo	Sim A. y col., 2013.
Cáncer				
HLA-A*0101	G8	Despliegue en fago	completo	Chames P. y col., 2000.

HLA-A*0201	38	Despliegue en fago	completo	Ahmed, M., y col., 2018.
Evaluación Inmunoterapéutica				
HLA-A0201	A6, C1 C y C7	Despliegue en fago	Fragmento de reconocimiento antigénico.(Fab)	Bewarder M. y col., 2020.

HCVM: Citomegalovirus humano, LMP2A: péptido de virus Epstein Bar, Fab: Fragment antibody

Para el desarrollo de anticuerpos tipo TCR, se ha utilizado la técnica de hibridoma que aporta anticuerpos con maduración de afinidad *in vivo*, sin embargo, debido al tipo de reconocimiento esperado, la probabilidad de seleccionar clonas específicas es muy baja y la estabilidad reducida de los complejos recombinantes para la inmunización, afectan negativamente su selección (Cohen M. y Reiter Y., 2013). Con el fin de sobreponer estas desventajas, nuevas propuestas metodológicas han permitido la selección de anticuerpos sin necesidad de inmunización. Siendo la técnica de despliegue en fago, una de las más exploradas (Høydahl L. y col., 2019). (Dahan, R., & Reiter, Y., 2012). (Tabla 2).

La fuente de anticuerpos usando esta metodología, son bibliotecas o bancos de anticuerpos recombinantes de diferentes tipos según su origen (naïve, inmunes, sintéticas), y 100% humanas. Permite explorar el uso de fragmentos de anticuerpo: región de reconocimiento antigénico-*fragment antibodies* (Fab_s), fragmentos de anticuerpos de cadena sencilla-*Single Chain Fragment Variable* (scFv) y anticuerpos de un solo dominio o más conocidos como *Nanobodies*. Esta versatilidad, ha permitido desarrollar nuevas opciones para alternar o complementar la aplicación de anticuerpos obtenidos de manera tradicional.

Dentro del grupo de fragmentos de anticuerpos, seleccionados para la construcción de bibliotecas, se han destacado los anticuerpos de un solo dominio o *Nanobodies*, representando el formato más pequeño de reconocimiento (Wang Y. y col., 2016).

D.6 Anticuerpos de un solo dominio

Su desarrollo y aplicación, se dio gracias al descubrimiento de Hamers-Casterman y colaboradores en 1992, quienes identificaron anticuerpos compuestos únicamente por cadenas pesadas, presentes en el suero de *Camelus dromedarius* (Hamers C. y col., 1993). Este tipo de anticuerpos, también ha sido descrito en algunas especies de tiburón (nodriza y

alfombra) y son conocidos como (IgNARs: *Immunoglobulin new antigen receptors*), (Nuttall S. y col, 2001). La estructura de estos anticuerpos, consiste en homodímeros de cadenas pesadas no asociados a cadenas ligeras, ausencia del dominio constante uno y una región bisagra extensa, unida a un dominio variable de reconocimiento antigénico por cada cadena (Figura 2). A estos dominios de reconocimiento, se les ha denominado VHH (*variable domain heavy chain*) para camélidos y V-NAR (*variable domain new antigen receptor*) para tiburones. Debido a su amplio desarrollo, también son conocidos como anticuerpos de un solo dominio (*sdAb: single domain antibodies*) o *nanobodies*, nombre que fue otorgado por Ablynx, una compañía que se enfoca en la producción de este tipo de formato de anticuerpos <https://www.ablynx.com/our-company/overview/>. Este formato tienen un peso molecular de (~15kDa), representando la estructura más pequeña con capacidad de reconocimiento. Definición asignada debido a su reducido tamaño en comparación con otros formatos como scFv de ~ 27kDa y Fab_s de ~57kDa)(Wang Y. y col, 2016). Los anticuerpos de un solo dominio, cuentan con característica estructurales particulares, donde la ausencia de la cadena ligera y la presencia de algunos residuos de aminoácidos específicos, están relacionados con un impacto positivo en su estabilidad y solubilidad (Muyldermans S. 2013). La longitud y número de sus regiones hipervariables, y la presencia de puentes disulfuro adicionales, dan lugar a una arquitectura alargada, relacionada con el reconocimiento de epítopes de difícil acceso para otros formatos de reconocimiento o anticuerpos completos (Govaert J. y col., 2012) (Siontorou C., 2013). Los anticuerpos de un solo dominio, además de su capacidad de reconocimiento, brindan la facilidad de construcción multimérica gracias a su reducido tamaño (Zhu, X. y col., 2010). Dada su alta especificidad han sido propuestos como moléculas de estabilización estructural (Korotkov K. y col., 2009). Todas estas propiedades biofísicas y su versatilidad de reconocimiento, los convierte en una herramienta idónea para investigación básica y también en moléculas con potencial terapéutico (Ingram J. y col., 2018) (Bannas P. y col., 2017) (Jovčevska, I. y col., 2020)

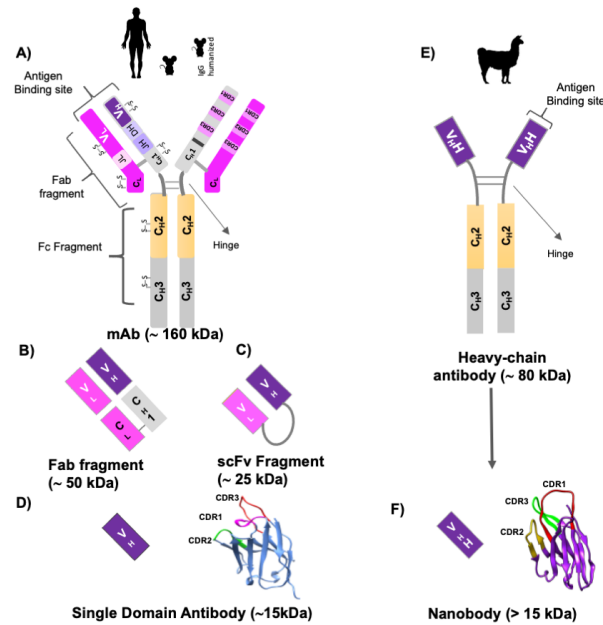


Figura 2: Esquema comparativo entre anticuerpos: A: tradicionales, E: de cadena pesada, B: fragmentos de reconocimiento antigénico, C: fragmentos variables de una sola cadena, D, F: Anticuerpos de un solo dominio-*Nanobody*. Tomada de: Valdez-Cruz N. y col., 2021.

D.6.1 Desarrollo y selección de anticuerpos de un solo dominio

Para su obtención, se ha explorado la inmunización de animales y a partir de bibliotecas no inmunes o sintéticas directamente (Liu W. y col., 2018). Su selección a partir de bibliotecas inmunes, implica la inmunización con el antígeno de interés en animales que generan naturalmente anticuerpos de cadena pesada (Camélidos-Llamas), seguido por la clonación específica de genes pertenecientes a las regiones variables, seguido por su ensamblaje en vectores como fagémidos, y finalmente ser seleccionados específicamente a través de metodologías como despliegue en fago.

La construcción de bibliotecas inmunes, usando anticuerpos de un solo dominio, ofrecen ventajas como: maduración de afinidad inmune desarrollada *in vivo* y mayor grado de conservación en la secuencia del dominio de reconocimiento antigénico, en comparación con el formato *scFv* donde se requiere del acoplamiento entre las secuencias de genes de cadenas variables pesadas y ligeras mediante un péptido adicional. La variabilidad reportada para este tipo de bibliotecas es $\sim 10^6$ a (partir de 50 ml de sangre) (Muyldermans S., 2013). En las bibliotecas de anticuerpos naïve, la variabilidad mínima requerida es $\sim 10^9$ lo que implica un mayor volumen de sangre, representando una limitante.

Para solucionar estos problemas, la construcción de bibliotecas sintéticas y semisintéticas ha sido propuesta. Estas son construidas utilizando menor volumen de sangre y mediante mutaciones se incrementa la variabilidad de las secuencias determinantes de complementariedad, conservando los marcos de lectura canónicos de los dominios variables de cadena pesada. Desarrollando bibliotecas de anticuerpos estables y con alta variabilidad, que pueden ser dirigidos contra diversos antígenos incluyendo aquellos con los cuales no es posible realizar una inmunización (Goldman E. y col., 2006). Aplicando estrategias similares, la construcción de bibliotecas de anticuerpos de origen humano desplegadas en fagos, ha sido posible, permitiendo una selección dirigida contra una amplia gama de antígenos de naturaleza infecciosa y no infecciosa; y gracias a su naturaleza, la aplicación como agentes terapéuticos en humanos se ve potenciada (Li W. y col., 2020). Algunas de las características más relevantes de las bibliotecas de anticuerpos recombinantes se encuentran en la siguiente tabla:

Tabla 3: Bibliotecas de fragmentos de anticuerpo:

Característica	Bibliotecas de fragmentos de anticuerpos		
	Inmune	Naïve	Semi/Sintéticas
Variabilidad	$\approx 10^6$	$\approx 10^9$	$\approx 10^{12}$
Inmunización	Sí	No	No
Sangre	0.05L	>1L	<0.01L
Origen humano	No	No	sí
Tiempo de construcción	prologado	corto	corto
Tipo de antígenos	limitada	No limitada	No limitada

Una de las técnicas más utilizadas para la selección de anticuerpos de un solo dominio, ha sido el despliegue en fago, la cual fue desarrollada en 1985, a quien a mediados del 2018, se le fue otorgado el premio nobel en química. La técnica de despliegue en fago o más conocida como “*phage display*”, consiste en la exposición de péptidos, proteínas y anticuerpos, en la superficie de partículas fágicas, incorporando al ADN foráneo en el genoma del fago (Barderas R. & Benito E., 2019). El despliegue de anticuerpos en el fago, se realiza mediante el acomplamiento a proteínas de la cubierta fágica. La proteína III es una de las más utilizadas, puesto que permite una plataforma idónea para la interacción biblioteca-molécula blanco y optimiza la selección de moléculas con mayor afinidad.

El uso de fagémidos para construir bibliotecas desplegadas en fagos, es uno de los más frecuentes, puesto que permite acoplar ADN foráneo de diversos tamaños, mayor eficiencia en transformación permitiendo mayor diversidad y suficiente estabilidad para tolerar múltiples ciclos de propagación (Qi H. y col., 2012). Además, tiene estratégicamente ubicado un codón de paro (TAG ámbar), entre la secuencia del ADN foráneo (anticuerpo de un solo dominio) y la proteína fágica de cubierta (proteína III), permitiendo la expresión independiente del anticuerpo. Para la expresión del anticuerpo de un solo dominio, se utilizan cepas bacterianas que si reconocen la secuencia de paro (*E. coli* HB2151), permitiendo su obtención soluble independiente de la proteínas III. Gracias a todas estas cualidades, la selección de anticuerpos de un solo dominio, a partir de bibliotecas, ha representado una estrategia ideal para el desarrollo de herramientas que cuenten con un amplio campo de aplicación.

D.6.2 Aplicación de anticuerpos de un solo dominio

La técnica de despliegue en fago, inició con la exposición de péptidos en la superficie fágica (Parmley S. y col., 1988), y posteriormente, fueron los Fab_s, dando lugar a una nueva plataforma de selección de anticuerpos (McCafferty J. y col., 1990), donde los anticuerpos de un solo dominio ha sido ampliamente explorados. Su aplicación diagnóstica y como herramienta para el seguimiento en cáncer mediante su acoplamiento con moléculas como el Galio, ha permitido la identificación de tejido tumoral y su evolución a lo largo del tratamiento, complementando así a las técnicas de imagenología existentes, representando una alternativa a la biopsia (Keyaerts M. y col., 2016).

Su potencial de tratamiento en cáncer, fue evidenciado gracias a la inducción de muerte de célula cancerígenas *in vitro* y a la disminución de tejido tumoral *in vivo* (Roshan R. y col., 2021). También se han evaluado como receptores de células T quiméricas, más conocidas como CAR-T (*Chimeric Antigen Receptor-T cells*), donde se optimizan los mecanismos de eliminación de células cancerígenas mediante el reconocimiento efectuado por el *nanobody* (Zhu L. y col., 2020) (Zhang G., y col., 2014) (Hajari T., y col., 2019). También se ha evaluado su aplicación en enfermedades de origen infeccioso, por ejemplo, los anticuerpos de un solo dominio 2TCE3 y ITC39, en formato divalente y acoplados a HRP, reconocieron

específicamente antígenos de secreción de *Toxocara canis*, en un inmunoensayo, e identificaron la infección en suero de ratones desde etapas más tempranas, en comparación con anticuerpos policlonales convencionales (Morales Y. y col., 2019). Siguiendo con el área de infecciosas, pero con un enfoque terapéutico, la aplicación vía oral del anticuerpo 2R215 dimérico, evidenció mejoría en la presentación clínica y disminución de invasión bacteriana tisular, post-exposición a enterotoxina de *Escherichia coli* en un modelo *in vivo* (Amcheslavsky A. y col., 2021).

Gracias a sus cualidades, actualmente está siendo explorado su potencial como anticuerpos neutralizantes frente al virus causante de la pandemia iniciada en el 2020. Para su desarrollo, las bibliotecas de *nanobodies* desplegadas en partículas fágicas tipo inmune (camélidos), sintéticas y de naturaleza humana, han sido utilizadas (Valdez-Cruz N. y col., 2021). La evaluación inicial consiste en su capacidad de reconocimiento y neutralización *in vitro* y algunos trabajos han evaluado su potencial profiláctico y de tratamiento en modelos *in vivo* (Li W. y col., 2020).

Su aplicación en el área industrial, fue explorada por el grupo de Chen F. y colaboradores, donde evaluaron la capacidad para detectar específicamente una proteína alergénica presente en el cacahuete mediante un inmunoensayo (Chen F. y col., 2019). El primer nanobody aprobado por la FDA en el 2018 fue el Caplacizumab, el cual impide la unión entre el factor de Von Willebrand y plaquetas, previniendo la formación de coágulos en microvasculatura de pacientes que padecen purpura trombocitopénica (Hollifield A. y col., 2020).

Tabla 4: Aplicación anticuerpos de un solo dominio

Anticuerpo de Un solo dominio	Multimerización/ Marcaje	Antígeno	Metodología selección	Potencial aplicación	Referencia
Enfermedades infecciosas					
2TCE39 1TC39	2TCE3- dimérico ITC39-HRP	Antígenos secreción <i>Toxocara canis</i> (ASTC)	Despliegue en fago/biblioteca inmune	Identificación específica de ASTC	Morales Y. y col., 2019.
2R215	Dimérico y trimérico	(Adhesina)factor de colonización- <i>Escherichia coli</i> .	Despliegue en fago	Tratamiento profiláctico	Amcheslavsky col., 2021.

			(biblioteca inmune)		
vH ab8	vH-fc ab8 fusión con fracción cristalizable de anticuerpos humano.	RBD-SARS CoV-2	Despliegue en fago (biblioteca de origen humano)	Neutralización de infección por SARS Cov-2	Lie W. y col., 2020.
n3130 n3988	Monomérico	RBD-SARS CoV-2	Despliegue en fago (biblioteca de origen humano)	Neutralización de infección por SARS Cov-2	Wu Y. y col., 2020.
Nb21 Nb20	Monomérico y Homotrimérico	RBD-SARS CoV-2	Despliegue en fago (biblioteca inmune llama)	Neutralización de infección por SARS Cov-2	Xiang Y. y col., 2020.
Cáncer					
⁶⁸ Ga-HER2-Nanobody	Acoplado a ⁶⁸ Galio	HER2	Despliegue en fago (biblioteca inmune)	Reemplazar biopsias para diagnóstico y seguimiento post tratamiento. (fase I)	Keyaerts M. y col., 2016.
Nb4	Monomérico	Moléculas de adhesión de células epiteliales.	Despliegue en fago (biblioteca inmune)	Agente terapéutico.	Roshan R. y col., 2021.
VHH-28z	VHH-28z-células T	RFCVE*	Despliegue en fago (biblioteca inmune)	Receptor de células T terapéuticas	Hajari y col., 2019.
GPA7-28z	GPA7-28z-Células T	Péptido de gp100/HLA-A2	Despliegue en fago (biblioteca inmune llama)	Receptor de células T terapéuticas.	Zhang G. y col., 2014.
Industria alimenticia					
Nb16	Monomérico	Ara h 3**	Despliegue en fago (biblioteca sintética-VHH)***	Identificación de alérgeno alimenticio	Chen F. y col., 2019.
Aprobado por FDA ♣					
Caplacizumab	Divalente	Factor Von Willebrand	Biblioteca inmune en llama.	Prevención de trombosis en purpura trombocitopénica	Holliefeld A. y col., 2020

*Receptor del Factor de Crecimiento Vascular Endotelial.**Proteína alergénica identificada en cacahuete.

***VHH: dominio variable de anticuerpo de cadena pesada de camello-humanizado. ♣Food and Drugs Administration.

E. JUSTIFICACIÓN

La búsqueda y desarrollo de alternativas para contrarrestar la infección causada por Mtb, va de la mano con el objetivo de la OMS de disminuir la epidemia de tuberculosis para el 2035. Antígenos micobacterianos como el Ag85B, tienen secuencias peptídicas reconocidas por linfocitos TCD8, las cuales son presentadas por la proteína HLA-A*0201 en modelo murino y humano de tuberculosis. Considerando la alta frecuencia de la proteína HLA-A*0201 a nivel mundial, su interacción altamente específica con péptidos inmunodominantes de Ag85B y la posibilidad de obtener anticuerpos de manera recombinante sin necesidad de inmunización, hacen que el desarrollo de anticuerpos con capacidad de reconocer el complejo HLA-A/péptido representen una valiosa herramienta, con potencial diagnóstico e inmunoterapéutico en tuberculosis.

F. HIPÓTESIS

“El anticuerpo de un solo dominio, seleccionado a partir de una biblioteca de origen humano, mediante la técnica de despliegue en fago, identificará a la proteína HLA-A*0201 plegada con el péptido Ag85B_{p199-207} de *Mycobacterium tuberculosis*, en la superficie de células T2”

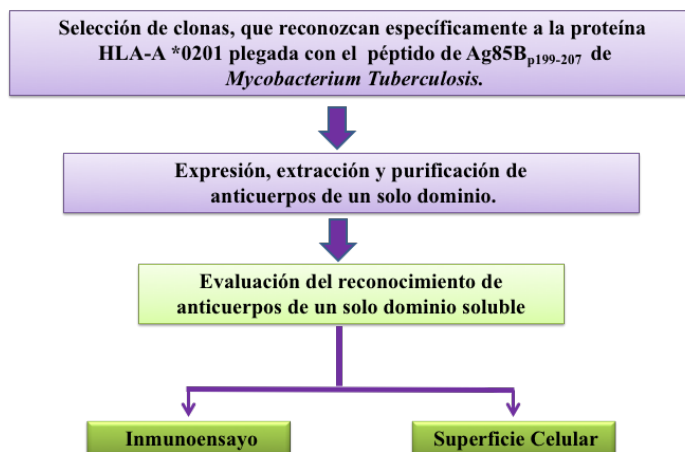
G. OBJETIVO GENERAL

Obtener un anticuerpo de un solo dominio con reconocimiento específico hacia la proteína HLA-A*0201 plegada con el péptido Ag85B_{p199-207} de *Mycobacterium tuberculosis*.

H. OBJETIVOS ESPECÍFICOS

1. Identificar clonas específicas dirigidas contra la proteína HLA-A*0201 plegada con el péptido Ag85B_{p199-207} de *Mycobacterium tuberculosis*.
2. Obtener los anticuerpos de un solo dominio en forma proteica.
3. Evaluar la especificidad de un anticuerpo de un solo dominio, hacia la proteína HLA-A*0201 y el péptido Ag85B_{p199-207} de *Mycobacterium tuberculosis*.
4. Determinar la afinidad de unión del anticuerpo de un solo dominio hacia la proteína HLA-A*0201 y el péptido Ag85B_{p199-207} de *Mycobacterium tuberculosis*.

I. DISEÑO EXPERIMENTAL



J. MATERIALES Y MÉTODOS

J.1 Complejos proteicos recombinante: HLA-A*0201/péptidos de *Mycobacterium tuberculosis*

Los péptidos de nueve residuos de aminoácidos, reconocidos por linfocitos TCD8 presentados en el contexto de la proteína HLA-A*0201, pertenecientes a tres antígenos de Mtb, Ag85B (199KLVANNTRL₂₀₇), Esat-6 (82AMASTEAGNV₉₀), Acr1(120 GILTVSVAV₁₂₈)(Comas I. y col., 2010), fueron sintetizados por ANASPEC (USA), con una pureza mayor al 90% y homogeneidad confirmada por cromatografía líquida en fase reversa. Los complejos recombinantes proteicos biotinilados, Ag85Bp₁₉₉₋₂₀₇/HLA-A*0201 (Ag85Bp/HLA-A*0201), Esat-6p₈₂₋₉₀/HLA-A*0201 (Esat-6p/HLA-A*0201), y Acr1p₁₂₀₋₁₂₈/HLA-A*0201 (Acr1p/HLA-A*0201), fueron desarrollados por el Department of Infectious Diseases, University Medical Centre Leiden, Leiden, Netherlands, con quienes se trabajó en colaboración. El complejo Ag85Bp/HLA-A*0201 fue usado como molécula blanco en las rondas de selección usando la técnica despliegue en fago, y los complejos Esat-6p/HLA-A*0201 y Acr1p/HLA-A*0201 como controles de especificidad. Todos los complejos recombinantes fueron recibidos y almacenados en PBS1x a -70°C.

J.1.2 Evaluación de los complejos recombinantes

La evaluación estructural de los tres complejos recombinante biotinilados, se realizó mediante un inmunoensayo, utilizando el anticuerpo W6/32 (Invitrogen/USA), el cual reconoce un epítipo conformacional sobre la cadena pesada alfa al estar correctamente plegada con la proteína β 2microglobulina (Denkberg G. y col., 2000) (De Lourdes M. y col., 2006). Para verificar el efecto de una correcta dirección de los complejos biotinilados, se usaron placas en presencia y ausencia de una cubierta de estreptavidina (ThermoScientific/USA). Ambas placas fueron sensibilizadas con 0.5 μ g de complejos biotinilados recombinantes en 100 μ l de PBS1x, toda la noche en agitación a 4°C, al siguiente día, las placas fueron lavadas dos veces con PBS1x e incubadas con el anticuerpo W6/32 (1/2000) en PBS1x Tween 0.05%-Bovin Serum Albumin (BSA) 2% (PBS-TBSA) en agitación a temperatura ambiente (TA) durante una hora, después de tres lavados con PBS1x-Tween20 0.05% (PBS-T0.05), los pozos fueron incubados con el anticuerpo anti-ratón IgG H+L acoplado a peroxidasa de rábano (HRP) (1/2000) (invitrogen/ USA), con agitación a TA durante una hora, todos los complejos biotinilados también fueron incubados con estreptavidina acoplada a peroxidasa (1/4000) (Biosource/China), con agitación a TA durante una hora, después de tres lavados con PBS-T0.05. Finalmente la reacción fue revelada con TMB (3,3',5,5'-tetramethylbenzidine)(ThermoScientific/USA), usando 25 μ l de ácido sulfúrico 0.16M, para detener la reacción, la absorbancia fue medida a 450 nm usando un lector de placas (Multiskan Go, Thermo)

J.2 Selección de anticuerpos de un solo dominio contra el complejo Ag85Bp/HLA-A*0201:

J.2.1 Rondas de selección usando despliegue en fago:

La biblioteca comercial de anticuerpos de un solo dominio de origen humano(Geneservice, Cambridge), fue utilizada como fuente. Su repertorio esta construido basado en la region variable de la cadena pesada (V3-23/D47), y cuenta con diversidad en las tres regiones determinantes de complementariedad, con aproximadamente 3×10^9 secuencias de anticuerpos. El protocolo de selección se realizó según (Lee CM. y col., 2007) con algunas modificaciones. En la primera ronda, se llevó a cabo una pre-absorción con el fin de eliminar fagos que reaccionaran con estreptavidina. Para esto un total de 5×10^{12} partículas fágicas

fusionadas con la biblioteca, fueron pre-incubadas con 30µl de perlas magnéticas cubiertas con estreptavidina M280(Invitrogen/Norway) previamente lavadas, durante 1 hora a 4°C en agitación, luego de exponer a un imán durante al menos dos minutos, se retiró el sobrenadante el cual fue incubado inmediatamente con 7.5µg del complejo biotinilado Ag85Bp/HLA-A*0201 en PBS1x-BSA2%, a 4°C en agitación durante 1 hora, pasado este tiempo, se adicionaron 200µl de perlas magnéticas cubiertas con estreptavidina y se incubaron durante 15 minutos, a 4°C en agitación. Después de separar las perlas y eliminar el sobrenadante, estas se sometieron a 15 lavados con PBS1x tween 0.1% y finalmente se realizó la elución con glicina-HCl pH 2.2 durante 15 minutos a TA, la muestra eluida (fagos que reconocieron al complejo recombinante blanco) fue neutralizada con Tris-HCl pH 9.0. Para la segunda y tercera ronda de selección, se utilizaron 2.5 y 1.25µg de la molécula blanco respectivamente, y el número de lavados previos a la elución, fueron 15 y 25 para la segunda y tercera ronda. Los fagos eluidos en cada ronda se usaron para infectar a *Escherichia coli* (E. coli) TG1 en 5ml de medio de cultivo 2xTY a una DO₆₀₀ 0.4-0.5, incubando en baño maria a 37°C sin agitación durante una hora, posteriormente se centrifugaron a 12300g durante 10 minutos. El botón celular se resuspendió en 1 ml de medio 2xTY, se sembraron en diluciones 1x10⁴–1x10⁶ todo el contenido bacteriano expuesto a partículas fágicas en medio sólido TYE suplementado con 4% glucosa y 100µg/ml de carbenicilina y se incubó toda la noche a 37°C, al siguiente día se cuantificaron las unidades formadoras de colonias (UFC_s), estas, representan el número de fagos eluidos que reconocieron al complejo biotinilado. Se recolectó con asa de vidrio todo el crecimiento bacteriano usando 5ml de medio de cultivo 2xTY, a partir del cual se guardaron glicerolos de cada ronda.

J.2.2 Fusión con partículas fágicas.

Las bacterias infectadas seleccionadas de J.2.1 se inocularon a una DO₆₀₀ de 0.1 en 200ml de medio liquido 2xTY, suplementado con 100µg/ml carbenicilina y 4% de glucosa, se incubó a 37°C, a 250 rpm, cuando la DO₆₀₀ llegó a 0.4-0.5, se expuso a 8x10¹¹ partículas del fago M13, se incubó en baño maria a 37°C, sin agitación durante una hora, se centrifugó la totalidad del volumen de cultivo a 12300g durante 15 minutos, el botón celular se resuspendió con 200ml de medio de cultivo liquido 2xTY, suplementado con carbenicilina

100µg/ml y kanamicina 50µg/ml, en ausencia de glucosa e incubando a 26°C, a 250rpm, entre 16-20 horas.

J.2.3 Precipitación de partícula fágica con PEG

Una vez se completó el paso (J.2.2), se centrifugó la totalidad del cultivo a 12300g durante 30 minutos y después de filtrar el sobrenadante por 0.45micras, se adicionaron 50ml de PEG6000(estéril) como agente precipitante y se incubó en hielo durante una hora, luego se repitió el ciclo de centrifugación y se resuspendió el sedimento en 5ml de PBS y 1ml de PEG6000 incubando en hielo durante 10 minutos, luego se centrifugó bajo las mismas condiciones y el sedimento fue resuspendido en 2ml PBS y centrifugado nuevamente, el sobrenadante se filtró por 0.45micras. Para su cuantificación, 10µl fueron diluidos 100 veces en PBS1x y se midió la DO₂₆₀ (las absorbancias en este paso se deben encontrar entre 0.1-1), aplicando la formula: Fagos/ml=DO₂₆₀ x(100) x (22.14x10¹⁰). Se almacenaron hasta por dos semanas a 4°C. Estas partículas fágicas fueron expuestas al complejo Ag85Bp/HLA-A*0201 en las siguientes rondas de selección.

J.3 Evaluación de clonas post rondas de selección.

J.3.1Selección y fusión de clonas con partículas fágicas:

Finalizada la tercera ronda, se evaluaron 94 clonas individuales al azar, seleccionadas con un palillo de madera estéril, cada clona fue inoculada en 200µl de medio de cultivo 2xTY suplementado con 4% de glucosa y 100µg/ml de carbenicilina en placas de 96 pozos, se incubaron toda la noche a 37°C a 200rpm, al siguiente día se tomaron 5µl de cada pozo y se transfirieron a una nueva placa con 200µl de medio 2xTY suplementado con 4% de glucosa y 100µg/ml de carbenicilina, se incubaron durante 3 horas a 37°C a 250rpm, pasado este tiempo, a cada pozo se le adicionaron 50µl de medio 2xTY suplementado con 4x10⁸ partículas fágicas, incubando sin agitación a 37°C durante una hora, posteriormente la placa se centrifugó a 7600g por 10 minutos, el sedimento de cada pozo fue resuspendido con 200µl de medio fresco 2xTY suplementado con 100µg/ml de carbenicilina y 100µg/ml de kanamicina, se incubaron a 26°C a 250rpm durante 16-20 horas. Pasado el tiempo de

incubación se centrifugaron a 7600g durante 10 minutos, y el sobrenadante de cada clona fue usado para su evaluación en un inmunoensayo.

J.3.2 Evaluación de clonas por inmunoensayo (anticuerpo de un solo dominio-fago)

Placas de ELISA cubiertas con estreptavidina (ThermoScientific/USA), fueron sensibilizadas con 0.5µg de complejo recombinante biotinilado Ag85B/HLA-A*0201 en 100µl de PBS1x, por pozo, durante toda la noche en agitación a 4°C, al siguiente día se lavaron 2 veces por 5 min con PBS1x con agitación, posteriormente, a cada pozo se le adicionaron 50µl del sobrenadante de los fagos de cada clona (J.3.1) con 50µl de PBS1x-Tween 0.05%-BSA 2% (PBS-TBSA) con agitación a temperatura ambiente (TA) durante una hora, luego se lavaron 4 veces con PBS1x-Tween 0.05% (PBS-T0.05) y 1 vez con PBS1x, 5 minutos c/u, posteriormente se adicionó el anticuerpo anti-M13 acoplado a HRP (GE Healthcare/USA) a una dilución de 1/2500 en PBS1x-BSA2% con agitación a TA durante una hora, después de repetir el ciclo de lavados, se adicionaron 100µl de sistema de revelado, OPD (o-Phenylenediamine dihydrochloride) (Sigma/USA) incubando en oscuridad por 30 minutos, se detuvo la reacción con 25µl de ácido sulfúrico 3M, y la DO fue medida a 492nm usando un lector de placas (Multiskan Go, Thermo). Los sobrenadante perteneciente a las clonas que reconocieron a la molécula blanco, también fueron evaluadas contra los complejos Esat-6/HLA-A*0201 y Acre1p/HLA-A*0201, como controles de especificidad de la misma forma anteriormente descrita. Las clonas que no evidenciaron un reconocimiento hacia los controles de especificidad, fueron seleccionadas para evaluar su secuencia de anticuerpo de un solo dominio.

J.4 Secuenciación de anticuerpos de un solo dominio

La extracción de ADN del fagémido de las clonas seleccionadas en *E. coli* cepa TG1, fue realizada usando GeneJET plasmid Miniprep Kit (ThermoScientific/Lithuania). A partir de 15ml de medio de cultivo 2xTY suplementado con 4% glucosa y 100µg/ml carbenicilina, previamente inoculado con una UFC de cada clona, este fue incubado toda la noche a 37°C a 200rpm, al siguiente día se extrajo el ADN siguiendo las instrucciones de fábrica. Posteriormente, su integridad fue evaluada mediante un gel de acrilamida 1% y su cuantificación usando NanoDrop ONE. Los oligonucleótidos usados para la secuenciación

fueron LMB3 (5' CAGGAAACAGCTATGAC 3') y pHEN (5'CTATGCGGCCCCATTCA 3'), esta fue realizada en el laboratorio de secuenciación, ubicado en el Instituto de Investigaciones Biomédicas (UNAM). Para la traducción se usó el software BioEdit 7.2 y para análisis de secuenciación y alineamiento Clustalw y Blast respectivamente.

J.5 Producción de anticuerpos de un solo dominio solubles

Una vez se seleccionaron las clonas, se indujo su expresión proteica con el fin de obtener anticuerpos de un solo dominio solubles independientes de la partícula fágica.

J.5.1 Transformación de *E. coli* cepa HB2151

Para este fin, se transformó a *E. coli* cepa HB2151 (cepa no supresora del codón de paro ámbar) mediante la exposición de la partícula fágica perteneciente a cada una de las clonas seleccionadas, este proceso se realizó según (Abou E. y col., 2016). *E. coli* cepa HB2151, fue sembrada por aislamiento en medio sólido M9 e incubada a 37°C durante 36 horas, luego se inoculó una UFC en 5ml de medio 2xTY a 37°C a 250 rpm durante toda la noche, al siguiente día se diluyó 100 veces en 5ml de cultivo 2xTY incubando a 37°C-250rpm cuando llegó a una DO₆₀₀ de 0.4-05, 10µl de partículas fágicas pertenecientes a las clonas seleccionadas fueron adicionados al medio de cultivo (para éste fin se repitió el proceso del numeral J.2.2), se incubó durante 30 minutos a 37°C sin agitación, luego se centrifugó el volumen total a 30000g durante 3 minutos y el botón celular fue resuspendido en 1ml de medio 2xTY, las diluciones 1x10²-1x10⁶ fueron sembradas en medio sólido TYE suplementado con 100µg/ml de carbenicilina y 4% glucosa, se incubaron a 37°C durante toda la noche.

J.5.2 Expresión, extracción y purificación de anticuerpos de un solo dominio

A partir de un pre-cultivo de toda la noche, se diluyó 100 veces, en 50ml de cultivo 2xTY suplementado con 100µg/ml de carbenicilina, incubando a 37°C a 250rpm, hasta una DO₆₀₀ de 0.6, se adicionó al medio 1mM de Isopropyl-b-D-1-thiogalactoside (IPTG) (Promega/USA), y se incubó a 26°C-250rpm, toda la noche. Al siguiente día el volumen total se centrifugó a 12200g durante 10 minutos, el sedimento fue sometido a extracción proteica mediante choque osmótico según (Liu J. y col., 2015). El sedimento bacteriano fue

resuspendido en 1/50 del volumen del cultivo inicial, en la solución (750mM sacarosa, 100mM Tris a pH 7.5 e inhibidores de proteasas) durante 30 minutos, incubando en hielo con agitación lenta, luego se adicionó 1 mL de MgCl₂ (500 mM) y se incubó por 15 minutos en las mismas condiciones, después de centrifugar a 30000g durante 30 minutos, el sobrenadante fue sometido a purificación por cromatografía de afinidad de forma manual, usando una columna con sefarosa acoplada a proteína-A(Roche/Germany). Se realizaron 2 lavados, el primero con 5 ml de 100mM Tris-HCl, pH 8.0 y el segundo con 5 ml de 10mM Tris-HCl, pH 8.0, la elución se realizó con 100mM glicina pH 3.0, en 5 fracciones de 1ml cada una, cada fracción fue neutralizada con ~200µl de 1M tris-HCl pH 8.0. El volumen total de las fracciones fue intercambiada a PBS1x pH 7.4 y concentrada a 500µl, usando tubos de 15ml con membranas de separación con punto de corte 10000 kDa (Merck/Ireland), la concentración fue determinada por colorimetría para cuantificación de proteínas totales, por el método de ácido bicinonínico BCA (Pierce/USA) siguiendo el protocolo de fábrica. Los anticuerpos purificados fueron almacenados a -20.

J.5.3 Evaluación purificación de anticuerpos de un solo dominio

Las fracciones obtenidas en el proceso de purificación, fueron evaluadas mediante electroforesis desnaturalizante en gel de poliacrilamida de sodio duodecil sulfato (SDS-PAGE) con gradiente de concentración 4-20%(ThermoScientific/USA), se realizó la transferencia del patrón de corrida proteico a una membrana de Polyvinylidene Difluoride (PVDF) con el objetivo de verificar la presencia de proteínas mediante tinción con Coomassie brillante blue R-250 y para identificar a los anticuerpos de dominio se realizó un Western blot. La membrana fue bloqueada con PBS1x-Tween20 al 0.05%- BSA 2% (PBS-TBSA) con agitación a TA por una hora, se realizaron tres lavados con PBS1x-Tween20 al 0.05%, (PBS-T0.05), posteriormente se incubó la membrana con el anticuerpo anti-cMyc (Sigma/USA) a una dilución de 1/750 en PBS-TBSA con agitación a TA durante una hora, luego de realizar tres lavados con PBS-T0.05, la membrana fue incubada con anticuerpo anti-ratón-IgG (H+L) acoplado a HRP en dilución 1/2000 en PBS-TBSA, con agitación a TA durante una hora, luego de realizar tres lavados con PBS-T0.05, se reveló la reacción mediante precipitación con una solución de PBS1x con 3mg/ml de 3-3diaminobenzidina (Sigma) y H₂O₂ al 30% dilución 1/1000.

J.6 Evaluación de anticuerpos de un solo dominio

J.6.1 Especificidad de anticuerpos de un solo dominio en un inmunoensayo

Placas de ELISA cubiertas con estreptavidina, fueron sensibilizadas con 1µg de los tres complejos recombinante biotinilados, donde Ag85B/HLA-A*0201 es la molécula blanco y los complejos Esat-6p/HLA-A*0201 y Acr1p/HLA-A*0201 fueron utilizados como controles de especificidad. Las placas fueron sensibilizadas durante toda la noche en agitación a 4°C, al siguiente día se lavaron 2 veces con PBS1x en agitación, 5 minutos cada lavado, luego, 5µg de los anticuerpos de un solo dominio fueron incubados en 100µl de PBS1x-Tween 0.05%-BSA2% (PBS-TBSA) en agitación a TA durante dos horas, después de lavar 3 veces con PBS-T0.05, los pozos fueron incubados con anticuerpo anti-cMyc acoplado a HRP (Sigma-Aldrich/Ireland Ltd.) a una dilución de 1/1000 en PBS-TBSA con agitación a TA durante una hora, luego de repetir el esquema de lavados, finalmente la reacción fue revelada con 100µL de TMB (ThermoScientific), usando 25µl de ácido sulfúrico 1M para detener la reacción, la absorbancia fue medida a DO_{450nm} usando un lector de placas (Tecan/Switzerland). Se realizaron tres experimentos independientes por duplicado.

J.6.2 Reconocimiento de anticuerpo de un solo dominio sobre superficie celular

Esta evaluación fue llevada a cabo mediante un ensayo *in vitro*, utilizando la línea celular linfoblástica humana T2, (Donada por la Dra. Patricia Gorocica - INER-México), estas células de naturaleza no adherente, son positivas para la proteína HLA-A*0201 y se caracterizan por exportar moléculas HLA-A clase I sin péptido en la superficie (DeMars R. y col., 1992). Las células fueron cultivadas en medio RPMI-1640 suplementado con 20% de suero fetal bovino (SFB) (Gibco/USA), aminoácidos esenciales 1x y antibiótico-antimicótico 1x de (Gibco 15-240 62) a 37°C, 5% CO₂. El mantenimiento de las células se realizó cambiando el medio de cultivo cada 72 horas, realizando lavados con medio de cultivo RPMI-1640 libre de suero, centrifugando a 1300g durante 5 minutos a TA, su cuantificación y determinación de viabilidad se hizo con la prueba de exclusión de colorante azul tripano en cámara de Neubauer.

J.6.2.1 Evaluación de la exposición de HLA-A*0201 en superficie de células T2

6x10⁵ células fueron incubadas en placas de cultivo-24 pozos (Costar/USA, ref: 3524) con RPMI-1640 libre de suero en presencia de β 2microglobulina (20 μ g/1x10⁶ células) y en ausencia o presencia de 80 μ g de los péptidos Ag85Bp₁₉₉₋₂₀₇ y Esat-6p₈₂₋₉₀, durante 4 horas a 37°C, 5% CO₂, pasado el tiempo de incubación, las células fueron lavadas con RPMI libre de suero, por centrifugación a 3200g durante 3 minutos, posteriormente, se bloquearon con PBS1x con 5% de SFB, con agitación en hielo durante 30 minutos, después de tres lavados con PBS1x-2% SFB centrifugando a 3200g por 3 minutos cada uno, se incubaron con el anticuerpo conformacional W6/32 (Denkberg G. y col., 2000) (De Lourdes M. y col., 2006)(Invitrogen/USA) (1 μ g/1x10⁶ células) en PBS1x-BSA2% con agitación en hielo durante 30 minutos, se lavaron tres veces con PBS1x-2% SFB centrifugando a 3200g durante 3 minutos, luego se incubaron con el anticuerpo secundario anti ratón-IgG H+L acoplado a Alexa Flúor 488 (Invitrogen/USA) a una dilución 1/2000 en PBS1x-BSA2% con agitación en hielo durante 30 minutos en oscuridad, se realizaron tres lavados de la misma manera anteriormente descrita, luego las células se fijaron con paraformaldehído (PFA) 0.5% en agitación a TA durante 10 minutos, luego se lavaron tres veces con PBS1x centrifugando a 3200g durante 3 minutos, finalmente se hizo tinción de los núcleos usando Hoechs (*Life technologies/USA*) en una dilución 1/9000 en PBS1x-BSA2% con agitación a TA por 10 minutos, después de realizar los últimos tres lavados de la misma forma anteriormente descrita, se realizó el montaje en un portaobjetos limpio usando vectashield (Vector-Laboratories), se cubrieron con un portaobjetos, sellando los extremos, una vez se verificó la presencia de las moléculas HLA-A*0201 en superficie celular, prosiguió la evaluación de los anticuerpo de un solo dominio.

J.6.2.2 Evaluación del reconocimiento de anticuerpos de un dominio en superficie de células T2

La incubación en ausencia y presencia de péptidos, se realizó de igual manera que en el numeral J.6.2.1, a excepción del tiempo de incubación que fueron 8 horas. Una vez pasó este tiempo, las células fueron lavadas con PBS1x estéril, fueron fijadas con PFA 0.5% en agitación a TA durante 15 minutos, luego se lavaron tres veces con PBS1x centrifugando a 3200g durante 3 minutos, posteriormente se bloquearon con PBS1x con 5% de SFB, con

agitación a TA durante 30 minutos, luego de tres lavados con PBS1x centrifugando a 3200 rpm 3 minutos cada uno, las células fueron incubadas con 10µg de anticuerpos de un solo dominio en PBS1x, con agitación a 4°C durante toda la noche, al siguiente día se lavaron dos veces con PBS1x centrifugando a 3200g durante 3 minutos y se incubaron con el anticuerpo anti cMyc (Santa cruz/Europa) a una dilución 1/200, en PBS1x-BSA2%, con agitación a TA durante una hora, luego de repetir tres lavados, se incubó con el anticuerpo anti ratón-IgG H+L acoplado a Alexa Flúor 488 (Invitrogen/USA) a una dilución 1/2000 en PBS1x-BSA2% con agitación durante 1 hora, luego se realizaron tres lavados de la mismas manera anteriormente descrita, finalmente se hizo tinción de núcleos y montaje de la lámina, en la misma forma que se describió en el numeral J.6.2.1. Para su observación se utilizó el microscopio de fluorescencia Olympus BX41, con aumento en 100x, la captura de imágenes y edición de las mismas se realizó con el programa Zen 2.6 blue edition. Se cuantificaron más de 300 campos por condición evaluada y se calculó el porcentaje de eventos positivos, los parámetros de captura aplicados para controles de montaje, especificidad y muestras problema fueron los mismos, se realizaron dos experimentos independientes.

J.7 Determinación de la constante de afinidad del anticuerpo de un solo dominio 2C

La cinética de unión y determinación de la constante de disociación (K_D) entre el anticuerpo de un solo dominio 2C y el complejo Ag85Bp/HLA-A*0201 fue evaluada usando interferometría de biocapa en tiempo real a 25°C. biosensores de estreptavidina en un sistema Octet RED96 (FortéBio Inc. San José, CA, USA) fueron usados. El ensayo fue realizado en placas negras de 96 pozos (Greiner Bio-One 655209), todos los ensayos fueron realizados en 200µl, de solución amortiguadora para determinaciones cinéticas de FortéBio Inc. San José, CA, USA). Los experimentos fueron monitoreados con el software (Data Acquisition 8.2 ForteBio, Inc.). 25ng del complejo biotinilado Ag85Bp/HLA-A*0201 fue expuesto al biosensor cubierto con estreptavidina durante 5 minutos, luego de realizar lavados usando la misma solución amortiguadora para eliminar uniones no específicas, el anticuerpo de un solo dominio 2C purificado fue expuesto al complejo blanco pre-acoplado al biosensor y las constante de asociación y disociación fueron medidas, al inicio y final de la interacción respectivamente. Se evaluaron seis diferentes concentraciones de 2C en los rangos (2.54 a 81.3mM) y como control negativo, un pozo en ausencia de anticuerpo fue evaluado, 10mM

de 2C también fue expuesto al complejo Esat-6/HLA-A*0201. Los datos fueron analizados usando el programa Octec Data Analysis versión 8.2, (FortéBio Inc. San José, CA, USA), Acorde al modelo 1:1. Esta evaluación se hizo en colaboración con el laboratorio de Bioquímica y Biología estructural, bajo la dirección del Dr. Alfredo Torres, del Instituto de Fisiología -UNAM.

J.8. Análisis estadístico

Los datos obtenidos fueron analizados usando el programa GraphPad Prism versión 6.0c, la determinación de las diferencias significativas del reconocimiento por parte del anticuerpo de un solo dominio hacia el complejo blanco en comparación con los complejos control de especificidad, fue realizada usando ANOVA de una vía, multiparamétrico corregido con Sidak's post. Hoc.

K. RESULTADOS

K.1. Evaluación de complejos recombinantes

Los tres complejos recombinantes biotinilados Ag85Bp/HLA-A*0201, Esat-6p/HLA-A*0201 y Acr1p/HLA-A*0201, inmovilizados en placas cubiertas con estreptavidina para inmunoensayo, fueron reconocidos por el anticuerpo conformacional W6/32, (Figura 3A), evidenciando un correcto plegamiento estructural, en contraste, los complejos unidos a placas sin estreptavidina no fueron reconocidos por el anticuerpo (Figura 3B). Para confirmar que los resultados negativos obtenidos, no fueron consecuencia de la ausencia de las moléculas evaluadas en la placa sin estreptavidina, los tres complejos biotinilados fueron evaluados usando estreptavidina acoplada a HRP. En la (Figura 3B), se observa que los complejos biotinilados únicamente fueron reconocidos en la placa sin estreptavidina, evidenciando exposición de la biotina. La diferencia en los resultados obtenidos, muestran que la unión de los complejos biotinilados a placas cubiertas con estreptavidina, brinda la dirección necesaria para permitir el reconocimiento por parte del anticuerpo conformacional W6/32, representando una plataforma idónea para optimizar la selección de anticuerpo que reconozcan la interacción péptido/HLA-A en los complejos evaluados.

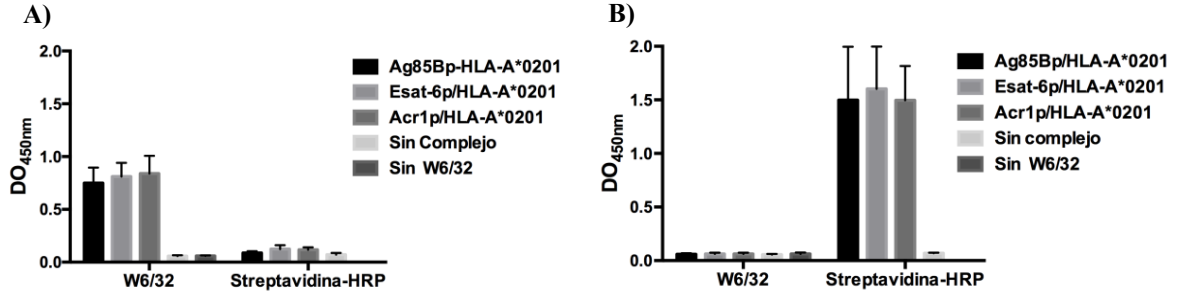


Figura 3: Evaluación de los complejos recombinantes (péptidos/HLA-A*0201): A) dos grupos de complejos recombinantes biotinilados fueron inmovilizados sobre placas cubiertas con estreptavidina, el grupo de la izquierda fue evaluado con el anticuerpo W6/32 y el grupo de la derecha fue evaluados con estreptavidina-HRP. B) ambos grupos de complejos biotinilados fueron unidos a placas sin estreptavidina y detectados con W6/32 y estreptavidina-HRP respectivamente. Los datos representan el promedio +/- desviación estándar de tres experimentos independientes.

K.2. Selección de anticuerpos de un solo dominio contra el complejo Ag85Bp/HLA A*0201

K.2.1 Rondas de selección por despliegue en fago:

Una biblioteca de anticuerpos de un solo dominio de origen humano desplegados en fagos, fue expuesta al complejo Ag85Bp/HLA-A*0201, mediante tres rondas de selección. Las condiciones y resultados de cada ronda se encuentran en la tabla 5:

Tabla 5: Rondas de selección por despliegue en fago:

Ronda	Ag85Bp/ HLA-A*0201	Fagos Ingresan	Fagos Eluidos /ml	Fagos eluidos/ Fagos ingresan	Factor de* rendimiento	Tween20/ N° Lavados
1	7.5µg	5x10 ¹²	6x10 ⁶	1.2x10 ⁻⁶	1	0.1%/15
2	2,5µg	5x10 ¹²	1.4x10 ⁸	2.8x10 ⁻⁵	20	0.1%/15
3	1,25µg	5x10 ¹²	1.5x10 ⁸	3x10 ⁻⁵	25	0.1%/25

* Factor de rendimiento: se calculó dividiendo el valor de fagos eluidos/fagos ingresan de cada ronda entre el resultado de fagos eluidos/fagos ingresan pero solo de la primera ronda. Ésta fórmula se aplicó según: Bagheri. M y col., 2017. Rangos - fagos eluidos por cada ronda: 1 y 2: 10⁵-10⁷ fagos/ml y 3: 10⁷- 10⁹ fagos/ml

El número de fagos eluidos de cada ronda, se encontró dentro de los rangos establecidos por el protocolo de fábrica de la biblioteca, a excepción de la ronda dos excediendo el valor

esperado, dado que los lavados en esta ronda se hicieron en igualdad de condiciones que para la primera, se decidió incrementar el número de lavados, obteniendo los resultados esperados. El factor de rendimiento fue acorde con el número de rondas, y el proceso de fusión y amplificación post elución, permitió obtener el número de partículas fágicas necesarias para realizar las tres rondas.

K.2.2 Evaluación y selección por inmunoensayo(anticuerpos de un solo dominio-fago):

94 UFC_s seleccionadas al azar, de la tercera ronda de bio-selección, fueron evaluadas de forma individual mediante un inmunoensayo. Como primer abordaje, se evaluó su capacidad para reconocer a Ag85Bp/HLA-A*0201 (Figura 4A), únicamente 7 clonas fueron seleccionadas, las cuales emitieron un señal de reconocimiento 10 veces mayor que la clona de control negativo (CN) y una DO_{492nm} mayor a 0.4. Posteriormente se expusieron a estreptavidina (pozos sin complejos recombinante)(figura 4B) donde, a las tres clonas que mostraron menor señal de reconocimiento, se les evaluó su especificidad frente a los complejos Esat-6p/HLA-A*0201 y Acr1p/HLA-A*0201(Figura 4C), (esta señal de reconocimiento fue casi 10 veces menor a la emitida hacia el complejo blanco). Los resultados obtenidos permitieron seleccionar a las clonas 2C, 3C y 7E por su capacidad de reconocimiento específico hacia el complejo blanco mediante un inmunoensayo.

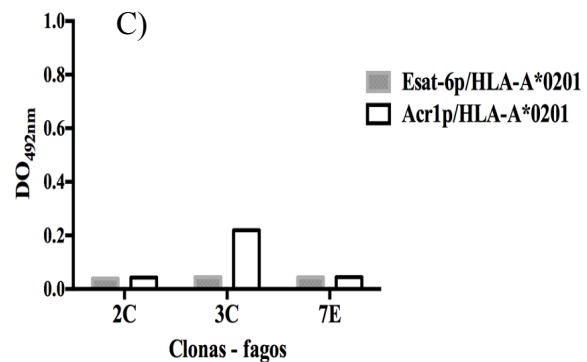
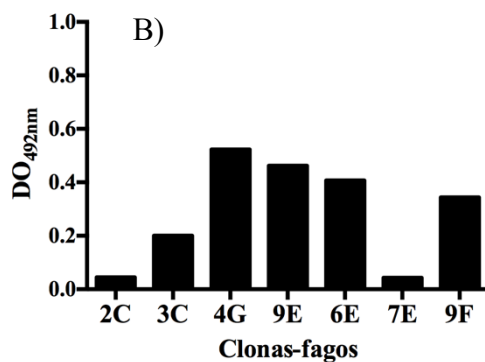
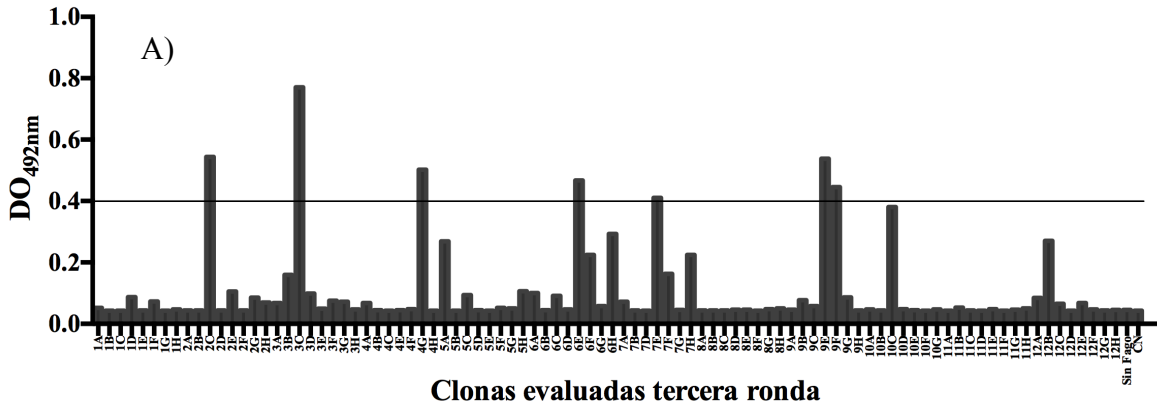


Figura 4: Evaluación de clonas post bio-selección mediante inmunoensayo: A) clonas evaluadas después de la tercera ronda de bio-selección, la línea indica el punto de corte establecido para definir clonas positivas. B) Las clonas que emitieron un señal de reconocimiento positivo hacia Ag85Bp/HLA-A*0201 fueron expuestas a placas cubiertas con estreptavidina (pozos sin complejos recombinante), donde 2C, 3C y 7E mostraron la menor señal de reconocimiento C) las tres clonas seleccionadas fueron evaluadas en presencia de los complejos Esat-6p/HLA-A*0201 y Acr1p/HLA-A*020, como prueba de especificidad.

K.3 Secuenciación de clonas seleccionadas

Los análisis mostraron que las secuencias de las tres clonas seleccionadas mediante un inmunoensayo, tienen similitud con 122 residuos de aminoácidos con el dominio variable de la cadena pesada, de una inmunoglobulina de origen humano (>ABM67233.1 Homo sapiens). Un total de 160 y 159 residuos de aminoácidos para 2C y 7E fueron identificados respectivamente, la secuencia proteica perteneciente a 3C, fue altamente similar a 2C, a excepción del número de aminoácidos que solo fueron 151 debido a la presencia de un codón de paro. A las tres secuencias se les identificaron las tres regiones determinantes de complementariedad, como también la secuencia c-Myc para su identificación. Con estos resultados las clonas 2C y 7E fueron seleccionada para continuar con la fase de expresión.

K.4. Expresión y purificación de anticuerpos de un solo dominio

La inducción de expresión proteica de las dos clonas seleccionadas 2C y 7E, se llevó a cabo en *E. coli* cepa HB2151. Esta fue evaluada en electroforesis, (figura 5A líneas 4 y 9), donde se identificó, una banda proteica con el peso molecular esperado (≈ 15 kDa) que también fue reconocida por el anticuerpo anti-cMyc mediante Western blot (WB), la reacción positiva estuvo presente únicamente en la biomasa del cultivo inducido. Un patrón similar de bandas proteicas fue identificado después de la purificación con proteína A (figura 5B líneas 4-8). El rendimiento de producción fue 1418 y 1800 μ g/ml para 2C y 7E respectivamente, a partir de 200ml de cultivo.

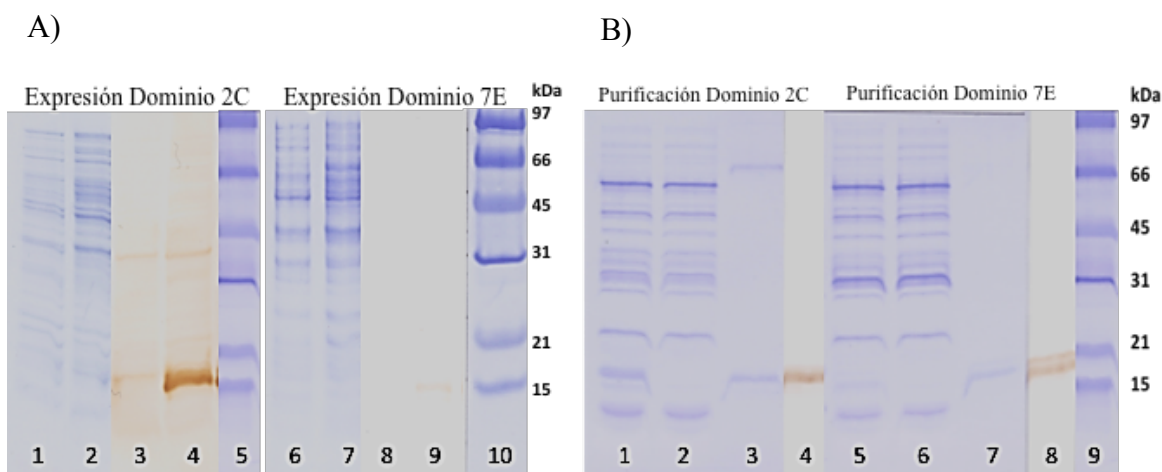


Figura 5 Expresión y Purificación de anticuerpos de un solo dominio 2C y 7E a partir de *E. coli* HB2151: **A) Expresión:** Pozos 1 y 6: (C) de biomasa no inducida, pozos 2 y 7: (C) biomasa inducida (3 μ l), pozos 3,8: WB biomasa no inducida, pozos 4,9: WB biomasa inducida, pozos 5,10: Peso Molecular en kDa. **B) Extracción y Purificación:** pozos 1,5: (C) fracción extraída, pozos 2,6: (C) fracción no unida a sefarsa-proteína A, pozos 3 y 7: (C) fracción purificada, pozos 4 y 8: WB fracciones purificadas. C: Coomassie, WB: Western Blot con anti c-Myc.

K.5. Evaluación de anticuerpos de un solo dominio

K.5.1 Especificidad de anticuerpos de un solo dominio en un inmunoensayo

Los resultados del anticuerpo 2C presentes en la (Figura 6A), evidenciaron un reconocimiento específico hacia la molécula blanco, mostrando diferencias significativas con respecto a los dos complejos Esat-6p/HLA-A*0201 y Acr1p/HLA-A*0201 usados como

controles de especificidad. Por otro lado, el patrón de reconocimiento del anticuerpo 7E, (Figura 6B), evidenció inespecificidad. Los controles evaluados en el inmunoensayo, se realizaron en ausencia de los anticuerpo 2C y 7E, como también en ausencia de los complejos recombinantes en cada pozo(Figura 6 A, B).

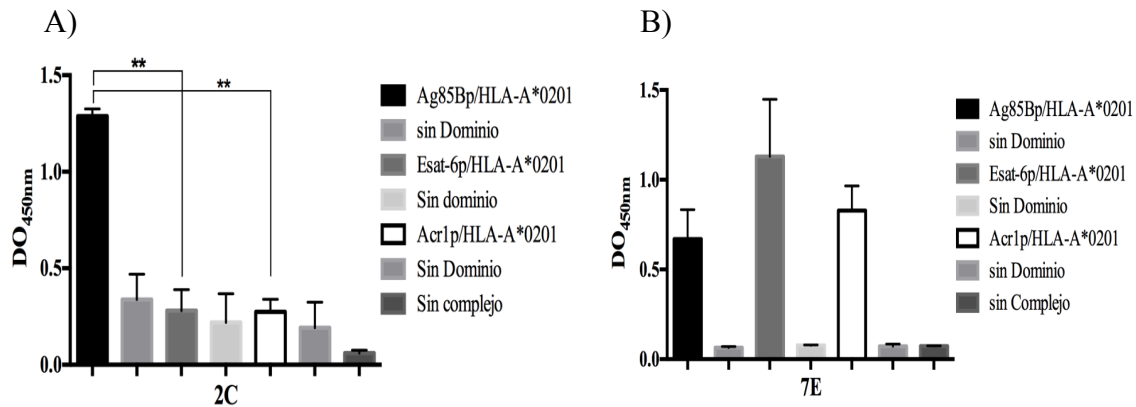


Figura 6: evaluación de Especificidad de los anticuerpos de un solo dominio 2C y 7E en un inmunoensayo: A)2C, especificidad de reconocimiento hacia Ag85Bp/HLA-A*0201, B) 7E reconocimiento no específico. Los resultados representan 3 experimentos independientes para 2C, con diferencias significativas * ($p < 0.05$), el anticuerpo 7E fue evaluado con 2 experimentos independientes.

K.5.2 Reconocimiento del anticuerpo de un solo dominio 2C sobre superficie celular

K.5.2.1 Expresión de HLA-A*0201 en superficie de células T2

Se verificó la exposición de HLA-A*0201 en superficie mediante inmunofluorescencia, en presencia y ausencia de péptidos exógenos, usando el anticuerpo conformacional W6/32. Los resultados se encuentran en la (Figura 7). Las imágenes capturadas de las condiciones evaluadas, permitieron verificar la expresión de las moléculas HLA-A*02 en superficie de las células T2.

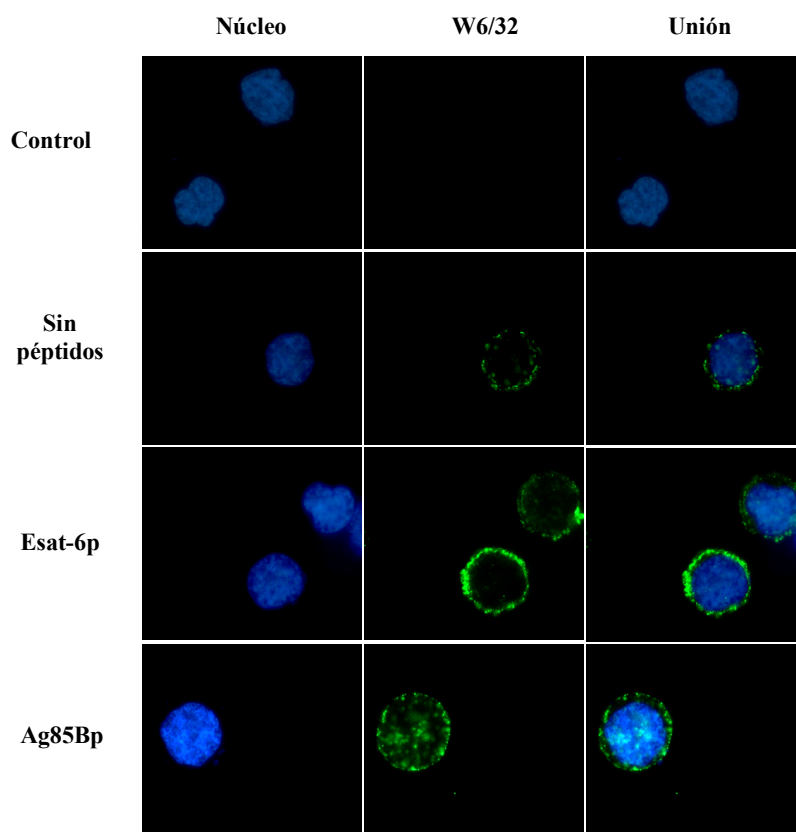


Figura 7: Expresión de HLA-A*02 en superficie de células T2: las células T2 fueron evaluadas en ausencia y presencia de los dos péptidos Esat-6p y Ag85Bp, la tinción se realizó con el anticuerpo primario W6/32, y con anti IgG H+L acoplado a Alexa flúor 488, como anticuerpo secundario. Control: en presencia de Ag85Bp, y todos sistema de tinción a excepción del anticuerpo primario. Más de 300 campos fueron observados por cada condición evaluada, lente aumento 100x, por microscopía de fluorescencia. las condiciones de captura de imágenes fueron iguales para todas condiciones.

K.5.2.2 Reconocimiento de 2C y 7E en superficie de células T2

Los resultados de la tinción usando a 2C como anticuerpo primario, se encuentran en la (figura 8A), las imágenes capturadas mediante microscopía de fluorescencia evidenciaron eventos positivos únicamente en la superficie de células expuestas a Ag85Bp. Los resultados obtenidos con el anticuerpo 7E, fueron contrastantes, dado que la fluorescencia se observó en la superficie celular en todas las condiciones evaluadas (Figura 8B). Estos resultados nos permitieron concluir que el anticuerpo de un solo dominio 2C reconoció al complejo Ag85Bp/HLA-A*02 en superficie células T2.

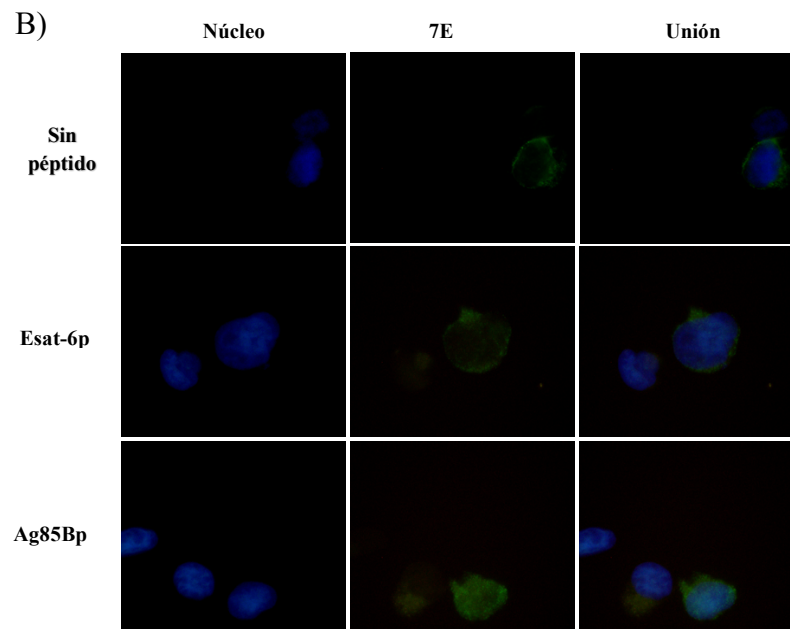
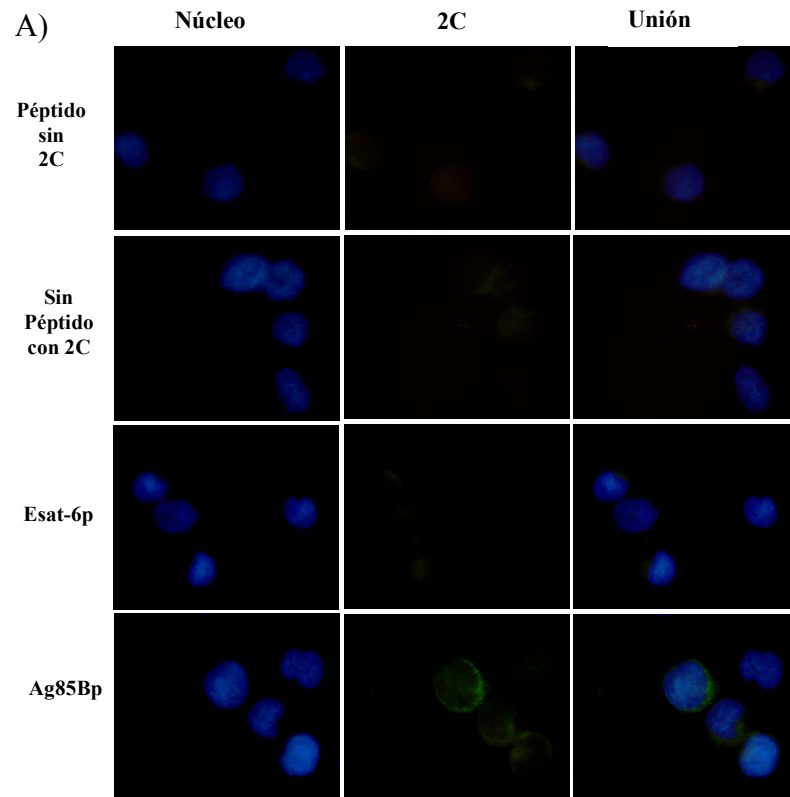


Figura 8: Reconocimiento de 2C y 7E en superficie de células T2: A) 2C, reconocimiento específico en superficie de células T2 expuestas a Ag85Bp con 6.4% de eventos positivos B) 7E reconocimiento no específico. Las células fueron evaluadas en ausencia y presencia de Ag85Bp y Esat-6p, los anticuerpos 2C y 7E fueron usados como anticuerpo primario en la tinción, seguido de anticuerpo anti-cMyc, y revelado con anticuerpo anti-IgG H+L acoplado a Alexa flúor 488. Control: en presencia de Ag85Bp, y todo el sistema de tinción a excepción de los anticuerpos primarios (2C y 7E). Más de 300 campos fueron observados por cada condición evaluada, aumento de lente 100x por microscopia de fluorescencia. Los parámetros de captura de imágenes fueron iguales para todas condiciones. Se realizaron dos experimentos independientes.

K.6 Determinación de la constante de afinidad del anticuerpo de un solo dominio 2C

Esta fue realizada mediante interferometría de biocapa, permitiendo la interacción entre diferentes concentraciones del anticuerpo de dominio 2C, con el complejo recombinante biotinilado Ag85Bp/HLA-A*0201 acoplado a un biosensor cubierto con estreptavidina. La afinidad fue calculada en términos de constante de equilibrio de disociación (k_d), siendo $15 \pm 0.20 \mu\text{M}$ (figura 9A). La interacción entre 2C y Esat-6/HLA-A*0201 fue muy baja, y no fue posible la determinación de parámetros de unión.

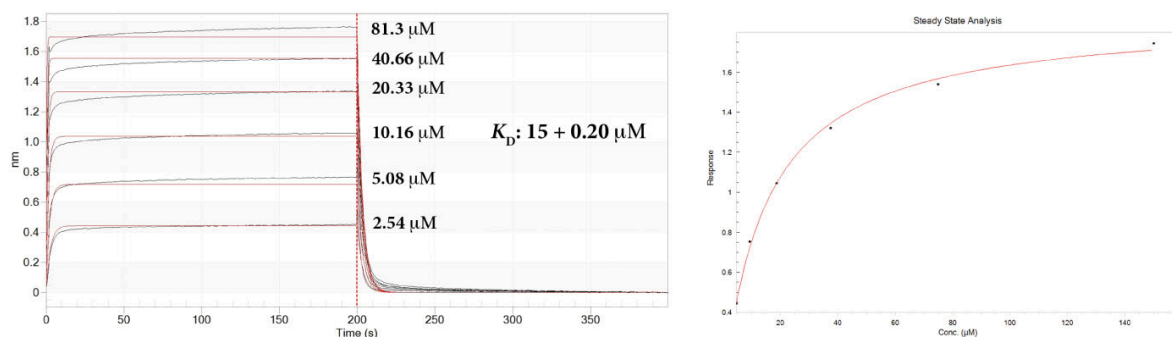


Figura 9: Determinación de constante de afinidad por interferometría de biocapa en tiempo real: A) sensograma muestra en la primera fase (0-200s) izquierda, la unión de diferentes concentraciones de 2C a 25ng de Ag85Bp/HLA-A*0201 (pre acoplado al biosensor cubierto con estreptavidina), la interacción se presentó en función de la concentración del anticuerpo de dominio. En la parte izquierda se ve la disociación, y el valor de $K_d: 15 \pm 0.20 \mu\text{M}$

L. DISCUSIÓN

Los linfocitos TCD8 que reconocen a los péptidos unidos a proteínas del complejo principal de histocompatibilidad clase I, tienen la capacidad de matar células infectadas por Mtb (Prezzemolo T. y col 2014) (Comas I. y col, 2010). Este reconocimiento se lleva a cabo mediante su receptor de superficie, que reconoce la interacción péptido-HLA-I, de manera altamente específica. Gracias a los avances biotecnológicos, es posible desarrollar anticuerpos tipo TCR, siendo ampliamente explorados en cáncer, enfermedades autoinmunes e infecciosas (Cohen M. y Reiter Y., 2013). Teniendo en cuenta que se han identificado linfocitos TCD8-péptido específicos en la infección por Mtb, el desarrollo de este tipo de anticuerpos, representa una herramienta con el potencial para contrarrestar la infección. Dass y colaboradores, realizaron uno de los primeros abordajes en cuanto a este tipo de anticuerpos en tuberculosis, generando anticuerpos dirigidos contra péptidos de la proteína alfa cristalina, antígeno de latencia en complejo con HLA-I (Dass S. y col., 2018) (Dass S. y col., 2020). En el presente trabajo, se desarrolló un anticuerpo dirigido contra un péptido perteneciente al antígeno inmunodominante Ag85Bp de Mtb, plegado con la proteína HLA-A*0201, a partir de una biblioteca de anticuerpos de un solo dominio de naturaleza humana.

Teniendo en cuenta que uno de los factores más importantes en el desarrollo de anticuerpos es la elección de la molécula blanco, nuestro criterio para seleccionar a Ag85B de la micobacteria, se basó en tres razones: es uno de los antígenos más abundantes de naturaleza secretora, está implicado en la síntesis de pared micobacteriana y gracias a su inmunodominancia, es uno de los antígenos más estudiados para el diseño de vacunas en diferentes formatos. Sin embargo, dado que uno de los principales objetivos de este trabajo, fue el desarrollo de anticuerpos tipo TCR, la selección de la secuencia peptídica $p_{199}KLVANNTRL_{p207}$, se basó en su interacción específica con la proteína HLA-A*0201 (Weichold R y col., 2007), su alto grado de conservación génica (Comas I. y col., 2010), y finalmente la identificación de linfocitos TCD8-péptido específicos en pacientes con tuberculosis activa y post-tratamiento (Axelsson R. y col., 2013), (Axelsson R. y col., 2015). En cuanto a la proteína HLA-A*0201, representa uno de los alelos identificados con mayor frecuencia en la población mundial (Neville M. y col., 2017), (Solberg O. y col., 2008) y en

México (Del Angel P. y col., 2020, sobreponiendo en parte el polimorfismo de HLA-I, lo cual representa un reto en la aplicación de anticuerpos tipo TCR. Todos los trabajos anteriormente mencionados convierten al complejo proteico Ag85Bp-HLA-A*0201 en un blanco idóneo para el desarrollo moléculas que tengan la capacidad de reconocerlo.

Los complejos proteicos biotinilados, usados en el proceso de selección, evidenciaron estabilidad estructural y el impacto positivo que tiene la presencia de estreptavidina en su dirección, demostrando que la interacción biotina-estreptavidina es una plataforma que favorece la selección de anticuerpos tipo TCR. Como estrategia metodológica, durante las tres rondas de selección, disminuimos la concentración del complejo blanco disponible y de forma alterna, un incremento en el número de lavados por cada ronda, nuestros resultados demostraron la importancia de este tipo de variables durante la selección, permitiendo optimizar el diseño de próximas estrategias al usar la técnica de despliegue en fago.

Para obtener anticuerpos de un solo dominio solubles, se indujo la expresión proteica a partir de la cepa *E. coli* HB2151. La extracción se realizó a partir del periplasma, puesto que es un ambiente oxidativo que optimiza el plegamiento de moléculas por formación de puentes disulfuro (Gupta S. y col., 2017), La purificación por afinidad a sefarosa acoplada a proteína A, permite seleccionar anticuerpos de un solo dominio plegados (Fridy P. y col., 2015), razón por la cual, ha sido utilizada en la purificación de fragmentos de anticuerpos (Fridy P. y col., 2014), (Abou E. y col., 2016), (Kunz P. y col., 2018). En cuanto al rendimiento de los anticuerpos de un solo dominio 2C y 7E, fue óptimo en comparación con trabajos previamente reportados (Abou E. y col., 2016), (Ruano G. y col., 2019). Todos los resultados anteriormente descritos, nos llevaron a concluir que la producción de los anticuerpos de un solo dominio solubles fue satisfactorio. No obstante, se deberá evaluar su producción en condiciones de escalamiento.

El cuanto a los resultados de reconocimiento, fueron controversiales con respecto a la primera evaluación. Para el anticuerpo 2C soluble, fue similar al obtenido cuando se encontraba unido a la partícula fágica, por otro lado, el anticuerpo 7E perdió la especificidad hacia el complejo Ag85Bp/HLA-A*0201, esta pérdida de especificidad, ha sido reportada en

fragmentos de anticuerpos seleccionados por despliegue en fago, al ser evaluados de forma soluble (Goswami P. y col., 2009), (Kaku Y. y col., 2012) la cual es adjudicada a la disminución en la estabilidad estructural cuando el anticuerpo es expresado de forma independiente a la partícula fágica. Otro factor a tener en cuenta, es el tipo de antígeno contra el cual se desarrolla un anticuerpo, por ejemplo, en los trabajos anteriores citados, hubo pérdida de especificidad de los fragmentos de anticuerpo, a pesar de que los antígenos fueron de naturaleza proteica independiente. En nuestro caso, el antígeno es un complejo recombinante, por esta razón, la pérdida de especificidad de uno de nuestros anticuerpos era de esperarse.

La evaluación en superficie celular del anticuerpos 2C, nos permitió evidenciar, la ausencia de reconocimiento tanto en el control de montaje como en ausencia y presencia del péptido Esat-6, implicando que el anticuerpo 2C no reconoce a HLA-A*02 plegadas con péptidos propios de la célula, ni tampoco con el control de especificidad. Para respaldar nuestros resultados, también se identificó la expresión de HLA-A*02 en superficie de las células T2, bajo las mismas condiciones, observando expresión tanto a nivel basal (ausencia de péptido) como en presencia de los péptidos de Ag85B y Esat-6. Estos resultados en conjunto nos permiten concluir que el dominio 2C, tiene la capacidad para reconocer al complejo Ag85p-HLA-A*0201 en superficie celular. Teniendo en cuenta que las secuencias peptídicas seleccionadas son reconocidas por linfocitos TCD8-péptido específicos, de pacientes con tuberculosis, nos permiten sugerir que el anticuerpo 2C, tiene el potencial de identificar células infectadas con Mtb.

La afinidad de reconocimiento hacia el complejo de interés por el anticuerpo 2C, se encuentra en el rango reportado para el receptor de linfocitos T (La G. y col., 2018) , (Rudolph M. y col., 2006). Previamente, fragmentos de anticuerpos *Fabs* tipo TCR, seleccionados por despliegue en fago, han mostrado constantes de afinidad en unidades de micromolaridad, conservando su capacidad de reconocimiento específico, e incluso, evidenciaron mecanismos de acción mediante eliminación de células blanco (Bewarder M. y col., 2020) Además, existen alternativas que permiten incrementar la afinidad sin afectar el reconocimiento, mediante la transformación monomérica a pentamérica (Zhu, X. y col., 2010) y mediante

mutaciones sobre regiones determinantes de complementariedad en combinación con una selección adicional usando despliegue en levaduras (Zhao Q. y col., 2015) .

La versatilidad en la construcción de bibliotecas de anticuerpos, al seleccionar al despliegue en fago, permite explorar el potencial de los fragmentos de anticuerpos, los cuales en las últimas décadas han tomado fuerza en el campo de desarrollo biotecnológico (Almagro J. y col., 2019). En este grupo se encuentran los anticuerpos de un solo dominio que por definición, representan el fragmento natural con capacidad de reconocimiento antigénica más pequeño (Ferrari A. y col., 2007), Además, cuentan con estabilidad, solubilidad y su tamaño casi 10 veces menor a un anticuerpo normal, brindan ventajas como la producción en sistema de expresión comunes como *E. coli*, fácil marcaje a nivel individual, y la construcción multimérica (Salvador J. y col., 2019), (Maass D. y col., 2007). Todas estas cualidades, hacen que actualmente, representen una de las moléculas de elección para el desarrollo de herramientas con el potencial de contrarrestar la pandemia causada por SARS-CoV-2 (Valdez-Cruz N. y col., 2021).

Con todos estos antecedentes de aplicación, contar con un anticuerpo de un solo dominio de origen humano, que reconozca al complejo Ag85Bp-HLA-A*0201, desarrollado mediante la técnica de despliegue en fago, deja un antecedente de diseño experimental para el desarrollo de este tipo anticuerpos contra otros antígenos y también, da lugar para continuar con su evaluación en células previamente infectadas por Mtb, lo cual representaría una valiosa herramienta con enfoques de aplicación en el área investigativa, como también, ser la base para el desarrollo de moléculas con potencial inmunoterapéutico.

M. CONCLUSIÓN

La estrategia utilizada para la selección de anticuerpos de un solo dominio, a partir de una biblioteca de origen humano, permitió identificar al anticuerpo 2C, el cual tiene la capacidad de reconocer a la proteína HLA-A*0201 plegada con el péptido Ag85Bp₁₉₉₋₂₀₇ de *Mycobacterium tuberculosis*, en un inmunoensayo y en la superficie de células T2.

N. PERSPECTIVAS

- El desarrollo de una molécula que tenga la capacidad de reconocer complejos péptido-HLA-I, brinda la posibilidad de estudiar más a fondo la dinámica entre células presentadoras de antígeno y linfocitos T en el desarrollo y establecimiento de la infección. Además, las cualidades exploradas de los anticuerpos de un solo dominio en cáncer, se acoplan muy bien a escenarios (granuloma) desarrollados en la infección por la micobacteria.

- La dinámica de expresión antigénica y el desarrollo de linfocitos T no polifuncionales, parecen favorecer el establecimiento y persistencia de la infección, sin embargo, esta situación, podría ser utilizada como un blanco de moléculas que simulen el reconocimiento del receptor de linfocitos T, actuando como puente entre la célula infectada y mecanismos de defensa para inducir muerte celular o potenciar la muerte de la micobacteria intracelular de manera específica.

Teniendo en cuenta este panorama, el siguiente paso consiste en evaluar al dominio 2C en superficie de células infectadas con Mtb e identificar la proteína HLA-A*0201 en donantes. Al obtener los resultados esperados, continuaría el diseño y desarrollo de propuestas de aplicación, tomando como referente la utilizadas en cáncer. A continuación se muestra un esquema que representa el potencial de aplicación de nanobodies en tuberculosis.

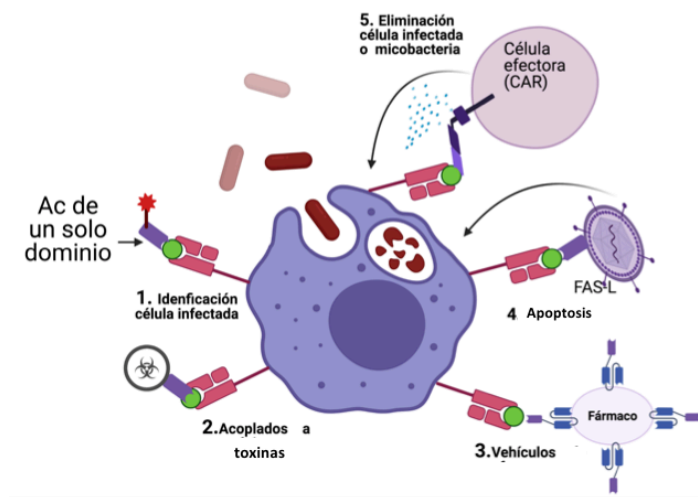


Figura 10: Potencial de aplicación de anticuerpos de un solo dominio en Tuberculosis.
Created with Bio Render.com

REFERENCIAS

Abou El-Magd, R. M., Vozza, N. F., Tuszynski, J. A., & Wishart, D. S. (2016). Isolation of soluble scFv antibody fragments specific for small biomarker molecule, L-Carnitine, using phage display. *Journal of immunological methods*, 428, 9-19.

Ahmed, M., Lopez-Albaitero, A., Pankov, D., Santich, B. H., Liu, H., Yan, S., Xiang, J., Wang, P., Hasan, A. N., Selvakumar, A., O'Reilly, R. J., Liu, C., & Cheung, N. V. (2018). TCR-mimic bispecific antibodies targeting LMP2A show potent activity against EBV malignancies. *JCI insight*, 3(4), e97805.

Almagro, J. C., Pedraza-Escalona, M., Arrieta, H. I., & Pérez-Tapia, S. M. (2019). Phage Display Libraries for Antibody Therapeutic Discovery and Development. *Antibodies (Basel, Switzerland)*, 8(3), 44.

Amcheslavsky, A., Wallace, A. L., Ejemel, M., Li, Q., McMahon, C. T., Stoppato, M., & Wang, Y. (2021). Anti-CfaE nanobodies provide broad cross-protection against major pathogenic enterotoxigenic *Escherichia coli* strains, with implications for vaccine design. *Scientific reports*, 11(1), 1-15.

Armitige, L. Y., Jagannath, C., Wanger, A. R., & Norris, S. J. (2000). Disruption of the genes encoding antigen 85A and antigen 85B of *Mycobacterium tuberculosis* H37Rv: effect on growth in culture and in macrophages. *Infection and immunity*, 68(2), 767-778.

Axelsson-Robertson, R., Ju, J. H., Kim, H. Y., Zumla, A., & Maeurer, M. (2015). *Mycobacterium tuberculosis*-specific and MHC class I-restricted CD8⁺ T-cells exhibit a stem cell precursor-like phenotype in patients with active pulmonary tuberculosis. *International Journal of Infectious Diseases*, 32, 13-22.

Axelsson-Robertson, R., Loxton, A. G., Walzl, G., Ehlers, M. M., Kock, M. M., Zumla, A., & Maeurer, M. (2013). A broad profile of co-dominant epitopes shapes the peripheral *Mycobacterium tuberculosis* specific CD8⁺ T-cell immune response in South African patients with active tuberculosis. *PloS one*, 8(3), e58309.

Axelsson-Robertson, R., Rao, M., Loxton, A. G., Walzl, G., Bates, M., Zumla, A., & Maeurer, M. (2015). Frequency of *Mycobacterium tuberculosis*-specific CD8⁺ T-cells in the course of anti-tuberculosis treatment. *International Journal of Infectious Diseases*, 32, 23-29.

Babaki, M. K. Z., Soleimanpour, S., & Rezaee, S. A. (2017). Antigen 85 complex as a powerful *Mycobacterium tuberculosis* immunogene: Biology, immunopathogenicity, applications in diagnosis, and vaccine design. *Microbial pathogenesis*, 112, 20-29.

Baena, A., & Porcelli, S. A. (2009). Evasion and subversion of antigen presentation by *Mycobacterium tuberculosis*. *Tissue antigens*, 74(3), 189-204.

Bagheri, S., Yousefi, M., Safaie Qamsari, E., Riazi-Rad, F., Abolhassani, M., Younesi, V., Sharifzadeh, Z. et al (2017). Selection of single chain antibody fragments binding to the extracellular domain of 4-1BB receptor by phage display technology. *Tumor Biology*, 39(3), 1010428317695924.

Bannas, P., Hambach, J., & Koch-Nolte, F. (2017). Nanobodies and Nanobody-Based Human Heavy Chain Antibodies as Antitumor Therapeutics. *Frontiers in immunology*, 8, 1603.

Barderas, R., & Benito-Peña, E. (2019). The 2018 Nobel Prize in Chemistry: Phage display of peptides and antibodies. *Analytical and bioanalytical chemistry*, 411(12), 2475-2479.

Bewarder, M., Held, G., Thurner, L., Stilgenbauer, S., Smola, S., Preuss, K. D., Carbon, G., Bette, B., Christofyllakis, K., Bittenbring, J. T., Felbel, A., Hasse, A., Murawski, N., Kaddu-Mulindwa, D., & Neumann, F. (2020). Characterization of an HLA-restricted and human cytomegalovirus-specific antibody repertoire with therapeutic potential. *Cancer immunology, immunotherapy: CII*, 69(8), 1535–1548.

Brewer, T. F. (2000). Preventing tuberculosis with bacillus Calmette-Guerin vaccine: a meta-analysis of the literature. *Clinical Infectious Diseases*, 31(Supplement_3), S64-S67.

Chames, P., Hufton, S. E., Coulie, P. G., Uchanska-Ziegler, B., & Hoogenboom, H. R. (2000). Direct selection of a human antibody fragment directed against the tumor T-cell epitope HLA-A1-MAGE-A1 from a nonimmunized phage-Fab library. *Proceedings of the National Academy of Sciences of the United States of America*, 97(14), 7969–7974.

Chen, F., Ma, H., Li, Y., Wang, H., Samad, A., Zhou, J., Zhu, L., Zhang, Y., He, J., Fan, X., & Jin, T. (2019). Screening of Nanobody Specific for Peanut Major Allergen Ara h 3 by Phage Display. *Journal of agricultural and food chemistry*, 67(40), 11219–11229.

Chow, A. Y., & Mellman, I. (2005). Old lysosomes, new tricks: MHC II dynamics in DCs. *Trends in immunology*, 26(2), 72-78.

Clay, H., Volkman, H. E., & Ramakrishnan, L. (2008). Tumor necrosis factor signaling mediates resistance to mycobacteria by inhibiting bacterial growth and macrophage death. *Immunity*, 29(2), 283–294.

Cohen, M., & Reiter, Y. (2013). T-cell receptor-like antibodies: targeting the intracellular proteome therapeutic potential and clinical applications. *Antibodies*, 2(3), 517-534.

Colditz, G. A., Berkey, C. S., Mosteller, F., Brewer, T. F., Wilson, M. E., Burdick, E., & Fineberg, H. V. (1995). The efficacy of bacillus Calmette-Guerin vaccination

of newborns and infants in the prevention of tuberculosis: meta-analyses of the published literature. *Pediatric*, (96), 20-35.

Comas, I., Chakravarti, J., Small, P. M., Galagan, J., Niemann, S., Kremer, K., & Gagneux, S. (2010). Human T cell epitopes of *Mycobacterium tuberculosis* are evolutionarily hyperconserved. *Nature genetics*, 42(6), 498-503.

Cooper, A. M., Dalton, D. K., Stewart, T. A., Griffin, J. P., Russell, D. G., Orme, I. M. et al. (1993). Disseminated tuberculosis in interferon gamma gene-disrupted mice. *The Journal of experimental medicine*, 178(6), 2243–2247.

Cosma, C. L., Humbert, O., Sherman, D. R., & Ramakrishnan, L. (2008). Trafficking of superinfecting *Mycobacterium* organisms into established granulomas occurs in mammals and is independent of the *Erp* and *ESX-1* mycobacterial virulence loci. *The Journal of infectious diseases*, 198(12), 1851-1855.

Court N, Vasseur V, Vacher R, Fremond C, Shebzukhov Y, Yeremeev VV, Maillet I, Nedospasov SA, Gordon S, Fallon PG, Suzuki H, Ryffel B, Quesniaux VF. (2010). Partial redundancy of the pattern recognition receptors, scavenger receptors, and C-type lectins for the long-term control of *Mycobacterium tuberculosis* infection. *J Immunol* 184:7057–7070.

Dahan, R., & Reiter, Y. (2012). T-cell-receptor-like antibodies-generation, function and applications. *Expert reviews in molecular medicine*, 14.

Dass, S. A., Norazmi, M. N., Acosta, A., Sarmiento, M. E., & Tye, G. J. (2020). TCR-like domain antibody against *Mycobacterium tuberculosis* (Mtb) heat shock protein antigen presented by HLA-A* 11 and HLA-A* 24. *International journal of biological macromolecules*, 155, 305-314.

Dass, S. A., Norazmi, M. N., Dominguez, A. A., Miguel, M., & Tye, G. J. (2018). Generation of a T cell receptor (TCR)-like single domain antibody (sDAb) against a *Mycobacterium Tuberculosis* (Mtb) heat shock protein (HSP) 16kDa antigen presented by Human Leukocyte Antigen (HLA)-A*02. *Molecular immunology*, 101, 189–196.

De los Ángeles Rojas-Alvarado, M., Díaz-Mendoza, M. L., Said-Fernández, S., Caballero-Olín, G., & Cerda-Flores, R. M. (2008). Asociación de la tuberculosis pulmonar con los antígenos del sistema HLA en el Noreste de México. *Gaceta médica de México*, 144(3), 233-238.

De Lourdes Mora-García, M., Duenas-González, A., Hernández-Montes, J., De la Cruz-Hernández, E., Pérez-Cárdenas, E., Weiss-Steider, B., ... & Monroy-García, A. (2006). Up-regulation of HLA class-I antigen expression and antigen-specific CTL response in cervical cancer cells by the demethylating agent hydralazine and the histone deacetylase inhibitor valproic acid. *Journal of translational medicine*, 4(1), 1-14.

De Sorrentino, A. H., Pardo, R., Marinic, K., Duarte, S. C., & Lotero, C. (2014). KIR-HLA clase I y tuberculosis pulmonar en población amerindia del Chaco, Argentina. *Enfermedades Infecciosas y Microbiología Clínica*, 32(9), 565-569.

Del Angel-Pablo, A. D., Juárez-Martín, A. I., Pérez-Rubio, G., Ambrocio-Ortiz, E., López-Flores, L. A., Camarena, A. E., & Falfán-Valencia, R. (2020). HLA Allele and Haplotype Frequencies in Three Urban Mexican Populations: Genetic Diversity for the Approach of Genomic Medicine. *Diagnostics (Basel, Switzerland)*, 10(1), 47.

DeMars, R., & Spies, T. (1992). New genes in the MHC that encode proteins for antigen processing. *Trends in cell biology*, 2(3), 81-86.

Denkberg, G., Cohen, C. J., Segal, D., Kirkin, A. F., & Reiter, Y. (2000). Recombinant human single-chain MHC-peptide complexes made from *E. coli* by in vitro refolding: functional single-chain MHC-peptide complexes and tetramers with tumor associated antigens. *European journal of immunology*, 30(12), 3522-3532.

Dirección general de epidemiología, Sistema nacional de vigilancia epidemiológica, Boletín epidemiológico, (2020), Número 53 | Volumen 37 | Semana 53. <https://www.gob.mx/salud/acciones-y-programas/historico-boletin-epidemiologico>.

Dulberger, C. L., Rubin, E. J., & Boutte, C. C. (2020). The mycobacterial cell envelope a moving target. *Nature Reviews Microbiology*, 18(1), 47-59.

Espinosa-Cueto, P., Magallanes-Puebla, A., Castellanos, C., & Mancilla, R. (2017). Dendritic cells that phagocytose apoptotic macrophages loaded with mycobacterial antigens activate CD8 T cells via cross-presentation. *PloS one*, 12(8), e0182126.

Ferrari, A., Rodríguez, M. M., Power, P., Weill, F. S., De Simone, E. A., Gutkind, G., & Leoni, J. (2007). Immunobiological role of llama heavy-chain antibodies against a bacterial β -lactamase. *Veterinary immunology and immunopathology*, 117(3-4), 173-182.

Flesch IE, Kaufmann SH. (1991) Mechanisms involved in mycobacterial growth inhibition by gamma interferon-activated bone marrow macrophages: role of reactive nitrogen intermediates. *Infect Immunology* 59:3213–3218.

Forrellad, M. A., Klepp, L. I., Gioffré, A., Sabio y Garcia, J., Morbidoni, H. R., Santangelo, M. D. L. P. & Bigi, F. (2013). Virulence factors of the *Mycobacterium tuberculosis* complex. *Virulence*, 4(1), 3-66.

Fridy, P. C., Li, Y., Keegan, S., Thompson, M. K., Nudelman, I., Scheid, J. F., Rout, M. P. et al. (2014). A robust pipeline for rapid production of versatile nanobody repertoires. *Nature methods*, 11(12), 1253-1260.

Fridy, P. C., Thompson, M. K., Ketaren, N. E., & Rout, M. P. (2015). Engineered high-affinity nanobodies recognizing staphylococcal Protein A and suitable for native isolation of protein complexes. *Analytical biochemistry*, 477, 92–94.

Fulton, S. A., Reba, S. M., Pai, R. K., Pennini, M., Torres, M., Harding, C. V., Boom, W. H., et al. (2004). Inhibition of major histocompatibility complex II expression and antigen processing in murine alveolar macrophages by *Mycobacterium bovis* BCG and the 19-kilodalton mycobacterial lipoprotein. *Infection and immunity*, 72(4), 2101-2110.

Geluk, A., Van Meijgaarden, K. E., Franken, K. L., Drijfhout, J. W., D'Souza, S., Necker, A. & Ottenhoff, T. H. (2000). Identification of major epitopes of *Mycobacterium tuberculosis* AG85B that are recognized by HLA-A* 0201-restricted CD8+ T cells in HLA-transgenic mice and humans. *The Journal of Immunology*, 165(11), 6463-6471.

Global tuberculosis report 2020. Geneva: World Health Organization; 2020. Licence: CC BY-NC-SA 3.0 IGO, available on line at: https://www.who.int/tb/publications/global_report/en/.

Goldman, E. R., Anderson, G. P., Liu, J. L., Delehanty, J. B., Sherwood, L. J., Osborn, L. E., & Hayhurst, A. (2006). Facile generation of heat-stable antiviral and antitoxin single domain antibodies from a semisynthetic llama library. *Analytical chemistry*, 78(24), 8245-8255.

Goswami, P., Saini, D., & Sinha, S. (2009). Phage displayed scFv: pIII scaffold may fine tune binding specificity. *Hybridoma*, 28(5), 327-331.

Govaert, J., Pellis, M., Deschacht, N., Vincke, C., Conrath, K., Muyldermans, S., & Saerens, D. (2012). Dual beneficial effect of interloop disulfide bond for single domain antibody fragments. *The Journal of biological chemistry*, 287(3), 1970–1979.

Gupta, S. K., & Shukla, P. (2017). Microbial platform technology for recombinant antibody fragment production: A review. *Critical reviews in microbiology*, 43(1), 31–42

Hajari Taheri, F., Hassani, M., Sharifzadeh, Z., Behdani, M., Arashkia, A., & Abolhassani, M. (2019). T cell engineered with a novel nanobody-based chimeric antigen receptor against VEGFR2 as a candidate for tumor immunotherapy. *IUBMB life*, 71(9), 1259–1267.

Hamers-Casterman, C., Atarhouch, T., Muyldermans, S., Robinson, G., Hamers, C., Songa, E. B., Bendahman, N., & Hamers, R. (1993). Naturally occurring antibodies devoid of light chains. *Nature*, 363(6428), 446–448.

Harth, G., Lee, B. Y., Wang, J., Clemens, D. L., & Horwitz, M. A. (1996). Novel insights into the genetics, biochemistry, and immunocytochemistry of the 30-

kilodalton major extracellular protein of *Mycobacterium tuberculosis*. *Infection and immunity*, 64(8), 3038-3047.

He, Q., Liu, Z., Liu, Z., Lai, Y., Zhou, X., & Weng, J. (2019). TCR-like antibodies in cancer immunotherapy. *Journal of hematology & oncology*, 12(1), 1-13.

Hollifield, A. L., Arnall, J. R., & Moore, D. C. (2020). Caplacizumab: an anti-von Willebrand factor antibody for the treatment of thrombotic thrombocytopenic purpura. *American journal of health-system pharmacy: AJHP: official journal of the American Society of Health-System Pharmacists*, 77(15), 1201–1207.

Horwitz, M. A., Harth, G., Dillon, B. J., & Masleša-Galić, S. (2000). Recombinant bacillus Calmette–Guérin (BCG) vaccines expressing the *Mycobacterium tuberculosis* 30-kDa major secretory protein induce greater protective immunity against tuberculosis than conventional BCG vaccines in a highly susceptible animal model. *Proceedings of the National Academy of Sciences*, 97(25), 13853-13858.

Høydahl, L. S., Frick, R., Sandlie, I., & Løset, G. Å. (2019). Targeting the MHC ligandome by use of TCR-like antibodies. *Antibodies*, 8(2), 32.

Hu, D., Wu, J., Zhang, R., & Chen, L. (2012). T-bet acts as a powerful adjuvant in Ag85B DNA-based vaccination against tuberculosis. *Molecular medicine reports*, 6(1), 139-144.

Hunter, R. L., Olsen, M. R., Jagannath, C., & Actor, J. K. (2006). Multiple roles of cord factor in the pathogenesis of primary, secondary, and cavitary tuberculosis, including a revised description of the pathology of secondary disease. *Annals of clinical and laboratory science*, 36(4), 371–386.

Huo, J., Le Bas, A., Ruza, R. R., Duyvesteyn, H. M., Mikolajek, H., Malinauskas, T., & Naismith, J. H. (2020). Neutralizing nanobodies bind SARS-CoV-2 spike RBD and block interaction with ACE2. *Nature structural & molecular biology*, 27(9), 846-854

Huygen, K. (2014). The immunodominant T-cell epitopes of the mycolyl-transferases of the antigen 85 complex of *M. tuberculosis*. *Frontiers in immunology*, 5, 321.

Indrigo, J., Hunter, R. L., & Actor, J. K. (2003). Cord factor trehalose 6,6'-dimycolate (TDM) mediates trafficking events during mycobacterial infection of murine macrophages. *Microbiology (Reading, England)*, 149(Pt 8), 2049–2059.

Ingram, J. R., Schmidt, F. I., & Ploegh, H. L. (2018). Exploiting Nanobodies' Singular Traits. *Annual review of immunology*, 36, 695–715.

Jovčevska, I., & Muyldermans, S. (2020). The Therapeutic Potential of Nanobodies. *BioDrugs: clinical immunotherapeutics, biopharmaceuticals and gene therapy*, 34(1), 11–26.

- Kadir, N. A., Sarmiento, M. E., Acosta, A., & Norazmi, M. N. (2016). Cellular and humoral immunogenicity of recombinant *Mycobacterium smegmatis* expressing Ag85B epitopes in mice. *International journal of mycobacteriology*, 5(1), 7-13.
- Kaku, Y., Noguchi, A., Okutani, A., Inoue, S., Tanabayashi, K., Yamamoto, Y., ... & Yamada, A. (2012). Altered specificity of single-chain antibody fragments bound to pandemic H1N1-2009 influenza virus after conversion of the phage-bound to the soluble form. *BMC research notes*, 5(1), 1-7.
- Kaufmann, S. H. E., Bloom, B., Brosch, R., Cardona, P. J., Dockrell, H., Fritzell, B., Schrager, L. et al (2015). Developing whole mycobacteria cell vaccines for tuberculosis: Workshop proceedings, Max Planck Institute for Infection Biology, Berlin, Germany, July 9, 2014. In *Vaccine* (Vol. 33, pp. 3047–3055).
- Keyaerts, M., Xavier, C., Heemskerk, J., Devoogdt, N., Everaert, H., Ackaert, C., & Lahoutte, T. (2016). Phase I study of ⁶⁸Ga-HER2-nanobody for PET/CT assessment of HER2 expression in breast carcinoma. *Journal of Nuclear Medicine*, 57(1), 27-33.
- Khan, A., Bakhru, P., Saikolappan, S., Das, K., Soudani, E., Singh, C. R., & Jagannath, C. (2019). An autophagy-inducing and TLR-2 activating BCG vaccine induces a robust protection against tuberculosis in mice. *NPJ vaccines*, 4(1), 1-19.
- Korotkov, K. V., Pardon, E., Steyaert, J., & Hol, W. G. (2009). Crystal structure of the N-terminal domain of the secretin GspD from ETEC determined with the assistance of a nanobody. *Structure*, 17(2), 255-265.
- Kunz, P., Zinner, K., Mücke, N., Bartoschik, T., Muyltermans, S., & Hoheisel, J. D. (2018). The structural basis of nanobody unfolding reversibility and thermoresistance. *Scientific reports*, 8(1), 1-10.
- Kuo, C. J., Bell, H., Hsieh, C. L., Ptak, C. P., & Chang, Y. F. (2012). Novel mycobacteria antigen 85 complex binding motif on fibronectin. *Journal of Biological Chemistry*, 287(3), 1892-1902.
- Kuo, C. J., Ptak, C. P., Hsieh, C. L., Akey, B. L., & Chang, Y. F. (2013). Elastin, a novel extracellular matrix protein adhering to mycobacterial antigen 85 complex. *Journal of Biological Chemistry*, 288(6), 3886-3896.
- Kwon, B. E., Ahn, J. H., Min, S., Kim, H., Seo, J., Yeo, S. G., & Ko, H. J. (2018). Development of new preventive and therapeutic vaccines for tuberculosis. *Immune network*, 18(2).
- La Gruta, N. L., Gras, S., Daley, S. R., Thomas, P. G., & Rossjohn, J. (2018). Understanding the drivers of MHC restriction of T cell receptors. *Nature Reviews Immunology*, 18(7), 467-478.

Lee, C. M., Iorno, N., Sierro, F., & Christ, D. (2007). Selection of human antibody fragments by phage display. *Nature protocols*, 2(11), 3001.

Li, C. P., Zhou, Y., Xiang, X., Zhou, Y., & He, M. (2015). Relationship of HLA-DRB1 gene polymorphism with susceptibility to pulmonary tuberculosis: updated meta-analysis. *The international journal of tuberculosis and lung disease: the official journal of the International Union against Tuberculosis and Lung Disease*, 19(7), 841–849.

Li, W., Schäfer, A., Kulkarni, S. S., Liu, X., Martinez, D. R., Chen, C., Dimitrov, D. S. et al. (2020). High potency of a bivalent human VH domain in SARS-CoV-2 animal models. *Cell*, 183(2), 429-441.

Lin, Y., Zhang, M., & Barnes, P. F. (1998). Chemokine production by a human alveolar epithelial cell line in response to *Mycobacterium tuberculosis*. *Infection and immunity*, 66(3), 1121-1126.

Liu, J. L., Goldman, E. R., Zabetakis, D., Walper, S. A., Turner, K. B., Shriver-Lake, L. C., & Anderson, G. P. (2015). Enhanced production of a single domain antibody with an engineered stabilizing extra disulfide bond. *Microbial cell factories*, 14(1), 1-8.

Liu, W., Song, H., Chen, Q., Yu, J., Xian, M., Nian, R., & Feng, D. (2018). Recent advances in the selection and identification of antigen-specific nanobodies. *Molecular immunology*, 96, 37-47.

Maass, D. R., Sepulveda, J., Pernthaler, A., & Shoemaker, C. B. (2007). Alpaca (*Lama pacos*) as a convenient source of recombinant camelid heavy chain antibodies (VHHs). *Journal of immunological methods*, 324(1-2), 13–25.

MacMicking JD, North RJ, LaCourse R, Mudgett JS, Shah SK, Nathan CF. (1997) Identification of nitric oxide synthase as a protective locus against tuberculosis. *Proc Natl Acad Sci U S A* 94:5243–5248.

Manangan, L. P., Pugliese, G., Jackson, M., Lynch, P., Sohn, A. H., Sinkowitz-Cochran, R. L., & Jarvis, W. R. (2001). Infection control dogma: top 10 suspects. *Infection control and hospital epidemiology*, 22(4), 243-247.

McCafferty, J., Griffiths, A. D., Winter, G., & Chiswell, D. J. (1990). Phage antibodies: filamentous phage displaying antibody variable domains. *nature*, 348(6301), 552-554.

Mearns, H., Geldenhuys, H. D., Kagina, B. M., Musvosvi, M., Little, F., Ratangee, F., & Steyn, M. (2017). H1: IC31 vaccination is safe and induces long-lived TNF- α + IL-2+ CD4 T cell responses in *M. tuberculosis* infected and uninfected adolescents: a randomized trial. *Vaccine*, 35(1), 132-141.

Morales-Yanez, F. J., Sariago, I., Vincke, C., Hassanzadeh-Ghassabeh, G., Polman, K., & Muyldermans, S. (2019). An innovative approach in the detection of *Toxocara canis* excretory/secretory antigens using specific nanobodies. *International journal for parasitology*, 49(8), 635–645.

Muyldermans S. (2013). Nanobodies: natural single-domain antibodies. *Annual review of biochemistry*, (82) 775–797.

Ndlovu, H., & Marakalala, M. J. (2016). Granulomas and Inflammation: Host-Directed Therapies for Tuberculosis. *Frontiers in immunology*, (7), 434.

Neville, M. J., Lee, W., Humburg, P., Wong, D., Barnardo, M., Karpe, F., & Knight, J. C. (2017). High resolution HLA haplotyping by imputation for a British population bioresource. *Human immunology*, 78(3), 242–251.

Nouailles G, Dorhoi A, Koch M, Zerrahn J, Weiner J 3rd, Fae KC, Arrey F, Kuhlmann S, Bandermann S, Loewe D, Mollenkopf HJ, Vogelzang A, Meyer-Schwesinger C, Mittrucker HW, McEwen G, Kaufmann SH. (2014). CXCL5-secreting pulmonary epithelial cells drive destructive neutrophilic inflammation in tuberculosis. *J Clin Invest* 124:1268–1282.

Nuttall, S. D., Krishnan, U. V., Hattarki, M., De Gori, R., Irving, R. A., & Hudson, P. J. (2001). Isolation of the new antigen receptor from wobbegong sharks, and use as a scaffold for the display of protein loop libraries. *Molecular immunology*, 38(4), 313–326.

Ocaña-Guzman, R., Tellez-Navarrete, N. A., Preciado-Garcia, M., Ponce-Gallegos, M. A., Buendia-Roldan, I., Falfán-Valencia, R., & Chavez-Galan, L. (2021). Multidrug-resistant tuberculosis patients expressing the HLA-DRB1*04 allele, and after treatment they show a low frequency of HLA-II⁺ monocytes and a chronic systemic inflammation. *Microbial pathogenesis*, 153, 104793.

Oliveira-Cortez, A., Melo, A. C., Chaves, V. E., Condino-Neto, A., & Camargos, P. (2016). Do HLA class II genes protect against pulmonary tuberculosis? A systematic review and meta-analysis. *European journal of clinical microbiology & infectious diseases* : official publication of the European Society of Clinical Microbiology, 35(10), 1567–1580.

Parmley, S. F., & Smith, G. P. (1988). Antibody-selectable filamentous fd phage vectors: affinity purification of target genes. *Gene*, 73(2), 305-318.

Pecora, N. D., Fulton, S. A., Reba, S. M., Drage, M. G., Simmons, D. P., Urankar-Nagy, N. J., Harding, C. V., et al. (2009). Mycobacterium bovis BCG decreases MHC-II expression in vivo on murine lung macrophages and dendritic cells during aerosol infection. *Cellular immunology*, 254(2), 94-104.

Prezzemolo, T., Guggino, G., La Manna, M. P., Di Liberto, D., Dieli, F., Caccamo, N. et al. (2014). Functional Signatures of Human CD4 and CD8 T Cell Responses to Mycobacterium tuberculosis. *Frontiers in immunology*, 5, 180.

Prezzemolo, T., van Meijgaarden, K. E., Franken, K. L., Caccamo, N., Dieli, F., Ottenhoff, T. H., & Joosten, S. A. (2018). Detailed characterization of human Mycobacterium tuberculosis specific HLA-E restricted CD8+ T cells. *European journal of immunology*, 48(2), 293-305.

Puissegur, M. P., Lay, G., Gilleron, M., Botella, L., Nigou, J., Marrakchi, H., Mari, B., Duteyrat, J. L., Guerardel, Y., Kremer, L., Barbry, P., Puzo, G., & Altare, F. (2007). Mycobacterial lipomannan induces granuloma macrophage fusion via a TLR2-dependent, ADAM9- and beta1 integrin-mediated pathway. *Journal of immunology (Baltimore, Md: 1950)*, 178(5), 3161–3169.

Qi, H., Lu, H., Qiu, H. J., Petrenko, V., & Liu, A. (2012). Phagemid vectors for phage display: properties, characteristics and construction. *Journal of molecular biology*, 417(3), 129–143.

Ramakrishnan L. Revisiting the role of the granuloma in tuberculosis. *Nat Rev Immunol.* (2012) Apr 20;12(5):352-66.

Reay, P. A., Matsui, K., Haase, K., Wulfig, C., Chien, Y. H., & Davis, M. M. (2000). Determination of the relationship between T cell responsiveness and the number of MHC-peptide complexes using specific monoclonal antibodies. *Journal of immunology (Baltimore, Md. : 1950)*, 164(11), 5626–5634.

Rogerson, B. J., Jung, Y. J., LaCourse, R., Ryan, L., Enright, N., North, R. J., (2006). Expression levels of Mycobacterium tuberculosis antigen-encoding genes versus production levels of antigen-specific T cells during stationary level lung infection in mice. *Immunology* 118(2):195-201.

Roshan, R., Naderi, S., Behdani, M., Cohan, R. A., Ghaderi, H., Shokrgozar, M. A., Golkar, M., & Kazemi-Lomedasht, F. (2021). Isolation and characterization of nanobodies against epithelial cell adhesion molecule as novel theranostic agents for cancer therapy. *Molecular immunology*, 129, 70–77.

Ruano-Gallego, D., Fraile, S., Gutierrez, C., & Fernández, L. Á. (2019). Screening and purification of nanobodies from E. coli culture supernatants using the hemolysin secretion system. *Microbial cell factories*, 18(1), 47.

Rudolph, M. G., Stanfield, R. L., & Wilson, I. A. (2006). How TCRs bind MHCs, peptides, and coreceptors. *Annu. Rev. Immunol.*, 24, 419-466.

Salvador, J. P., Vilaplana, L., & Marco, M. P. (2019). Nanobody: outstanding features for diagnostic and therapeutic applications. *Analytical and bioanalytical chemistry*, 411(9), 1703–1713.

- Scanga, C. A., Mohan, V. P., Yu, K., Joseph, H., Tanaka, K., Chan, J., Flynn, J. L. et al. (2000). Depletion of CD4⁺ T cells causes reactivation of murine persistent tuberculosis despite continued expression of interferon γ and nitric oxide synthase 2. *The Journal of experimental medicine*, 192(3), 347-358.
- Sendide, K., Deghmane, A. E., Pechkovsky, D., Av-Gay, Y., Talal, A., Hmama, Z., et al. (2005). Mycobacterium bovis BCG attenuates surface expression of mature class II molecules through IL-10-dependent inhibition of cathepsin S. *The Journal of Immunology*, 175(8), 5324-5332.
- Sendide, K., Deghmane, A. E., Reyrat, J. M., Talal, A., Hmama, Z., et al. (2004). Mycobacterium bovis BCG urease attenuates major histocompatibility complex class II trafficking to the macrophage cell surface. *Infection and immunity*, 72(7), 4200–4209.
- Sharma, S. K., Turaga, K. K., Balamurugan, A., Saha, P. K., Pandey, R. M., Jain, N. K., Katoch, V. M., & Mehra, N. K. (2003). Clinical and genetic risk factors for the development of multi-drug resistant tuberculosis in non-HIV infected patients at a tertiary care center in India: a case-control study. *Infection, genetics and evolution: journal of molecular epidemiology and evolutionary genetics in infectious diseases*, 3(3), 183–188.
- Sim, A. C. N., Too, C. T., Oo, M. Z., Lai, J., Eio, M. Y., Song, Z., & MacAry, P. A. (2013). Defining the expression hierarchy of latent T-cell epitopes in Epstein-Barr virus infection with TCR-like antibodies. *Scientific reports*, 3(1), 1-7.
- Siontorou C. G. (2013). Nanobodies as novel agents for disease diagnosis and therapy. *International journal of nanomedicine*, 8, 4215–4227.
- Solberg, O. D., Mack, S. J., Lancaster, A. K., Single, R. M., Tsai, Y., Sanchez-Mazas, A., & Thomson, G. (2008). Balancing selection and heterogeneity across the classical human leukocyte antigen loci: a meta-analytic review of 497 population studies. *Human immunology*, 69(7), 443–464.
- Soto, M. E., Vargas-Alarcón, G., Cicero-Sabido, R., Ramírez, E., Alvarez-León, E., & Reyes, P. A. (2007). Comparison distribution of HLA-B alleles in mexican patients with takayasu arteritis and tuberculosis. *Human immunology*, 68(5), 449–453.
- Souza de Lima, D., Morishi Ogusku, M., Porto Dos Santos, M., de Melo Silva, C. M., Alves de Almeida, V., Assumpção Antunes, I., Boechat, A. L., Ramasawmy, R., & Sadahiro, A. (2016). Alleles of HLA-DRB1*04 Associated with Pulmonary Tuberculosis in Amazon Brazilian Population. *PloS one*, 11(2), e0147543.
- Sreejit, G., Ahmed, A., Parveen, N., Jha, V., Valluri, V. L., Ghosh, S., Mukhopadhyay, S., et al. (2014). The ESAT-6 protein of Mycobacterium tuberculosis interacts with beta-2-microglobulin (β 2M) affecting antigen presentation function of macrophage. *PLoS pathogens*, 10(10), e1004446.

Suliman, S., Luabeya, A. K. K., Geldenhuys, H., Tameris, M., Hoff, S. T., Shi, Z., & Hatherill, M. (2019). Dose optimization of H56: IC31 vaccine for tuberculosis-endemic populations. A double-blind, placebo-controlled, dose-selection trial. *American Journal of Respiratory and Critical Care Medicine*, 199(2), 220-231.

Terán-Escandón, D., Terán-Ortiz, L., Camarena-Olvera, A., González-Avila, G., Vaca-Marín, M. A., Granados, J., & Selman, M. (1999). Human leukocyte antigen-associated susceptibility to pulmonary tuberculosis: molecular analysis of class II alleles by DNA amplification and oligonucleotide hybridization in Mexican patients. *Chest*, 115(2), 428-433.

Valdez-Cruz, N. A., García-Hernández, E., Espitia, C., Cobos-Marín, L., Altamirano, C., Bando-Campos, C. G., & Trujillo-Roldán, M. A. (2021). Integrative overview of antibodies against SARS-CoV-2 and their possible applications in COVID-19 prophylaxis and treatment. *Microbial cell factories*, 20(1), 1-32.

Van der Wel, N., Hava, D., Houben, D., Fluitsma, D., van Zon, M., Pierson, J., Brenner, M., Peters, P. J., et al. (2007). *M. tuberculosis* and *M. leprae* translocate from the phagolysosome to the cytosol in myeloid cells. *Cell*, 129(7), 1287-1298.

Van Zyl-Smit, R. N., Esmail, A., Bateman, M. E., Dawson, R., Goldin, J., van Rikxoort, E., & Bateman, E. D. (2017). Safety and immunogenicity of adenovirus 35 tuberculosis vaccine candidate in adults with active or previous tuberculosis. A randomized trial. *American journal of respiratory and critical care medicine*, 195(9), 1171-1180.

Volkman, H. E., Clay, H., Beery, D., Chang, J. C., Sherman, D. R., & Ramakrishnan, L. (2004). Tuberculous granuloma formation is enhanced by a mycobacterium virulence determinant. *PLoS Biol*, 2(11), 367.

Wang, Y., Fan, Z., Shao, L., Kong, X., Hou, X., Tian, D., Sun, Y., Xiao, Y., & Yu, L. (2016). Nanobody-derived nanobiotechnology tool kits for diverse biomedical and biotechnology applications. *International journal of nanomedicine*, 11, 3287-3303.

Weichold, F. F., Mueller, S., Kortsik, C., Hitzler, W. E., Wulf, M. J., Hone, D. M., & Maeurer, M. J. (2007). Impact of MHC class I alleles on the *M. tuberculosis* antigen-specific CD8⁺ T-cell response in patients with pulmonary tuberculosis. *Genes & Immunity*, 8(4), 334-343.

Wilkinson, R. J., DesJardin, L. E., Islam, N., Gibson, B. M., Kanost, R. A., Wilkinson, K. A., & Toossi, Z. (2001). An increase in expression of a *Mycobacterium tuberculosis* mycolyl transferase gene (*fbpB*) occurs early after infection of human monocytes. *Molecular microbiology*, 39(3), 813-821.

Wolf, A. J., Desvignes, L., Linas, B., Banaiee, N., Tamura, T., Takatsu, K., Ernst, J. D. et al. (2008). Initiation of the adaptive immune response to *Mycobacterium*

tuberculosis depends on antigen production in the local lymph node, not the lungs. *The Journal of experimental medicine*, 205(1), 105-115.

Wolf, A. J., Linas, B., Trevejo-Nuñez, G. J., Kincaid, E., Tamura, T., Takatsu, K., Ernst, J. D. et al. (2007). *Mycobacterium tuberculosis* infects dendritic cells with high frequency and impairs their function in vivo. *Journal of immunology* (Baltimore, Md. : 1950), 179(4), 2509–2519.

Wu, Y., Li, C., Xia, S., Tian, X., Kong, Y., Wang, Z., Ying, T. et al (2020). Identification of human single-domain antibodies against SARS-CoV-2. *Cell host & microbe*, 27(6), 891-898.

Xiang, Y., Nambulli, S., Xiao, Z., Liu, H., Sang, Z., Duprex, W. P., Shi, Y. et al. (2020). Versatile and multivalent nanobodies efficiently neutralize SARS-CoV-2. *Science*, 370(6523), 1479-148.

Zhang, G., Wang, L., Cui, H., Wang, X., Zhang, G., Ma, J., Han, H., He, W., Wang, W., Zhao, Y., Liu, C., Sun, M., & Gao, B. (2014). Anti-melanoma activity of T cells redirected with a TCR-like chimeric antigen receptor. *Scientific reports*, 4, 3571.

Zhao, Q., Ahmed, M., Tassev, D. V., Hasan, A., Kuo, T. Y., Guo, H. F., O'Reilly, R. J., & Cheung, N. K. (2015). Affinity maturation of T-cell receptor-like antibodies for Wilms tumor 1 peptide greatly enhances therapeutic potential. *Leukemia*, 29(11), 2238–2247.

Zhu, L., Yang, X., Zhong, D., Xie, S., Shi, W., Li, Y., Hou, X., Yao, H., Zhou, H., Ding, Z., Zhao, X., Mo, F., Yin, S., Liu, A., & Lu, X. (2020). Single-Domain Antibody-Based TCR-Like CAR-T: A Potential Cancer Therapy. *Journal of Immunology Research*, 2020.

Zhu, X., Wang, L., Liu, R., Flutter, B., Li, S., Ding, J., Tao, H., Liu, C., Sun, M., & Gao, B. (2010). COMBODY: one-domain antibody multimer with improved avidity. *Immunology and cell biology*, 88(6), 667–675.



Selection of a Single Domain Antibody, Specific for an HLA-Bound Epitope of the Mycobacterial Ag85B Antigen

Paola A. Ortega¹, Mayra Silva-Miranda^{1,2}, Alfredo Torres-Larios³, Eduardo Campos-Chávez³, Kees C. L. C. M. Franken⁴, Tom H. M. Ottenhoff⁴, Juraj Ivanyi⁵ and Clara Espitia^{1,5*}

¹ Departamento de Inmunología, Instituto de Investigaciones Biomédicas, Universidad Nacional Autónoma de México, Ciudad de México, México, ² CONACYT-Instituto de Investigaciones Biomédicas, Universidad Nacional Autónoma de México, Ciudad de México, México, ³ Department of Biochemistry and Structural Biology, Instituto de Fisiología Celular, Universidad Nacional Autónoma de México, Ciudad de México, México, ⁴ Department of Infectious Diseases, University Medical Centre Leiden, Leiden, Netherlands, ⁵ Center for Host-Microbiome Interactions, King's College London, London, United Kingdom

OPEN ACCESS

Edited by:

Mario Alberto Flores-Valdez,
CONACYT Centro de Investigación y
Asistencia en Tecnología y Diseño del
Estado de Jalisco (CIATEJ), Mexico

Reviewed by:

Eddie A. James,
Benaroya Research Institute,
United States
Armando Acosta,
Universiti Sains Malaysia Health
Campus, Malaysia

*Correspondence:

Clara Espitia
espitia@iibiomedicas.unam.mx

Specialty section:

This article was submitted to
Microbial Immunology,
a section of the journal
Frontiers in Immunology

Received: 30 June 2020

Accepted: 14 September 2020

Published: 02 October 2020

Citation:

Ortega PA, Silva-Miranda M,
Torres-Larios A, Campos-Chávez E,
Franken KCLCM, Ottenhoff THM,
Ivanyi J and Espitia C (2020) Selection
of a Single Domain Antibody, Specific
for an HLA-Bound Epitope of the
Mycobacterial Ag85B Antigen.
Front. Immunol. 11:577815.
doi: 10.3389/fimmu.2020.577815

T cells recognizing epitopes on the surface of mycobacteria-infected macrophages can impart protection, but with associated risk for reactivation to lung pathology. We aimed to identify antibodies specific to such epitopes, which carry potentials for development toward novel therapeutic constructs. Since epitopes presented in the context of major histocompatibility complex alleles are rarely recognized by naturally produced antibodies, we used a phage display library for the identification of monoclonal human single domain antibody producing clones. The selected 2C clone displayed T cell receptor-like recognition of an HLA-A*0201 bound ₁₉₉KLVANNT₂₀₇ peptide from the Ag85B antigen, which is known to be an immunodominant epitope for human T cells. The specificity of the selected domain antibody was demonstrated by solid phase immunoassay and by immunofluorescent surface staining of peptide loaded cells of the T2 cell line. The antibody affinity binding was determined by biolayer interferometry. Our results validated the used technologies as suitable for the generation of antibodies against epitopes on the surface of *Mycobacterium tuberculosis* infected cells. The potential approaches forward the development of antibody in immunotherapy of tuberculosis have been outlined in the discussion.

Keywords: tuberculosis, single domain antibodies, peptide-human leukocyte antigen complex, mycobacterial Ag85B, T cell receptor-like antibodies

INTRODUCTION

Current problems of Tuberculosis (TB) control are due to the emergence of drug resistant strains, the failure of the existing BCG vaccination and the persistence of factors associated with poverty-stricken populations. Consequently, there is a global morbidity of 10 million people with the mortality of 1.2 million in HIV-negative people and 0.25 million in HIV positive subjects (1) New

approaches toward the control of TB involve the shortening of the current chemotherapy regimen (2) and prophylaxis for HIV-related TB without interfering with antiretroviral therapy (3). This pilot study, aiming at the immunotherapy of TB had an initial objective to identify monoclonal antibodies with T cell receptor (TCR)-like specificity, binding to peptide epitope/human leukocyte antigen (HLA) class I complexes on the surface of *M. tuberculosis* infected cells. This approach has been based in the evidence, that such antibodies can be developed for the specific killing of malignant and virus-infected cells (4–10).

The mycobacterial peptides epitopes complexed with MHC class I molecules on the surface of infected cells are known to be recognized and leading to the activation of CD8+ T cells (11–13). Therefore, antibodies with TCR-like specificity following conjugation with suitable apoptosis-inducing ligands could potentially become mycobactericidal and a suitable adjunct to the chemotherapy of TB. The identification of TCR-like antibodies with specificity against *M. tuberculosis* Acr1 peptides/HLA.A*0201, HLA.A*011 and HLA.A*24 class I complexes has recently been reported, using peptide/MHC complexes generated *via* UV-induced peptide exchange. The complexes were panned against human DAb (domain antibody) phage display library (14, 15). This approach can be expanded by testing immunodominant epitopes from other *M. tuberculosis* antigens recognized in the context of HLA class I alleles (16, 17). Our interest focused on the HLA-A*0201 restricted CD8+T-cell epitopes of Ag85B, a major secreted *M. tuberculosis* protein. Two Ag85B peptides ₁₄₃FIYAGLSA₁₅₁ and ₁₉₉KLVANNTRL₂₀₇ had previously been identified in healthy humans and in immunized HLA-A2 transgenic mice (18), while HLA-A*0201 allele specific recognition of ₃₇YLLDGLRAQ₄₅ and ₁₉₉KLVANNTRL₂₀₇, was observed in patients with active TB (19). Since epitopes from Esat-6 and TB10.4, are recognized in the context of various HLA-A alleles, the HLA-A*0201 restricted, ₁₉₉KLVANNTRL₂₀₇ epitope from Ag85B appeared to be the most immunodominant (17) and was therefore chosen as our target for the selection and characterization of a TCR-like antibody. Using a human DAb phage display library, we selected a clone producing a single domain antibody (sdAb) against the Ag85B_{p199-207}/HLA-A*0201 complex (Ag85Bp/HLA-A*0201). Its specificity was determined by ELISA, and by its binding capacity to the Ag85Bp/HLA-A*0201 expressed on cells of the human HLA-A*0201 positive T2 cell line.

MATERIALS AND METHODS

Mycobacterium tuberculosis Peptides/HLA-A*0201 Complexes

Three nonamer peptides, known to be HLA-A*0201 restricted CD8+T cell epitopes from: Ag85B (₁₉₉KLVANNTRL₂₀₇), Esat-6 (₈₂AMASTEGNV₉₀), or Acr1 (₁₂₀GILTVSVAV₁₂₈) proteins of *M. tuberculosis* (16) were synthesized by Anaspec, Inc. (USA). The peptides were of > 90% purity, and their homogeneity was confirmed by analytical reverse-phase high-performance liquid

chromatography. The biotinylated recombinant complexes of Ag85Bp/HLA-A*0201, Esat-6_{p82-90}/HLA-A*0201 (Esat-6p/HLA-A*0201), and Acr1_{p120-128}/HLA-A*0201 (Acr1p/HLA-A*0201), were produced using extracellular HLA class I molecules, with C-terminal BirA recognition site, and β 2-microglobulin (20). The insoluble aggregates expressed in *Escherichia coli* in the form of inclusion bodies were solubilized in urea and folded with peptide by dilution. Monomers were biotinylated using the BirA enzyme and purified by gel filtration on a Hiload 16/60 Superdex 75 prep grade.

Evaluation of Refolding of Peptide/HLA-A*0201 Complexes by ELISA

An ELISA was carried out to evaluate the correct conformation of the complexes by using the W6/32 mAb (Invitrogen/USA) which recognizes a conformational epitope on the intact heavy chain/ β 2microglobulin complex (21–23). Briefly, 0.5 μ g/well of the biotinylated complexes in Phosphate Buffer Saline (PBS), were immobilized on streptavidin coated (ThermoScientific/USA) and on uncoated high protein-binding (ThermoScientific) plates. Samples were incubated overnight (ON) at 4°C. Next day, plates were washed twice with PBS and then incubated 1 h at room temperature (RT) with W6/32 mAb diluted 1/2,000 in PBS-tween-20 0.05%, Bovine Serum Albumin BSA 2% (PBS-TBSA). After 3 washes with PBS-T, wells were incubated by 1 h with Horseradish peroxidase conjugated goat anti-mouse IgG H+L antibody (anti-mouse IgG-HRP)[1/2,000 (Invitrogen/USA)]. Then, complexes on both streptavidin coated and uncoated plates, were incubated with streptavidin-HRP (Biosource/China), diluted 1/4,000 1 h at RT. Finally the reaction was revealed with TMB (3,3',5,5'-tetramethylbenzidine) (ThermoScientific), and stopped with 100 μ l of 0.16M H₂SO₄. Absorbance values were measured at 450 nm using an ELISA plate reader (Multiskan Go, Thermo).

Panning of the Human Single Domain Antibody Phage Library Against the Ag85B_{p199-207}/HLA-A*0201 Complex

A human DAb phage display library, containing approximately 3×10^9 sdAb clones (Geneservice, Cambridge) was used following a modified protocol (24). A negative panning was carried out for elimination of the background reactivity against streptavidin as follow: 5×10^{12} phage library particles were pre-incubated at 4°C for 1h with 30 μ l of streptavidin magnetic beads M280 (Invitrogen/Norway), then tube was placed in a magnet and phage supernatant was incubated with a 7.5 μ g of biotinylated Ag85Bp/HLA-A*0201 in PBS at 4°C for 1h. After that, 200 μ l of streptavidin beads were added and sample was incubated for 15 min at 4°C with shaking. Beads were pulled down with the magnet and washed 15 times with PBS-T 0.1%. Finally, sdAb phage complexes were eluted by incubation with glycine-HCl pH 2.2 for 15 min at RT and sample was neutralized with Tris-HCl pH 9.0. For the second and the third round of selection, 2.5 and 1.25 μ g of complexes were exposed to streptavidin beads and washed 15 and 25 times with PBS-T 0.1% respectively. After the third final round of panning, the eluted sdAb phages were used

to infect 5 ml freshly prepared *E. coli* TG1 culture. Bacteria were plated onto TYE medium supplemented with 4% glucose and carbenicillin 100 µg/ml (TYG_{4%}C₁₀₀). After ON culture, 94 individual clones were picked onto a 96 wells plate, containing 200 µl of 2xTYG_{4%}C₁₀₀. Plates were incubated ON at 37°C, with shaking at 200 rpm. Next day, 5 µl of ON culture from each well was transferred to a new plate with 200 µl of fresh 2xTYG_{4%}C₁₀₀. After 3 h of culture at 37°C, 50 µl 2xTY supplemented with 4x10⁸ M13 phage was added to each well and plates were incubated for 1 h at 37°C. After centrifugation to 2,800 rpm during 10 min, pellet was re suspended in 200 µl of 2xTYC₁₀₀K₁₀₀ (Kanamycin 100 µg/ml). Cultures were grown at 26°C with shaking at 250 rpm, during 16-24 h.

ELISA Phage

Phage supernatants from each well were collected and evaluated by ELISA. Biotinylated complexes at 0.5 µg/well were bound to coated streptavidin plates as described before, and incubated with 100 µl of phage supernatant for 1 h at RT. After several washes with PBS-T 0.05%, wells were incubated with anti-M13 HRP antibody (1/2,500) for 1 h at RT (GE Healthcare/USA). The reaction was developed with o-Phenylenediamine dihydrochloride OPD (SigmaAldrich/USA), and stopped adding 25 µl of 3M H₂SO₄. Absorbance values were measured at 492 nm using an ELISA plate reader Multiskan-GO. Phage supernatants from positive clones were also evaluated by phage ELISA against non-target complex; Esat-6p/HLA-A*0201 and Acr1p/HLA-A*0201 as described above.

Domain Antibody Sequencing

Double strand phagemid DNA extraction was performed from 3 selected clones in *E. coli* strain TG1 by using GeneJET Plasmid Miniprep kit (ThermoScientific/Lithuania), The primers used for sequencing were LMB3 (5' CAGGAAACAGCTATGAC 3') and pHEN (5'CTATGCGGCCCCATTCA 3'). Sequencing was carried out in the sequencing facility at Instituto de Investigaciones Biomédicas. For translation BioEdit 7.2 software was used and BLAST and Clustalw tools for sequences analysis and alignment.

Production of Soluble Domain Antibody

Transformation of *E. coli* HB2151 by phage infection and expression of sdAb were done with minor modifications according to (25). Once bacteria were transformed with phages, the positive clones (2C, 3C, and 7E), 50 µl of 1:10¹² to 1:10⁶ cell dilutions were sub-cultured in TYEC₁₀₀ plates and incubated overnight at 37°C. Three random unit forming colony (UFC) were picked up from each sample and inoculated in a culture flask containing 2xTYC₁₀₀. The culture was grown with shaking (250 rpm) at 37°C until OD_{600nm}=0.6 (26). Then, Isopropyl-β-D-1-thiogalactoside (IPTG) (Promega/USA) was added to a final concentration of 1 mM, culture was continued, at 26°C with shaking (250 rpm), ON. Cells were harvest by centrifugation at 4,500 rpm, and bacterial sediment was treated with an osmotic buffer (750 mM sucrose, 100 mM Tris pH 7.5) as described by (27). The periplasmic fractions obtained from each clone were subjected to affinity chromatography on Protein-A-

agarose (Roche/Germany), in order to purify the sdAbs following the manufacturer protocol. The eluted protein fractions were shuffled and concentrated to 500 µl in PBS pH 7.4, using amicon-15ml, 10.000 WM (Merck/Ireland). Protein quantification was determined by BCA assay (Pierce/USA).

SDS-PAGE and Western Blot

Ten µg/well of recombinant periplasmic extracts and 1.4 µg/well from 2C and 7E clones, were resolved on pre-made SDS-PAGE 4%–20%, (ThermoScientific/USA) and transferred to PVDF membranes. After 1 h blocking with PBS-BSA at RT, membranes were incubated with anti-c-Myc mAb (Sigma/USA) diluted 1/750 in PBS-T-BSA and then after washes with PBS-T, membranes were incubated with anti-mouse IgG HRP diluted (1/2,000)(Invitrogen/USA) for 1 h, washed with PBS-T, and developed with 3 mg/ml of 3,3-diaminobenzidine in PBS and 30% hydrogen peroxide diluted 1:1,000.

Evaluation of Specificity of Single Domain Antibodies by ELISA

The specificity of the purified sdAb 2C and 7E, were evaluated by ELISA using 1µg of target Ag85Bp/HLA-A*0201 and non-targets Esat-6p/HLA-A*0201 and Acr1p/HLA-A*0201 as which were immobilized on streptavidin plates. Complexes were incubated with 5 µg of sdAb followed by incubation with 1/1,000 dilution of anti-c-Myc Ab labelled with HRP (Sigma-Aldrich/Ireland Ltd) by 1h. After several washes with PBS-T, the reaction was developed with 50 µl of TMB. The reaction was stopped with 1M of H₂SO₄. OD_{450nm} was measured in an Infinium F50 microplate ELISA reader (Tecan/Switzerland). Three experiments were carried out by duplicated for 2C and 2 experiments for 7E.

Ex Vivo Specificity of Single Domain 2C on the Surface of T2 Cells

To assess the ability to sdAb 2C to recognize the Ag85Bp/HLA-A*0201 an *ex vivo* assay was performed, by using the HLA-A*0201 positive T2 lymphoblastic human cell line (kindly donate by Dr. Patricia Gorocica INER-México). These cells are characterized by export empty HLA class I molecules due to a processing defect by homozygous deletion of the MHC class II region located on chromosome 6 including the TAP1 and TAP2 (transporters associated with antigen processing) genes which encode the transporter proteins (28). Cells were maintained in RPMI-1640 medium supplemented with 20% (vol/vol) fetal bovine serum (FBS) (Gibco/USA), at 37°C, 5% CO₂. T2 cells (6x10⁵) were placed on flat bottom, 24 well cell culture plates (Costar/USA) in RPMI free serum in absence and presence of peptides from Ag85B and Esat-6.

In order to confirm the presence of HLA-ABC on T2 cells, they were incubated with W6/32 mAb (1µg/million cells), for 30 min on ice, after 3 washes, goat anti-mouse IgG Alexa fluor 488 (Invitrogen/USA) at 1/2,000 dilution was added. Samples were fixating with 0.5% PFA and the slides were mounted with vectashield (Vector Laboratories/USA). Then, cells (6x10⁵) were incubated with 80 µg of either Ag85Bp₍₁₉₉₋₂₀₇₎ target peptide and Esat-6p₍₈₂₋₉₀₎ as non-target. Twenty µg/ml of β2m (Sigma) was

added according to (29). Cells were incubated for 8 h at 37°C in 5% CO₂ atmosphere, after that cells were washed twice with PBS and incubated with 10 µg of sdAb 2C ON at 4°C in agitation, and then washed 2 times, with PBS, following by incubation with anti-c-Myc Ab (Santa Cruz-/Europe) (1/100) for 1 h at RT. After three washes, anti-mouse IgG Alexa fluor 488 (Invitrogen/USA) (1/2,000) was added and samples were incubated for 1 h at RT. After three washes, Hoechst 33343 (Life technologies/USA) diluted 1/9,000 was used for 10 min for nucleus staining. sdAb 2C was evaluated on cells in the absence of peptides and as a staining control in one condition, no domain was added. Fluorescence images were acquired with Olympus BX41, (Fluorescence-Microcopy) using the 100x magnifying lens, the digital images were captured with Zen 2.6 blue edition software, and the capture parameters, exposure time and intensity for each staining system, were applied in both control and problem samples.

Kinetic Binding Assays for the Assessment of the Interaction of sdAb 2C With Ag85Bp/HLA-A*0201 Complex by Biolayer Interferometry

The binding kinetics and the determination of the dissociation constant (K_D) for the sdAb 2C against the Ag85Bp/HLA-A*0201 complex were performed using Biolayer Interferometry (BLI) at 25°C. Streptavidin biosensors in an Octet RED96 system (FortéBio Inc. San Jose, CA, USA) were used. The assays were performed on black bottom 96-well microplates (Greiner Bio-One 655209) in a total volume of 200 µl with orbital shaking at 1000 rpm. Experiments were controlled with the software Data Acquisition 8.2 (FortéBio, Inc.) For the BLI experiment, a baseline was established using 1x Kinetics buffer (FortéBio Inc. San Jose, CA, USA). Then, the biotinylated Ag85Bp/HLA-A*0201 complex at 25 ng was allowed to bind to streptavidin sensor for 5 min, followed by washing with the same buffer to eliminate nonspecific binding. Next, the purified sdAb was bound to the Ag85Bp/HLA-A*0201 complex in the biosensor and the association rate was measured (k_a). In the last step, the dissociation rate (k_d) of the antibody-complex was obtained. The BLI experiment was done with six different concentrations of the sdAb 2C from (2.54 to 81.3 µM), one well with 200 µl without sdAb was used as a negative control.

New streptavidin biosensors were used for each experiment. The binding of sdAb 2C at 10 µM, to non-target Esat-6p/HLA-A*0201 was also tested. The data were processed using the Octet Data Analysis Software version 8.2 (FortéBio Inc. San Jose, CA, USA) according to a 1:1 model.

Statistical Analysis

GraphPad Prism version 6.0c software was used to analyze the results. For the statistical analysis, one-way ANOVA multiple comparisons with Sidak's post Hoc correction was used.

RESULTS

Evaluation of Peptide HLA-A Complexes With W6/32 Antibody

Ag85Bp/HLA-A*0201, Esat-6p/HLA-A*0201, and Acr1p/HLA-A*0201 immobilized on streptavidin plates were recognized by W6/32 mAb (Figure 1A), indicating this result that peptides HLA-A*0201 complexes were correctly folded. In contrast, the mAb did not recognize the complexes bound to non-coated streptavidin control plate (Figure 1B), showing the results that direct binding of the complexes in the plates could lead to a loss of conformation. The biotinylated complexes bound to streptavidin plates were not recognized for streptavidin-HRP, an indication that biotinylated complexes were correctly oriented by streptavidin on coated plates (Figure 1A). In contrast, the positive signal obtained with the complexes bound to the non-coated streptavidin plate (Figure 1B), was an indication that exposed biotin in unfolded complexes was being recognized by streptavidin-HRP.

Screening of the Human Single DAb Phage Library Binding to Ag85B_{p199-207} HLA-A*0201/Complexes

The number of phage particles from sdAb library during the three rounds of selection was consistent with the published protocol (24). The final output titers of phage particles showed an enrichment factor of 25 (Table 1). From 94 clones evaluated by monoclonal phage-ELISA, only 7 clones showed absorbance 10 fold higher than the negative control (clone not reactive to the

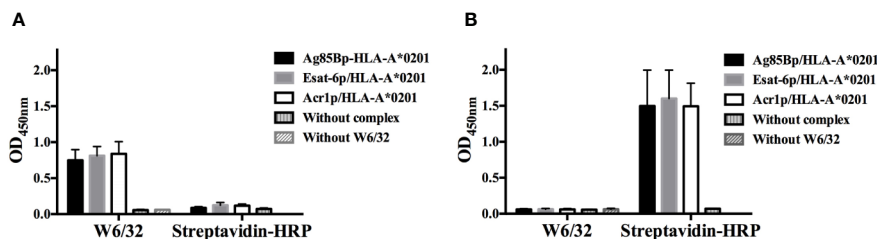


FIGURE 1 | Evaluation of complexes with conformational antibody W6/32. **(A)** Two groups of biotinylated complexes were immobilized on streptavidin coated plates, the group on the left was detected with W6/32 and the group on the right, was incubated with HRP-streptavidin. **(B)** The same as A, but both groups of biotinylated complexes were bound to uncoated streptavidin plates and detected with W6/32 and HRP-streptavidin respectively. The dates represent the media +/- standard deviation from three independent experiments.

TABLE 1 | Selective enrichment of phage domain antibody after 3 rounds of biopanning.

SelS Selection Round	Ag85Bp/HLA-A*0201	Phages Input	Eluted phages/ml	Eluted/input	Enrichment Factor*	Amplified Phages/ml	Tween 20/ # washes
1	7.5µg	5.0×10 ¹²	6.0×10 ⁶	1.2×10 ⁻⁶	1.0	84×10 ¹²	1.0%/15
2	2.5µg	5.0×10 ¹²	1.4×10 ⁸	2.8×10 ⁻⁵	23	7×10 ¹²	0.1%/15
3	1.25µg	5.0×10 ¹²	1.5 ×10 ⁸	3.0×10 ⁻⁵	25	—	0.1%/25

*Enrichment factor was determined by dividing the eluted/input ratio in each round by the ratio in the first round. according to Bagheri et al. (30) Zhang et al. (31).

Ag85Bp/HLA-A*0201) (**Figure 2A**). From those, clones 2C, 3C, and 7E did not recognized streptavidin (**Figure 2B**) and all of them showed specific binding by ELISA to the target complex and but none bound to non-target complexes, Esat-6p/HLA-A*0201, and Acr1p/HLA-A*0201 (**Figure 2C**).

Domain Antibody Sequencing

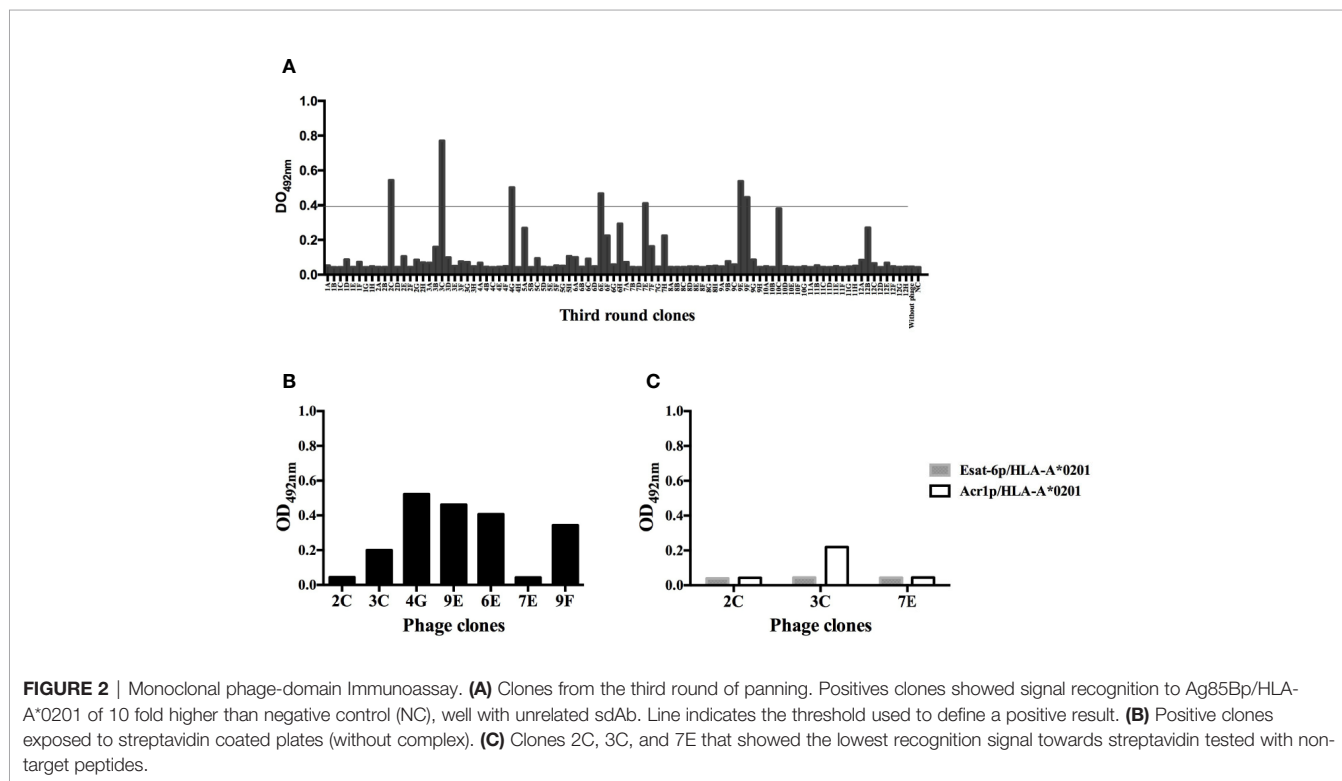
BLAST search analysis of sdAb 2C, 3C, and 7E sequences, showed that all them matched with 122 amino acids length of immunoglobulin heavy chain variable region, partial (>ABM67233.1 Homo sapiens). Sequences corresponded to a human dAb with a length of 160 and 159 amino acids residues for 2C and 7E domains, respectively, the protein sequence of the 3C domain was exactly the same as 2C but shorter in length, 3C had only 151 amino acids due to the presence of a stop codon. For all sequences, the three complementarity determining regions (CDR) and the c-Myc tag sequence were identified. Clones 2C and 7E were selected to continue with de antibody expression phase.

Production of Single Domain Antibodies

sdAb 2C was produced in *E. coli* HB2151. The expression and purification of sdAb 2C is shown in **Figure 3A**. Purified sdAb 2C with the expected molecular mass of ≈15 kDa was detected by Coomassie blue staining (**Figure 3A**, line 3) and antibody was recognized by anti-c-Myc Ab on Western blot (**Figure 3A**, line 4). The yield of production of 2C was 1418 µg from 50 ml of culture, (Results obtained with 7E are not shown).

Specificity of Single Domain Antibodies by ELISA

The recognition of the Ag85Bp/HLA-A*0201 complex by sdAb 2C was evaluated by ELISA, using Esat-6p/HLA-A*0201 and Acr1p/HLA-A*0201 as non-targets. The results are shown in **Figure 3B**. The binding of sdAb 2C to Ag85Bp/HLA-A*0201 complex was highly specific, showing statistically significant differences with respect to non-targeted complexes. On the other hand, sdAb 7E, showed a nonspecific signal absorbance ratios for both target and non-target complexes (Results not shown).



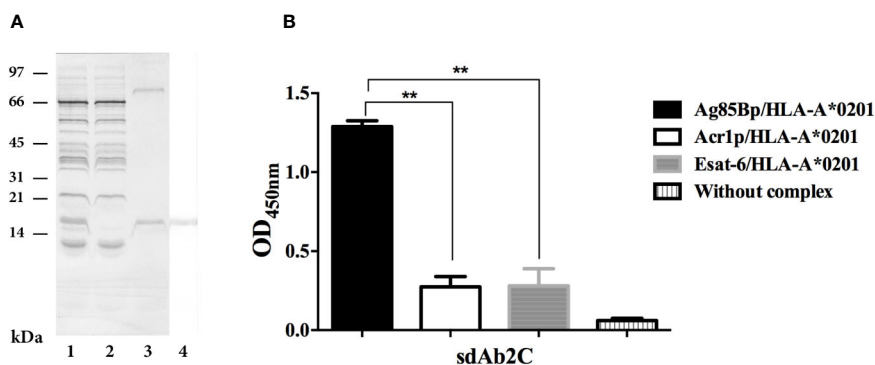


FIGURE 3 | Expression, purification and specificity evaluation of sdAb 2C. **(A)** Lanes 1 to 3. Line 1, Coomassie blue stained of periplasmic extract. Line 2, unbound fraction to protein A sepharose column. Line 3, purified domain. Lane 4, Western blot of purified sdAb 2C recognized by anti-c-Myc Ab. **(B)** Evaluation of specificity of sdAb 2C by ELISA with target Ag85Bp/HLA-A*0201 and non-target (Esat-6p/HLA-A*0201 and Acr1p/HLA-A*0201) complexes. The results represent 3 independent experiments and significant differences are indicated by asterisk ($p < 0.05$).

Ex Vivo Specificity of Soluble Domain 2C on T2 Cells Surface

Surface expression of HLA-A molecules in T2 cells was demonstrable by binding of the W6/32 mAb in absence and in presence of either Ag85Bp₁₉₉₋₂₀₇ or Esat-6p₈₂₋₉₀ peptides (**Supplementary Figure S1**). However, sdAbs 2C showed different recognition patterns, whereby the sdAb 2C fluorescence signal was observed only on T2 cells exposed to the Ag85Bp₁₉₉₋₂₀₇ (**Figure 4**). About 6.4% of positive events were observed, but no positive signals were detected without sdAb 2C, or without Ag85Bp₁₉₉₋₂₀₇, or by incubation with the no-target Esat-6 peptide.

sdAb 2C Binding Affinity by Biolayer Interferometry

The association of sdAb 2C to Ag85Bp/HLA-A*0201 was measured by BLI. The affinity constant was calculated in terms of equilibrium dissociation constant (K_D) to be $15 + 0.20 \mu\text{M}$ (**Figure 5A**). The sdAb interacts with the target complex in a concentration dependent manner and confirms the dissociation constant value (**Figure 5B**). The interaction of sdAb with Esat-6p/HLA-A*0201 was very low and the binding parameters could not be determined.

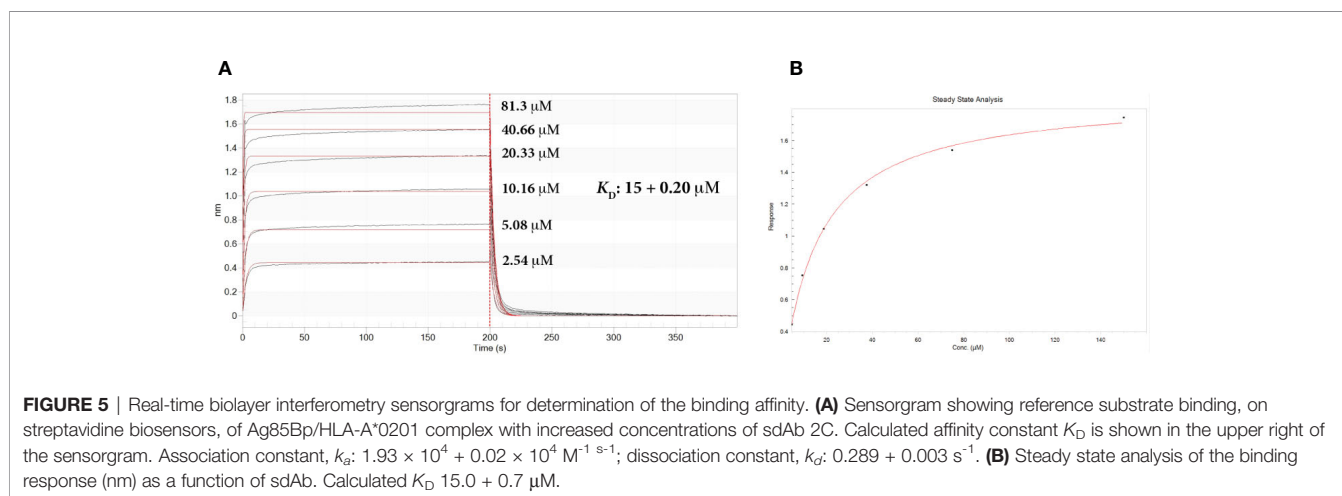
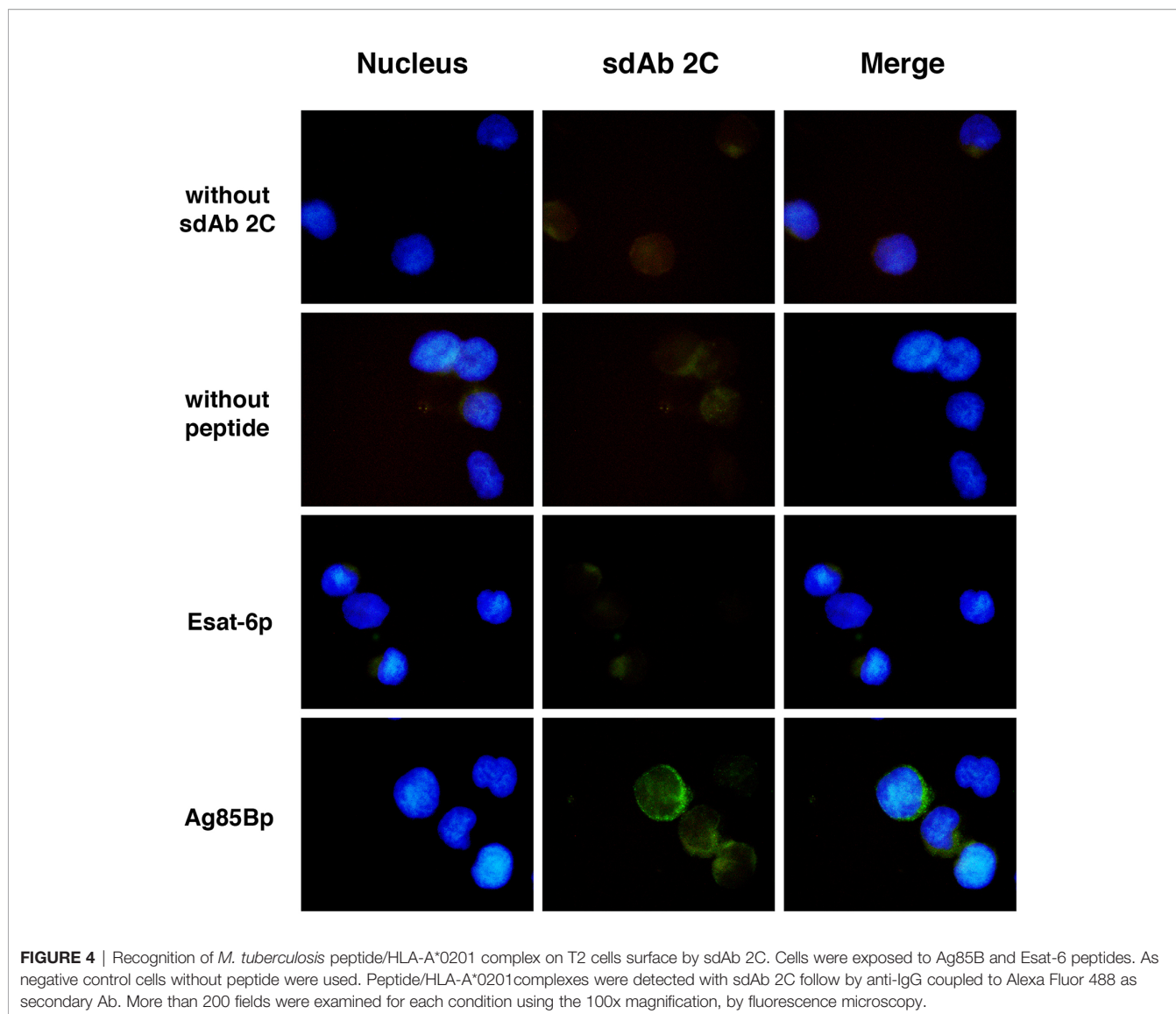
DISCUSSION

CD8+ T cells recognizing peptide epitopes bound to MHC/HLA class I molecules have the capacity to lyse the *M. tuberculosis* infected cells, thus contributing to the intracellular killing of the infecting organisms (16). Hence, binding of antibodies with TCR-like recognition specificity seemed desirable for developing antibody constructs, with mycobactericidal potentials. TCR-like Ab recognizing MHC class I bound antigenic peptides on antigen presenting cells, have previously been reported for the treatment of cancer, viral infections and autoimmune diseases (6). The aim toward TB immunotherapy has recently been

initiated by the selection of antibodies against the latency expressed Acr1/HLA class I restricted epitopes (14, 15). We report here on a TCR-like sdAb against an immunodominant HLA-A*0201 binding epitope of the Ag85B, selected by screening and selection from a human DAb phage display library. The secreted, fibronectin binding, mycolyl transferase protein is a strong immunogen in both infected and active TB cases and it has been used in several recombinant vaccine constructs (32–35). We chose the p₁₉₉KLVANNT₂₀₇ peptide as the target epitope in this study, because its known immunodominance for the human CD8+ T cell responses in the context of HLA-A*0201 and it's a conserved sequence in the genome (16, 17, 19). These properties favoured the previous application of TCR-like sdAbs for targeting tumors and cells infected with other pathogens (36, 37).

The procedures used for the selection and evaluation of TCR-like sdAbs ensure the specificity of recognition between for the target and non-target molecules. In this work, all the biotinylated complexes were first evaluated through a comparative ELISA, using plates with or without streptavidin. The results showed that the streptavidin coated plates ensured an adequate arrangement and orientation of p/HLA-A complexes, which is necessary for finding the specific TCR-like sdAbs. Similarly, Ag85Bp/HLA-A*0201 was bound to magnetic pearl cover with streptavidin for the selection of recombinant phages (26). From the third-round of selection, clones, 2C and 3C of identical sequence and clone 7E bound to the target complex. However, after conversion to the soluble form, sdAb 7E lost its specificity for the target complex. Such a change in specificity was previously reported to be due to loss of structural support by the phage scaffold pIII protein for the anti-H1N1 influenza virus antibody's antigen-binding site (38). The production of sdAb 2C and 7E in *E. coli* HB2151 from periplasmic extracts was satisfactory, compared with the previously reported production outputs (25, 39).

Although sdAb 2C was highly specific against the target complex, its affinity is low, i.e., in the range of 1–100 μM



corresponding to the affinity binding interaction of TCR ligands. The low binding affinity known for TCR-like antibody fragments selected from human libraries can be improved using complementary technologies (40). An increased up to 100 fold of the initial affinity from scFv (single chain variable fragment) directed against the HLA-A2-pWT1₁₂₆ complex, was achieved by mutagenesis combined with yeast display based on one specific scFv-clone (41). The affinity could also be improved by re-cloning and re-selection of clones or by conversion of sdAbs into multivalent formats with higher avidity (4, 42). Though antibody affinity can be significant for its potential for immunotherapy, most interestingly however, it was found that low, rather than high antibody affinity has been reported to be essential for the passive antibody therapy of a drosophila based model of Alzheimer's disease (43, 44). This was interpreted on the grounds that the low affinity anti-tau antibody may loosen up intracellular tau aggregates allowing better access of lysosomal degrading enzymes, while high affinity antibody may make these aggregates more compact and therefore more difficult to degrade. Such interpretation may be relevant also for the desired intracellular mycobactericidal action on *M. tuberculosis* infected macrophages.

Antibodies generated in animals against MHC-I recombinant tetramers are rarely TCR-like, because many of them recognize the $\alpha 3$ domain of MHC-I and $\beta 2$ microglobulin ($\beta 2m$) (5) and also due to the reduced stability of recombinant p/HLA-A complex (45). However, the phage display antibody libraries have the advantage that the fusion proteins are exposed on the surface of phage particles, and recombinant p/HLA-A complex targets can be used through several selection rounds (37). The structure of human sdAbs also known as nanobodies, used in the present work represents a single variable domain based on the VH3-23 germline segment heavy chain with synthetic diversity introduced by PCR mutagenesis into all tree complementary determining regions (24). They are highly stable, easily produced in large quantity by *E. coli*, they are of low immunogenicity, small size (15 kDa), and can be fused with multiple tags (46–48). Consequently, sdAbs have been used for virus detection (49–51), for imaging *in vivo*, mainly in cancer due to their bio distribution, high tumor penetrance and fast clearance from the blood circulation (52). The immunotherapeutic potentials include therapeutic targets in cancer (53), antagonism of angiogenesis (54) and acting as metastasis inhibitors.

CONCLUSIONS AND PERSPECTIVES

The TCR-like identity of the sdAb 2C has been validated by its specific recognition of Ag85Bp/HLA-A*0201 on the surface of human T2 cell line. It will be of further interest to test, if the sdAb 2C can detect the expression of the HLA-A*0201-bound Ag85B peptide on human macrophages, which contain either replicating or dormant *M. tuberculosis* infection. A positive result would justify further engineering of the sdAb 2C to become an

immunotoxin, by conjugation with suitable apoptosis inducing ligands, i.e., *Pseudomonas* exotoxin A, Granzyme B or BH3 peptide (55, 56), in endeavour to develop a mycobactericidal immunotherapeutic agent.

Further, development of sdAb 2C will need evaluation in both HLA-A*0201 transgenic mice and in humans with active TB disease. The obtained results are showing the feasibility of selecting TCR-like sdAbs to other immunodominant epitopes of *M. tuberculosis* and their future development as potential immunotherapeutic adjuncts to the chemotherapy of TB.

DATA AVAILABILITY STATEMENT

The raw data supporting the conclusions of this article will be made available by the authors, without undue reservation.

AUTHOR CONTRIBUTIONS

CE and JI conceived and supervised the study. CE, PO, MS-M, and KF performed experiments. TO, KF, MS-M, and PO designed experiments, analyzed data, and provided new tools and reagents. CE, JI, and PO wrote the manuscript. All authors contributed to the article and approved the submitted version.

ACKNOWLEDGMENTS

We thank Cristina Parada for technical assistance, the University program PASPA-UNAM for a scholarship to CE to take out a Sabbatical stay in the Center for Host-Microbiome Interactions at the Guy's Campus of King's College London. This project was funded by a Research Institutional program "NUATEI" from Instituto de Investigaciones Biomédicas UNAM, México and by the EC/H2020-PHC-2014/EMI-TB grant entitled: Eliciting Mucosal Immunity to Tuberculosis. PO is a PhD student from Doctorado en Ciencias Bioquímicas at Universidad Nacional Autónoma de México (UNAM), and has a scholarship from the Consejo Nacional de Ciencia y 417 Tecnología (CONACYT), (CVU/707238).

SUPPLEMENTARY MATERIAL

The Supplementary Material for this article can be found online at: <https://www.frontiersin.org/articles/10.3389/fimmu.2020.577815/full#supplementary-material>

SUPPLEMENTARY FIGURE 1 | Recognition of HLA-A molecules on T2 cell surface. Cells were loaded with Ag85B and Esat-6 peptides and cells without peptide as negative control. HLA-A molecules were detected with W6/32 as primary Ab, by anti c-Myc Ab and anti IgG coupled to Alexa Fluor 488 as secondary Abs. More than 200 fields were observed for each condition evaluated using the 100x magnification, by fluorescence microscopy.

REFERENCES

- World Health Organization. *Global tuberculosis report* (2018). Available at: <https://www.who.int/es/news-room/fact-sheets/detail/tuberculosis> (Accessed Jun 16, 2018).
- Hoagland DT, Liu J, Lee RB, Lee RE. New agents for the treatment of drug-resistant *Mycobacterium tuberculosis*. *Adv Drug Deliv Rev* (2016) 102:55–72. doi: 10.1016/j.addr.2016.04.02
- Pawlowski A, Jansson M, Sköld M, Rottenberg ME, Källenius G. Tuberculosis and HIV co-infection. *PLoS Pathog* (2012) 8(2):e1002464. doi: 10.1371/journal.ppat.1002464
- Chames P, Hufton SE, Coulie PG, Uchanska-Ziegler B, Hoogenboom HR. Direct selection of a human antibody fragment directed against the tumor T-cell epitope HLA-A1-MAGE-A1 from a nonimmunized phage-Fab library. *Proc Natl Acad Sci* (2000) 97(14):7969–74. doi: 10.1073/pnas.97.14.796
- Wittman VP, David W, Tiffany N, Francisca AN, Stephen W and Jon AW. Antibody targeting to a class I MHC-peptide epitope promotes tumor cell death. *J Immunol* (2006) 177:4187–95. doi: 10.4049/jimmunol.177.6.4187
- Dahan R, Reiter Y. T-cell-receptor-like antibodies generation, function and applications. *Expert Rev Mol Med* (2012) 14:e6. doi: 10.1017/erm.2012.2
- Saeed M, van BM, Zalba S, Schooten E, Rens JA, Koning GA, et al. Targeting melanoma with immunoliposomes coupled to anti-MAGE A1 TCR-like single-chain antibody. *Int J Nanomed* (2016) 11:955–75. doi: 10.2147/IJN.S96123
- Porgador A, Yewdell JW, Deng Y, Bennink JR, Germain RN. Localization, quantitation, and in situ detection of specific peptide-MHC class I complexes using a monoclonal antibody. *Immunity* (1997) 6:715–26. doi: 10.1016/s1074-7613(00)80447-1
- Cohen CJ, Sarig O, Yamano Y, Tomaru U, Jacobson S, Reiter Y. Direct phenotypic analysis of human MHC class I antigen presentation: visualization, quantitation, and in situ detection of human viral epitopes using peptide-specific, MHC-restricted human recombinant antibodies. *J Immunol* (2003) 170(8):4349–61. doi: 10.4049/jimmunol.170.8.4349
- Denkberg G, Cohen CJ, Lev A, Chames P, Hoogenboom HR, Reiter Y. Direct visualization of distinct T cell epitopes derived from a melanoma tumor-associated antigen by using human recombinant antibodies with MHC-restricted T cell receptor-like specificity. *Proc Natl Acad Sci* (2002) 99(14):9421–6. doi: 10.1073/pnas.132285699
- Shams H, Klucar P, Weis SE, Lavani A, Moonan PK, Safi H, et al. Characterization of a *Mycobacterium tuberculosis* peptide that is recognized by human CD4+ and CD8+ T cells in the context of multiple HLA alleles. *J Immunol* (2004) 173(3):1966–77. doi: 10.4049/jimmunol.173.3.1966
- Klein MR, Smith SM, Hammond AS, Ogg GS, King AS, Vekemans J, et al. HLA-B*35-restricted CD8 T cell epitopes in the antigen 85 complex of *Mycobacterium tuberculosis*. *J Infect Dis* (2001) 183(6):928–34. doi: 10.1086/319267
- Lewinsohn DA, Winata E, Swarbrick GM, Tanner KE, Cook MS, Null MD, et al. Immunodominant tuberculosis CD8 antigens preferentially restricted by HLA-B. *PLoS Pathog* (2007) 13(9):1240–9. doi: 10.1371/journal.ppat.0030127
- Dass SA, Norazmi MN, Dominguez AA, Miguel MESSG, Tye GJ. Generation of a T cell receptor (TCR)-like single domain antibody (sDAb) against a *Mycobacterium tuberculosis* (Mtb) heat shock protein (HSP) 16kDa antigen presented by Human Leukocyte Antigen (HLA)-A*02. *Mol Immunol* (2018) 101:189–96. doi: 10.1016/j.molimm.2018.07.001
- Dass SA, Norazmi MN, Acosta A, Sarmiento ME, Tye GJ. TCR-like domain antibody against *Mycobacterium tuberculosis* (Mtb) heat shock protein antigen presented by HLA-A*11 and HLA-A*24. *Int J Biol Macromol* (2020) 155:305–14. doi: 10.1016/j.ijbiomac.2020.03.229
- Comas I, Chakravarti J, Small PM, Galagan J, Niemann S, Kremer K, et al. Human T cell epitopes of *Mycobacterium tuberculosis* are evolutionarily hyperconserved. *Nat Genet* (2010) 42:498–503. doi: 10.1038/ng.590
- Axelsson R, Loxton AG, Walzl G, Ehlers MM, Kock MM, Zumla A, et al. Broad profile of co-dominant epitopes shapes the peripheral *Mycobacterium tuberculosis* specific CD8+ T-cell immune response in South African patients with active tuberculosis. *PLoS One* (2013) 3:e58309. doi: 10.1371/journal.pone.0058309
- Geluk A, van Meijgaarden KE, Franken KL, Drijfhout JW, D'Souza S, Necker A, et al. Identification of major epitopes of *Mycobacterium tuberculosis* AG85B that are recognized by HLA-A*0201-restricted CD8+ T cells in HLA-transgenic mice and humans. *J Immunol* (2000) 165(11):6463–71. doi: 10.4049/jimmunol.165.11.6463
- Weichold FF, Mueller S, Kortsik C, Hitzler WE, Wulf MJ, Hone DM, et al. Impact of MHC class I alleles on the *M. tuberculosis* antigen-specific CD8+ T-cell response in patients with pulmonary tuberculosis. *Genes Immun* (2007) 8(4):334–43. doi: 10.1038/sj.gene.6364392
- Prezzemolo T, van Meijgaarden KE, Franken KLMC, Caccamo N, Dieli F, Ottenhoff, et al. Detailed characterization of human *Mycobacterium tuberculosis* specific HLA-E restricted CD8+ T cells. *Eur J Immunol* (2018) 48(2):293–305. doi: 10.1002/eji.201747184
- Denkberg G, Cohen CJ, Segal D, Kirkin AF, Reiter Y. Recombinant human single-chain MHC-peptide complexes made from *E. coli* By in vitro refolding: functional single-chain MHC-peptide complexes and tetramers with tumor associated antigens. *Eur J Immunol* (2000) 30(12):3522–32. doi: 10.1002/1521-4141(200012)30:12
- Parham P, Barnstable CJ, Bodmer WF. Use of a monoclonal antibody (W6/32) in structural studies of HLA-A,B,C, antigens. *J Immunol* (1979) 23(1):342–9.
- Mora GM de L, Duenas GA, Hernández MJ, De la Cruz HE, Pérez CE, Weiss SB, et al. Up-regulation of HLA class-I antigen expression and antigen-specific CTL response in cervical cancer cells by the demethylating agent hydralazine and the histone deacetylase inhibitor valproic acid. *J Transl Med* (2006) 4:55. doi: 10.1186/1479-5876-4-55
- Lee CM, Iorno N, Siervo F, Christ D. Selection of human antibody fragments by phage display. *Nat Protoc* (2007) 2(11):3001–8. doi: 10.1038/nprot.2007.448
- Abou El-Magd RM, Voza NF, Tuszyński JA, Wishart DS. Isolation of soluble scFv antibody fragments specific for small biomarker molecule, L-Carnitine, using phage display. *J Immunol Methods* (2016) 428:9–19. doi: 10.1016/j.jim.2015.11.006
- Santich BH, Liu H, Liu C, Cheung NK. “Generation of TCR-Like Antibodies Using Phage Display”. In: G Houen, editor. *Methods in molecular biology*, vol. 1348. New York: NY human Press (2015). p. 191–204.
- Liu JL, Goldman ER, Zabetakis D, Walper SA, Turner KB, Shriver-Lake LC, et al. Enhanced production of a single domain antibody with an engineered stabilizing extra disulfide bond. *Microb Cell Fact* (2015) 14:158. doi: 10.1186/s12934-015-0340-3
- DeMars R, Spies T. New genes in the MHC that encode proteins for antigen processing. *Trends Cell Biol* (1992) 3:81–6. doi: 10.1016/0962-8924(92)90077-z
- Atzin-Méndez JA, López-González JS, Báez R, Arenas-Del Angel MC, Montaña LF, Silva-Adaya, et al. Expansion of quiescent lung adenocarcinoma CD8+ T cells by MUC1-8-mer peptide-T2 cell-β2 microglobulin complexes. *Oncol Rep* (2016) 1:33–42. doi: 10.3892/or.2015.4328
- Bagheri S, Yousefi M, Safaie Qamsari E, Riazzi-Rad F, Abolhassani M, Younesi V, et al. Selection of single chain antibody fragments binding to the extracellular domain of 4-1BB receptor by phage display technology. *Tumour Biol* (2017) 39(3):1010428317695924. doi: 10.1177/1010428317695924
- Zhang F, Chen Y, Ke Y, Zhang L, Zhang B, Yang L, et al. Single Chain Fragment Variable (scFv) Antibodies Targeting the Spike Protein of Porcine Epidemic Diarrhea Virus Provide Protection against Viral Infection in Piglets. *Viruses* (2019) 11(1):58. doi: 10.3390/v11010058
- Kadir NA, Sarmiento ME, Acosta A, Norazmi MN. Cellular and humoral immunogenicity of recombinant *Mycobacterium smegmatis* expressing Ag85B epitopes in mice. *Int J Mycobacteriol* (2016) 5(1):7–13. doi: 10.1016/j.ijmyco.2015.09.006
- Babaki M, Soleimanpour S, Rezaee SA. Antigen 85 complex as a powerful *Mycobacterium tuberculosis* immunogene: Biology, immune-pathogenicity, applications in diagnosis, and vaccine design. *Microb Pathog* (2017) 112:20–9. doi: 10.1016/j.micpath.2017.08.040
- Horwitz MA, Harth G, Dillon BJ, Maslesa-Galic' S. Recombinant bacillus calmette-guerin (BCG) vaccines expressing the *Mycobacterium tuberculosis* 30-kDa major secretory protein induce greater protective immunity against tuberculosis than conventional BCG vaccines in a highly susceptible animal model. *Proc Natl Acad Sci U S A* (2000) 25:13853–8. doi: 10.1073/pnas.250480397
- Olsen WA, van PLA, Meng OL, Birk RP, Andersen P. Protection of mice with a tuberculosis subunit vaccine based on a fusion protein of antigen 85b and esat-6. *Infect Immun* (2001) 5:2773–8. doi: 10.1128/IAI.69.5.2773-2778.2001

36. De Groeve K, Deschacht N, De Koninck C, Caveliers V, Lahoutte T, Devoogdt N, Muyltermans S, De Baetselier P, Raes G. Nanobodies as tools for in vivo imaging of specific immune cell types. *J Nucl Med* (2010) 51:782–9. doi: 10.2967/jnumed.109.070078
37. Ingram JR, Schmidt FI, Ploegh HL. Exploiting Nanobodies' Singular Traits. *Annu Rev Immunol* (2018) 36:695–715. doi: 10.1146/annurev-immunol-042617-053327
38. Kaku Y, Noguchi A, Okutani A, Inoue S, Tanabayashi K, Yamamoto Y, et al. Altered specificity of single-chain antibody fragments bound to pandemic H1N1-2009 influenza virus after conversion of the phage-bound to the soluble form. *BMC Res Notes* (2012) 5:483. doi: 10.1186/1756-0500-5-483
39. Ruano-Gallego D, Fraile GC, Fernández LÁ. Screening and purification of nanobodies from *E. coli* culture supernatants using the hemolysin secretion system. *Microb Cell Fact* (2019) 18(1):47. doi: 10.1186/s12934-019-1094-0
40. Høydahl L, Frick R, Sandlie I, Løset GÅ. Targeting the MHC Ligandome by Use of TCR-Like Antibodies. *Antibodies Basel* (2019) 8(2):32. doi: 10.3390/antib8020032
41. Zhao Q, Ahmed M, Tassev DV, Hasan A, Kuo TY, Guo HF, et al. Affinity maturation of T-cell receptor-like antibodies for Wilms tumor 1 peptide greatly enhances therapeutic potential. *Leukemia* (2015) 29(11):2238–47. doi: 10.1038/leu.2015.125
42. Zhu X, Wang L, Liu R, Flutter B, Li S, Ding J, et al. COMBODY: one-domain antibody multimer with improved avidity. *Immunol Cell Biol* (2010) 88(6):667–75. doi: 10.1038/icb.2010.21
43. Krishnaswamy S, Huang HW, Marchal IS, Ryoo HD, Sigurdsson EM. Neuronally expressed anti-tau scFv prevents tauopathy-induced phenotypes in *Drosophila* models. *Neurobiol Dis* (2020) 137:104770. doi: 10.1016/j.nbd.2020.104770
44. Congdon E, Chukwu J, Shamir D, Deng J, Ujla D, Sait H, et al. Tau antibody chimerization alters its charge and binding, thereby reducing its cellular uptake and efficacy. *EBioMedicine* (2019) 42:157–73. doi: 10.1016/j.ebiom.2019.03.033
45. Cohen M, Reiter Y. T-Cell Receptor-Like Antibodies: Targeting the Intracellular Proteome Therapeutic Potential and Clinical Applications. *Antibodies* (2013) 2(3):517–34. doi: 10.3390/antib2030517
46. Salvador JP, Vilaplana L, Marco MP. Nanobody: outstanding features for diagnostic and therapeutic applications. *Anal Bioanal Chem* (2019) 411(9):1703–13. doi: 10.1007/s00216-019-01633-4
47. Wang P, Li G, Yan J, Hu Y, Zhang C, Liu X, et al. Bactrian camel nanobody-based immunoassay for specific and sensitive detection of Cry1Fa toxin. *Toxicon* (2014) 92:186–92. doi: 10.1016/j.toxicon.2014.10.024
48. Mass DR, Sepulveda J, Pernthaner A, Shoemaker CB. Alpaca (Lama pacos) as a convenient source of recombinant camelid heavy chain antibodies (VHHs). *J Immunol Methods* (2007) 324(1-2):13–25. doi: 10.1016/j.jim.2007.04.008
49. Ma Z, Tianyu W, Zhiwei L, Xuyang G, Yangsheng T, Li Y, et al. A novel biotinylated nanobody-based blocking ELISA for the rapid and sensitive clinical detection of porcine epidemic diarrhea virus. *J Nanobiotechnol* (2019) 17(1):96. doi: 10.1186/s12951-019-0531-x
50. Gelpok S, Sobarzo A, Brangel P, Vincke C, Romão E, Fedida-Metula S, et al. The Development and Validation of a Novel Nanobody-Based Competitive ELISA for the Detection of Foot and Mouth Disease 3ABC Antibodies in Cattle. *Front Vet Sci* (2018) 5:250. doi: 10.3389/fvets.2018.00250
51. Zhu M, Gong X, Hu Y, Ou W, Wan Y. Streptavidin-biotin-based directional double Nanobody sandwich ELISA for clinical rapid and sensitive detection of influenza H5N1. *J Transl Med* (2014) 12:352. doi: 10.1186/s12967-014-0352-5
52. Oliveira S, Heukers R, Sornkom J, Kok RJ, van Bergen En Henegouwen PM. Targeting tumors with nanobodies for cancer imaging and therapy. *J Control Release* (2013) 172(3):607–17. doi: 10.1016/j.jconrel.2013.08.298
53. Ji L, Dong C, Fan R, Qi S. A high affinity nanobody against endothelin receptor type B: a new approach to the treatment of melanoma. *Mol Biol Rep* (2020) 47(3):2137–47. doi: 10.1007/s11033-020-05313-w
54. Ebrahimzadeh W, Mousavi SL, Javidan Z, Rajabibazl M. Production of Novel VHH Nanobody Inhibiting Angiogenesis by Targeting Binding Site of VEGF. *Appl Biochem Biotechnol* (2015) 176(7):1985–95. doi: 10.1007/s12010-015-1695-y
55. Rosenblum M. Immunotoxins and toxin constructs in the treatment of leukemia and lymphoma. *Adv Pharmacol* (2004) 51:209–28. doi: 10.1016/S1054-3589(04)51009-8
56. Walensky LD, Kung AL, Escher I, Malia TJ, Barbuto S, Wright RD, et al. Activation of apoptosis in vivo by a hydrocarbon-stapled BH3 helix. *Science* (2004) 305(5689):1466–70. doi: 10.1126/science.1099191

Conflict of Interest: The authors declare that the research was conducted in the absence of any commercial or financial relationships that could be construed as a potential conflict of interest.


Copyright © 2020 Ortega, Silva-Miranda, Torres-Larios, Campos-Chávez, Franken, Ottenhoff, Ivanyi and Espitia. This is an open-access article distributed under the terms of the Creative Commons Attribution License (CC BY). The use, distribution or reproduction in other forums is permitted, provided the original author(s) and the copyright owner(s) are credited and that the original publication in this journal is cited, in accordance with accepted academic practice. No use, distribution or reproduction is permitted which does not comply with these terms.

REVIEW

Open Access



Integrative overview of antibodies against SARS-CoV-2 and their possible applications in COVID-19 prophylaxis and treatment

Norma A. Valdez-Cruz^{1*}, Enrique García-Hernández², Clara Espitia³, Laura Cobos-Marín⁴, Claudia Altamirano⁵, Carlos G. Bando-Campos¹, Luis F. Cofas-Vargas², Enrique W. Coronado-Aceves³, Ricardo A. González-Hernández¹, Pablo Hernández-Peralta⁴, Daniel Juárez-López¹, Paola A. Ortega-Portilla³, Sara Restrepo-Pineda¹, Patricio Zelada-Cordero¹ and Mauricio A. Trujillo-Roldán^{1*} 

Abstract

SARS-CoV-2 is a novel β -coronavirus that caused the COVID-19 pandemic disease, which spread rapidly, infecting more than 134 million people, and killing almost 2.9 million thus far. Based on the urgent need for therapeutic and prophylactic strategies, the identification and characterization of antibodies has been accelerated, since they have been fundamental in treating other viral diseases. Here, we summarized in an integrative manner the present understanding of the immune response and physiopathology caused by SARS-CoV-2, including the activation of the humoral immune response in SARS-CoV-2 infection and therefore, the synthesis of antibodies. Furthermore, we also discussed about the antibodies that can be generated in COVID-19 convalescent sera and their associated clinical studies, including a detailed characterization of a variety of human antibodies and identification of antibodies from other sources, which have powerful neutralizing capacities. Accordingly, the development of effective treatments to mitigate COVID-19 is expected. Finally, we reviewed the challenges faced in producing potential therapeutic antibodies and nanobodies by cell factories at an industrial level while ensuring their quality, efficacy, and safety.

Introduction

The recent disease outbreak caused by the new severe acute respiratory syndrome coronavirus 2 (SARS-CoV-2) is a global health emergency, as april 2021 affecting more

than 134 million people and leading to almost 2.9 million deaths until date [1]. In the last two decades, other SARS-CoV-2-related pathogenic β -coronaviruses have caused syndromes such as severe acute respiratory syndrome (SARS-CoV) and Middle East respiratory syndrome (MERS-CoV). SARS-CoV-2 is the causative agent of coronavirus disease (COVID-19). As the most transmissible coronavirus (CoV) identified to date, its vertiginous spread has led to the current COVID-19 pandemic [2–5]. This emphasizes the urgency in the research, design, innovation, and large-scale production of new prophylactic and therapeutic drugs.

CoVs are enveloped single-stranded positive-sense RNA viruses that can infect an extensive number of

*Correspondence: adri@biomedicas.unam.mx; maurotru@biomedicas.unam.mx

¹ Programa de Investigación de Producción de Biomoléculas, Departamento de Biología Molecular y Biotecnología, Instituto de Investigaciones Biomédicas, Universidad Nacional Autónoma de México, Ciudad Universitaria, 04510 Ciudad de México, México

Full list of author information is available at the end of the article

This article is dedicated to the memory of Dr. José de Jesús García Valdés of the Facultad de Química, Universidad Nacional Autónoma de México, a pioneer in the study of ion-channels and scorpion toxins in México.



© The Author(s) 2021. This article is licensed under a Creative Commons Attribution 4.0 International License, which permits use, sharing, adaptation, distribution and reproduction in any medium or format, as long as you give appropriate credit to the original author(s) and the source, provide a link to the Creative Commons licence, and indicate if changes were made. The images or other third party material in this article are included in the article's Creative Commons licence, unless indicated otherwise in a credit line to the material. If material is not included in the article's Creative Commons licence and your intended use is not permitted by statutory regulation or exceeds the permitted use, you will need to obtain permission directly from the copyright holder. To view a copy of this licence, visit <http://creativecommons.org/licenses/by/4.0/>. The Creative Commons Public Domain Dedication waiver (<http://creativecommons.org/publicdomain/zero/1.0/>) applies to the data made available in this article, unless otherwise stated in a credit line to the data.

hosts. Human CoVs (order Nidovirales, family Coronaviridae, subfamily Coronavirinae) are zoonotic pathogens, i.e., they can infect humans via interspecies transmission [6–8]. SARS-CoV-2 is a β -coronavirus that has four structural proteins: the nucleocapsid (N), membrane (M), envelope (E), and surface-anchored spike glycoprotein (S), which is proteolytically processed, generating a trimmer with three S_1 subunit heads sitting on top of a trimeric S_2 subunit, that allow the subsequent virus fusion [9–11]. The S protein, through its three receptor binding domains (RBDs), interacts with the human angiotensin-converting enzyme (hACE2), as an entry receptor, and the S_2 subunit induces fusion to the cell membrane [10, 12–15]. For this reason, the S protein represents an interesting target for the rational production of vaccines or therapeutic antibodies (Abs) preventing infection [16–18]. Due to the extensive transmission worldwide, the genetic diversity of the virus is dynamic. Recurrent mutations may indicate a convergent evolution for adaptation in humans, similar to those occurring in the S protein [19].

Since the beginning of the SARS-CoV-2 infectious outbreak, diverse antiviral chemical compounds have been tested in the clinic, showing different efficacies. For instance, the antiviral remdesivir is authorized in the United States for emergency use in humans [20, 21], although some trials do not show substantive benefits [22]. Moreover, approximately 180 vaccine candidates are under development awaiting expedited approval, upon demonstration of proof of quality, safety, and efficacy. More than four different vaccines are approved for emergency use by the Food and Drug Administration (FDA) and other regulatory agencies [23–25]. In addition, various recombinant monoclonal antibodies (mAbs) are being tested in therapy, with targets such as C5a, IL-6, and PD-1, among others, to curb some of the responses caused by SARS-CoV-2 [23]. Similarly, various mAbs developed and tested against other CoVs, including SARS-CoV and MERS-CoV, have been tested against SARS-CoV-2 to treat COVID-19 [3, 12, 26–30]. Alternatively, the World Health Organization recommends the use of plasma from convalescent patients as a therapy to treat critically ill patients globally [5, 31, 32]. Therefore, there is a need for the development of effective and safe COVID-19-specific vaccines or therapeutic drugs. Neutralizing Abs are one of the best candidates for neutralizing virus infection due to their antigenic specificity [12, 29, 30, 32]. Artificial passive immunization was born as a therapy based on antibodies transference from serum of immunized animals or humans to a recipient, conferring an immune state against the target [33]. Furthermore, this is one of the most employed immunotherapies in medicine history, supported by a long list of uses based

on its neutralization activities upon infectious diseases as produced by bacterial toxins as *Corynebacterium diphtheriae* [34], *Clostridium tetani* [35], *Staphylococcus aureus* [36], *Clostridium difficile* [37], *Bordetella pertussis* [38], among others. Also, successful viral neutralization had been described such as Enterovirus [39], Hepatitis B virus [40], Measles virus [41], Parvovirus [42], Rabies virus [43], Respiratory syncytial virus (RSV) [44] and Varicella-zoster virus [45]. Nowadays, there is technology to produce monoclonal high-specific and long-lasting antibodies from in vitro systems [46], which means a relevant therapeutic weapon to fight a wide spectrum of infections and other pathologies. Whilst active immunization by infection or vaccination requires a period of time to generate its own system antibodies, passive immunity represents an instantly effective source which induces immunological events as neutralization, opsonization, complement activation and antibody dependent cellular cytotoxicity (ADCC). Furthermore, passive immunity does not depend on recipient immune response which implies a critical instrument to treat immunocompromised patients and other vulnerable groups who cannot be exposed to the antigen itself. In front of COVID-19 pandemic, antibody-based humoral passive immunization treatment is a promising route to treat severe cases, or people who do not respond to vaccination or cannot be vaccinated.

There are several reviews on specific aspects of Abs or its formats as alternative treatments for COVID-19 [47–51]. Moreover, information about Abs is updated daily and is tremendously enriched, then different public databases have compiled information, allowing quick searches [52, 53]. Here, we update the knowledge regarding the immune response associated with COVID-19, the formation of neutralizing Abs towards SARS-CoV-2 in the plasma of patients, which could be useful in prophylactic and therapeutic treatments. Moreover, we discuss on the development and isolation of Abs from different sources (hybridomas production, the generation of nanobodies, and the recombinant production of fully humanized mAbs) against different SARS-CoV-2 targets, in an integrative form. This review also incorporates a comprehensive view of the challenges that faces the cell factories at an industrial level to produce therapeutic Abs and their formats, guaranteeing the corresponding quality, efficacy and safety attributes in the bioprocess. Due to the importance of certain references, 18 preprints were considered.

The immune response and physiopathology of COVID-19

COVID-19 is highly contagious, and oral-respiratory droplet contamination as well as aerosols, have been implicated in its transmission [54, 55]. A wide spectrum of associated clinical symptoms have been described, such as gastrointestinal issues, diarrhea, shortness of breath, headache, sore throat, cold, breathing difficulties, myalgia, nasal congestion and inflammation of the mucous membranes, and central nervous system injuries [56], and patients present with asymptomatic to severe infections, or even succumb to the disease [57]. There is an important relationship between the COVID-19 severity and activation/suppression of the immune response elements. SARS-CoV-2 is a virus with the ability to generate an acute and destructive inflammatory response affecting the tissues and various cell types that express the hACE2 receptor [10, 58, 59]. hACE2 is a type I membrane protein present in the human organs, including the lungs, heart, kidney, and intestine [60]. The inflammatory response is induced by different immunological mechanisms associated with the innate and adaptive immune responses.

Innate immune response against SARS-CoV-2 infection

The innate immune response to SARS-CoV-2 is characterized by not only the activation of epithelial cells, but also the hyperactivity of macrophages. In the presence of the virus, macrophages and respiratory epithelial cells have the ability to release proinflammatory and inflammatory mediators by activating the inflammasome, and pattern recognition receptors induced by virus pathogen-associated molecular patterns (PAMPs) [61]. RNA from different viruses, such as CoVs, acts as a PAMP that can be detected by various toll-like receptors (TLRs), such as TLR3, TLR7, TLR8, and TLR9 [62], activating the nuclear factor kappa light chain enhancer of activated B cells (NF-κB) pathway and proinflammatory cytokines [61]. During COVID-19 infection, it has been observed that monocytes have a relevant contribution in the progression of the disease towards severe manifestations, because the systemic profiles of cytokines in patients are similar to that in some of the syndromes, such as macrophage activation syndrome [63], or cytokine storm [64, 65]. This immune response is related to a high production of cytokines (IL-6, IL-7, and TNF-α) and inflammatory chemokines, including CCL2, CCL3, and CXCL10, as well as the IL-2 receptor α-chain in the soluble form [64, 66]. Multiple organ failures and complications such as acute respiratory distress syndrome (ARDS), which

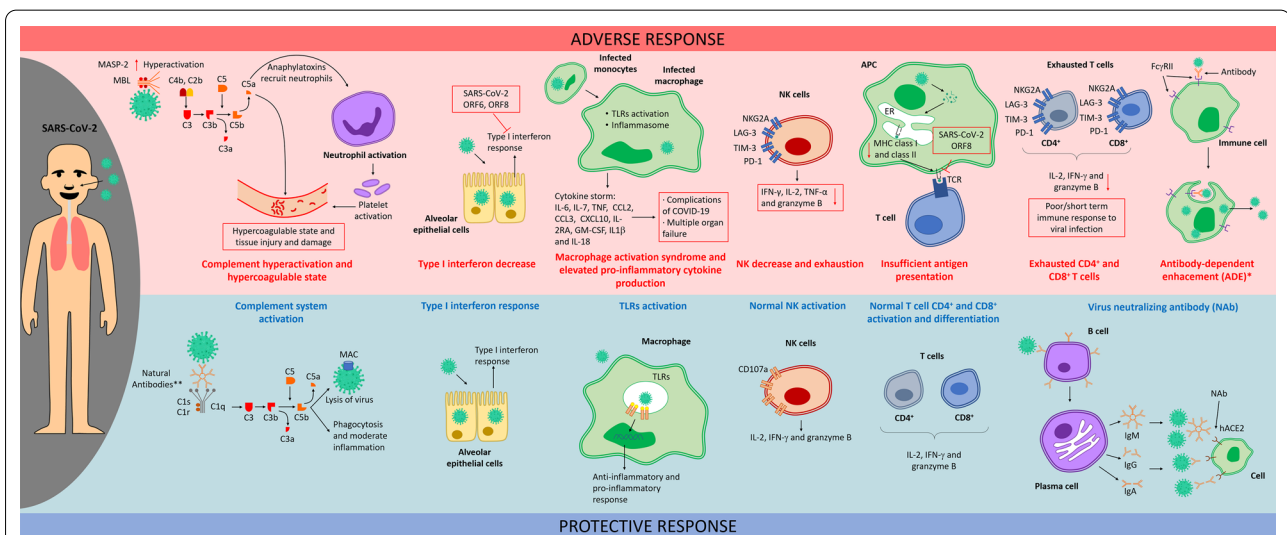


Fig. 1 Mechanisms in adverse and protective immune response for SARS-CoV-2. Upper panel (red). Adverse immune response in the presence of SARS-CoV-2 include mechanisms like complement hyperactivation and hypercoagulable state, excessive macrophage migration, macrophage activation syndrome, NK exhaustion, insufficient antigen presentation, exhausted CD4⁺ and CD8⁺ T cell and antibody-dependent enhancement (ADE) *This response has been described by in vitro models. Lower panel (blue). Protective immune response is characterized by complement system activation trough IgM natural antibodies (** this has been suggested as an initial barrier for SARS-CoV-2 infection), TLRs activation, NK and T cell normal activation and antibody virus neutralization by B cells. APC antigen presenting cell, ER endoplasmic reticulum, FcγRIII receptor II for the Fc region of immunoglobulin G, GM-CSF Granulocyte–macrophage colony-stimulating factor, MAC membrane attack complex, MBL mannan-binding lectin, MHC major histocompatibility complex, MSP mannose-associated serine proteases, Nab neutralizing antibody, TCR T-cell receptor, TLR Toll-like receptor

could cause the death in patients (Fig. 1, Additional file 1: Table S1), have been related with the systemic overproduction of cytokines [65, 67].

The role of macrophages can be deduced from the immune response noted in other CoV infections, such as that for SARS-CoV, which has an accessory protein open reading frame 8 (ORF8) that activates a family of PAMPs called nucleotide-binding domain and leucine-rich repeat pyrin domain 3 (NLRP3) [68]. NLRP3 can form multiprotein complexes, termed “inflammasomes” that activate caspase-1, which leads to the maturation of proinflammatory cytokines (IL-1 β and IL-18), and induction of pyroptosis [69]. Moreover, this protein is present in SARS-CoV-2, and although its participation in the immune response has not been described, it is likely that NLRP3 could be associated with the aberrant activation of macrophages and elevated levels of IL-1 β and IL-18 in some of the patients with COVID-19 [70] (Fig. 1 and Additional file 1: Table S1).

Forty-two percent of patients with pneumonia due to COVID-19 present severe ARDS [71]. This is reflected by the macrophage infiltration in the lung tissues observed *post mortem* [72]. Several studies have reported that macrophage hyperactivation results in pathological effects; this led us to hypothesize that a balance between anti-inflammatory and proinflammatory activities may be related to a protective immune response (Fig. 1 and Additional file 1: Table S1).

In severe cases, there is a decrease in natural killer (NK) cell populations [73]. Moreover, in patients infected with SARS-CoV-2, their NK cell population have shown lower percentages of intracellular CD107a, IFN- γ , IL-2, TNF- α , and granzyme B compared with that in healthy subjects, and an exhaustive phenotype characterized by the overexpression of NK group 2 member A (NKG2A) [74]. An inhibitory receptor related to the dysfunctional NK cell phenotype [75] has also been observed in chronic viral infections [74, 76] as well as in COVID-19 patients with other NK cell exhaustive phenotype molecules, such as lymphocyte-activation gene-3 (LAG-3), programmed cell death protein 1 (PD-1), mucin domain-3 (TIM-3), and T-cell immunoglobulin [77] (Fig. 1 and Additional file 1: Table S1).

Another element of the innate immune response participating in COVID-19 pathophysiology is the complement system, which can be activated by an antibody-independent mechanism, termed the “lectin pathway”. This mechanism uses, among other proteins, mannan-binding lectin-associated serine protease 2 (MASP-2), which can generate fragments of complement components, such as C5a that are potent mediators of inflammation and chemoattractants for neutrophils and monocytes. Since the SARS-CoV-2N protein can activate

MASP-2 [78], it may lead to the hyperactivation of the complement system that can cause significant damage, specifically damage related to neutrophil migration and activation in the lung tissues [79], and lead to hypercoagulation, as observed in critical patients [78]. Proteins of the complement system can also participate in coagulation [80] (Fig. 1 and Additional file 1: Table S1). Remarkably, MASPs have been shown to cleave prothrombin into thrombin [81]. The C5a receptor in neutrophils leads to the induction of the blood coagulation cascade [82], and C5b-9 stimulates procoagulant activity through platelet prothrombinase [83]. Some studies have suggested the potential SARS-CoV-2-specific antiviral effects of natural IgM Abs against A blood group produced by B1, in a complement-dependent manner, thereby proposing natural Abs as an initial barrier to infection and speculating a relationship between the reduced antibody diversity present in older patients [84] with severe illness [85] (Fig. 1 and Additional file 1: Table S1).

It has been suggested in different animal models infected with other viruses that an acute lung injury can be caused due to monocyte activation through mechanisms that could occur in SARS-CoV-2 infection. For example, viruses such as H5N1 avian influenza and SARS-CoV can activate macrophages by oxidative stress in a murine model [86, 87]; IgG anti-SARS-CoV S protein immune complexes can polarize the macrophage response into an inflammatory response in macaques [88].

Type I and III IFNs can control viral infection [89], but delayed interferon signaling in SARS-CoV-2 infection is related to robust virus replication and severe complications [90]. The decrease in IFN production is associated with ORF6, ORF8, and nucleocapsid proteins that inhibit the type I IFN signaling pathway [70] (Fig. 1 and Additional file 1: Table S1).

Effective adaptive immune response against SARS-CoV-2 infection

In COVID-19 the immune response associated with lymphocytes present heterogeneity as human diversity, but in many cases correlates with the severity of the disease. In adaptive cellular immune response patients with COVID-19 show a dramatic reduction in total T cells, which is negatively related to patient survival; these T cells express exhaustive signatures, such as PD-1, TIM-3, and LAG-3 [91, 92], all of which are immune-inhibitory factors [93, 94]. Evidence shows that CD8⁺T numbers are low in patients with severe COVID-19 compared with less severe cases [95, 96]. CD8⁺ T cells also express exhaustive-type cell phenotypes similar to NK cells (high expression of NKG2A and low expression of intracellular CD107a, IFN- γ , IL-2, TNF- α , and granzyme B+) [74,

97]. In addition, the T_{reg} and $CD4^{+}T$ memory lymphocyte counts are reduced [56, 73, 96]. In the same sense, older patients with some comorbidity had a higher number of activated virus-specific $CD4^{+}T$ cells compared to patients who had fewer risk factors. Moreover, these cells show an increase in IL-2 secretion and a diminishing in the IFN- γ production [98]. Furthermore, lymphopenia has been associated with an increase in mortality [99], this probably caused by the infection of SARS-CoV-2 to lymphocytes, which express hACE2 [100]. In addition, exhaustion of lymphocytes, has been observed in severe cases [101]. While in mild disease, an increased number of active $CD8^{+}T$ cells and greater clonal expansion has been observed [101], as well as more IFN- γ -producing T helper 1 (TH1) cells. Notably, in recovered patients a strong memory T cell response in peripheral blood has been detected, being wider and intense in patients with severe condition compared to mild cases [102]. As well as the COVID-19 recovered patients have virus-specific memory $CD4^{+}T$ and $CD8^{+}T$ cells [103], which could be an indicative of protective immunity (Fig. 1, Additional file 1: Table S1).

Other cell populations, such as plasmacytoid dendritic cells and $\gamma\delta$ T cells, have been reported to be almost depleted in SARS-CoV-2 infection [77]. Regarding antigen (Ag) presentation for T-cell activation, the ORF8 protein of SARS-CoV-2 can interact with the major histocompatibility complex class I (MHC-I) molecule, causing its downregulation and provoking the conjugate internalization to lysosome for its further degradation, avoiding the Ag presentation, being proposed as a via of immune evasion through ORF8 [104]. Furthermore, there is also evidence of downregulation of at least eight genes encoding MHC-II molecules in peripheral monocytes isolated from ventilation-dependent patients, relative to that in healthy subjects [77] (Fig. 1 and Additional file 1: Table S1). In contrast, the humoral arm of the adaptive response may facilitate, on rare occasions, the entry of viruses into host cells and enhancement of viral infection by a process independent of their specific cell receptors, known as “antibody-dependent enhancement (ADE)” [105, 106]. ADE comprises the production of sub-neutralizing or non-neutralizing Abs with a paradoxical effect associated with the virus-antibody interaction, with Fc receptors on different immune cells improving viral infection and replication [107, 108]. This event has been described to be related to other CoVs, such as MERS-CoV, SARS-CoV, and feline CoVs [88–112]. However, in the case of SARS-CoV-2, this association has not been demonstrated in patients [113]. Nevertheless, there is evidence from in vitro models that show ADE promoted by Abs isolated from severely affected patients’ plasma, relating to the Fc γ R2 engagement [114] (Fig. 1

and Additional file 1: Table S1). Hence, ADE should be monitored in vaccination or therapeutic strategies against SARS-CoV-2 infection.

The controversy about the exacerbation of the disease and the appropriate response to resolve COVID-19 is still under discussion. However, hospital patients coincide in an insufficient or excessive immune response, compared to those individuals without serious consequences. This remarks that the set of innate and adaptive responses and their balance is important for a favorable progression, being highlighted that the humoral immune response points out that specialized neutralizing antibodies are the most important molecules for the protection against infection.

Abs and their isotypes

Dating back to the 1790s, Abs have been described as a protective substance in the serum after vaccination [115, 116]. Abs are used by the immune system to identify and neutralize elements, such as bacteria and viruses [117]. Abs are composed of proteins (82–96%) and carbohydrates (4–18%), and are divided into five immunoglobulin isotypes (IgG, IgA, IgM, IgE, and IgD), which differ in structure, abundance/distribution, specificity, and half-life [118].

Serum IgA is present in the plasma, and its secreted form (sIgA) is present in the mucous membrane, tears, and saliva, which prevents the colonization of pathogens in the respiratory, gastrointestinal, and urogenital tracts [119]. The sIgA is capable of inducing the synthesis of IL-6, IL-8, monocyte chemoattractant protein-1 (MCP-1), and the granulocyte-macrophage colony-stimulating factor (GM-CSF) in the lung fibroblasts [120], which leads to hypothesizing its participation in severe cases of COVID-19 [121]. IgD is an antigen receptor localized at the surface of different B-cells, and its expression is balanced with IgM depending on the antigens sensed [122, 123]. The secreted IgD is produced by mucosal B cells such as plasmablasts or plasma cells and improves mucosal homeostasis and prepares basophils and mast cells to protect the system against antigens, producing cytokines [122]. IgE has antiparasitic activity and responds to allergens, releasing histamine from mast cells and basophils [124]. IgM is also an Ag receptor in B cells and is the first to be secreted during the primary humoral immune response, before IgG synthesis [117, 124]. IgG is the most prevalent isotype, specialized to recognize and neutralize Ags [125].

Humoral response

It is well recognized that the neutralizing humoral immune response is the main mechanism for preventing viral infections [126]. Particularly, antibody-mediated

responses against SARS-CoV-2, as well as their kinetics have been described in COVID-19 patients. The appearance of IgM, IgA, and IgG that recognize SARS-CoV-2 has been determined [127]. The seroconversion of patients with COVID-19 is attained following the onset of symptoms, producing IgM, IgA, and IgG [127, 128]. IgM accumulation is observed within 7 days post symptom onset (PSO), which is useful as a marker of acute infection. In contrast, IgA titer increases principally between 8 and 21 days PSO [127]. Importantly, the median time of IgG appearance has been recorded as 14 days PSO [127]. Hence, the detection of anti-SARS-CoV-2 Abs IgM and IgG is a diagnostic. However, the IgG and IgM levels are found to be widely variable, and no correlation between the Ab titers and clinical characteristics of the patients has been found [128].

The response of serum IgA against the S protein is detectable from 6 to 8 days PSO, with a mean period of 13 days PSO [121], followed by attainment of a peak on days 20–22 and maintenance for at least 40 days [129]. Furthermore, patients with COVID-19 establish the seroconversion of IgM and IgG that recognize mainly N and S (RBD) proteins, within 20 days PSO (median, 13 days PSO) [128]. A correlation has been observed between the increase in serum blood concentrations of IgA and IgG anti-S proteins and decrease in the viral counts, as well as the time between the onset of symptoms and admission to the intensive care unit. Moreover, a significant relationship between the serum titers of anti-S IgA and IgG and the survival of patients in a critical condition has been demonstrated [130]. In addition to neutralization, Abs can result in antiviral protection through other mechanisms, like antibody-dependent cell cytotoxicity (ADCC) resulting from FcγRIIIa cross-linking in NK cells, antibody-dependent phagocytosis (ADCP) mediated by mononuclear and granulocyte phagocytes that bind to antibody-coated viruses through different Fc receptors, and complement activation by the classical route with the participation of IgM and IgG [131]. However, sometimes these same mechanisms can enhance the pathogenic condition, as previously described [107, 108]. In the case of COVID-19, there are studies that demonstrate that the plasma of convalescent patients contains Abs capable of mediating ADCC, phagocytosis, and complement activation [132].

Insights from Ab therapeutic strategies against SARS-CoV-2 infection

Immunoglobulins

Immunoglobulins are heterodimeric proteins comprising two identical 55-kDa heavy (H) chains and two identical 25-kDa light (L) chains linked by inter-chain disulfide bonds between conserved cysteine residues (Fig. 2)

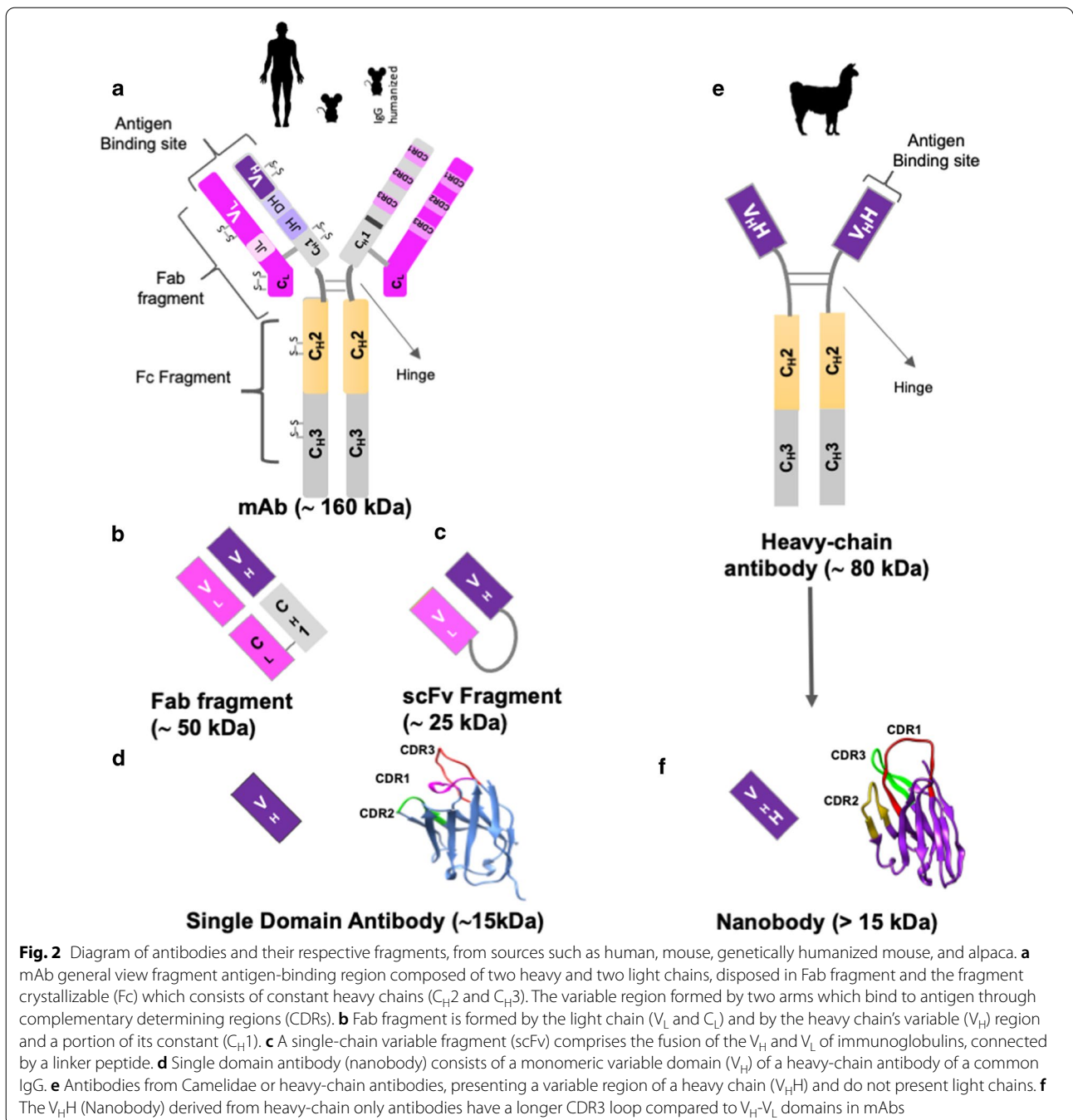
[133]. The evaluation of the immune response in patients infected with SARS-CoV-2 is of great importance to understand the production of Abs. One study showed that 13 of 14 patients presented IgG1 anti-S-RBD, and in two patients, the presence of IgG3 was observed, while IgG2 was not found [134]. Immunoglobulins from patients with non-severe and severe COVID-19 have affinity for the S protein or RBD that could block its interaction with hACE2, thereby preventing virus replication [16, 17, 32, 134–138]. An IgM response against the N protein, with a change in isotype to IgG after 15 days has been observed [13]. Although the titers of neutralizing Abs against SARS-CoV-2 in the human plasma decrease over time, these remain for at least three months until seroconversion [139].

A variety of anti-S or anti-RBD immunoglobulins generated from low somatic mutations are consistent with acute infection [13, 16, 17, 135, 140–144] due to low maturation of the affinity of Abs produced by B lymphocytes [17]. The neutralizing Abs have different epitopes, but many of them share the heavy-chain coding genes originating from similar germ lines of V-segments belonging to the VH3 family (VH3-23, VH3-30, VH3-53, or VH3-66), as well as VH169, VH2-70, and VH5-51 [16, 32, 135, 136, 138, 140, 142, 144, 145]. The light chains are preferably encoded by KV1-5, KV1-17, KV1-33, KV1-39, KV3-15, KV3-20, KV2-28, LV2-14, LV3-21, LV1-40, LV2-23, and LV6-57, among others [140, 142, 146]. Of note, these light chains predominantly pair with the long CDR H3 segment in the RBD region (15 amino acids or longer) [28, 135, 136, 138, 142, 145]. Whereas the other light chains pair with the short CDR H3 segment, which is 7–11 amino acids long [16, 32, 135, 136, 142, 145, 146].

Convalescent plasma therapy: one of the ways to fight COVID-19

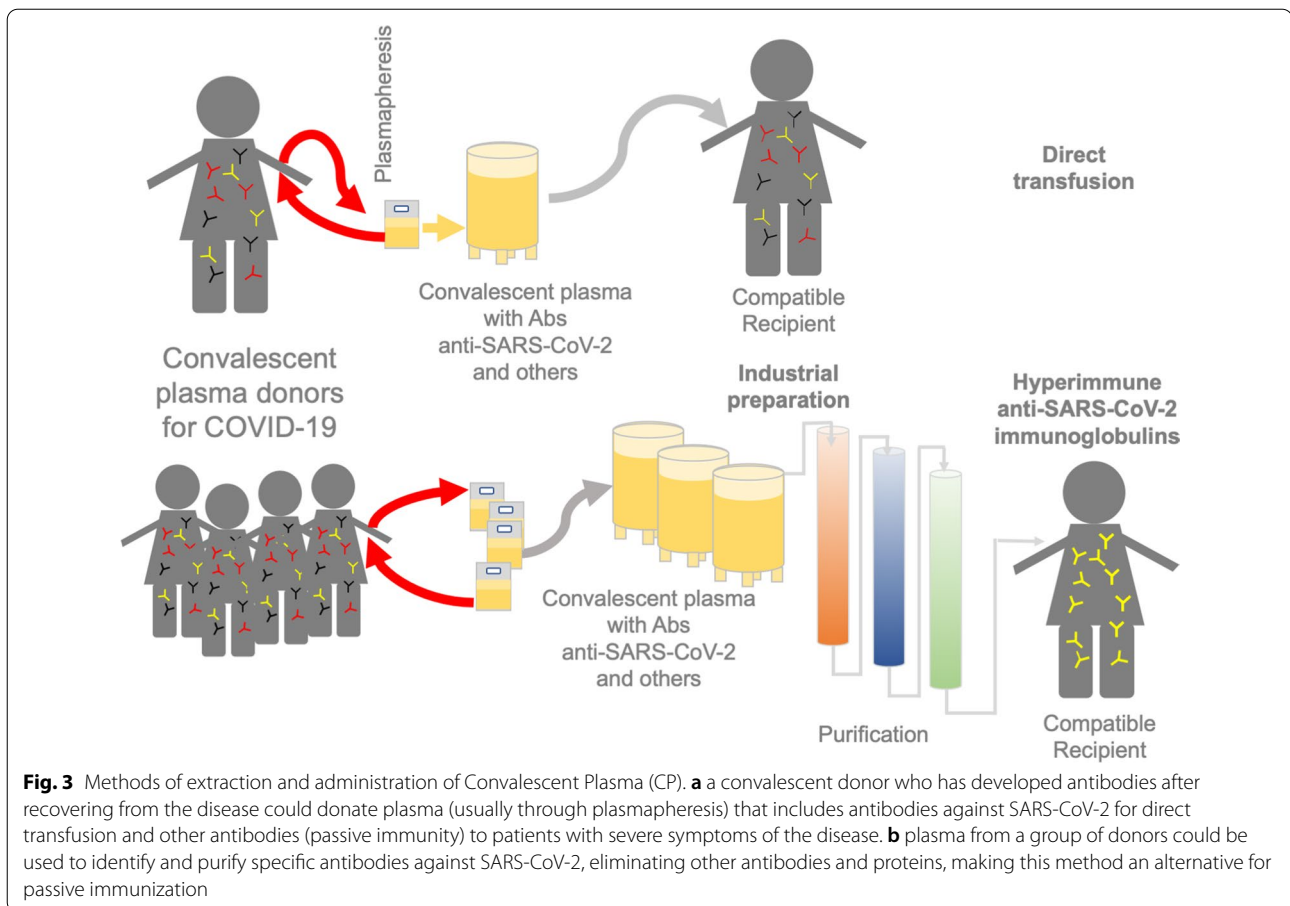
The implementation of the use of convalescent plasma (CP) has been a strategy to confer immunity or to treat individuals who acquire COVID-19. CP is collected from patients with neutralizing Abs after recovery and used to generate passive immunization [147–162].

The treatment involves collection of plasma from recovering patients, i.e., those who have faced an infectious disease and been cured successfully (known as convalescent patient), with the intention for it to be administered to recipient patients who have not yet developed an effective adaptive immune response (Fig. 3a) [163, 164]. The main objective of this alternative treatment is to reduce the viral load (viremia) in the recipient by the action of neutralizing Abs produced by the donor, which can occur between 10- and 14-days post infection [165, 166]. A crucial factor for the success of CP therapy is the selection of donors, since one of the main



problems that have been identified is the diversity of virus variants found in the population, and the neutralizing Ab titer in different plasma samples [167]. Thus, it is necessary to ensure that the plasma contains an appropriate concentration of neutralizing Abs, determine the antibody titer, and use a neutralization test in vitro with the virus variants. However, the potential side effects of CP therapy must be considered, particularly the serum

incompatibility in recipients [153, 154, 168–170]. The CP therapy used to treat SARS-CoV and MERS-CoV patients in the critical stage of infection has been shown to reduce the viral load and death rate [165, 171]. Based on the findings in the treatment of these diseases caused by other CoVs, CP from SARS-CoV-2-infected patients is administered as an experimental therapy in critically ill patients (Fig. 3a) (Additional file 1: Table S2). In addition, the use



of polyclonal immunoglobulins and plasma derivatives isolated and purified from the blood of COVID-19 survivors has been discussed [172, 173] (Fig. 3b). CP administration in patients leads to an increment in IgG, IgM, and neutralizing Ab titers [147, 149, 150, 152], a decrease in short-term mortality in patients with severe respiratory failure [155] and hospital mortality, and the shortening of duration of admission in hospital for severely ill patients [156]. It is also suggested that CP treatment can be more efficient when it is administered to patients with no critical or life-threatening conditions [148, 160, 162]. CP therapy is accompanied by the supplementation of different medications, including antivirals, antibiotics, antifungals, corticosteroids, and anticoagulants [147–159], according to the patients needs, resulting in variations relative to the healthy subjects. Due to the simultaneous use of CP and other medications, it is inappropriate to determine the beneficial or adverse effects of CP therapy conclusively.

In a study administering CP to a group of 22 critically ill patients, the hospital mortality rate reduced by 55% compared with that observed in other studies (Additional file 1: Table S2), and the hospitalization length was

reduced [156]. This is probably due to the high SARS-CoV-2 Abs titer of plasma administered more than once [156]. However, this study represents a compassionate bias when applying therapy to critically ill patients with little possibilities of success [162], unlike the treatment outcomes reported in other studies [148, 150, 160, 162], which showed no positive effects in such patients. Nonetheless, a precise design of controlled studies, randomized trials, and a high number of subjects are paving the way to further assess the benefits of CP therapy [152, 153, 156–158, 161]. It is important to mention that CP treatments depend on plasma collecting time. The neutralizing Abs from CP of COVID-19 patients are enriched between 31 and 35 days after the first symptoms presenting a higher neutralization titer [174], but decreases in titers over time (42 days after first symptoms) [175]. Hence, FDA recommends a minimum titer of neutralizing Abs of 1:160.

Importantly, the presence of different Abs with the ability to neutralize specific epitopes of the virus, as well as their biotechnological production and application as a life-saving therapeutic agent, still requires investigation.

Neutralizing Abs against SARS-CoV-2

Due to their high Ag specificity and potency, Abs have been used for the treatment of different illnesses. Hence, identification and production of the best candidate Abs against the key epitopes of SARS-CoV-2 will be vital [12, 176]. Therefore, different strategies have been used to capture and obtain neutralizing Abs from patients with COVID-19 [16, 46, 177–180], such as combinatorial display libraries, humanized mice, single B cell cloning, memory B cell immortalization, and B cell culture, until the production of recombinant antibody fragments [46, 181–183] in different formats (Fig. 2). In this sense, Abs have shown a neutralizing effect in vitro and in vivo [18] (Table 1, Additional file 1: Table S3), although their safety and efficacy in vivo, as well as their contributions in ADCC, antibody-dependent genotoxicity, and even antibody-dependent risks are under evaluation, and there is scarce information on attempts of production on an industrial scale.

Targets and classification of Abs against SARS-CoV-2

A variety of Abs targeting different epitopes of SARS-CoV-2 have been described, principally those against the β -coronavirus envelope (Table 1, Additional file 1: Table S3), conformed more externally by S protein [19, 177]. The S protein is a highly glycosylated homotrimeric protein of ~180–200 kDa (Fig. 4). As an inactive precursor, each S protomer (1273 residues) comprises two functional regions that become active after cleavage by the human protease TMPRSS2 [9–11]. The S1 subunit (14–685 residues) triggers the invasion process by mediating virus binding to the N-terminal domain (NTD) of hACE2, while the S2 subunit (686–1273 residues) drives the fusion of the viral and cellular membranes (Fig. 4), similar to that noted for other CoVs [9–11, 184].

The S1 subunit is composed of two domains, the NTD (14–305 residues) bearing a galectin-like motif and an RBD (319–541 residues) having a core comprising five-stranded antiparallel β -sheets (β 1–4 and β 7) connected to helices (α 1– α 3) and loops. The receptor-binding motif (RBM) within the RBD interacts with hACE2 at the 446–505 residue segment (Fig. 4) [12, 185–187]. The three RBDs undergo a hinge-like conformational equilibrium change from a “down” or closed pre-fusion state to an “up” or open fusion-prone state [14, 36, 188–190]. In the pre-fusion conformation, each RBD contacts extensively with the other RBDs and its own intracatenary NTD partially burying the RBM. Therefore, hACE2 binding is only possible in the active S protein conformation, with RBDs in the “up” state [184, 188, 191–193].

The neutralizing anti-SARS-CoV-2 Abs isolated from CP often recognize the RBD, particularly the RBM, and

thus, interfere with the virus-hACE2 interaction and prevent viral particle entry into the target cell [12, 17, 32, 135, 194]. Approximately 78% and 70% of COVID-19 CPs have been found to present anti-RBD and anti-S IgG, with those in hospitalized individuals having high neutralizing activities [142]. This interaction bias is due to the RBM being an immunodominant region [178] and the RBD/spike protein-based strategies used to isolate many of these Abs. To date, several dozen structures of different Abs bound to the isolated RBD or S protein have been resolved experimentally (Table 1). According to their mode of binding to the viral protein, they have been grouped into four classes [194] (Fig. 5, Table 1). Class 1 comprises the largest group of Abs. These are characterized by a short CDRH3 loop and a binding pose that resembles the angle of interaction with hACE2, largely overlapping the RBM (Fig. 5a). Thus, these Abs can only bind to the “up”-state RBDs. Class 2 comprises Abs that partially overlap with the hACE2 footprint and can recognize both “up”- and “down”-state RBDs (Fig. 5a, b). As with Class 1, the binding poses of Class 2 Abs show that the neutralization effect is due to direct competition with hACE2, consistent with the competitive binding assay findings. The ability of Class 2 Abs to bind RBDs in both the conformations results from their different angles of interaction with hACE2, avoiding any steric hindrance with the other RBDs even in the “down” conformation. Class 2 includes Abs with a long CDRH3 loop. Interestingly, some Class 2 Abs simultaneously bind two RBDs. Different interaction patterns have been observed for these “quaternary Abs.” For example, the long CDRH3 loop of the mAb C144 interacts with two “down”-state RBDs. In this way, three C144 Abs lock the S protein in the pre-fusion conformation [194]. Additionally, of the three C002 Abs that bind to the S protein, one links the other two “down”-state RBDs, the second binds one “down”-state and one “up”-state RBD, while the third binds only the “up”-state RBD (Fig. 5b) [194].

Classes 3 and 4 include Abs that bind outside the RBM. Some of these Abs compete directly with hACE2 because of the relative proximity of their epitope to the RBM. In the case of the mAb EY6A, steric hindrance occurs because of collision with hACE2 glycans [13]. Other mAbs do not interfere with the binding of hACE2 to the same RBD to which it is bound, but rather with that to a neighboring RBD. Class 3 Abs recognize a solvent-exposed protein/glycan epitope in both “up”- and “down”-state RBDs (Fig. 5c). This epitope is highly conserved in *Sarbecovirus* clades 1, 2, and 3 [27, 195], making it more difficult for the viruses to develop escape mutations. Class 4 Abs bind cryptic epitopes that become accessible only in “up”-state RBDs (Fig. 5c). One of these epitopes is buried by the contact between “down”-state

Table 1 Anti-SARS-CoV-2 antibodies whose structure and interaction with their respective epitopes have been described and based on them classified into the groups defined by Barnes et al. [194]

General view	Class [194]	Binding mode	Binding description	Sub-groups	mAb	K_D (nM)	$I_{C_{50}}$ (PSV-CoV-2) ng/mL	$I_{C_{50}}$ (AV-CoV-2) ng/mL	Status	PDB code	References
Overlap with hACE2-binding site	Class 1	hACE2-like binding mode	The binding to RBD in up conformation that mimics the interaction with hACE2	298 (multibody)		NR	28,000 (IgG) 0.11 (MB)	2200 (IgG) 5.7 (MB)	NR	7k9z	[196]
				910–30		0.162	66	180	NR	7ks9	[292]
				15,033		0.3 (IgG)	NR	489	NR	7klg	[293]
				15,033–7		0.039 (IgG)	NR	83	NR	7klh	[293]
				B38		70.1	NR	177	with H4 Protect hACE2 transgenic mice	7bz5	[146]
				BD-236		2.8	37	NR	NR	7chb	[140]
				BD-604		0.15	5	NR	NR	7ch4	[140]
				BD-629		0.14	4	NR	NR	7ch5	[140]
				C102		27	34	NR	NR	7k8m	[142, 194]
				C105		14	26.1	NR	NR	6xcn	[142, 194]
				C1A-B3		76.3 (RBD)	53	441,000	NR	7kfw	[180]
				C1A-B12		4.2 (RBD)	81.0	62	NR	7kfv	[180]
				C1A-C2		14.1 (RBD)	118	184,000	NR	7kfx	[180]
				C1A-F10		55.7 (RBD)	8	184,000	NR	7kfy	[180]
				CB6		2.49	41.0 (ND ₅₀)	36.0 (ND ₅₀)	CB6-LALA protects rhesus macaques	7c01	[204]
				CC12.1		5.92	19	22	Protect a hamster model	6xc2	[16]
				CC12.3		8.59	18	26	NR	6xc4	[16]
			COVA2-04		2.3	220	2.5	NR	7jmo	[136]	
			CV07-250		0.056	NR	3.5	NR	6xkq	[17]	
			CV30		3.63	NR	30	NR	6xe1	[144, 294]	
			REGNI 0933 ^a		0.041	0.042	0.037	Clinical trials	6xdg	[145, 201]	
			S2E12		1.6 (RBD) 2.5 (S)	NR	5.29	NR	7k4n	[223]	
			S2H14		75 (RBD) 90.1 (S)	900	NR	NR	7jx3	[178]	

Table 1 (continued)

General view	Class [194]	Binding mode	Binding description	Sub-groups	mAb	K _D (nM)	I _{C50} (PSV-CoV-2) ng/mL	I _{C50} (AV-CoV-2) ng/mL	Status	PDB code	References
Class 2	Overlap with hACE2-binding site	RBD binding mode in "up/down" conformation, that partially overlaps with hACE2 site, with angle of attack and positioning different from Class 1	Tertiary epitope	BD-368-2	0.82	1.2	15	Protect hACE2 transgenic mice	7chh	[32]	
				C110	1.3	18.4	NR	NR	NR	7k8v	[142, 194]
				COVA2-39	1.1 (RBD) 0.1(S)	36	54	NR	NR	7jmp	[136]
				CV07-270	NR	NR	82.3	NR	NR	6xkp	[17]
				DH1047	NR	90	124	NR	NR	7ld1	[294]
				H11-D4 ^b	39.0	NR	18 nM	NR	NR	6yz5	[30]
				H11-H4 ^b	12.0	NR	6 nM	NR	NR	6zhd	[13]
				LY-COV555	1.45 (FAB)	12,103	20–49	Clinical trials	Clinical trials	7kmg	[200]
				MR17 ^c	83.7 (RBD)	12,320	NR	NR	NR	7c8w	[249]
				P2B-2F6	5.14	50	410	Preclinical	Preclinical	7bwj	[135]
				REGN10987 ^a	0.042	40	42	Clinical trials	Clinical trials	6xdg	[145, 201]
				S2H13	149(RBD) 119 (S)	500	NR	NR	NR	7jv6	[178]
				SB23 ³	4.9 (Sb23 vs S) 0.225 (Sb23-Fc vs RBD)	NR	600.0 (Sb23) 7 (Sb23-Fc)	NR	NR	7a29,7a25	[250]
				SR4 ^d	14.5 (RBD)	5900	NR	NR	NR	7c8v	[249]
				2–4 Fab	NR	394	3	NR	NR	6xey	[205]
				2–15	0.114	5	1	NR	NR	7l5b	[206]
				BD23	NR	4800	NR	NR	NR	7byr	[32, 189]
				C002	11.0	8.9	NR	NR	NR	7k8t	[142]
				C104	19.0	23.3	NR	Promising candidate	Promising candidate	7k8u	[142, 194]
				C119	10.0	9.12	NR	NR	NR	7k8w	[142, 194]
				C121	0.5	6.73	1.64	Promising candidate	Promising candidate	7k8x	[142, 194]
				C144	18.0	6.91	2.55	Promising candidate	Promising candidate	7k90	[142, 194]
				mNB6 ^d	0.56 (RBD) 0.45 (S)	6.3	12	NR	NR	7kkl	[252]

Table 1 (continued)

General view	Class [194]	Binding mode	Binding description	Sub-groups	mAb	K_D (nM)	IC_{50} (PSV-CoV-2) ng/mL	IC_{50} (AV-CoV-2) ng/mL	Status	PDB code	References
No overlap with any residue of hACE2	Class 3	No cryptic epitopes	The epitope is exposed in RBD in up or down conformation	S2M11		66.0 (RBD) 68 (S)	NR	1.66	NR	7k43	[223]
				2-51		3.6	5	0.7	NR	7l2c	[207]
Class 4	Cryptic epitopes	Epitope exposed only in RBD up configuration	C135		6.0 (RBD)	6.91	2.98	Promising candidate	7k8z	[142]	
			DH11050.1		16 (Fab)	39	161		7lcn	[295]	
			S309		0.3 (RBD) ~0.2 (S)	NR	79.0	Fc variant fast-tracked for clinical trials	6wpt	[4, 27]	
			52 ^a (multibody)		NR	17 (IgG) 0.2 (MB)	6200 270.0 (MB)	NR	7k9z	[196]	
			CR3022		6.3 (RBD)	NR	93 nM	Preclinical	6yor	[28-30]	
			EY6A		2	NR	390	Promising candidate	6zdh	[13]	
				H014f		0.09	3 nM	38 nM	Preclinical	7cak	[4]
				S304		4.58 (RBD)	NR	> 5000	NR	7jw0	[27]
				S2A4		7.5 (RBD) 10 (S)	3500	NR	NR	7jvc	[178]

AV authentic virus, IC_{50} half-maximal inhibitory concentration, K_D dissociation constant, MB multibody, ND_{50} 50% neutralization dose, NR not reported, PSV pseudovirus

^a Human/IV mice

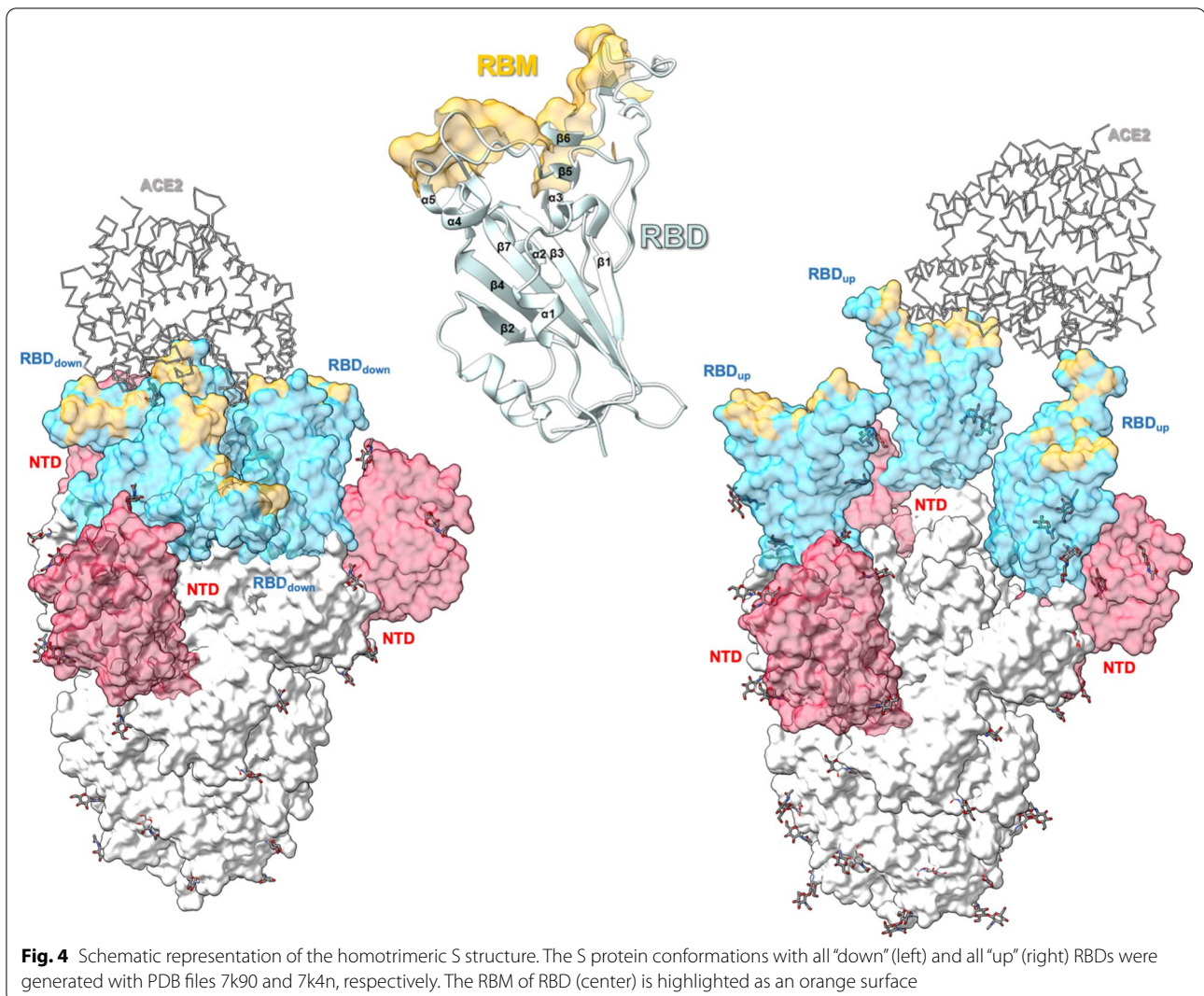
^b Llama source

^c Sybody

^d Nanobody

^e New fusion antibody protein

^f Obtained by phage display

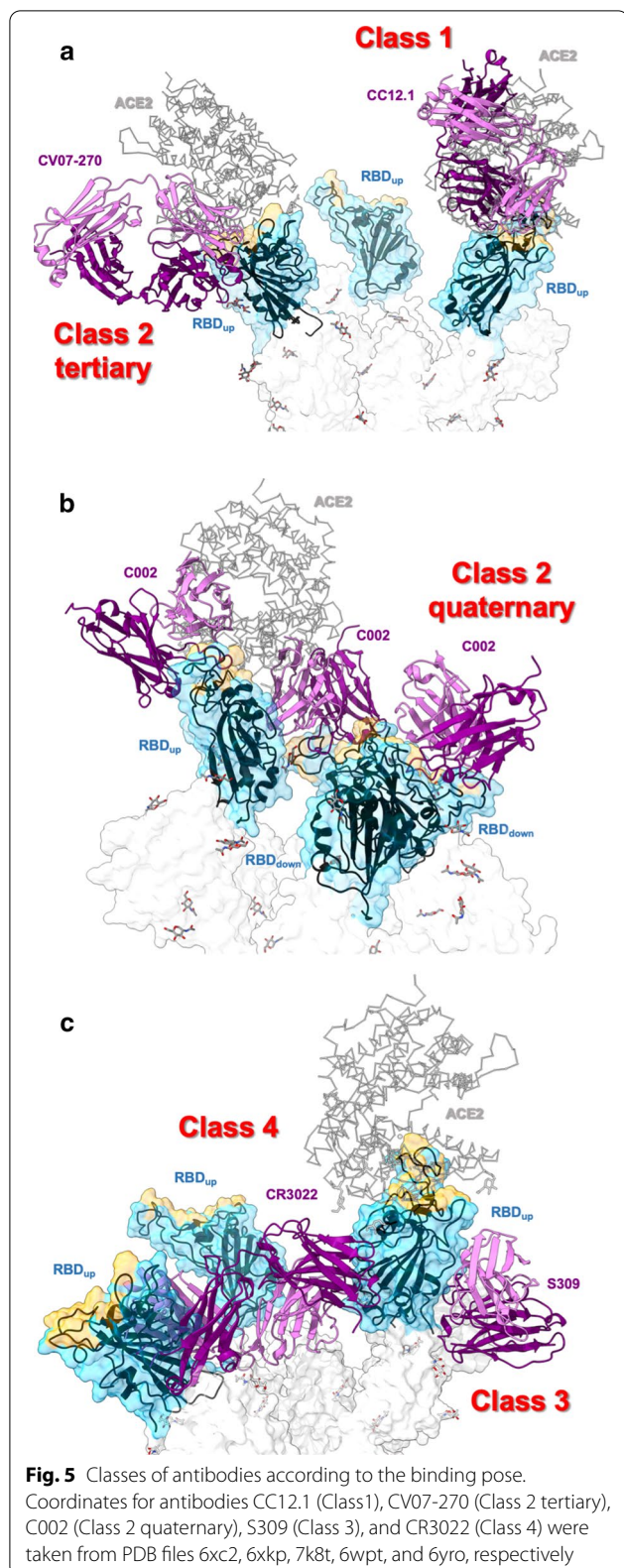


RBDs. Therefore, Abs that recognize this epitope tend to affect the conformation and/or binding capacity of adjacent RBDs. An extreme case is represented by the mAb CR3022, which promotes destruction of the pre-fusion S protein trimer by perturbing the folding of both NTDs and RBDs [30, 33, 36]. mAb 52 recognizes a different cryptic epitope that is buried by the NTD in the pre-fusion conformation [196]. Although most Abs recognize epitopes consisting of only peptide moieties, some of them bind to protein/glycan moieties, sometimes with very high neutralizing potency [197, 198].

Abs with cross-neutralizing activity against SARS-CoV-2

The battery of neutralizing Abs described so far has been the result of intensified research using samples from various sources (Additional file 1: Table S3, S4). Since the RBDs of SARS-CoV and SARS-CoV-2 are ~75% identical

in their primary sequence, only a relatively small number of Abs have shown cross-reactivity with these two Ags [12, 23]. The first set of anti-SARS-CoV-2 Abs was obtained from the blood of patients with anti-SARS-CoV Abs [13, 27]. In the initial studies, cross-neutralization was scarcely noted [15, 27, 29, 197, 198]. However, some anti-SARS-CoV Abs have shown cross-neutralizing activity against SARS-CoV-2 [12, 27]. For instance, the neutralizing Ab S309 obtained from B cells from a patient infected with SARS-CoV [27] and CR3022 IgG and Fab isolated from SARS-CoV CP present cross-reactivity with the SARS-CoV-2 RBD [28, 29, 36] (Additional file 1: Table S3). Another study has reported a 47D11 SARS-CoV-neutralizing Ab that also neutralized SARS-CoV-2 [12, 33]. Data suggest a cross-neutralizing epitope shared between both the CoVs, which is directly related to some of the epitopes conserved in the RBD [194]. Despite this,



the Fab 2G12 developed as anti-HIV-1 presents cross reactivity towards the S2 domain via glycan recognition, being of interest for the design of new therapies [199].

Useful Abs with therapeutic or prophylactic efficacy

At least 80 mAbs have been shown to block the interaction of the RBD with the hACE2 receptor in vitro, with a neutralizing effect against a pseudovirus or the authentic SARS-CoV-2 (Additional file 1: Table S3), and around 30 mAbs are under clinical trials (Additional file 1: Table S4) [52, 53]. Among these, bamlanivimab (LY-CoV555) developed by Eli Lilly and Company (Indianapolis, IN, USA) has been granted emergency use authorization by the FDA [52, 200]. Similarly, two potent Abs, REGN10933/casirivimab and REGN10987/imdevimab (Regeneron, Tarrytown, NY, USA), developed and recovered from VelocImmune[®] (Regeneron), a genetically modified mouse with a human immune system, form part of the REGN-COV2 treatment, which is authorized by the FDA for emergency use [48, 52, 53, 145]. Each Ab recognizes the RBD at distinct sites, increasing the protection against and avoiding the escape of the virus by most of mutations [145, 201]. The REGN-COV2 cocktail or LY-CoV555 have demonstrated that decrease viral load and reduce the risk of progression to severe COVID-19 and hospitalization, each one with a particular dose [52, 202]. Although a recent study of LY-CoV555 did not demonstrate efficacy coupled with supportive care (remdesivir and, when indicated, supplemental oxygen and glucocorticoids) in hospitalized patients without end-organ failure, using a high dose (7000 mg per patient) [203].

Furthermore, several mAbs have demonstrated effectiveness in preclinical studies, and are currently under clinical trials of different phases (Additional file 1: Table S4). Some of these include sotrovimab, AZD7442, regdanvimab, DXP-593, DXP-604, etesevimab, STI-1499/COVI-SHIELD, CT-P59, TY027, SCTA01, MW33, HFB30132A, BRII-196, BRII-198, ABBV-47D11, ABBV-2B04, COVI-GUARD (STI-1499), COVI-AMG (STI-2020), ADM03820, DZIF-10c, AD-20, JMB2002, LY-CovMab, C-144-LS, C-135-LS, COR-101, JS016, and HLX70 (Additional file 1: Table S4). The human Ab VIR-7831 (or GSK4182136), developed by Vir Biotechnology Inc. (San Francisco, CA, USA) and GlaxoSmithKline (Brentford, UK), presents an epitope similar to that of S309 (Table 1, Fig. 5) and is presently under phase 3 evaluation [52, 53]. CT-P59 (Celtrium) and ADG20 (Adagio Therapeutics) is under phase 2/3 clinical trial. The Abs AZD8895 and AZD1061, developed by Vanderbilt

University and licensed by AstraZeneca (Cambridge, UK), TY027 (Tychan Pte., Ltd., Singapore), are in phase 3 clinical trial. In addition to etesevimab (LY-CoV016 or JS016) developed by Eli Lilly and Company, another related Ab CB6LALA is under phase 3 clinical trial [204]. Bamlanivimab (700 mg/dose) in combination with etesevimab (1400 mg/dose) won FDA authorization for emergency use. Other Abs, such as DXP-593 related to BD-368-2 and SCTA01, are close to completing phase 2 or phase 2/3 clinical trials. Whereas Abs such as STI-1499/COVI-SHIELD (Sorrento Therapeutics Inc., San Diego, CA, USA), BR11-96 (Brii Biosciences, Durham, NC, USA), BR11-98 (Brii Biosciences), ABBV-47D11 (AbbVie, North Chicago, IL, USA), COVI-GUARD (STI-1499; Sorrento Therapeutics Inc.), COVI-AMG (STI-2020; Sorrento Therapeutics Inc.), MW33 (Mabwell Bioscience Co., Ltd., Shanghai), HFB30132A (HiFiBiO Therapeutics, Cambridge, MA, USA), and HLX70 (Hengenix Biotech Inc., Fremont, CA, USA) are under phase 1 clinical trials (Additional file 1: Table S4). Among the Abs in clinical trials, the characterization of Abs such as CB6-LALA and BD-368-2 [32, 204] has been fundamental. CB6-LALA is a neutralizing mAb isolated from B cells from the CP of patients with COVID-19, and it blocks the binding between the SARS-CoV-2 RBD and hACE2 through steric hindrance and competition for the interface amino acid interaction, without inducing conformational changes in the RBD. It has been proposed as a potential therapeutic agent against SARS-CoV-2 in rhesus macaques because it reduces the viral titer and infection [204]. This Ab has been modified via leucine-to-alanine mutations at residues 234 and 235 (LALA mutation) in the Fc region to diminish the possibility of Fc-mediated acute lung injury [204]. In addition, BD-368-2 effectively neutralizes the pseudovirus of SARS-CoV-2 and authentic SARS-CoV-2 (IC_{50} of 1.2 ng/mL and 15 ng/mL, respectively) [32] (Table 2). BD-368-2 binds the RBD in the “down” conformation, localizing between the NTD and RBD and adjacent to an RBD in the “up” conformation. Moreover, BD-368-2 can bind RBDs in the “up” and “down” conformations, to reach complete occupancy of the S protein trimer [140] (Table 1, Table 2). BD-368-2 can interact with the RBD in combination with CR3022 and S309 [27, 29]. Furthermore, BD-368-2 shows prophylactic and therapeutic efficacy (Additional file 1: Table S3) in hACE2 transgenic mice [32].

Potent neutralizers mAbs against SARS-CoV-2

At least 21 Abs published present a potent neutralizing effect against the pseudovirus or authentic SARS-CoV-2 infection, with an IC_{50} lower than 0.01 μ g/mL (Table 2). Among these, CV07-250, BD-604, BD-629, COVA1-18,

CC6.29, COV2-2196 are Class 1 Abs (Table 2). Class 2 Abs such as BD-368-2, COV2-2130, COVA2-04, C119, C121, C144, COVA2-15, 2-15 and C002 are the most potent (Table 2). The Class 3 Ab C135 and 2-51, and Class 4 Ab H014 present an elevated neutralizing effect (Table 2). The mAb 5-24 that binds the NTD, and Abs CV07-209, 2-15, 1-57, and 2-7 that interact with the RBD, also present potent neutralizing activities (Table 2). The diversity in amongst the potent neutralizing Abs is crucial, considering their probable combinational use to achieve rational therapeutic effectiveness, as well as their usefulness in reducing or preventing evasion by the present or future virus variants.

The Abs CV07-250 and CV07-209 have been isolated from the B cells of patients with COVID-19, with CV07-209 being the most potent mAb that neutralizes authentic SARS-CoV-2 (IC_{50} : 3.1 ng/mL) and CV07-250 presenting close enough activity (IC_{50} : 3.5 ng/mL). The crystal structure of CV07-250 in complex with the SARS-CoV-2 RBD has been resolved at 2.55 Å. Prophylactic and therapeutic evaluations have shown CV07-209 to protect hamsters from SARS-CoV-2 infection [17]. CV07-250 (Class 1 Ab) binds the RBD, at a site overlapping with the hACE2-binding site, via an unusual light chain-dominated interaction. On the contrary, BD-604 and BD-629 (Class 1 Abs) also show a potent neutralizing effect against the SARS-CoV-2 pseudovirus with an IC_{50} of 5 ng/mL and 4 ng/mL, respectively. Both Abs interact with the RBD, with the binding of BD-629 dominated by the heavy chain in comparison with that of BD-604 [140]. The crystal structures of BD-604 and BD-629 resolved at 3.2 Å and 2.7 Å, respectively, show that they bind the RBD in a manner similar to that of other Class 1 Abs [140], such as C105 [142, 194] and CB6 [204] (Table 2).

A family of Abs obtained from the B cells of patients with COVID-19, including 2-15, 1-57, 2-7, and 5-24, have been found to have potent neutralizing activities against authentic SARS-CoV-2 in vitro with an IC_{50} of 0.7 ng/mL, 8 ng/mL, 3 ng/mL, and 8 ng/mL, respectively [205, 206]. The 1-57, and 2-7 Abs belong to Class 1. The 5-24 and 2-51 Ab binds the NTD and exerts a powerful neutralizing effect [205, 207]. The 2-15 Ab (Class 2) has been evaluated in vivo in protection experiments using golden Syrian hamster as a model of SARS-CoV-2 infection. Virus challenge showed a reduction in infectious viral particle titers with 1.5 mg/kg of 2-15 [205].

The Abs COVA1-18, COVA2-04, and COVA2-15 are also obtained from B cells of patients with COVID-19, and these present strong competition for hACE2 with an IC_{50} against authentic SARS-CoV-2 of 7.0, 2.0, and 9.0 ng/mL, respectively [136]. COVA1-18 appears to be a Class 1 Ab, and the cryogenic electron microscopy (cryo-EM) reconstructions reveal that COVA2-15 is

Table 2 Antibodies with a potent neutralizing effect against pseudovirus or authentic virus SARS-CoV-2 infection

Name/class	Source	K_D (nM)	IC_{50} μ g/mL	Target	Observations	References
CV07-250/C1	B cells from C-CoV-2	0.056	0.0035 (AV-CoV-2)	RBD	Reduced hACE2 binding and showed no binding to murine tissue	[17]
BD-604/C1	B cells from C-CoV-2	0.15	0.005 (PSV-CoV-2)	RBD up	BD-604 binds to RBD ~ 19-fold higher than BD-236 and is more potent against the SARS-CoV-2 pseudovirus, compared to BD-236	[140]
BD-629/C1	B cells from C-CoV-2	0.006	0.004 (PSV-CoV-2)	RBD up	Genes coding for BD-629 are different compared to BD-604. However, its affinity and neutralization against the SARS-CoV-2 pseudovirus are similar	[140]
CV07-209/C1	B cells from C-CoV-2	0.056	0.003 (AV-CoV-2)	RBD	Prophylactic and therapeutic efficacy in golden Syrian hamsters. Therapeutic mAb reduced signs of COVID-19, although 1/3 animals presented mild bronchopulmonary, pneumonia and endothelialitis	[17]
COVA1-18/C1	B cells from C-CoV-2	0.03 (S) 0.9 (RBD)	0.008 (PSV-CoV-2) 0.007 (AV-CoV-2)	RBD	A strong competition with hACE2 was observed, suggesting blocking hACE2 is its mechanism of neutralization	[136]
CC6.29/C1	B cells from C-CoV-2	1.2	0.002 (PSV-CoV-2) 0.0071 (AV-CoV-2)	RBD-A	mAb exhibited a potent neutralization	[16]
COV2-2196/C1	B cells from C-CoV-2	–	0.0007 (PSV-CoV-2) 0.015 (AV-CoV-2)	S2P _{ecto} open	A strong competition with hACE2. Prophylactic efficacy in rhesus macaques (50 mg/Kg) and mice (200 μ g per mouse) reducing lung disease. Therapeutic efficacy in mice (20 mg kg ⁻¹)	[208]
BD-368–2/C2	B cells from C-CoV-2	0.82	0.0012 (PSV-CoV-2) 0.015 (AV-CoV-2)	RBD "up/down"	Changes the S trimer conformation contributing to its neutralizing activity. Prophylactic efficacy: IP 20 mg/kg mAb 24 h before infection. Therapeutic efficacy: IP 20 mg/kg of mAb 2 h after infection into hACE2 transgenic mice	[32]
COV2-2130/C2	B cells from C-CoV-2	–	0.0016 (PSV-CoV-2) 0.107 (AV-CoV-2)	S2P _{ecto} closed	Blocked the binding of SARS-CoV-2 to hACE2. Prophylactic efficacy in rhesus macaques (50 mg/Kg) and mice (200 μ g per mouse) developing less lung disease. Therapeutic (20 mg kg ⁻¹) efficacy in mice	[208]
C12-04/C2	B cells from C-CoV-2	2.3 (S) 11.2 (RBD)	0.220 (PSV-CoV-2) 0.002 (AV-CoV-2)	RBD "up"/"down"	Potent neutralizing mAb, suggest the blocks the engagement of hACE2 as a main mechanism of neutralization	[136]
C119/C2	PMBC's from C-CoV-2	10.0 (RBD)	0.009 (PSV-CoV-2)	RBD "up"/"down"	It was proposed a quaternary interaction with RBD in down conformation adjacent to an "up" RBD, as well could interact between two adjacent down RBD domains. Showed a binding pose similar to REGN10987's	[142, 194]
C121/C2	PMBC's from C-CoV-2	0.5 (RBD)	0.0067 (PSV-CoV-2) 0.00164 (AV-CoV-2)	RBD "up"/"down"	Quaternary binding with RBD in down adjacent to an "up" RBD was proposed, and could interact between two adjacent down RBD, with a binding pose similar to REGN10987's	[142, 194]
C144/C2	PMBC's from C-CoV-2	18.0 (RBD)	0.0069 (PSV-CoV-2) 0.0025 (AV-CoV-2)	RBD "up"/"down"	Quaternary binding, in the "down" RBD conformation. different from C002, C121, C119, C104	[142, 194]
COVA2-15/C2	B cells from C-CoV-2	0.6 (S) 3.1 (RBD)	0.008 (PSV-CoV-2) 0.009 (AV-CoV-2)	RBD "up"/"down"	A strong competition with hACE2 binding, binding RBD in "up" and "down" conformations, while its epitope is partially overlapped with the hACE2-binding site	[136]

Table 2 (continued)

Name/class	Source	K_D (nM)	IC_{50} μ g/mL	Target	Observations	References
2-15/C2	B cells from C-CoV-2	0.056	0.005 (PSV-CoV-2) 0.0007 (AV-CoV-2)	RBD "up"/"down"	Exhibited high potency in neutralizing in vitro, in a protection experiments using golden Syrian hamster reduced the infectious virus titres by 4 logs (1.5 mg/kg)	[205, 206]
C002/C2	PBMC from C-CoV-2	11 (RBD)	0.009 (PSV-CoV-2)	RBD "up"/"down"	Quaternary binding to "up/down" RBDs like C121, but different to C144. Interaction with RBD in down conformation adjacent to an "up" RBD, probably interacts between two adjacent "down" RBD domains	[142, 194]
C135/C3	PMBC's from C-CoV-2	6.0 (RBD)	0.016 (PSV-CoV-2) 0.0029 (AV-CoV-2)	RBD "up"/"down"	Three C135 Fabs bound with 2 "down" and 1 "up" RBDs (interaction weakly resolved), recognizing the glycosylated epitope N343RBD, interacting with R346 and N440, without steric hindrance between hACE2 / RBD	[142, 194]
2-51/C3	B cells from C-CoV-2	3.6	0.005 (PSV-CoV-2) 0.0007 (AV-CoV-2)	NTD	Potent neutralizing antibody against PSV-CoV-2 and AV-CoV-2 in vitro	[207]
H014/C4	phage display antibody library	0.09	3 nM (PSV-CoV-2) 38 nM (AV-CoV-2)	RBD up class 4	hACE2-humanized mice injected IP 50 mg per kilogram either 4 h after (one dose, therapeutic) or 12 h before and 4 h after (two doses, prophylactic plus therapeutic) with SARS-CoV-2 infection. No lesions of alveolar epithelial cells	[4]
5-24/WO	B cells from C-CoV-2		0.013 (PSV-CoV-2) 0.008 (AV-CoV-2)	NTD	nAb with high potency against AV-CoV-2 in vitro	[205]
1-57/WO	B cells from C-CoV-2	0.056	0.009 (PSV-CoV-2) 0.008 (AV-CoV-2)	RBD	mAb exhibited high potency in neutralizing AV-CoV-2 in vitro	[205]
2-7/WO	B cells from C-CoV-2	0.056	0.010 (PSV-CoV-2) 0.003 (AV-CoV-2)	RBD	mAb exhibited high potency in neutralizing AV-CoV-2 in vitro	[205]

SARS-CoV Severe acute respiratory syndrome–coronavirus, SARS-CoV-2 respiratory syndrome–coronavirus 2, RBD Receptor binding domain, PBMCs Fresh peripheral blood mononuclear cells, IP Intraperitoneally, PSV Pseudovirus, AV-CoV-2 authentic virus SARS-CoV-2, AV-CoV authentic virus SARS-CoV, SdAb single-domain antibodies, CPE Cytopathic effect, N-t amino-terminus, C-CoV-2 Convalescent SARS-CoV-2, NTD N-terminal domain ((residue 1–290), S2P_{ecto} S ectodomain trimer (S_{ecto}), C1 Class 1, C2 Class 2, C3 Class 3, C4 Class 4, WO those without structure analysis

able to bind RBDs in the "up" and "down" conformations and therefore, belongs to Class 2 [136]. The epitope and approach of binding to the RBD used by COVA2-04 is similar to that by CR3022, and hence, is categorized to Class 4 [28–30, 136] (Table 2).

The mAbs COV2-2196 and COV2-2130, which bind near the hACE2-binding site, exhibit powerful neutralizing activities. These mAbs present, in pseudovirus neutralization assays, an IC_{50} of 0.07 ng/mL and 1.6 ng/mL, respectively, although they are less sensitive for neutralization of the authentic virus (IC_{50} : 15 ng/mL and 107 ng/mL, respectively). Both mAbs recognize the RBD in the "up" configuration, although they do not compete with the virus for binding with hACE2. Furthermore, COV2-2130 presents different competitive binding sites and is able to interact with an RBD in the "down" state, indicating that it could recognize the RBD in the "up" or "down" conformations by probably binding to three distinct sites

on the S protein trimer [208]. Due to their differences in binding, COV2-2196 and COV2-2130 has been tested for prophylactic efficacy using a mouse-adapted SARS-CoV-2 model [208]. A cocktail of COV2-2196 (16 ng/mL) and COV2-2130 (63 ng/mL) presents a synergistic effect on virus neutralization in vitro compared with the effect observed by using 250 ng/mL of the Abs individually [208].

The Abs C002, C119, C121, C135, and C144 obtained from peripheral blood mononuclear cell of patients with COVID-19, interact with the RBD using different binding modes and present a strong pseudovirus neutralization effect (IC_{50} : 9.0 ng/mL, 9.0 ng/mL, 6.7 ng/mL, 16.0 ng/mL, and 6.9 ng/mL, respectively). Moreover, the Abs C121, C135, and 144 also neutralize authentic SARS-CoV-2 (IC_{50} : 1.6 ng/mL, 2.9 ng/mL, and 2.5 ng/mL, respectively) [142]. C002, C119, and C121 bind both the "up"- and "down"-state RBDs, where the Fab-S structures

suggest a quaternary epitope, including the neighboring RBDs, to also support bivalent interactions with two “down”-state RBDs. Additionally, C002 seems to be in contact with glycans in the RBD [142]. C135 and C144 bind the same “up” RBD conformation. In addition, C135 binds a “down”-state RBD regardless of the conformation of the neighboring RBDs. The conformational changes in the RBD allow the configuration of a quaternary epitope, which is formed by neighboring “down”-state RBDs that are recognized by C144 through its long CDRH3 loop. This unique interaction locks the S protein domains in a pre-fusion conformation, thereby avoiding the S protein-open conformation, in which it engages with hACE2 [142, 194] (Table 2).

The humanized mAb H014 has been obtained from an Ab library constructed by phage display from immunized mice with recombinant RBD from SARS-CoV [4]. H014 neutralizes the SARS-CoV-2 pseudovirus infection (IC₅₀: 3 nM) and authentic SARS-CoV-2 infection (IC₅₀: 38 nM). Cryo-EM characterization of H014 Fab in complex with the SARS-CoV-2 S protein trimer suggests a novel conformational RBD epitope accessible in an “open” conformation, where the mAb interacts with the S protein and blocks the hACE2 engagement by steric hindrance and the associated protein–protein interactions, different to the RBM interaction [4]. Interestingly, H014 is capable of neutralizing *in vivo* in a hACE2 mouse model with a prophylactic dose [4] (Table 2). This Ab is categorized in Class 4, together with CR3022, EY6A, S304, and S2A4 [4, 13, 27, 28, 178]. In general, Abs grouped in Class 4 need the highest concentration to reach the neutralization effect compared with Abs from the other classes.

Mutants could reduce Abs neutralization

RBD mutations have been related with the reduction of the sensitivity or confer resistance to neutralizing Abs. For instance, mutations N439K, L452R, A475V, V483A, E484K, G485D, F486A, F490L, and Y508H weaken the binding of mAbs, such as 157, 247, CB6, P2C-1F11, B3SCA1, X593, 261–262, H4, P2B-2F6, H014, and H00S022 [4, 19, 30, 135]. The V483A variant, with a mutation frequency greater than 0.1%, elicits a loss of activity of mAbs, such as P2B-2F6 and X593 [19, 135]. While V_H-Fc ab8 loss neutralizing activity against F486A mutant [209]. As well as REGN10933 showed a reduction of the sensitivity against E484K and G485D [145]. Similarly, RBD variants such as Q414E, N439K, G446V, K458N, I472V, A475V, T478I, V483I, and F490L cause viral resistance to CP [19]. In addition, variants such as N439K and Y508H are increasing in circulation [19]. Moreover, variants in the RBD or S₁ subunit, which allow the viral particle to increase its transmissibility,

pathogenicity, infectivity, and resistance, will continue to occur. D614G is a frequent mutation that does not occur in the RBD [48]. Although it has been related to SARS-CoV-2 infectivity and worsened COVID-19 symptoms, its participation in virus resistance has scarcely been demonstrated [48]. In contrast, Abs such as 2H2, 3C1, CC6, CC12, and CC25 neutralize the D614G variant [16, 48, 210, 211]. As well as STE90-C11 recognized with elevated affinity RBD mutations like V367F, N439K, G476S, V483A, E484K, G485R, F486V [212]. These data indicate the importance of using different Abs to achieve therapeutic effectiveness.

Cocktails of Abs

Based on distinct epitopes conserved in the S protein domain, a cocktail of neutralizing Abs has been used to mitigate the risk of COVID-19. Such cocktails can significantly enhance the neutralizing abilities [48, 143, 213, 214]. For example, to complement the neutralizing effect of H014 it was combined with the non-competitive antibody P17 obtained from a library of naive human antibodies. P17 has high affinity for RBD, and a potent neutralizing activity with pseudovirus (IC₅₀: 0.165 nM) and highest IC₅₀ against the authentic virus than H014. According to the authors, the cocktail of P17 and H014 improves (two to ten-fold) the protective effect against SARS-CoV-2 in mouse model [213].

Other combinations such as B38+H4, REGN10933+REGN10987, AZD8895+AZD1061, 414-1+555-63+553-15, COV2-2196+COV2-2130, and CR3022+CR3014 have been evaluated [26, 48, 214]. In fact, the addition of 553-15 to 414-1+555-63 or the combination of COV2-2196 with COV2-2130 has been shown to provide a synergistic neutralization effect [208, 214]. Furthermore, cocktails may have therapeutic potential in a possible SARS-CoV-2 reinfection, which has not been noted for other therapies [34, 215].

Abs Fc-mediated effector functions

The Fc-mediated effector functions, such as ADCC or ADCP, can contribute to virus clearance independent of the mAb neutralization effect [216, 217]. Briefly, infected cells may expose the Ags on the pathogen surface that can also be recognized by IgG, which through its Fc region binds the Fcγ receptors (FcγRs) and can attract other cells. In addition, IgGs bind C1q, drifting away from the complement-dependent cytotoxicity (CDC) pathway, which involves the IgG-bound Ag and recognition of the C1 complex [218]. Cytotoxic Abs, such as alemtuzumab, dinutuximab, and ofatumumab, present their main mechanism of action through ADCC and CDC. In fact, the Fc region of an Ab determines its serum half-life and effector functions, which are associated with the N-glycan structure

[219, 220]. In particular, the absence of the fucose residue at the core increases the ADCC [221, 222].

Pinto et al. [27] demonstrated that S309 mediates ADCC in SARS-CoV-2 S protein-transfected cells, along with the strongest ADCP response by monocytes, among the immune cells, via FcγRIIIa and FcγRIIa engagement and affinity for an FcγRIIIa variant (V158). It also activates the CDC pathway [178]. S306 activates ADCC and ADCP with intensity lesser than that of S309. S2M11 promotes FcγRIIIa-dependent ADCC in a dose-dependent manner and does not promote FcγRIIa-mediated ADCC, with a high affinity towards the V158 variant comparable to that of S309 [27]. Moreover, S2M11 also exerts ADCP. S2E12 triggers FcγRIIa but not FcγRIIIa signaling, unlike S2M11 and S309. Furthermore, a combination of S2M11 with S2E12 or S309 activates effector functions [223]. S2H13 promotes ADCC through FcγRIIIa (V158) activation, but presents a weak activation of FcγRIIa. Additionally, S2H13 is effective in killing Chinese hamster ovary (CHO) cells stably transfected with SARS-CoV-2 S protein via CDC. A superior ADCC response by REGN10987 compared with REGN1089, REGN10933, and REGN10934 has been observed, but all Abs have been shown to induce ADCP [145]. These findings highlight the differences in Abs and their relationship with FcγRIIIa and FcγRIIa receptors, or C1q, which can be decisive in displaying their protective mechanisms [27, 178, 223].

Hybridoma Abs

The recent discovery of potent antibodies has been driven using different technologies [46] instead of the traditional hybridoma production, although some Abs were also obtained by this strategy. Hybridomas were introduced in 1975 by Köhler and Milstein [224], and these are cloned cell lines produced by the fusion of a B lymphocyte of interest and an immortalized myeloma cell, which are capable of secreting large quantities of pure Abs [225]. Although hybridoma development represents a labor-intensive and time-consuming process [226], research related to hybridomas has continued over time. Accordingly, COVID-19 research has not excluded hybridomas, as there are multiple studies using this strategy for treating SARS-CoV-2 infection [12, 227–230]. In recent studies, Abs from hybridomas with the ability to cross-neutralize SARS-CoV and SARS-CoV-2 *in vitro* have been identified [12, 227, 229], similar to those previously reported in terms of cross-neutralization amongst different CoVs (SARS-CoV, MERS-CoV, and SARS-CoV-2) [3, 29, 135, 231, 232].

The mAb 47D11 obtained from SARS-S hybridoma supernatants has been humanized [12]. Importantly, mAb 47D11 does not interfere with the recognition and

binding of the S protein with hACE2, owing to a mechanism that remains unknown [12, 47]. In addition, it has been demonstrated that its ability to perform a cross-neutralization is possibly by interactions with the conserved central region of the S protein from the RBD domain [12] (Additional file 1: Table S3). Another Ab obtained by the hybridoma technique is MAB362, whose variable sequences are expressed as IgG or monomeric IgA isotypes. IgA-type Ab presents higher neutralizing activity than its IgG homolog due to its “longer arms” and “greater flexibility” in the hinge domain, which allows the neutralization of S proteins from other CoVs. Additionally, IgA is proposed to have a greater persistence in mucosal secretions compared with the other isotypes [227]. Another mAb obtained from hybridoma cells is mAb#11/9, which binds the S protein irrespective of its glycosylation pattern [228], being also recognized by Abs SiD7h and S3D8h (IC₅₀ of 113.3 ng/mL and 137.2 ng/mL, respectively) [229]. Furthermore, six groups of mice hybridoma Abs with neutralizing capacity that recognized different epitopes on RBD has been described and can be employed as diagnostic tools in SARS-CoV-2 infection [230]. Using the same technique, the Abs 2H2 and 3C1 were developed, targeting different regions of S. Both have the ability to neutralize infection by SARS-CoV-2 virus. In particular 2H2, potently neutralize SARS-CoV-2 pseudovirus (IC₅₀: 0.025 μg/mL) and authentic SARS-CoV-2 (IC₅₀: 0.007 μg/mL). Interestingly, the human–mouse chimeric Abs c2H2 and the c2H2/c3C1 cocktail (with the same IC₅₀ of 0.054 μg/mL) could significantly reduce viral loads in Balb/c mice, showing therapeutic efficacy [210].

Neutralization of SARS-CoV-2 by nanobodies

In mammals, Abs present two chains (heavy and light), whereas in camelids, Abs containing homodimeric heavy chain with no C_H1 but a conserved Ag-binding domain (V_HH) can be found (Fig. 2e). The V_HH is also known as a single-domain Ab (sdAb) or nanobody (Nb) (Fig. 2d, f), which can be selected from synthetic, naive, or immunized cDNA libraries using phage, bacterial, yeast, or ribosomal display technologies [233–235]. Nbs have the smallest structures (~13 kDa) compared with other Abs, present with antigenic recognition, can act in a monomeric form or fusion protein, and show high specificity, stability, and solubility [236]. Therefore, Nbs are valuable in biomedical research. The first therapeutically active Nb caplacizumab-yhdp designed for treating thrombotic thrombocytopenic purpura and thrombosis (Abylnx, a Sanofi Company, Ghent, Belgium) was approved by the European Medicines Agency (EMA) in 2018 and the U.S. Food and Drug Administration (FDA) in 2019 [237]. Accordingly, Nbs with high affinity against SARS-CoV-2

S proteins, and the RBD could emerge as potential therapeutics in the fight against COVID-19, in line with the repertoire of potent neutralizing Nbs previously reported (Additional file 1: Table S5).

Camelid immune libraries

Distinct Nbs have been developed against SARS-CoV and MERS-CoV, such as V_HH-55 and V_HH-72 [238]. V_HH-72 when converted into a bivalent Fc (human IgG1) fusion form neutralizes the S protein of SARS-CoV-2 pseudovirus (IC₅₀ of ~0.2 µg/mL). Pretreatment with V_HH-72-Fc has been observed to reduce the viral load in the lungs of Syrian hamsters by ~10⁵-fold compared with that in the untreated control animals [239] (Additional file 1: Table S5). According to the differing neutralization effects noted for V_HH-72 and V_HH-72-Fc, there exists different epitopes between them, and the crystal structures indicate that V_HH-72-Fc interacts with the RBD as a Class 4 Ab [240]. ExeVir Company (Ghent, Belgium) has advanced with the development of V_HH-72-Fc through preclinical and clinical trials. The NIH-CoVnb-112 Nb has been obtained from a llama immunized with the SARS-CoV-2 S protein, and it blocks the SARS-CoV-2 RBD and hACE2 engagement [240]. W25UACH obtained from a V_HH library using *E. coli* display, is able to recognize beads coated with the S protein [241]. Ty1 binds the RBD with a high affinity and present neutralization activity against SARS-CoV-2 pseudovirus (IC₅₀: 77 ng/mL), avoiding hACE2 interaction; cryo-EM reconstruction revealed this complex with the RBD in both the “up” and “down” conformations as belonging to Class 2 having Abs with a quaternary epitope [242] (Additional file 1: Table S5). Ty1 multimeric constructs as the tetramer 4-arm PEG Ty1 increased its neutralizing capacity dramatically (IC₅₀: 13 pM) [243].

In contrast, Nbs such as Nb-Set1, NM1226, NM1228, NM1230, and NM1224, also derived from an immunized camelid, present high neutralization potencies against authentic SARS-CoV-2 (IC₅₀: ~15 nM, ~7 nM, ~37 nM, and ~256 nM, respectively). Furthermore, these Nbs block the RBD-hACE2 interaction and target different epitopes within the RBD [244]. Moreover, the Nbs 89, 20, and 21 obtained from the RBD-immunized camelid serum present high neutralization activities against authentic SARS-CoV-2 (IC₅₀: 20.154 nM, 0.048 nM, and 0.22, respectively) [237] (Additional file 1: Table S5). By modeling the Nbs 20 and 21, it has been revealed that they probably interact with the RBD in the “down” conformation [245]. On the other hand, Nb11-59, was obtained from camels immunized with the recombinant RBD of SARS-CoV-2, and present neutralizing activity against the authentic SARS-CoV-2 with neutralizing dose 50 (ND₅₀) of 0.55 µg/mL, and inhibit the replication of

eight RBD SARS-CoV-2 mutants (Q321L, V341I, N354D, V367F, K378R, V483A, Y508H, H519P) [246].

Camelid naïve libraries

H11 has been identified in a naïve llama V_HH library using phage display and found to target the RBD. Later, using random mutagenesis, Nbs H11-D4 and H11-H4 have been generated. Both Nbs are able to block the attachment of the S protein to hACE2 in vitro, recognizing different epitopes compared with CR3022 [30]. H11-D4-Fc and H11-H4-Fc fusions show neutralizing activity against authentic SARS-CoV-2 (ND₅₀: 18 nM and 6 nM, respectively) [30]. Cryo-EM reveals that both Nbs bind RBDs in the “up” and “down” conformations in the S protein trimer and hence, these are categorized as Class 2 Abs [30].

Three synthetic V_HH camelid libraries using ribosome and phage displays have allowed the generation of synthetic Nbs, termed as “sybodies” (Sbs) [247]. Sixty-three anti-RBD Sbs have been obtained from three libraries, screened by one round of ribosome display and two rounds of phage display against the RBD [248]. Other Sbs have been isolated from libraries such as SR4, MR17, MR3, and MR4, presenting high neutralization potencies against SARS-CoV-2 pseudovirus (IC₅₀: 5.9, 12.32, 0.40, and 0.74 µg/mL, respectively). Crystal structures of the complexes of Sbs and the RBD reveal a common neutralizing mechanism, suggesting that SR4, MR17, and probably MR3 interfere with the interaction between the RBD and hACE2 [249]. Divalent-engineered Sbs used to synthesize the MR3-MR3-albumin binding domain have been demonstrated to be the best for improving neutralization activities against pseudotyped virus (IC₅₀: 0.012 µg/mL). These Sbs have also been evaluated in SARS-CoV-2-infected C57BL/6J female mice, and the lung viral titers were found to be 50-fold lower than that in the control mice [249]. In the Sb-treated group, the alveolar wall structures were normal, although mild bronchopneumonia was observed; whereas, the lung viral load was reduced [249]. Sb23 has been isolated from a synthetic library, and interferes with the RBD and hACE2 interaction showing neutralizing activity against SARS-CoV-2-S pseudotyped virus (IC₅₀: 0.6 µg/mL) [250]. The cryo-EM structure suggested Sb23 as a Class 2 indicating that interacts with the S protein, wherein two RBDs are in the “up” conformation [250]. SR31, another Sb isolated from a synthetic library, interacts with the RBD, distorting it, and does not neutralize SARS-CoV-2 pseudovirus [251]. Since SR31 displays high affinity, its fusion with other neutralizing Sbs, such as SR31-MR17 or SR31-MR6, increases the neutralization activity against SARS-CoV-2 pseudovirus (IC₅₀: 52.8 µg/mL or 2.7 µg/mL, respectively) [251].

The synthetic Nbs Nb3, Nb6, and Nb11 have been obtained through screening of a yeast surface-displayed library using multiple S protein epitopes [252]. Particularly, Nb6 has a potent neutralization activity against pseudovirus infection (IC_{50} : 2.0 μ M). Cryo-EM revealed that Nb6 binds to the RBD in the open and closed S conformations, and belongs to Class 2 according to the Barnes classification [194]. Furthermore, the trivalent version of Nb6 (Nb6-tri) has shown an improvement in the neutralization activity against the authentic SARS-CoV-2 (IC_{50} : 140 pM) [252]. In addition, multi-specific V_H H Abs fused to human IgG1 Fc domains are able to activate the Fc-dependent functions, such as tri-specific V_H H-Fc 3F-1B-2A, which has been designed to neutralize SARS-CoV-2 [253]. The tri-specific V_H H-Fc 3F-1B-2A Ab, which in a docking model has been observed to interact with the RBD, exhibits higher pseudovirus neutralization activity than that by other V_H H-Fc combinations (IC_{50} : 3.0 nM) [253] (Additional file 1: Table S5). Other Nbs have been obtained from camelid V_H H naïve and synthetic libraries. Nbs were fused with IgG1 Fc domains to obtain two monoclonal V_H H-Fc named as 1B and 3F and one bi-specific 1B-3F-Fc, which block the binding of hACE2 with S, being 1B-3F-Fc the best in blocking function [254]. In the same sense, the Nb nanosota-1C was obtained from naïve camelid Nb phage display library, which presents high RBD affinity. The same Nb in Fc format (Nanosota-1C-Fc) increases the RBD affinity and presents strong neutralizing effect against SARS-CoV-2 pseudovirus (ND_{50} : 270 ng/mL) and against authentic virus (ND_{50} : 160 ng/mL). Interestingly, it protected prophylactically, and therapeutically Syrian hamsters infected with SARS-CoV-2 [255].

Human Nbs against SARS-CoV-2

Humanization of camelid Nbs has been aimed to reduce their immunogenicity. Nbs against the SARS-CoV-2 RBD have been detected in a library of phage-displayed sdAbs that uses naïve CDR regions together with human germline frameworks, with varied arrangements [256]. Among them, n3088 and n3130 inhibit SARS-CoV-2 pseudovirus infection (IC_{50} : 3.3 and 3.7 μ g/mL, respectively), and neutralize the authentic SARS-CoV-2 (IC_{50} : 2.6 and 4.0 μ g/mL respectively) [256]. Both n3088 and n3130 share some residues with the cryptic epitope recognized by CR3022, as suggested by binding models [28, 256]. Another study identified V_H ab8 fused with human IgG1 Fc (V_H -Fc ab8), and this bivalent form shows a potent neutralization activity against pseudotyped SARS-CoV-2 (IC_{50} : 0.03 μ g/mL), as well as the authentic SARS-CoV-2 (IC_{50} : 0.04 μ g/mL). V_H -Fc ab8 is categorized as Class 2 Ab, and it competitively inhibits the hACE2-RBD interaction by occupying three RBDs (two in the “down”

and one in the “up” conformation) [209]. Furthermore, V_H -Fc ab8 binds several RBD mutants found in patients with COVID-19, and its prophylactic and therapeutic efficacy has been demonstrated against SARS-CoV-2 infection in hamsters [209].

Other synthetic humanized sdAbs (1E2, 2F2, 3F11, 4D8, and 5F8) in a bivalent form fused with human IgG1 Fc have been shown to inhibit the association between the RBD and hACE2, presenting superior neutralization potencies against pseudotyped SARS-CoV-2-S (EC_{50} : 0.54, 0.40, 0.01, 0.46, and 0.05 μ g/mL, respectively) (Additional file 1: Table S5) [257]. Moreover, from a library of engineered human V_H S, V_H ab6 and V_H m397 have been obtained, which compete with the RBD for hACE2 binding. Both V_H S fused with Fc (V_H -Fc ab6 and V_H -Fc m397) have been shown to neutralize the authentic SARS-CoV-2 (IC_{50} : 0.35 μ g/mL and 1.5 μ g/mL, respectively) and present differences in competition probably due to different target S protein epitopes [258]. Biparatopic and trivalent Nbs against RBD were obtained from human VH-phage library. VH monomers were used to design bi-paratopic or multivalent VHs, with the aim to recognize different RBD epitopes simultaneously [179]. New formats improved the viral neutralization, being the most potent the trivalent VH3 B01 against over authentic SARS-CoV-2 (IC_{50} : 3.98 nM), which seems to block simultaneously the hACE2 and RBD interaction through the attack of three RBDs [179].

The diversity of Nbs found and the variety of neutralization mechanisms indicate their promising application in the therapy or prophylaxis of SARS-CoV-2 infection.

Remarks on the production of mAbs for COVID-19 treatment

Antibodies obtention from patients with COVID-19 is a fruitful strategy to recover human specialized neutralizing Abs. However, few discussions have been conducted on mAb production technologies in order to obtain quality mAbs that are safe, efficient, and accessible to the population [259]. The tetrameric nature of an IgG molecule and its glycosylation is essential for its functioning, making it a challenging protein for expression [260]. In this sense, mammalian cells, such as CHO cells, have become one of the most widely used cell factories for the industrial production of mAbs [261, 262] and are considered the workhorse of the industry [263–265]. Among the 68 mAbs approved between 2014 and 2018, 84% were produced in CHO cells and 16% in cells derived from myelomas (13% in NS0 and 3% in Sp2/0) [262]. Even during the pandemic in 2020, 10 Ab therapeutics had been approved by EMA or FDA [259]. Furthermore, over 60 previously known Abs are under evaluation for possible COVID-19 treatments [259]. Compared with bacteria and yeasts, the

yields and productivities of processes based on mammalian cells are low due to the slow rate of cell growth, their tendency to undergo apoptosis, and a low production capacity per cell [260, 261]. Therefore, developing cells with superior production characteristics has been aimed in the field [264, 266–268]. Nevertheless, owing to cell engineering, the time for the establishment of productive cell lines of fully humanized mAbs has sharply reduced, limiting it to some months, with increased productivities (up to 100 pg/cell day, representing bioreactor titers of nearly 10 g/L), which is presently crucial for the production of anti-SARS-CoV-2 mAbs [264, 269–271]. Elevated productive-mAb titres have also been achieved by extensive improvements in the production schemes [272]. Similarly, improvements in the recovery and purification of mAbs have achieved yields of up to 80% of that produced in bioreactors, and consequently, the manufacturing costs of goods have dropped to 20–100 US\$ per gram of the active pharmaceutical ingredient [270, 273].

Evidently, with the search for tools to attend the COVID-19 pandemic, and since the start-up of production of mAbs at industrial scale can take at least 6 months, Nbs production became an alternative. Due to the fact that Nbs are smaller and not glycosylated proteins they can be produced in cell factories such as bacteria or yeasts, at lower costs, with a larger scale of production [274]. Moreover, monomeric or multimeric V_H Hs can be produced without implying major changes in the bioprocess unit operations. However, as they are new molecules with complex and novel structural characteristics, the quality, safety and efficacy tests must be highly rigorous, and the regulatory approval could be longer and intensive than a complete mAb [274, 275]. The humanized Nb11-59 (Additional file 1: Table S4) was expressed in *Pichia pastoris* in small-scale and in 7 L bioreactor, reaching almost 20 g/L of the Nb. HuNb11-59 was also purified by affinity chromatography and hydrophobic chromatography reaching around 95% purity [246].

CHO cells as producers of anti-SARS-CoV-2 mAbs

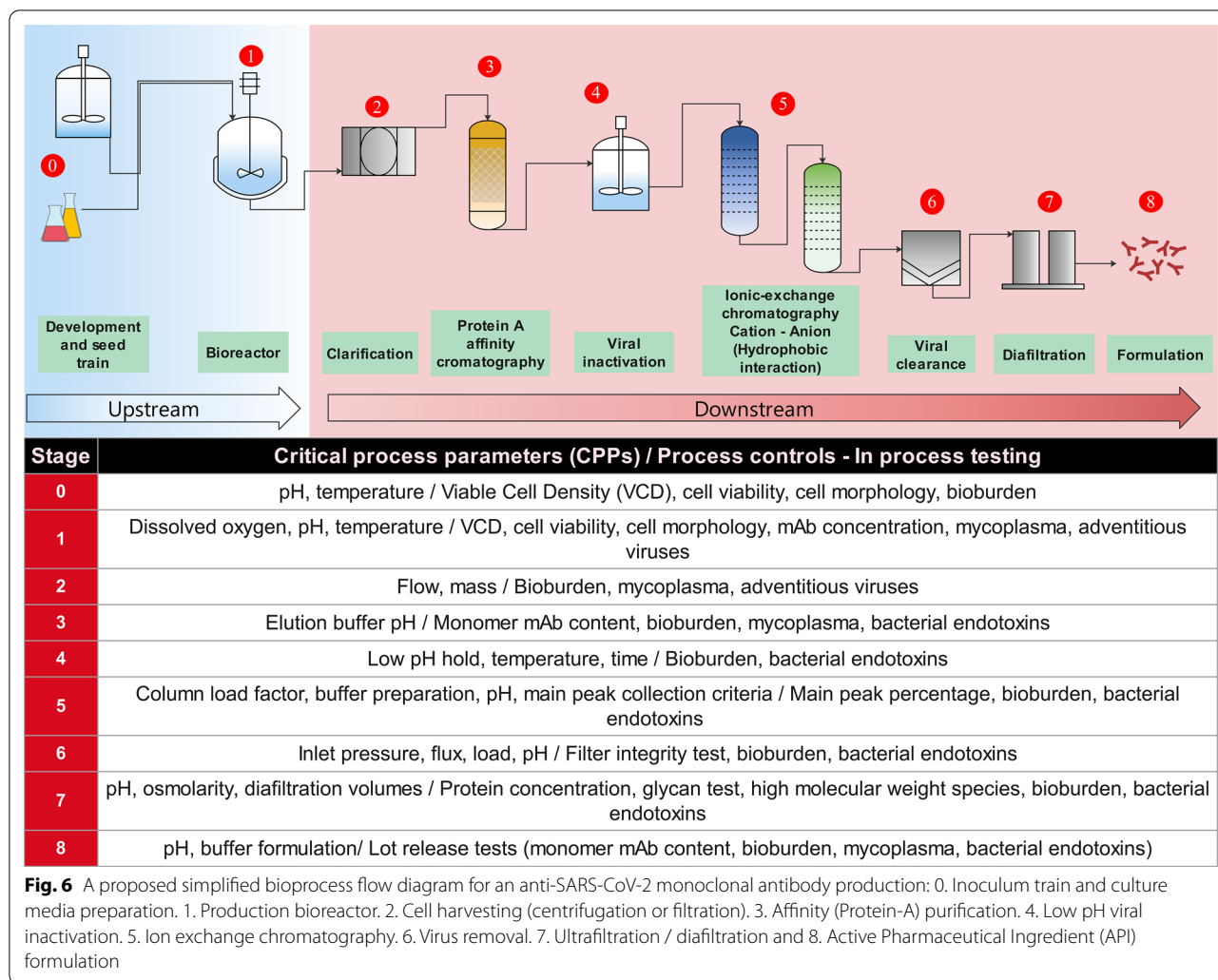
CHO cells were established and considered “immortal” by the end of the 1950s [264]. CHO cells present several advantages over other cell types for the production of mAbs: (i) a capacity to perform complex post-translational modifications (PTMs), such as “human”-like glycosylations, protein processing (e.g., phosphorylation) and folding, (ii) robust cell culture in chemically-defined and serum-free media that facilitates scaling-up, (iii) a safe host with a high rate of regulatory approval, and (iv) optimized transfection/selection systems that enable stable expression of heterologous genes [261, 263–265, 276].

Efforts have been made to optimize recombinant protein production in CHO cells, reduce manufacturing costs, and increase accessibility of life-changing drugs to patients [264, 266]. In this sense, mAb production involves a series of processes dictated by transcription (strength of the promoter, integration site for the gene of interest, and mRNA turnover), but also by the translation rate, protein turnover, and protein folding and processing [266]. Limited studies indicate the expression of recombinant anti-SARS-CoV-2 mAbs in CHO cell lines [145] some using transient expression [17, 178, 184, 277] with low utility at an industrial scale. Moreover, there are some studies on the production of the His-tagged SARS-CoV-2 S protein trimer or the S protein by CHO cells [27, 278]. Furthermore, to date there are at least 21 clinical studies evaluating anti-SARS-CoV-2 mAbs (Additional file 1: Table S4); however, information of large-scale production of mAbs has not been reported [52, 53, 279].

Challenges in the production of anti-SARS-CoV-2 mAbs

Although there are more than 70 mAbs licensed, only few of them have been approved or are under review in the EU or USA to treat or prevent diseases caused by viruses, such as human immunodeficiency virus infection, lower respiratory tract disease caused by syncytial virus in children, Ebola, and recently, COVID-19 [52, 53, 259]. Moreover, there are just one therapeutically active Nb approved in USA and EU [237]. Some of the mAb products are a combination of two or three mAbs. Accordingly, therapeutic Abs against SARS-CoV-2 should be combined cocktails that they recognize different epitopes in S including varied Abs formats and classes [52, 53, 144, 280]. Hence, the current challenges in large-scale production of Abs necessary to fight the pandemic are related to achieving production of all formats of Abs in cell factories with elevated productivities, as well as the scaling-up bioprocesses to generate enough amounts of the active pharmaceutical ingredient (API) to cover the world population.

Moreover, the location and optimum operation of production plants with stringent quality control practices worldwide, including Africa and Latin America, needs to be determined, along with the recruitment of skilled labor. Furthermore, multiproduct facilities should be considered to produce Ab cocktails. In addition to the quality assurance, it is necessary to demonstrate batch-by-batch reproducibility in bioprocesses. The production of anti-SARS-CoV-2 mAbs in CHO cells can be seen as a feasible strategy for implementation on an industrial scale in conjunction with high-density cultures [272], single-use technologies [267], design/selection techniques for highly productive clones [264, 281], and bioprocess optimization [266]. To achieve this, it is necessary that



companies with large biotechnological developments provide insights to the bio-pharmacological industry to combat this global pandemic.

Upstream and downstream bioprocesses in mAb production

The upstream production of mAbs in CHO cells is widely conducted using suspension cultures in stirred tank bioreactors under different modes: batch, fed-batch, and perfusion (continuous culture with retention of cells), although in the process of increasing the cell number (inoculum train) to reach the production volume, other types of bioreactors are also used, such as shake flasks and wave bioreactors, with preference for single-use systems [267, 282]. While, the production Nbs bioprocesses can be carried out in bacterial or yeasts conventional biopharmaceutical plants, where the inoculum train and the production bioreactors are generally made of stainless steel, with economical culture media, implying larger

industrial scales than those of animal cells. In general, upstream process development also includes scaling-up the culture process for reproduction on a large scale. An in-depth understanding of the process and its critical process parameters (CPPs) is essential to achieve a successful scale-up. The scale-up strategy involves keeping one or two parameters constant (scale-up criterion) across the different production scales [283]. In the case of mammalian cells, the aim is usually to keep the shear forces or oxygen transfer constant [283]. Moreover, technological, analytical, and regulatory advances promote biopharmacies to implement continuous culture systems to meet the growing demand for mAb production [275, 282, 284]. mAb isolation and purification (downstream) represent a significant portion of the production effort and costs [270, 285]. Hence, improvements in these aspects are relevant [285]. Furthermore, the downstream mAb manufacturing processes do not have a standard framework (Fig. 6); all processes rely on biomass clarification

(biomass removal) and protein-A chromatography as the initial capture steps (providing in some cases > 98% purity in a single purification step). Subsequently, low-pH viral particle inactivation, viral particle removal, and polishing chromatographic steps are used to obtain the API [270]. The Nbs downstream can follow the procedures typically used for human therapeutic recombinant proteins (such as hormones, cytokines or stimulatory factors) produced in bacteria and yeast [246, 286].

The production level and the quality of Abs are highly sensitive to the operating conditions of the production process [287]. Ab production implies identification of the critical stages and variables in the process (Fig. 6), as well as determination of the critical quality attributes (CQAs) of the Ab to ensure its quality, safety, and efficacy (Additional file 1: Table S6). Then, CQAs are physical, chemical, biological, or microbiological properties with defined statistical limits, ranges, or distributions [287] (Additional file 1: Table S6). Given the relevance of the CQAs, the concept of quality by design (QbD) emerges as an experimental strategy that requires a deep understanding of the bioprocess to determine the CPPs and the in-process testing parameters of the unit operations (Fig. 6) [287]. The implementation of process analytical technologies (PAT) is the most helpful strategy to ensure the quality, safety, and efficacy of mAbs [282]. CQAs should be carefully controlled and measured during both, upstream and downstream bioprocesses (Additional file 1: Table S6). Finally, the CQAs for an Ab finished pharmaceutical product must be taken into account, such as the pH, protein amount, formulation, freezing/thawing, dose, color, lyophilization, drug delivery, and logistics, all of which, depend on the final product presentation.

Conclusions and perspectives

mAbs have revolutionized the treatment of different diseases, including viral diseases. Their applications in human therapy have improved with the development of completely human mAbs, thereby ensuring their quality, efficacy, and safety with reduced immunogenicity. However, the cost of Abs has always been a limiting factor in their use in the clinical settings, as well as their large-scale distribution. This limitation has been overcome by improving the production processes, as well as the purification strategies.

Until now, different studies have shown that the immune response in many COVID-19 patients leads to the production of CP, which contains specialized neutralizing Abs that can protect the patient against SARS-CoV-2, in conjunction with a series of other favorable immune responses. The recovery of the genetic and protein information on the Abs produced in COVID-19 patients and other immunized animals has allowed the

identification of hundreds of Abs with neutralizing activity. Furthermore, these discoveries have led to the expression and production of Abs in different formats (mAbs, Fabs, Nbs, and sdAbs) to be characterized physically, chemically, and structurally. Some of these Abs are being tested in animal models, undergoing clinical trials, or recently mAbs approved for emergency use in humans. A cascade of information has been generated in this regard, which will surely lead to the generation of therapeutic and prophylactic solutions for the treatment of COVID-19, an unprecedented disease that remains uncontrolled globally. Thus, the search for neutralizing Abs that can serve in the control and therapy of SARS-CoV-2 infection needs to be exhaustive and remains urgent.

In COVID-19 patients, neutralizing Ab titers are correlated with the severity of the infection [12, 128, 178] and low somatic hypermutation [137, 138, 142, 180]. The RBD region is found to be immunodominant and the target of approximately 90% of the neutralizing Abs present in the sera of SARS-CoV-2-infected people. Furthermore, it has been determined that the anti-RBD IgG titers decrease with time post symptom onset, presenting a half-life of approximately 49 days. Importantly, avidity increases over time, probably due to increased maturation. In the serum of hospitalized COVID-19 patients, there is a greater number of IgG against the protein S and the RBD, compared with that in non-serious and asymptomatic patients [178]. Therefore, all patients present anti-RBD IgGs, from patients with severe (most of them older than 50 years), high, medium, low, or atypical symptoms to asymptomatic patients (diverse age group with most of them between 20 and 60 years of age). The pediatric antibody production is different, since they produce anti-S but not anti-N Abs and present untrained T-cell responses together with a strong immune response acquired at birth that allows faster virus elimination [192, 288, 289]. In contrast, hospitalized adult patients present a high titer of Abs that block the interaction between the RBD and hACE2 [178]. Therefore, CP therapy using plasma from adult patients could increase the Ab content, and accordingly, it has been used as treatment in different clinical trials [147, 152, 153]. However, many concerns around the safety and efficacy of CP against COVID-19 exist. Consequently, the possibility of identifying neutralizing Abs and their characterization will avoid application of the whole CP.

Hence, in-depth analyses, isolation, characterization, and production of neutralizing Abs found in COVID-19 patients would allow for rational proposals of immunological protection [178]. Moreover, generation of polyvalent antivirals with at least four targets, as described by the four different Ab classes, using mAbs, Fabs, multibodies, Nbs, Sbs, or fusion proteins that interact with

the RBD in the “up” and “down” conformations could broaden the spectrum of their therapeutic potential and prevent viral escape through mutations. In addition, combination of Abs, targeting different RBD epitopes or the new variants integrated in cocktails [145, 215, 290], can ensure successful COVID-19 therapy. Of note, although recombinant mAbs have generally been used in human therapies for more than 20 years and are generally well tolerated, adverse effects (skin reactions, pyrexia, anaphylaxis even a systemic inflammatory response and ADE reaction, among others) must be well studied and characterized [48, 50, 101, 102, 291]. Thus, passive immunization treatment could be one strategy to treat severe cases, people who do not respond to vaccination or cannot be vaccinated. Therefore, the vast amount of information generated will allow for the development of safe and effective treatments and vaccines for COVID-19, providing the molecular basis for the neutralization of pathogenic CoVs by Abs.

Abbreviations

Ab: Antibody; ADCC: Antibody-dependent cell cytotoxicity; ADCP: Antibody-dependent cellular phagocytosis; ADE: Antibody-dependent enhancement; Ag: Antigen; ARDS: Acute respiratory distress syndrome; CDC: Complement-dependent cytotoxicity; CDR: Complementarity-determining region; CHO: Chinese Hamster Ovary cells; CP: Convalescent plasma; cryo-EM: Cryogenic electron microscopy; EC₅₀: Half-maximal effective concentration; ND₅₀: Neutralizing dose 50; Fab: Fragment antigen-binding; GM-CSF: Granulocyte-macrophage colony-stimulating factor; hACE2: Human angiotensin-converting enzyme; IC₅₀: Half maximal inhibitory concentration; IGHV: Immunoglobulin heavy chain variable region; mAb: Monoclonal antibody; MASP-2: Mannan-binding lectin-associated serine protease 2; MERS-CoV: Middle East respiratory syndrome coronavirus; Nbs: Nanobodies; NK: Natural killer; NKG2A: Natural Killer Group Protein 2; NTD: N-terminal domain; PAMPs: Pathogen-associated molecular patterns; PDB: Protein data bank; PMTs: Post-translational modifications; PSO: Days-post symptoms onset; RBD: Receptor binding domain; RBM: Receptor-binding motif; RT-PCR: Reverse transcription polymerase chain reaction; SARS-CoV-2: Severe acute respiratory syndrome coronavirus 2; S_b: Sybody; sdAb: Single domain antibody; TLR: Toll-like receptor; VDJ: Variable (V), diversity (D), and joining (J) genes segments; V-NAR: Variable domain new antigen receptor; V_HH: Variable domain heavy chain.

Supplementary Information

The online version contains supplementary material available at <https://doi.org/10.1186/s12934-021-01576-5>.

Additional file 1: Table S1. Participation of the immune system in the infection by SARS-CoV-2. **Table S2.** Summary of outcomes regarding the use of convalescent plasma from COVID-19 patients. **Table S3.** Binding affinity of monoclonal antibodies that block or neutralize interaction between SARS-CoV-2 and hACE2. **Table S4.** Clinical evaluation of mAbs against SARS-CoV-2. **Table S5.** Binding affinity of nanobodies that block or neutralize interaction between SARS-CoV-2 and hACE2. **Table S6.** Process and product related potential critical quality attributes (pCQAs) to be taken into account for the production of anti-SARS-CoV-2 mAbs to obtain a pure active pharmaceutical ingredient.

Acknowledgements

Bando-Campos C.G. (fellowship 366135), Ortega-Portilla P.A. (fellowship 707238), Cofas-Vargas L.F. (fellowship 508395), and Zelada-Cordero P.

(fellowship 749447) are doctoral students from Programa de Doctorado en Ciencias Bioquímicas, Universidad Nacional Autónoma de México (UNAM). González-Hernández R.A. (fellowship 717832), Juárez-López D. (fellowship 388590), and Restrepo-Pineda S. (fellowship 589949) are doctoral students from Programa de Doctorado en Ciencias Biológicas, UNAM. Hernández-Peralta P. (fellowship 394569) is a student from Doctorado en Ciencias de la Producción y de la Salud Animal, UNAM. All received fellowships from “Consejo Nacional de Ciencia y Tecnología” CONACYT. Coronado-Aceves E.W. thanks “Dirección General de Asuntos del Personal Académico (UNAM)” for the post-doctoral fellowship.

Authors' contributions

Conceptualization: MATR, NAVC. Funding acquisition: LC, CE, EGH, MATR, NAVC. Project administration: MATR, NAVC. Supervision: MATR, NAVC. Writing—original draft: All authors contributed equally. Writing—review & editing: All authors contributed equally. All authors read and approved the final manuscript.

Funding

This work was supported by “Programa de Apoyo a Proyectos de Investigación e Innovación Tecnológica, Universidad Nacional Autónoma de México” (PAPIIT-UNAM IV-201220, Identification of antibody sequences from recovered and asymptomatic Mexican COVID-19 patients, and development of recombinant monoclonal antibodies as a possible treatment -Identificación de secuencias de anticuerpos de pacientes COVID-19 mexicanos recuperados y asintomáticos, y desarrollo de anticuerpos monoclonales recombinantes: posible tratamiento -). Funding sources had no role in study design, data collection and analysis, decision to publish, or preparation of the manuscript. This work was supported by project 1200962 FONDECYT (Chile) to CA.

Availability of data and materials

Not applicable.

Declarations

Ethics approval and consent to participate

Not applicable.

Consent for publication

Not applicable.

Competing interests

Authors declare that they have no conflict of interest.

Author details

¹ Programa de Investigación de Producción de Biomoléculas, Departamento de Biología Molecular y Biotecnología, Instituto de Investigaciones Biomédicas, Universidad Nacional Autónoma de México, Ciudad Universitaria, 04510 Ciudad de México, México. ² Instituto de Química, Universidad Nacional Autónoma de México, Ciudad Universitaria, 04510 Ciudad de México, México. ³ Departamento de Inmunología, Instituto de Investigaciones Biomédicas, Universidad Nacional Autónoma de México, Ciudad Universitaria, 04510 Ciudad de México, México. ⁴ Facultad de Medicina Veterinaria Y Zootecnia, Universidad Nacional Autónoma de México, Ciudad Universitaria, 04510 Ciudad de México, México. ⁵ Escuela de Ingeniería Bioquímica, Pontificia Universidad Católica de Valparaíso, Av. Brasil N° 2950, Valparaíso, Chile.

Received: 27 January 2021 Accepted: 3 April 2021

Published online: 22 April 2021

References

- Dong E, Du H, Gardner L. An interactive web-based dashboard to track COVID-19 in real time. *Lancet Infect Dis.* 2020;20(5):533–4.
- Petersen E, Koopmans M, Go U, Hamer DH, Petrosillo N, Castelli N, et al. Comparing SARS-CoV-2 with SARS-CoV and influenza pandemics. *Lancet Infect Dis.* 2020;20(9):e238–44.

3. Zhu Z, Chakraborti S, He Y, Roberts A, Sheahan T, Xiao X, et al. Potent cross-reactive neutralization of SARS coronavirus isolates by human monoclonal antibodies. *Proc Natl Acad Sci USA*. 2007;104(29):12123–8.
4. Lv Z, Deng YQ, Ye Q, Cao L, Sun CY, Fan C, et al. Structural basis for neutralization of SARS-CoV-2 and SARS-CoV by a potent therapeutic antibody. *Science*. 2020;369(6510):1505–9.
5. Cheng ZJ, Qu HQ, Tian L, Duan Z, Hakonarson H. COVID-19: look to the future, learn from the past. *Viruses*. 2020;12(11):1226.
6. Forni D, Cagliari R, Clerici M, Sironi M. Molecular evolution of human coronavirus genomes. *Trends Microbiol*. 2017;25:35–48.
7. Song Z, Xu Y, Bao L, Zhang L, Yu P, Qu Y, et al. From SARS to MERS, thrusting Coronaviruses into the spotlight. *Viruses*. 2019;11(1):59.
8. Kandeel M, Ibrahim A, Fayed M, Al-Nazawi M. From SARS and MERS CoVs to SARS-CoV-2: moving toward more biased codon usage in viral structural and nonstructural genes. *J Med Virol*. 2020;92(6):660–6.
9. Bestle D, Heindl MR, Limburg H, van Van Lam T, Pilgram O, Moulton H, et al. TMPRSS2 and furin are both essential for proteolytic activation of SARS-CoV-2 in human airway cells. *Life Sci Alliance*. 2020;3(9):e202000786.
10. Hoffmann M, Kleine-Weber H, Schroeder S, Krüger N, Herrler T, Erichsen S, et al. SARS-CoV-2 cell entry depends on ACE2 and TMPRSS2 and is blocked by a clinically proven protease inhibitor. *Cell*. 2020;181(2):271–280.e8.
11. Matsuyama S, Nao N, Shirato K, Kawase M, Saito S, Takayama I, et al. Enhanced isolation of SARS-CoV-2 by TMPRSS2-expressing cells. *Proc Natl Acad Sci USA*. 2020;117(13):7001–3.
12. Wang C, Li W, Drabek D, Okba NMA, van Haperen R, Osterhaus ADME, et al. A human monoclonal antibody blocking SARS-CoV-2 infection. *Nat Commun*. 2020;11(1):2251.
13. Zhou D, Duyvesteyn HME, Chen CP, Huang CG, Chen TH, Shih SR, et al. Structural basis for the neutralization of SARS-CoV-2 by an antibody from a convalescent patient. *Nat Struct Mol Biol*. 2020;27(10):950–8.
14. Shang J, Ye G, Shi K, Wan Y, Luo C, Aihara H, Geng Q, Auerbach A, Li F. Structural basis of receptor recognition by SARS-CoV-2. *Nature*. 2020;581(7807):221–4.
15. Lan J, Ge J, Yu J, Shan S, Zhou H, Fan S, et al. Structure of the SARS-CoV-2 spike receptor-binding domain bound to the ACE2 receptor. *Nature*. 2020;581(7807):215–20.
16. Rogers TF, Zhao F, Huang D, Beutler N, Burns A, He WT, et al. Isolation of potent SARS-CoV-2 neutralizing antibodies and protection from disease in a small animal model. *Science*. 2020;369(6506):956–63.
17. Kreye J, Reincke SM, Kornau HC, Sánchez-Sendin E, Corman VM, Liu H, et al. A therapeutic non-self-reactive SARS-CoV-2 antibody protects from lung pathology in a COVID-19 hamster model. *Cell*. 2020;183(4):1058–69.e19.
18. Chen X, Li R, Pan Z, Qian C, Yang Y, You R, Zhao J, Liu P, Gao L, et al. Human monoclonal antibodies block the binding of SARS-CoV-2 spike protein to angiotensin converting enzyme 2 receptor. *Cell Mol Immunol*. 2020;17(6):647–9.
19. Li Q, Wu J, Nie J, Zhang L, Hao H, Liu S, et al. The impact of mutations in SARS-CoV-2 spike on viral infectivity and antigenicity. *Cell*. 2020;182(5):1284–94.e9.
20. Malin JJ, Suárez I, Priesner V, Fätkenheuer G, Rybniker J. Remdesivir against COVID-19 and other viral diseases. *Clin Microbiol Rev*. 2020;34(1):e00162–e220.
21. Beigel JH, Tomashek KM, Dodd LE, Mehta AK, Zingman BS, Kalil AC, et al. Remdesivir for the treatment of Covid-19—final report. *N Engl J Med*. 2020;383(19):1813–26.
22. Wang Y, Zhang D, Du G, Du R, Zhao J, Jin Y. A Remdesivir in adults with severe COVID-19: a randomised, double-blind, placebo-controlled, multicentre trial. *Lancet*. 2020;395(10236):1569–78. [Erratum in: *Lancet*. 2020;395(10238):1694].
23. Prompetchara E, Ketloy C, Palaga T. Immune responses in COVID-19 and potential vaccines: lessons learned from SARS and MERS epidemic. *Asian Pac J Allergy Immunol*. 2020;38(1):1–9.
24. Johnson AR, McDonald AR, Malay DS. In Pursuit of a SARS-CoV-2 vaccine. *J Foot Ankle Surg*. 2020;59(6):1133–4.
25. Krammer F. SARS-CoV-2 vaccines in development. *Nature*. 2020;586(7830):516–27.
26. ter Meulen J, van den Brink EN, Poon LL, Marissen WE, Leung CS, Cox F, et al. Human monoclonal antibody combination against SARS coronavirus: synergy and coverage of escape mutants. *PLoS Med*. 2006;3(7):e237.
27. Pinto D, Park YJ, Beltramello M, Walls AC, Tortorici MA, Bianchi S, et al. Cross-neutralization of SARS-CoV-2 by a human monoclonal SARS-CoV antibody. *Nature*. 2020;583(7815):290–5.
28. Yuan M, Wu NC, Zhu X, Lee CD, So RTY, Lv H, et al. A highly conserved cryptic epitope in the receptor binding domains of SARS-CoV-2 and SARS-CoV. *Science*. 2020;368(6491):630–3.
29. Tian X, Li C, Huang A, Xia S, Lu S, Shi Z, et al. Potent binding of 2019 novel coronavirus spike protein by a SARS coronavirus-specific human monoclonal antibody. *Emerg Microbes Infect*. 2020;9(1):382–5.
30. Huo J, Le Bas A, Ruza RR, Duyvesteyn HME, Mikolajek H, Malinauskas T, et al. Neutralizing nanobodies bind SARS-CoV-2 spike RBD and block interaction with ACE2. *Nat Struct Mol Biol*. 2020;27(9):846–54. [Erratum in: *Nat Struct Mol Biol*. 2020;27(11):1094].
31. Maradei J, Vanesa-Castanó V, Luján-Jaureguibehère M. Terapia con plasma de donantes convalecientes en enfermos graves con COVID-19: un llamado a la acción. *Revista del Hospital Dr Emilio Ferreyra*. 2020;1(1):e25–30.
32. Cao Y, Su B, Guo X, Sun W, Deng Y, Bao L, et al. Potent neutralizing antibodies against SARS-CoV-2 identified by high-throughput single-cell sequencing of convalescent patients' B Cells. *Cell*. 2020;182(1):73–84.e16.
33. Hey A. History and practice: antibodies in infectious diseases. In: Crowe JE, Boraschi D, Rappuoli R, editors. *Antibodies for infectious diseases*. Hoboken: Wiley; 2015. p. 1–21. <https://doi.org/10.1128/9781555817411.ch1>.
34. Both L, White J, Mandal S, Efstratiou A. Access to diphtheria antitoxin for therapy and diagnostics. *Euro surveill*. 2014;19:20830.
35. Blake PA, Feldman RA, Buchanan TM, Brooks GF, Bennett JV. Serologic therapy of tetanus in the United States, 1965–1971. *JAMA*. 1976;235:42–4.
36. Menzies BE, Kernodle DS. Passive immunization with antiserum to a nontoxic alpha-toxin mutant from *Staphylococcus aureus* is protective in a murine model. *Infect Immun*. 1996;64:1839–41.
37. Lyerly DM, Bostwick E, Binion S, Wilkins T. Passive immunization of hamsters against disease caused by *Clostridium difficile* by use of bovine immunoglobulin G concentrate. *Infect Immun*. 1991;59:2215–8.
38. McGuinness AC, Armstrong JG, Felton HM. Hyperimmune whooping cough serum: further studies. *J Pediatr*. 1944;24:249–58.
39. Bodensteiner JB, Morris H, Howell J, Schochet S. Chronic ECHO type 5 virus meningoencephalitis in X-linked hypogammaglobulinemia: treatment with immune plasma. *Neurol*. 1979;29:815.
40. McGory RW, Ishitani MB, Oliveira WM, Stevenson WC, McCullough CS, Dickson RC, et al. Improved outcome of orthotopic liver transplantation for chronic hepatitis B cirrhosis with aggressive passive immunization. *Transplantation*. 1996;61(9):1358–64.
41. Gallagher JR. Use of convalescent measles serum to control measles in a preparatory school. *Am J Public Health Nations Health*. 1935;25:595–8.
42. Frickhofen N, Abkowitz JL, Safford M, Berry JM, Antunez-de-Mayolo J, Astrow A, et al. Persistent B19 parvovirus infection in patients infected with human immunodeficiency virus type 1 (HIV-1): a treatable cause of anemia in AIDS. *Ann Intern Med*. 1990;113(12):926–33.
43. Hattwick MA, Corey L, Creech WB. Clinical use of human globulin immune to rabies virus. *J Infect Dis*. 1976;133(S2):A266–72.
44. Groothuis JR, Simoes EA, Levin MJ, Hall CB, Long CE, Rodriguez WJ, et al. Prophylactic administration of respiratory syncytial virus immune globulin to high-risk infants and young children. *N Engl J Med*. 1993;329:1524–30.
45. Weech A. The prophylaxis of varicella with convalescents' serum. *JAMA*. 1924;82:1245–6.
46. Walker LM, Burton DR. Passive immunotherapy of viral infections: "super-antibodies" enter the fray. *Nat Rev Immunol*. 2018;18:297.
47. Levi-Schaffer F, de Marco A. COVID-19 and the revival of passive immunization: antibody therapy for inhibiting SARS-CoV-2 and preventing host cell infection: IUPHAR review: 31. *Br J pharmacol*. 2020. <https://doi.org/10.1111/bph.15359>.

48. Gavor E, Choong YK, Er SY, Sivaraman H, Sivaraman J (2020) Structural basis of SARS-CoV-2 and SARS-CoV-antibody interactions. *Trends Immunol.* 2020;41(11):1006–22.
49. Rajendran K, Krishnasamy N, Rangarajan J, Rathinam J, Natarajan M, Ramachandran A. Convalescent plasma transfusion for the treatment of COVID-19: systematic review. *J Med Virol.* 2020;92(9):1475–83.
50. Renn A, Fu Y, Hu X, Hall MD, Simeonov A. Fruitful neutralizing antibody pipeline brings hope to defeat SARS-CoV-2. *Trends Pharmacol Sci.* 2020;41(11):815–29.
51. Zare H, Aghamollaei H, Hosseindokht M, Heiat M, Razei A, Bakherad H. Nanobodies, the potent agents to detect and treat the Coronavirus infections: a systematic review. *Mol Cell Probes.* 2021;2021(55):101692.
52. Raybould MJ, Kovaltsuk A, Marks C, Deane CM. CoV-AbDab: the coronavirus antibody database. *Bioinformatics.* 2020. <https://doi.org/10.1093/bioinformatics/btaa739>.
53. Yang L, Liu W, Yu X, Wu M, Reichert JM, Ho M. COVID-19 antibody therapeutics tracker: a global online database of antibody therapeutics for the prevention and treatment of COVID-19. *Antib Ther.* 2020;3(3):205–12.
54. Lednický JA, Lauzardo M, Fan ZH, Jutla A, Tilly TB, Gangwar M, et al. Viable SARS-CoV-2 in the air of a hospital room with COVID-19 patients. *Int J Infect Dis.* 2020;100:476–82.
55. Rodriguez-Palacios A, Cominelli F, Basson AR, Pizarro TT, Ilic S. Textile masks and surface covers-A spray simulation method and a "Universal Droplet Reduction Model" against respiratory pandemics. *Front Med (Lausanne).* 2020;7:260.
56. Chen G, Wu D, Guo W, Cao Y, Huang D, Wang H, et al. Clinical and immunological features of severe and moderate coronavirus disease 2019. *J Clin Invest.* 2020;130(5):2620–9.
57. García LF. Immune response, inflammation, and the clinical spectrum of COVID-19. *Front Immunol.* 2020;11:1441.
58. Gu J, Han B, Wang J. COVID-19: gastrointestinal manifestations and potential fecal–oral transmission. *Gastroenterology.* 2020;158:1518–9.
59. Lamers MM, Beumer J, van der Vaart J, Knoops K, Puschhof J, Breugem TI, et al. SARS-CoV-2 productively infects human gut enterocytes. *Science.* 2020;369(6499):50–4.
60. Yan R, Zhang Y, Li Y, Xia L, Guo Y, Zhou Q. Structural basis for the recognition of SARS-CoV-2 by full-length human ACE2. *Science.* 2020;367(6485):1444–8.
61. Conti P, Ronconi G, Caraffa A, Gallenga CE, Ross R, Frydas I, Kritas SK. Induction of pro-inflammatory cytokines (IL-1 and IL-6) and lung inflammation by Coronavirus-19 (COVI-19 or SARS-CoV-2): anti-inflammatory strategies. *J Biol Regul Homeost Agents.* 2020;34(2):327–31.
62. Guillot L, Le Goffic R, Bloch S, Escρίου N, Akira S, Chignard M, Si-Tahar M. Involvement of toll-like receptor 3 in the immune response of lung epithelial cells to double-stranded RNA and influenza A virus. *J Biol Chem.* 2005;280:5571–80.
63. Merad M, Martin JC. Pathological inflammation in patients with COVID-19: a key role for monocytes and macrophages. *Nat Rev Immunol.* 2020;20(6):355–62.
64. Mehta P, McAuley DF, Brown M, Sanchez E, Tattersall RS, Manson JJ, et al. COVID-19: consider cytokine storm syndromes and immunosuppression. *Lancet.* 2020;395(10229):1033–4.
65. Hu B, Huang S, Yin L. The cytokine storm and COVID-19. *J Med Virol.* 2020. <https://doi.org/10.1002/jmv.26232>.
66. Schulert GS, Grom AA. Pathogenesis of macrophage activation syndrome and potential for cytokine-directed therapies. *Annu Rev Med.* 2015;66:145–59.
67. Jafarzadeh A, Chauhan P, Saha B, Jafarzadeh S, Nematı M. Contribution of monocytes and macrophages to the local tissue inflammation and cytokine storm in COVID-19: lessons from SARS and MERS, and potential therapeutic interventions. *Life Sci.* 2020;257:118102.
68. Shi CS, Nabar NR, Huang NN, Kehrl JH. SARS-Coronavirus Open Reading Frame-8b triggers intracellular stress pathways and activates NLRP3 inflammasomes. *Cell Death Discov.* 2019;5:101.
69. Freeman TL, Swartz TH. Targeting the NLRP3 Inflammasome in Severe COVID-19. *Front Immunol.* 2020;11:1518.
70. Li JY, Liao CH, Wang Q, Tan YJ, Luo R, Qiu Y, Ge XY. The ORF6, ORF8 and nucleocapsid proteins of SARS-CoV-2 inhibit type I interferon signaling pathway. *Virus Res.* 2020;286:198074.
71. Wu C, Chen X, Cai Y, Xia J, Zhou X, Xu S, et al. Risk factors associated with acute respiratory distress syndrome and death in patients with coronavirus disease 2019 pneumonia in Wuhan, China. *JAMA Intern Med.* 2020;180(7):934–43.
72. Barton LM, Duval EJ, Stroberg E, Ghosh S, Mukhopadhyay S. COVID-19 Autopsies, Oklahoma, USA. *Am J Clin Pathol.* 2020;153(6):725–33. [Erratum in: *Am J Clin Pathol.* 2020;153(6):852]
73. Zhang W, Zhao Y, Zhang F, Wang Q, Li T, Liu Z, et al. The use of anti-inflammatory drugs in the treatment of people with severe coronavirus disease 2019 (COVID-19): the perspectives of clinical immunologists from China. *Clin Immunol.* 2020;214:108393.
74. Zheng M, Gao Y, Wang G, Song G, Liu S, Sun D, Xu Y, Tian Z. Functional exhaustion of antiviral lymphocytes in COVID-19 patients. *Cell Mol Immunol.* 2020;17(5):533–5.
75. André P, Denis C, Soulas C, Bourbon-Caillet C, Lopez J, Arnoux T, et al. Anti-NKG2A mAb is a checkpoint inhibitor that promotes anti-tumor immunity by unleashing both T and NK cells. *Cell.* 2018;175:1731–43.
76. Li F, Wei H, Wei H, Gao Y, Xu L, Yin W, Sun R, Tian Z. Blocking the natural killer cell inhibitory receptor NKG2A increases activity of human natural killer cells and clears hepatitis B virus infection in mice. *Gastroenterology.* 2013;144:392–401.
77. Wilk AJ, Rustagi A, Zhao NQ, Roque J, Martínez-Colón GJ, McKechnie JL, et al. A single-cell atlas of the peripheral immune response in patients with severe COVID-19. *Nat Med.* 2020;26(7):1070–6.
78. Gao T, Hu M, Zhang X, Li H, Zhu L, Liu H, et al. Highly pathogenic coronavirus N protein aggravates lung injury by MASP-2-mediated complement over-activation. *MedRxiv.* 2020. <https://doi.org/10.1101/2020.03.29.20041962>.
79. Barnes BJ, Adrover JM, Baxter-Stoltzfus A, Borczuk A, Cools-Lartigue J, Crawford JM, et al. Targeting potential drivers of COVID-19: Neutrophil extracellular traps. *J Exp Med.* 2020;217(6):e20200652.
80. Dzik S. Complement and coagulation: cross talk through time. *Transf Med Rev.* 2019;33(4):199–206.
81. Krarup A, Wallis R, Presanis JS, Gál P, Sim RRB. Simultaneous activation of complement and coagulation by MBL-associated serine protease 2. *PLoS ONE.* 2007;2:e623.
82. Ritis K, Doumas M, Mastellos D, Micheli A, Giaglis S, Magotti P, et al. A novel C5a receptor-tissue factor cross-talk in neutrophils links innate immunity to coagulation pathways. *J Immunol.* 2006;177(7):4794–802.
83. Wiedmer T, Esmon CT, Sims PJ. Complement proteins C5b–9 stimulate procoagulant activity through platelet prothrombinase. *Blood.* 1986;68(4):875–80.
84. Rodriguez-Zhurbenko N, Quach TD, Hopkins TJ, Rothstein TL, Hernandez AM. Human B-1 Cells and B-1 cell antibodies change with advancing age. *Front Immunol.* 2019;10:483.
85. Java A, Apicelli AJ, Liszewski MK, Coler-Reilly A, Atkinson JP, Kim AH, Kulkarni HS. The complement system in COVID-19: friend and foe? *JCI Insight.* 2020;5(15):e140711.
86. Imai Y, Kubo K, Neely GG, Yaghubian-Malhami R, Perkmann T, van Loo G, et al. Identification of oxidative stress and Toll-like receptor 4 signaling as a key pathway of acute lung injury. *Cell.* 2008;133(2):235–49.
87. Vijay R, Hua X, Meyerholz DK, Miki Y, Yamamoto K, Gelb M, et al. Critical role of phospholipase A2 group IID in age-related susceptibility to severe acute respiratory syndrome-CoV infection. *J Exp Med.* 2015;212(11):1851–68.
88. Liu L, Wei Q, Lin Q, Fang J, Wang H, Kwok H, et al. Anti-spike IgG causes severe acute lung injury by skewing macrophage responses during acute SARS-CoV infection. *JCI Insight.* 2019;4(4):e123158.
89. Felgenhauer U, Schoen A, Gad HH, Hartmann R, Schaubmar AR, Failing K, et al. Inhibition of SARS-CoV-2 by type I and type III interferons. *J Biol Chem.* 2020;295(41):13958–64.
90. Sa Ribero M, Jouvenet N, Dreux M, Nisole S. Interplay between SARS-CoV-2 and the type I interferon response. *PLoS Pathog.* 2020;16(7):e1008737.
91. Diao B, Wang C, Tan Y, Chen X, Liu Y, Ning L, et al. Reduction and functional exhaustion of T cells in patients with Coronavirus Disease 2019 (COVID-19). *Front Immunol.* 2020;11:827.
92. Herrmann M, Schulte S, Wildner NH, Wittner M, Brehm TT, Ramharter M, et al. Analysis of co-inhibitory receptor expression in COVID-19 infection compared to acute *Plasmodium falciparum* malaria: LAG-3

- and TIM-3 Correlate with T Cell activation and course of disease. *Front Immunol.* 2020;11:1870.
93. Wherry EJ, Kurachi M. Molecular and cellular insights into T cell exhaustion. *Nat Rev Immunol.* 2015;15(8):486–99.
 94. Anderson AC, Joller N, Kuchroo VK. Lag-3, Tim-3, and TIGIT: co-inhibitory receptors with specialized functions in immune regulation. *Immunity.* 2016;44:989–1004.
 95. Kalpakci Y, Hacibekiroglu T, Trak G, Karacaer C, Demirci T, Kocayigit H, et al. Comparative evaluation of memory T cells in COVID-19 patients and the predictive role of CD4+ CD8+ double positive T lymphocytes as a new marker. *Rev Assoc Med Bras.* 2020;66(12):1666–72.
 96. Chen Z, Wherry EJ. T cell responses in patients with COVID-19. *Nat Rev Immunol.* 2020;20(9):529–36.
 97. Moon C. Fighting COVID-19 exhausts T cells. *Nat Rev Immunol.* 2020;20(5):277.
 98. Sattler A, Angermair S, Stockmann H, Heim KM, Khadzhyrov D, Treskatsch S, et al. SARS-CoV-2-specific T cell responses and correlations with COVID-19 patient predisposition. *J Clin Invest.* 2020;130(12):6477–89.
 99. Terpos E, Ntanasis-Stathopoulos I, Elalamy I, Kastritis E, Sergentanis TN, Politou M, et al. Hematological findings and complications of COVID-19. *Am J Hematol.* 2020;2020(95):834–47.
 100. Xu H, Zhong L, Deng J, Peng J, Dan H, Zeng X, et al. (2020) High expression of ACE2 receptor of 2019-nCoV on the epithelial cells of oral mucosa. *Int J Oral Sci.* 2020;12(1):1–5.
 101. Liao M, Liu Y, Yuan J, Wen Y, Xu G, Zhao J, et al. Single-cell landscape of bronchoalveolar immune cells in patients with COVID-19. *Nat Med.* 2020;26(6):842–4.
 102. Peng Y, Mentzer AJ, Liu G, Yao X, Yin Z, Dong D, et al. Broad and strong memory CD4+ and CD8+ T cells induced by SARS-CoV-2 in UK convalescent individuals following COVID-19. *Nat Immunol.* 2020;21(11):1336–45.
 103. Neidleman J, Luo X, Frouard J, Xie G, Gill G, Stein ES, et al. SARS-CoV-2-specific T cells exhibit phenotypic features of helper function, lack of terminal differentiation, and high proliferation potential. *Cell Reports Med.* 2020;1(6):100081.
 104. Zhang Y, Zhang J, Chen Y, Luo B, Yuan Y, Huang F, et al. The ORF8 protein of SARS-CoV-2 mediates immune evasion through potently downregulating MHC-I. *bioRxiv.* 2020. <https://doi.org/10.1101/2020.05.24.111823>.
 105. Tirado SMC, Yoon KJ. Antibody-dependent enhancement of virus infection and disease. *Viral Immun.* 2003;16:69–86.
 106. Takada A, Kawaoka Y. Antibody-dependent enhancement of viral infection: molecular mechanisms and in vivo implications. *Rev Med Virol.* 2003;13:387–98.
 107. Kam YW, Kien F, Roberts A, Cheung YC, Lamirande EW, Vogel L, et al. Antibodies against trimeric S glycoprotein protect hamsters against SARS-CoV challenge despite their capacity to mediate FcγRII-dependent entry into B cells in vitro. *Vaccine.* 2007;25:729–40.
 108. Yip MS, Leung NH, Cheung CY, Li PH, Lee HH, Daëron M, et al. Antibody-dependent infection of human macrophages by severe acute respiratory syndrome coronavirus. *Virology.* 2014;11:82.
 109. Agrawal AS, Tao X, Algaissi A, Garron T, Narayanan K, Peng BH, et al. Immunization with inactivated Middle East Respiratory Syndrome coronavirus vaccine leads to lung immunopathology on challenge with live virus. *Hum Vaccin Immunother.* 2016;12(9):2351–6.
 110. Vennema H, De Groot R, Harbour D, Dalderup M, Gruffydd-Jones T, Horzinek M, Spaan W. Early death after feline infectious peritonitis virus challenge due to recombinant vaccinia virus immunization. *J Virol.* 1990;64:1407–9.
 111. Takada A, Watanabe S, Okazaki K, Kida H, Kawaoka Y. Infectivity-enhancing antibodies to Ebola virus glycoprotein. *J Virol.* 2001;75:2324–30.
 112. Beck Z, Prohászka Z, Füst G. Traitors of the immune system—enhancing antibodies in HIV infection: their possible implication in HIV vaccine development. *Vaccine.* 2008;26:3078–85.
 113. Negro F. Is antibody-dependent enhancement playing a role in COVID-19 pathogenesis? *Swiss Med Wkly.* 2020;150:w20249.
 114. Wu F, Yan R, Liu M, Liu Z, Wang Y, Luan D, et al. Antibody-dependent enhancement (ADE) of SARS-CoV-2 infection in recovered COVID-19 patients: studies based on cellular and structural biology analysis. *MedRxiv.* 2020. <https://doi.org/10.1101/2020.10.08.20209114>.
 115. Kaufmann SH. Immunology's foundation: the 100-year anniversary of the Nobel Prize to Paul Ehrlich and Elie Metchnikoff. *Nature Immunol.* 2008;9:705–12.
 116. Ehrlich P. Experimentelle untersuchungen über immunität. I. Ueber ricin. *DMW-Deutsche Medizinische Wochenschrift.* 1981;17:976–9.
 117. Muhammed Y. The best IgG subclass for the development of therapeutic monoclonal antibody drugs and their commercial production: a review. *Immunome Res.* 2020;16:1–12.
 118. Le Basle Y, Chennell P, Tokhadze N, Astier A, Sautou V. Physico-chemical stability of monoclonal antibodies: a review. *J Pharm Sci.* 2020;109(1):169–90.
 119. Harris R. Heterogeneity of recombinant antibodies: linking structure to function. Mire-Sluis AR, editor. State of the art analytical methods for the characterization of biological. Products and assessment of comparability. (Dev Biol, Basel, Karger, 2005, vol 122, pp 117–127; 2005).
 120. Arakawa S, Suzukawa M, Watanabe K, Kobayashi K, Matsui H, Nagai H, et al. Secretory immunoglobulin A induces human lung fibroblasts to produce inflammatory cytokines and undergo activation. *Clin Exp Immunol.* 2019;195(3):287–301.
 121. Yu HQ, Sun BQ, Fang ZF, Zhao JC, Liu XY, Li YM, et al. Distinct features of SARS-CoV-2-specific IgA response in COVID-19 patients. *Eur Respir J.* 2020;56(2):2001526.
 122. Gutzeit C, Chen K, Cerutti A. The enigmatic function of IgD: some answers at last. *Eur J Immunol.* 2018;48(7):1101–13.
 123. Chen K, Xu W, Wilson M, He B, Miller NW, Bengtén E, et al. Immunoglobulin D enhances immune surveillance by activating antimicrobial, proinflammatory and B cell-stimulating programs in basophils. *Nat Immunol.* 2009;10(8):889–98.
 124. Pier GB, Lyczak JB, Wetzler LM. Immunology, infection, and immunity. Washington: ASM press; 2004.
 125. Vidarsson G, Dekkers G, Rispens T. IgG subclasses and allotypes: from structure to effector functions. *Front Immunol.* 2014;5:520.
 126. Zinkernagel RM, LaMarre A, Ciurea A, Hunziker L, Ochsenbein AF, McCoy KD, et al. Neutralizing antiviral antibody responses. *Adv Immunol.* 2001;79:1–53.
 127. Guo L, Ren L, Yang S, Xiao M, Chang D, Yang F, et al. Profiling early humoral response to diagnose novel coronavirus disease (COVID-19). *Clin Infect Dis.* 2020;71(15):778–85.
 128. Long QX, Liu BZ, Deng HJ, Wu CG, Deng K, Chen YK, et al. Antibody responses to SARS-CoV-2 in patients with COVID-19. *Nat Med.* 2020;26(6):845–8.
 129. Padoan A, Sciacovelli L, Basso D, Negrini D, Zuin S, Cosma C, et al. IgA-Ab response to spike glycoprotein of SARS-CoV-2 in patients with COVID-19: a longitudinal study. *Clin Chim Acta.* 2020;507:164–6.
 130. Fourati S, Hue S, Pawlotsky JM, Mekontso-Dessap A, de Prost N. SARS-CoV-2 viral loads and serum IgA/IgG immune responses in critically ill COVID-19 patients. *Intensive Care Med.* 2020;46(9):1781–3.
 131. Lu LL, Suscovich TJ, Fortune SM, Alter G. Beyond binding: antibody effector functions in infectious diseases. *Nat Rev Immunol.* 2018;18:46.
 132. Natarajan H, Crowley AR, Butler SE, Xu S, Weiner JA, Bloch EM, et al. SARS-CoV-2 antibody signatures robustly predict diverse antiviral functions relevant for convalescent plasma therapy. *medRxiv.* 2020. <https://doi.org/10.1101/2020.09.16.20196154>.
 133. Schroeder HW Jr, Cavacini L. Structure and function of immunoglobulins. *J Allergy Clin Immunol.* 2010;125(2 Suppl 2):S41–52.
 134. Ni L, Ye F, Cheng ML, Feng Y, Deng YQ, Zhao H, et al. Detection of SARS-CoV-2-specific humoral and cellular immunity in COVID-19 convalescent individuals. *Immunity.* 2020;52(6):971–7.e3.
 135. Ju B, Zhang Q, Ge J, Wang R, Sun J, Ge X, et al. Human neutralizing antibodies elicited by SARS-CoV-2 infection. *Nature.* 2020;584(7819):115–9.
 136. Brouwer PJM, Caniels TG, van der Straten K, Snitselaar JL, Aldon Y, Bangaru S, et al. Potent neutralizing antibodies from COVID-19 patients define multiple targets of vulnerability. *Science.* 2020;369(6504):643–50.
 137. Kreer C, Zehner M, Weber T, Ercanoglu MS, Gieselmann L, Rohde C, et al. Longitudinal isolation of potent near-germline SARS-CoV-2-neutralizing antibodies from COVID-19 patients. *Cell.* 2020;182(4):843–54.e12.
 138. Barnes CO, West AP Jr, Huey-Tubman KE, Hoffmann MAG, Sharaf NG, Hoffman PR, et al. Structures of human antibodies bound to

- SARS-CoV-2 spike reveal common epitopes and recurrent features of antibodies. *Cell*. 2020;182(4):828–42.e16.
139. Shu H, Wang S, Ruan S, Wang Y, Zhang J, Yuan Y, et al. Dynamic changes of antibodies to SARS-CoV-2 in COVID-19 patients at early stage of outbreak. *Viral Sin*. 2020;27:1–8.
 140. Du S, Cao Y, Zhu Q, Wang G, Du X, He R, et al. Structures of potent and convergent neutralizing antibodies bound to the SARS-CoV-2 spike unveil a unique epitope responsible for exceptional potency. *bioRxiv*. 2020. <https://doi.org/10.1101/2020.07.09.195263>.
 141. Chi X, Yan R, Zhang J, Zhang G, Zhang Y, Hao M, et al. A neutralizing human antibody binds to the N-terminal domain of the spike protein of SARS-CoV-2. *Science*. 2020;369(6504):650–5.
 142. Robbiani DF, Gaebler C, Muecksch F, Lorenzi JCC, Wang Z, Cho A, et al. Convergent antibody responses to SARS-CoV-2 in convalescent individuals. *Nature*. 2020;584(7821):437–42.
 143. Zost SJ, Gilchuk P, Chen RE, Case JB, Reidy JX, Trivette A, et al. Rapid isolation and profiling of a diverse panel of human monoclonal antibodies targeting the SARS-CoV-2 spike protein. *Nat Med*. 2020;26(9):1422–7.
 144. Seydoux E, Homad LJ, MacCamy AJ, Parks KR, Hurlburt NK, Jennewein MF, et al. Analysis of a SARS-CoV-2-infected individual reveals development of potent neutralizing antibodies with limited somatic mutation. *Immunity*. 2020;53(1):98–105.e5.
 145. Hansen J, Baum A, Pascal KE, Russo V, Giordano S, Wloga E, et al. Studies in humanized mice and convalescent humans yield a SARS-CoV-2 antibody cocktail. *Science*. 2020;369(6506):1010–4.
 146. Wu Y, Wang F, Shen C, Peng W, Li D, Zhao C, et al. A noncompeting pair of human neutralizing antibodies block COVID-19 virus binding to its receptor ACE2. *Science*. 2020;368(6496):1274–8.
 147. Shen C, Wang Z, Zhao F, Yang Y, Li J, Yuan J, et al. Treatment of 5 critically ill patients with COVID-19 with convalescent plasma. *JAMA*. 2020;323(16):1582–9.
 148. Zeng QL, Yu ZJ, Gou JJ, Li GM, Ma SH, Zhang GF, et al. Effect of convalescent plasma therapy on viral shedding and survival in patients with coronavirus disease 2019. *J Infect Dis*. 2020;222(1):38–43.
 149. Zhang B, Liu S, Tan T, Huang W, Dong Y, Chen L, et al. Treatment with convalescent plasma for critically ill patients with severe acute respiratory syndrome coronavirus 2 infection. *Chest*. 2020;158(1):e9–13.
 150. Ye M, Fu D, Ren Y, Wang F, Wang D, Zhang F, Xia X, Lv T. Treatment with convalescent plasma for COVID-19 patients in Wuhan. *China J Med Virol*. 2020;92(10):1890–901.
 151. Ahn JY, Sohn Y, Lee SH, Cho Y, Hyun JH, Baek YJ, et al. Use of convalescent plasma therapy in two COVID-19 patients with acute respiratory distress syndrome in Korea. *J Korean Med Sci*. 2020;35(14):e149.
 152. Duan K, Liu B, Li C, Zhang H, Yu T, Qu J, et al. Effectiveness of convalescent plasma therapy in severe COVID-19 patients. *Proc Natl Acad Sci USA*. 2020;117(17):9490–6.
 153. Li L, Zhang W, Hu Y, Tong X, Zheng S, Yang J, et al. Effect of convalescent plasma therapy on time to clinical improvement in patients with severe and life-threatening COVID-19: a randomized clinical trial. *JAMA*. 2020;324(5):460–70.
 154. Salazar E, Kuchipudi SV, Christensen PA, Eagar TN, Yi X, Zhao P, et al. Relationship between anti-spike protein antibody titers and SARS-CoV-2 in vitro virus neutralization in convalescent plasma. *bioRxiv*. 2020. <https://doi.org/10.1101/2020.06.08.138990>.
 155. Perotti C, Baldanti F, Bruno R, del Fante C, Seminari E, Casari S, et al. Covid-19 plasma task force, Mortality reduction in 46 severe Covid-19 patients treated with hyperimmune plasma. A proof of concept single arm multicenter trial. *Haematologica*. 2020; 23:haematol.2020.261784.
 156. Ibrahim D, Dulipsingh L, Zapatka L, Eadie R, Crowell R, Williams K, et al. Factors associated with good patient outcomes following convalescent plasma in COVID-19: a prospective phase II clinical trial. *Infect Dis Ther*. 2020;20:1–14.
 157. Abolghasemi H, Eshghi P, Cheraghali AM, Imani Fooladi AA, Bolouki Moghaddam F, Imanizadeh S, et al. Clinical efficacy of convalescent plasma for treatment of COVID-19 infections: results of a multicenter clinical study. *Transf Apher Sci*. 2020;59(5):102875.
 158. Hegerova L, Gooley TA, Sweerus KA, Maree C, Bailey N, Bailey M, et al. Use of convalescent plasma in hospitalized patients with COVID-19: case series. *Blood*. 2020;136(6):759–62.
 159. Liu STH, Lin HM, Baine I, Wajnberg A, Gumprecht JP, Rahman F, et al. Convalescent plasma treatment of severe COVID-19: a propensity score-matched control study. *Nat Med*. 2020;26(11):1708–13.
 160. Xia X, Li K, Wu L, Wang Z, Zhu M, Huang B, et al. Improved clinical symptoms and mortality among patients with severe or critical COVID-19 after convalescent plasma transfusion. *Blood*. 2020;136(6):755–9.
 161. Joyner MJ, Wright RS, Fairweather D, Senefeld JW, Bruno KA, Klassen SA, et al. Early safety indicators of COVID-19 convalescent plasma in 5000 patients. *J Clin Invest*. 2020;130(9):4791–7.
 162. Hartman WR, Hess AS, Connor JP. Hospitalized COVID-19 patients treated with convalescent plasma in a mid-size city in the Midwest. *Transl Med Commun*. 2020;5(1):17.
 163. Brown BL, McCullough J. Treatment for emerging viruses: convalescent plasma and COVID-19. *Transf Apher Sci*. 2020;59(3):102790.
 164. Luke TC, Kilbane EM, Jackson JL, Hoffman SL. Meta-analysis: convalescent blood products for Spanish influenza pneumonia: a future H5N1 treatment? *Ann Intern Med*. 2006;145(8):599–609.
 165. Cheng Y, Wong R, Soo YO, Wong WS, Lee CK, Ng MH, et al. Use of convalescent plasma therapy in SARS patients in Hong Kong. *Eur J Clin Microbiol Infect Dis*. 2005;24(1):44–6.
 166. Focosi D, Anderson AO, Tang JW, Tuccori M. Convalescent plasma therapy for COVID-19: state of the art. *Clin Microbiol Rev*. 2020;33(4):e00072–e120.
 167. Cunningham AC, Goh HP, Koh D. Treatment of COVID-19: old tricks for new challenges. *Crit Care*. 2020;24(1):91.
 168. Arabi YM, Hajeer AH, Luke T, Raviprakash K, Balkhy H, Johani S, et al. Feasibility of using convalescent plasma immunotherapy for MERS-CoV Infection. *Saudi Arabia Emerg Infect Dis*. 2016;22(9):1554–61.
 169. Klein SL, Pekosz A, Park HS, Ursin RL, Shapiro JR, Benner SE, et al. Sex, age, and hospitalization drive antibody responses in a COVID-19 convalescent plasma donor population. *J Clin Invest*. 2020;130(11):6141–50.
 170. Franchini M, Marano G, Velati C, Pati I, Pupella S, Liumbardo GM. Operational protocol for donation of anti-COVID-19 convalescent plasma in Italy. *Vox Sang*. 2020. <https://doi.org/10.1111/vox.12940>.
 171. Mair-Jenkins J, Saavedra-Campos M, Baillie JK, Cleary P, Khaw FM, Lim WS, et al. The effectiveness of convalescent plasma and hyperimmune immunoglobulin for the treatment of severe acute respiratory infections of viral etiology: a systematic review and exploratory meta-analysis. *J Infect Dis*. 2015;211(1):80–90.
 172. Lung T, Kazatchkine MD, Risch L, Risch M, Nydegger UE. A consideration of convalescent plasma and plasma derivatives in the care of Severely-ill patients with COVID-19. *Transfus Apher Sci*. 2020;59(5):102936.
 173. Singh N, Pandey A. Blood plasma from survivors of COVID-19: a novel and next frontier approach to fight against pandemic coronavirus. *Int J Immunol Immunother*. 2020;7:045.
 174. Lee WT, Girardin RC, Dupuis AP, Kulas KE, Payne AF, Wong SJ, et al. Neutralizing antibody responses in COVID-19 convalescent sera. *J Infect Dis*. 2021;223(1):47–55.
 175. Girardin RC, Dupuis AP, Payne AF, Sullivan TJ, Strauss D, Parker MM, McDonough KA. Temporal analysis of serial donations reveals decrease in neutralizing capacity and justifies revised qualifying criteria for COVID-19 convalescent plasma. *J Inf Dis*. 2021. <https://doi.org/10.1093/infdis/jiaa803>.
 176. Shanmugaraj B, Siri wattananon K, Wangkanont K, Phoolcharoen W. Perspectives on monoclonal antibody therapy as potential therapeutic intervention for Coronavirus disease-19 (COVID-19). *Asian Pac J Allergy Immunol*. 2020;38(1):10–8.
 177. Hassan AO, Case JB, Winkler ES, Thackray LB, Kafai NM, Bailey AL, et al. A SARS-CoV-2 infection model in mice demonstrates protection by neutralizing antibodies. *Cell*. 2020;182(3):744–753.e4.
 178. Piccoli L, Park YJ, Tortorici MA, Czudnochowski N, Walls AC, Beltramello M, et al. Mapping neutralizing and immunodominant sites on the SARS-CoV-2 Spike Receptor-Binding Domain by structure-guided high-resolution serology. *Cell*. 2020;183(4):1024–1042.e21.
 179. Bracken CJ, Lim SA, Solomon P, Rettko NJ, Nguyen DP, Zha BS, et al. Biparatopic and multivalent VH domains block ACE2 binding and neutralize SARS-CoV-2. *Nat Chem Biol*. 2021;17:113–21.
 180. Clark SA, Clark LE, Pan J, Coscia A, McKay LGA, Shankar S, et al. Molecular basis for a germline-biased neutralizing antibody response to SARS-CoV-2. *bioRxiv*. 2020. <https://doi.org/10.1101/2020.11.13.381533>.

181. El Debs B, Utharala R, Balyasnikova IV, Griffiths AD, Merten CA. Functional single-cell hybridoma screening using droplet-based microfluidics. *Proc Natl Acad Sci USA*. 2012;109(29):11570–5.
182. Niu X, Zhao L, Qu L, Yao Z, Zhang F, Yan Q. Convalescent patient-derived monoclonal antibodies targeting different epitopes of E protein confer protection against Zika virus in a neonatal mouse model. *Emerg Microbes Infect*. 2019;8(1):749–59.
183. Walker LM, Phogat SK, Chan-Hui PY, Wagner D, Phung P, Goss JL, et al. Broad and potent neutralizing antibodies from an African donor reveal a new HIV-1 vaccine target. *Science*. 2009;326(5950):285–9.
184. McCallum M, Walls AC, Bowen JE, Corti D, Veessler D. Structure-guided covalent stabilization of coronavirus spike glycoprotein trimers in the closed conformation. *Nat Struct Mol Biol*. 2020;27(10):942–9.
185. Duan L, Zheng Q, Zhang H, Niu Y, Lou Y, Wang H. The SARS-CoV-2 spike glycoprotein biosynthesis, structure, function, and antigenicity: implications for the design of spike-based vaccine immunogens. *Front Immunol*. 2020;11:576622.
186. Sternberg A, Naujokat C. Structural features of coronavirus SARS-CoV-2 spike protein: targets for vaccination. *Life Sci*. 2020;257:118056.
187. Zhang T, Wu Q, Zhang Z. Probable pangolin origin of SARS-CoV-2 associated with the COVID-19 outbreak. *Curr Biol*. 2020;30(7):1346–1351.e2. [Erratum in: *Curr Biol*. 2020;30(8):1578].
188. Wrapp D, Wang N, Corbett KS, Goldsmith JA, Hsieh CL, Abiona O, et al. Cryo-EM structure of the 2019-nCoV spike in the prefusion conformation. *Science*. 2020;367(6483):1260–3.
189. Xu C, Wang Y, Liu C, Zhang C, Han W, Hong X, et al. Conformational dynamics of SARS-CoV-2 trimeric spike glycoprotein in complex with receptor ACE2 revealed by cryo-EM. *Sci Adv*. 2020;7:eabe5575.
190. Henderson R, Edwards RJ, Mansouri K, Janowska K, Stalls V, Gobeil SMC, et al. Controlling the SARS-CoV-2 spike glycoprotein conformation. *Nat Struct Mol Biol*. 2020;27(10):925–33.
191. Bruhns P, Iannascoli B, England P, Mancardi DA, Fernandez N, Jorieux S, Daéron M. Specificity and affinity of human Fcγ receptors and their polymorphic variants for human IgG subclasses. *Blood*. 2009;113(16):3716–25.
192. Walls AC, Park YJ, Tortorici MA, Wall A, McGuire AT, Veessler D. Structure, function, and antigenicity of the SARS-CoV-2 spike glycoprotein. *Cell*. 2020;181(2):281–292.e6. [Erratum in: *Cell* 2020;183(6):1735]
193. Yu F, Xiang R, Deng X, Wang L, Yu Z, Tian S, et al. Receptor-binding domain-specific human neutralizing monoclonal antibodies against SARS-CoV and SARS-CoV-2. *Signal Transduct Target Ther*. 2020;5(1):212.
194. Barnes CO, Jette CA, Abernathy ME, Dam KA, Esswein SR, Gristick HB, et al. SARS-CoV-2 neutralizing antibody structures inform therapeutic strategies. *Nature*. 2020;588(7839):682–7.
195. Lu R, Zhao X, Li J, Niu P, Yang B, Wu H, et al. Genomic characterisation and epidemiology of 2019 novel coronavirus: implications for virus origins and receptor binding. *Lancet*. 2020;395(10224):565–74.
196. Rujas E, Kucharska I, Tan YZ, Benlekber S, Cui H, Zhao T, et al. Multivalency transforms SARS-CoV-2 antibodies into broad and ultrapotent neutralizers. *bioRxiv*. 2020. <https://doi.org/10.1101/2020.10.15.341636>.
197. Prabakaran P, Gan J, Feng Y, Zhu Z, Choudhry V, Xiao X, et al. Structure of severe acute respiratory syndrome coronavirus receptor-binding domain complexed with neutralizing antibody. *J Biol Chem*. 2006;281(23):15829–36.
198. Hwang WC, Lin Y, Santelli E, Sui J, Jaroszewski L, Stec B, et al. Structural basis of neutralization by a human anti-severe acute respiratory syndrome spike protein antibody, 80R. *J Biol Chem*. 2006;281(45):34610–6.
199. Acharya P, Williams W, Henderson R, Janowska K, Manne K, Parks R, et al. A glycan cluster on the SARS-CoV-2 spike ectodomain is recognized by Fab-dimerized glycan-reactive antibodies. *bioRxiv*. 2020. <https://doi.org/10.1101/2020.06.30.178897>.
200. Jones BE, Brown-Augsburger PL, Corbett KS, Westendorp K, Davies J, Cujec TP, et al. LY-CoV555, a rapidly isolated potent neutralizing antibody, provides protection in a non-human primate model of SARS-CoV-2 infection. *bioRxiv*. 2020. <https://doi.org/10.1101/2020.09.30.318972>.
201. Baum A, Fulton BO, Wloga E, Copin R, Pascal KE, Russo V, et al. Antibody cocktail to SARS-CoV-2 spike protein prevents rapid mutational escape seen with individual antibodies. *Science*. 2020;369(6506):1014–8.
202. Chen P, Nirula A, Heller B, Gottlieb RL, Boscia J, Morris J, et al. SARS-CoV-2 neutralizing antibody LY-CoV555 in outpatients with Covid-19. *N Engl J Med*. 2021;384(3):229–37.
203. ACTIV-3/TICO LY-CoV555 Study Group, Lundgren JD, Grund B, Barkauskas CE, Holland TL, Gottlieb RL, et al. A neutralizing monoclonal antibody for hospitalized patients with Covid-19. *N Engl J Med*. 2021;384(10):905–14.
204. Shi R, Shan C, Duan X, Chen Z, Liu P, Song J, et al. A human neutralizing antibody targets the receptor-binding site of SARS-CoV-2. *Nature*. 2020;584(7819):120–4.
205. Liu L, Wang P, Nair MS, Yu J, Rapp M, Wang Q. Potent neutralizing antibodies against multiple epitopes on SARS-CoV-2 spike. *Nature*. 2020;584(7821):450–6.
206. Rapp M, Guo Y, Reddem ER, Liu L, Wang P, Yu J, et al. Modular basis for potent SARS-CoV-2 neutralization by a prevalent VH1-2-derived antibody class. *Cell Rep*. 2021. <https://doi.org/10.1016/j.celrep.2021.108950>.
207. Cerutti G, Guo Y, Zhou T, Gorman J, Lee M, Rapp M, et al. Potent SARS-CoV-2 neutralizing antibodies directed against spike N-terminal domain target a single supersite. *Cell Host Microbe*. 2021. <https://doi.org/10.1016/j.chom.2021.03.005>.
208. Zost SJ, Gilchuk P, Case JB, Binshtein E, Chen RE, Nkolola JP, et al. Potently neutralizing and protective human antibodies against SARS-CoV-2. *Nature*. 2020;584(7821):443–9.
209. Li W, Schäfer A, Kulkarni SS, Liu X, Martinez DR, Chen C, et al. High potency of a bivalent human VH domain in SARS-CoV-2 animal models. *Cell*. 2020;183(2):429–441.e16.
210. Zhang C, Wang Y, Zhu Y, Liu C, Gu C, Xu S, et al. Development and structural basis of a two-MAB cocktail for treating SARS-CoV-2 infections. *Nat Commun*. 2021;12(1):264.
211. Korber B, Fischer WM, Gnanakaran S, Yoon H, Theiler J, Abfalterer W, et al. Tracking changes in SARS-CoV-2 Spike: evidence that D614G increases infectivity of the COVID-19 virus. *Cell*. 2020;182(4):812–827.e19.
212. Bertoglio F, Fühner V, Ruschig M, Heine PA, Rand U, Klünemann T, et al. A SARS-CoV-2 neutralizing antibody selected from COVID-19 patients by phage display is binding to the ACE2-RBD interface and is tolerant to known RBD mutations. *bioRxiv*. 2020. <https://doi.org/10.1101/2020.12.03.409318>.
213. Yao H, Sun Y, Deng YQ, Wang N, Tan Y, Zhang NN, et al. Rational development of a human antibody cocktail that deploys multiple functions to confer Pan-SARS-CoVs protection. *Cell Res*. 2021;31:25–36.
214. Wan J, Xing S, Ding L, Wang Y, Gu C, Wu Y, et al. Human-IgG-neutralizing monoclonal antibodies block the SARS-CoV-2 infection. *Cell Rep*. 2020;32(3):107918.
215. Shervani Z, Khan I, Khan T, Qazi UY. World's fastest supercomputer picks COVID-19 drug. *Adv Infect Dis*. 2020;10(3):211.
216. Bournazos S, Ravetch JV. Anti-retroviral antibody FcγR-mediated effector functions. *Immunol Rev*. 2017;275(1):285–95.
217. Shields RL, Namenuk AK, Hong K, Meng YG, Rae J, Briggs J, et al. High resolution mapping of the binding site on human IgG1 for FcγRI, FcγRII, FcγRIII, and FcRn and design of IgG1 variants with improved binding to the FcγRIII. *J Biol Chem*. 2001;276(9):6591–604.
218. Wang B, Yang C, Jin X, Du Q, Wu H, Dall'Acqua W, Mazor Y. Regulation of antibody-mediated complement-dependent cytotoxicity by modulating the intrinsic affinity and binding valency of IgG for target antigen. *MAbs*. 2020;12(1):1690959.
219. Popp O, Moser S, Zielonka J, Rieger P, Hansen S, Plöttner O. Development of a pre-glycoengineered CHO-K1 host cell line for the expression of antibodies with enhanced Fc mediated effector function. *MAbs*. 2018;10(2):290–303.
220. Krammer F, Palese P, Steel J. Advances in universal influenza virus vaccine design and antibody mediated therapies based on conserved regions of the hemagglutinin. *Curr Top Microbiol Immunol*. 2015;386:301–21.
221. Shields RL, Lai J, Keck R, Oconnell LY, Hong K, Meng YG, et al. Lack of fucose on human IgG1 N-linked oligosaccharide improves binding to human FcγRIII and antibody-dependent cellular toxicity. *J Biol Chem*. 2002;277(30):26733–40.
222. Shinkawa T, Nakamura K, Yamane N, Shoji-Hosaka E, Kanda Y, Sakurada M, et al. The absence of fucose but not the presence of galactose or bisecting N-acetylglucosamine of human IgG1 complex-type

- oligosaccharides shows the critical role of enhancing antibody-dependent cellular cytotoxicity. *J Biol Chem*. 2003;278:3466–73.
223. Tortorici MA, Beltramello M, Lempp FA, Pinto D, Dang HV, Rosen LE, et al. Ultrapotent human antibodies protect against SARS-CoV-2 challenge via multiple mechanisms. *Science*. 2020;370(6519):0950–7.
 224. Köhler G, Milstein C. Continuous cultures of fused cells secreting antibody of predefined specificity. *Nature*. 1975;256(5517):495–7.
 225. Kwakkenbos MJ, van Helden PM, Beaumont T, Spits H. Stable long-term cultures of self-renewing B cells and their applications. *Immunol Rev*. 2016;270(1):65–77.
 226. Listek M, Hönow A, Gossen M, Hanack K. A novel selection strategy for antibody producing hybridoma cells based on a new transgenic fusion cell line. *Sci Rep*. 2020;10(1):1664.
 227. Ejemel M, Li Q, Hou S, Schiller ZA, Tree JA, Wallace A, et al. A cross-reactive human IgA monoclonal antibody blocks SARS-CoV-2 spike-ACE2 interaction. *Nat Commun*. 2020;11(1):4198.
 228. Antipova NV, Larionova TD, Siniavin AE, Nikiforova MA, Gushchin VA, Babichenko II, et al. Establishment of murine hybridoma cells producing antibodies against spike protein of SARS-CoV-2. *Int J Mol Sci*. 2020;21(23):9167.
 229. Guo Y, Kawaguchi A, Takeshita M, Sekiya T, Hirohama M, et al. Potent mouse monoclonal antibodies that block SARS-CoV-2 infection. *J Biol Chem*. 2021;296:100346.
 230. Chapman AP, Tang X, Lee JR, Chida A, Mercer K, Wharton RE, et al. Rapid development of neutralizing and diagnostic SARS-CoV-2 mouse monoclonal antibodies. *bioRxiv*. 2020. <https://doi.org/10.1101/2020.10.13.338095>.
 231. Menachery VD, Yount BL Jr, Debbink K, Agnihothram S, Gralinski LE, Plante JA, et al. A SARS-like cluster of circulating bat coronaviruses shows potential for human emergence. *Nat Med*. 2015;21(12):1508–13. [Erratum in: *Nat Med* 2016;22(4):446].
 232. Ma Z, Li P, Ikram A, Pan Q. Does cross-neutralization of SARS-CoV-2 only relate to high pathogenic coronaviruses? *Trends Immunol*. 2020;41(10):851–3.
 233. Hamers-Casterman C, Atarhouch T, Muyldermans S, Robinson G, Hamers C, Songa EB, et al. Naturally occurring antibodies devoid of light chains. *Nature*. 1993;363(6428):446–8.
 234. Nuttall SD, Krishnan UV, Hattarki M, De Gori R, Irving RA, Hudson PJ. Isolation of the new antigen receptor from wobbegong sharks, and use as a scaffold for the display of protein loop libraries. *Mol Immunol*. 2001;38(4):313–26.
 235. Lee CM, Iorno N, Sierro F, Christ D. Selection of human antibody fragments by phage display. *Nat Protoc*. 2007;2(11):3001–8.
 236. Chames P, Rothbauer U. Special Issue: Nanobody. *Antibodies (Basel)*. 2020;9(1):6.
 237. Morrison C. Nanobody approval gives domain antibodies a boost. *Nat Rev Drug Discov*. 2019;18(7):485–8.
 238. Wrapp D, De Vlieger C, Corbett KS, Torres GM, Wang N, Van Breedam W, et al. Structural basis for potent neutralization of Betacoronaviruses by single-domain camelid antibodies. *Cell* 2020;181(5):1004–1015.e15. [Erratum in: *Cell* 2020;181(6):1436–1441].
 239. Boudewijns R, Thibaut HJ, Kaptein SJF, Li R, Vergote V, Seldeslachts L, Van Weyenbergh J, et al. STAT2 signaling restricts viral dissemination but drives severe pneumonia in SARS-CoV-2 infected hamsters. *Nat Commun*. 2020;11(1):5838.
 240. Esparza TJ, Martin NP, Anderson GP, Goldman ER, Brody DL. High affinity nanobodies block SARS-CoV-2 spike receptor binding domain interaction with human angiotensin converting enzyme. *Sci Rep*. 2020;10(1):22370.
 241. Valenzuela Nieto G, Jara R, Watterson D, Modhiran N, Amarilla AA, Himelreichs J, et al. Potent neutralization of clinical isolates of SARS-CoV-2 D614 and G614 variants by a monomeric, sub-nanomolar affinity nanobody. *Sci Rep*. 2021;11:3318.
 242. Hanke L, Vidakovic Perez L, Sheward DJ, Das H, Schulte T, Moliner-Morro A, et al. An alpaca nanobody neutralizes SARS-CoV-2 by blocking receptor interaction. *Nat Commun*. 2020;11(1):4420.
 243. Moliner-Morro A, Sheward D, Karl V, Perez Vidakovic L, Murrell B, McNerney GM, Hanke L. Picomolar SARS-CoV-2 neutralization using multi-arm PEG nanobody constructs. *Biomolecules*. 2020;10(12):1661.
 244. Wagner TR, Kaiser PD, Gramlich M, Becker M, Traenkle B, Junker D, et al. NeutrobodyPlex-Nanobodies to monitor a SARS-CoV-2 neutralizing immune response. *bioRxiv*. 2020. <https://doi.org/10.1101/2020.09.22.308338>.
 245. Xiang Y, Nambulli S, Xiao Z, Liu H, Sang Z, Duprex WP, et al. Versatile and multivalent nanobodies efficiently neutralize SARS-CoV-2. *Science*. 2020;370(6523):1479–84.
 246. Gai J, Ma L, Li G, Zhu M, Qiao P, Li X, et al. A potent neutralizing nanobody against SARS-CoV-2 with inhaled delivery potential. *MedComm*. 2021;2:101–13.
 247. Zimmermann I, Egloff P, Hutter CAJ, Kuhn BT, Bräuer P, Newstead S, et al. Seeger, generation of synthetic nanobodies against delicate proteins. *Nat Protoc*. 2020;15(5):1707–41.
 248. Walter JD, Hutter CAJ, Zimmermann I, Earp J, Egloff P, Sorgenfrei M, et al. Synthetic nanobodies targeting the SARS-CoV-2 receptor-binding domain. *bioRxiv*. 2020. <https://doi.org/10.1101/2020.04.16.045419>.
 249. Li T, Cai H, Yao H, Zhou B, Zhang N, Gong Y, et al. A potent synthetic nanobody targets RBD and protects mice from SARS-CoV-2 infection. *bioRxiv*. 2020. doi.org/<https://doi.org/10.21203/rs.3.rs-75540/v1>. PPR:PPR218472.
 250. Custódio TF, Das H, Sheward DJ, Hanke L, Pazicky S, Pieprzyk J, et al. Selection, biophysical and structural analysis of synthetic nanobodies that effectively neutralize SARS-CoV-2. *Nat Commun*. 2020;11(1):5588.
 251. Yao H, Cai H, Li T, Zhou B, Qin W, Lavillette D, Li D. A high-affinity RBD-targeting nanobody improves fusion partner's potency against SARS-CoV-2. *PLoS pathog*. 2021;17(3):e1009328.
 252. Schoof M, Faust B, Saunders RA, Sangwan S, Rezelj V, Hoppe N, et al. An ultra-high affinity synthetic nanobody blocks SARS-CoV-2 infection by locking Spike into an inactive conformation. *bioRxiv*. 2020. <https://doi.org/10.1101/2020.08.08.238469>.
 253. Dong J, Huang B, Wang B, Titong A, Gallolu Kankanamalage S, Jia Z, et al. Development of humanized tri-specific nanobodies with potent neutralization for SARS-CoV-2. *Sci Rep*. 2020;10(1):17806.
 254. Dong J, Huang B, Jia Z, Wang B, Gallolu Kankanamalage S, Titong A, Liu Y. Development of multi-specific humanized llama antibodies blocking SARS-CoV-2/ACE2 interaction with high affinity and avidity. *Emerg Microbes Infect*. 2020;9(1):1034–6.
 255. Ye G, Gallant JP, Massey C, Shi K, Tai W, Zheng J, et al. The development of a novel nanobody therapeutic for SARS-CoV-2. *bioRxiv*. 2020. <https://doi.org/10.1101/2020.11.17.386532>.
 256. Wu Y, Li C, Xia S, Tian X, Kong Y, Wang Z, et al. Ying, Identification of human single-domain antibodies against SARS-CoV-2. *Cell Host Microbe*. 2020;27(6):891–898.e5.
 257. Chi X, Liu X, Wang C, Zhang X, Li X, Hou J, et al. Humanized single domain antibodies neutralize SARS-CoV-2 by targeting the spike receptor binding domain. *Nat Commun*. 2020;11(1):4528.
 258. Sun Z, Chen C, Li W, Martinez DR, Drelich A, Baek DS, et al. Potent neutralization of SARS-CoV-2 by human antibody heavy-chain variable domains isolated from a large library with a new stable scaffold. *MABs*. 2020;12(1):1778435.
 259. Kaplon H. Reichert Antibodies to watch in 2021. *MABs*. 2021;13:1.
 260. Al-Rubeai M. Antibody expression and production. *Cell engineering*, vol. 7; 2007.
 261. Bandaranayake AD, Almo SC. Recent advances in mammalian protein production. *FEBS Lett*. 2014;588(2):253–60.
 262. Walsh G. Biopharmaceutical benchmarks 2018. *Nat Biotechnol*. 2018;36(12):1136–45.
 263. Jayapal KP, Wlaschin KF, Hu WS, Yap MGS. Recombinant protein therapeutics from CHO cells—20 years and counting. *Chem Eng Prog*. 2007;103(10):40–7.
 264. Wurm FM, Wurm MJ. Cloning of CHO cells, productivity and genetic stability—a discussion. *Processes*. 2017;5(2):20.
 265. Sharker SM, Rahman MA. Review of the current methods of Chinese Hamster Ovary (CHO) cells cultivation for production of therapeutic protein. *Curr Drug Discov Technol*. 2020;17:1.
 266. Kuo CC, Chiang AW, Shamie I, Samoudi M, Gutierrez JM, Lewis NE. The emerging role of systems biology for engineering protein production in CHO cells. *Curr Opin Biotechnol*. 2018;51:64–9.
 267. Sarsaiya S, Shi J, Che J. Bioengineering tools for the production of pharmaceuticals: current perspective and future outlook. *Bioengineered*. 2019;10:469–92.

268. Pérez-Rodríguez S, Ramírez-Lira MJ, Trujillo-Roldán MA, Valdez-Cruz NA. Nutrient supplementation strategy improves cell concentration and longevity, monoclonal antibody production and lactate metabolism of Chinese hamster ovary cells. *Bioengineered*. 2020;11(1):463–71.
269. Golabgir A, Gutierrez JM, Hefzi H, Li S, Palsson BO, Herwig C, Lewis NE. Quantitative feature extraction from the Chinese hamster ovary bioprocess bibliome using a novel meta-analysis workflow. *Biotechnol Adv*. 2016;34(5):621–33.
270. Kelley B. Industrialization of mAb production technology: the bioprocessing industry at a crossroads. *MAbs*. 2009;1:443–52.
271. Welch JT, Arden NS. Considering “clonality”: a regulatory perspective on the importance of the clonal derivation of mammalian cell banks in biopharmaceutical development. *Biologicals*. 2019;62:16–21.
272. Radhakrishnan D, Wells EA, Robinson AS. Strategies to enhance productivity and modify product quality in therapeutic proteins. *Curr Opin Chem Eng*. 2018;22:81–8.
273. Klutz S, Holtmann L, Lobedann M, Schembecker G. Cost evaluation of antibody production processes in different operation modes. *Chem Eng Sci*. 2016;141:63–74.
274. Wu Y, Jiang S, Ying T. Single-domain antibodies as therapeutics against human viral diseases. *Front Immunol*. 2017;8:1802.
275. Steeland S, Vandenbroucke RE, Libert C. Nanobodies as therapeutics: big opportunities for small antibodies. *Drug Discov Today*. 2016;21(7):1076–113.
276. Mead EJ, Chiverton LM, Smales CM, von der Haar T. Identification of the limitations on recombinant gene expression in CHO cell lines with varying luciferase production rates. *Biotechnol Bioeng*. 2009;102(6):1593–602.
277. Wu NC, Yuan M, Liu H, Lee CD, Zhu X, Bangaru S, et al. An alternative binding mode of IGHV3-53 antibodies to the SARS-CoV-2 receptor binding domain. *Cell Rep*. 2020;33(3):108274.
278. Johari YB, Jaffé SRP, Scarrott JM, Johnson AO, Mozzanino T, Pohle TH, et al. Production of trimeric SARS-CoV-2 spike protein by CHO cells for serological COVID-19 testing. *Biotechnol Bioeng*. 2020. <https://doi.org/10.1002/bit.27615>.
279. DeFrancesco L. COVID-19 antibodies on trial. *Nat Biotechnol*. 2020;38(11):1242–52.
280. Marovich M, Mascola JR, Cohen MS. Monoclonal antibodies for prevention and treatment of COVID-19. *JAMA*. 2020;324(2):131–2.
281. Fischer S, Handrick R, Otte K. The art of CHO cell engineering: a comprehensive retrospect and future perspectives. *Biotechnol Adv*. 2015;33:1878–96.
282. Maruthamuthu MK, Rudge SR, Ardekani AM, Ladisch MR, Verma MS. Process analytical technologies and data analytics for the manufacture of monoclonal antibodies. *Trends Biotechnol*. 2020;38(10):1169–86.
283. He C, Ye P, Wang H, Liu X, Li F. A systematic mass-transfer modeling approach for mammalian cell culture bioreactor scale-up. *Biochem Eng J*. 2019;141:173–81.
284. Karst DJ, Steinebach F, Soos M, Morbidelli M. Process performance and product quality in an integrated continuous antibody production process. *Biotechnol Bioeng*. 2017;114:298–307.
285. Challener CA. Process Chromatography: continuous Optimization, Improved resin chemistries and customized separation solutions are enabling more efficient separations. *BioPharm Int*. 2017;30(8):14–7.
286. Bando-Campos G, Juárez-López D, Román-González SA, Castillo-Rodal AI, Olvera C, López-Vidal Y, et al. Recombinant O-mannosylated protein production (PstS-1) from *Mycobacterium tuberculosis* in *Pichia pastoris* (*Komagataella phaffii*) as a tool to study tuberculosis infection. *Microb Cell Fact*. 2019;18(1):1–19.
287. Alt N, Zhang TY, Motchnik P, Taticek R, Quarby V, Schlothauer T, et al. Determination of critical quality attributes for monoclonal antibodies using quality by design principles. *Biologicals*. 2016;44(5):291–305.
288. Bellino S, Punzo O, Rota MC, Del Manso M, Urdiales AM, Andrianou X, COVIS-19 WORKING GROUP, et al. COVID-19, disease severity risk factors for pediatric patients in Italy. *Pediatrics*. 2020;146(4):e2020009399.
289. Nogrady B. How kids' immune systems can evade COVID. *Nature*. 2020;588(7838):382.
290. Cathcart AL, Havenar-Daughton C, Lempp FA, Ma D, Schmid M, Agostini ML, et al. The dual function monoclonal antibodies VIR-7831 and VIR-7832 demonstrate potent in vitro and in vivo activity against SARS-CoV-2. *bioRxiv*. 2021. <https://doi.org/10.1101/2021.03.09.434607>.
291. Singh S, Kumar NK, Dwiwedi P, Charan J, Kaur R, Sidhu P, Chugh VK. Monoclonal antibodies: a review. *Curr Clin Pharmacol*. 2018;13(2):85–99.
292. Banach BB, Cerutti G, Fahad AS, Shen CH, de Souza MO, Katsamba PS, et al. Paired heavy and light chain signatures contribute to potent SARS-CoV-2 neutralization in public antibody responses. *bioRxiv*. 2021. <https://doi.org/10.1101/2020.12.31.424987>.
293. Miersch S, Li Z, Saberianfar R, Ustav M, Case JB, Blazer L, et al. Tetravalent SARS-CoV-2 neutralizing antibodies show enhanced potency and resistance to escape mutations. *bioRxiv*. 2020. <https://doi.org/10.1101/2020.10.31.362848>.
294. Hurlburt NK, Seydoux E, Wan YH, Edara VV, Stuart AB, Feng J, et al. Structural basis for potent neutralization of SARS-CoV-2 and role of antibody affinity maturation. *Nat Commun*. 2020;11(1):1–7.
295. Li D, Edwards RJ, Manne K, Martinez DR, Schäfer A, Alam SM, et al. The functions of SARS-CoV-2 neutralizing and infection-enhancing antibodies in vitro and in mice and nonhuman primates. *bioRxiv*. 2021. <https://doi.org/10.1101/2020.12.31.424729>.

Publisher's Note

Springer Nature remains neutral with regard to jurisdictional claims in published maps and institutional affiliations.

Ready to submit your research? Choose BMC and benefit from:

- fast, convenient online submission
- thorough peer review by experienced researchers in your field
- rapid publication on acceptance
- support for research data, including large and complex data types
- gold Open Access which fosters wider collaboration and increased citations
- maximum visibility for your research: over 100M website views per year

At BMC, research is always in progress.

Learn more biomedcentral.com/submissions

